

The University of Sheffield

Department of Biomedical Science

Centre for Stem Cell Biology



The Role of Jagged1 As a Pivotal Regulator of Neural Stem Cell Differentiation in the Neurogenic Niche

Robert Joseph Beattie

Inaugural-dissertation to obtain the degree of Doctor of Science from
the Department of Biomedical Science, The University of Sheffield,
Sheffield, England

Supervisor: Prof. Verdon Taylor

Advisors: Prof. Marysia Placzek and Prof. Marcelo Rivolta

External Examiner: Prof. Charles French-Constant

Internal Examiner: Prof. Peter Andrews

| | | |
|----------|--|-----------|
| 1 | SUMMARY | 9 |
| 2 | INTRODUCTION | 10 |
| 2.1 | DEVELOPMENT OF THE MAMMALIAN CENTRAL NERVOUS SYSTEM | 10 |
| 2.1.1 | <i>Neurulation: formation of the central nervous system anlage.....</i> | <i>10</i> |
| 2.1.2 | <i>Neurulation and the formation of the neural tube.....</i> | <i>11</i> |
| 2.1.3 | <i>Molecular basis of regionalization of the mammalian neural tube.....</i> | <i>12</i> |
| 2.1.4 | <i>Structural organization and function of the developing neural tube</i> | <i>13</i> |
| 2.2 | EMBRYONIC NEUROGENESIS..... | 15 |
| 2.2.1 | <i>Onset of Neurogenesis in the Telencephalon.....</i> | <i>15</i> |
| 2.2.2 | <i>The transition of the neuroepithelium to NSCs</i> | <i>15</i> |
| 2.2.3 | <i>Asymmetric versus symmetric cell divisions</i> | <i>18</i> |
| 2.2.4 | <i>Post-transcriptional Control of Neurogenesis in RGCs.....</i> | <i>20</i> |
| 2.2.5 | <i>Pathways and transcription Factors involved in embryonic neurogenesis</i> | <i>21</i> |
| 2.2.6 | <i>Progenitor fate commitment and restriction through sequential expression of transcription factors during cortical neurogenesis.....</i> | <i>22</i> |
| 2.2.7 | <i>The role of Wnt Signalling in embryonic neurogenesis and NSC proliferation.....</i> | <i>23</i> |
| 2.2.8 | <i>The direct regulation of target genes by Wnt signaling in Neurogenesis.....</i> | <i>25</i> |
| 2.2.9 | <i>The dual role of bHLH transcription factors in maintenance of NSCs and neuronal differentiation.....</i> | <i>26</i> |
| 2.2.10 | <i>Notch Signaling as a critical regulator in maintenance of NSCs.....</i> | <i>27</i> |
| 2.2.11 | <i>The essential role of canonical DSL Notch ligands in the CNS.....</i> | <i>33</i> |
| 2.3 | ADULT NEUROGENESIS..... | 41 |
| 2.3.1 | <i>The Neurogenic Regions in the Adult.....</i> | <i>41</i> |
| 2.3.2 | <i>The SVZ neurogenic niche.....</i> | <i>43</i> |
| 2.3.3 | <i>Molecular factors and signaling pathways involved in maintenance of the adult neurogenic niche</i> | <i>46</i> |
| 2.4 | OLIGODENDROGENESIS IN MAMMALS..... | 48 |
| 2.4.1 | <i>Signaling pathways involved in oligodendrocyte maturation.....</i> | <i>48</i> |
| 2.4.2 | <i>Origin of Oligodendrocytes in the SVZ.....</i> | <i>49</i> |
| 2.4.3 | <i>Oligodendrocyte maturation in the developing forebrain.....</i> | <i>50</i> |
| 2.4.4 | <i>The role of Wnt signaling in maturation of oligodendrocytes.....</i> | <i>55</i> |
| 2.4.5 | <i>The role of Notch signaling in maturation of oligodendrocytes</i> | <i>56</i> |
| 2.4.6 | <i>Multiple Sclerosis: The demyelinating disease.....</i> | <i>57</i> |
| 2.4.7 | <i>Putative role of Jag1 in remyelination.....</i> | <i>59</i> |
| 3 | RESULTS..... | 62 |

| | | |
|----------|---|------------|
| 3.1 | PROJECT 1: THE ROLE OF JAG1 FULL LENGTH IN MAINTAINING THE NSC NICHE | 62 |
| 3.1.1 | <i>Background</i> | 62 |
| 3.1.2 | <i>AAV-Jag1FL particles are able to package Jag1FL transcript and transduce cells in vitro</i> | 62 |
| 3.1.3 | <i>Retro-Jag1FL particles are highly efficient at transducing cells in vitro</i> .. | 63 |
| 3.1.4 | <i>Jag1FL-IRES-GFP transduction into the postnatal SVZ niche results in a fate shift to Sox10⁺ oligodendrocytes</i> | 64 |
| 3.1.5 | <i>Jag1FL-IRES-GFP⁺ Sox10⁺ cells express the early OPC marker NG2</i> ... | 65 |
| 3.1.6 | <i>Jag1FL-IRES-GFP⁺ NSCs lose sphere-forming capacity but do not change rate of proliferation</i> | 66 |
| 3.1.7 | <i>Under differentiating conditions, Jag1FL-IRES-GFP⁺ NSCs can upregulate essential genes involved in oligodendrocyte maturation</i> | 67 |
| 3.1.8 | <i>Next generation RNA sequencing of the transcriptome profiles of Jag1FL-IRES-GFP⁺ NSCs</i> | 67 |
| 3.1.9 | <i>Jag1FL-IRES-GFP⁺ NSCs upregulate genes involved in oligodendrocyte maturation</i> | 68 |
| 3.1.10 | <i>Current experiments studying the role of Jag1FL in the NSC Niche</i> | 68 |
| 3.2 | PROJECT 2: JAG1 AND THE ROLE OF THE JICD IN BI-DIRECTIONAL SIGNALING..... | 70 |
| 3.2.1 | <i>Background</i> | 70 |
| 3.2.2 | <i>JICD induces a cell autonomous loss of progenitor markers and stimulates differentiation genes in a PDZ dependent manner</i> | 70 |
| 3.2.3 | <i>Molecular components of JICD identified through TAP and Y2H screens</i> | 71 |
| 3.2.4 | <i>Basis for ChIP-Seq experiments</i> | 75 |
| 3.2.5 | <i>Analysis of JICD ChIP experiments</i> | 76 |
| 3.2.6 | <i>Confirmed targets identified by the JICD ChIP</i> | 77 |
| 3.2.7 | <i>Figures</i> | 78 |
| 3.2.8 | <i>Figure Legends</i> | 119 |
| 4 | DISCUSSION | 129 |
| 4.1 | JAG1FL IN THE ROLE OF NSC NICHE MAINTENANCE | 129 |
| 4.1.1 | <i>Jag1FL as a key regulator of stem cell fate</i> | 129 |
| 4.1.2 | <i>Regulation of genes involved in oligodendrocyte maturation identified by the Jag1FL-IRES-GFP⁺ NSC RNA-Seq</i> | 132 |
| 4.1.3 | <i>Hypothesis: Wnt signal regulation by Jag1 determines OPC specification</i> | 135 |
| 4.1.4 | <i>Interaction partners of JICD pertaining to the phenotype observed in Jag1FL NSC niche gain-of-function experiments</i> | 136 |

| | | |
|----------|--|------------|
| 4.1.5 | <i>Hypothesis: Regulation of CD4⁺ T-Cell development at the site of lesions by competition between the Notch ligands Jag1 and Dll</i> | 137 |
| 4.1.6 | <i>Conclusions</i> | 137 |
| 5 | THE CELL AUTONOMOUS ROLE OF JICD IN NSC MAINTENANCE | 141 |
| 5.1.1 | <i>Significant findings of this project</i> | 141 |
| 5.1.2 | <i>JICD can directly regulate the transcription of known Wnt targets by binding to the promoter regions</i> | 141 |
| 5.1.3 | <i>Future outlooks</i> | 142 |
| 6 | MATERIALS AND METHODS | 146 |
| 6.1 | METHODS | 146 |
| 6.1.1 | <i>Animals and husbandry</i> | 146 |
| 6.1.2 | <i>Preparation of tissue</i> | 146 |
| 6.1.3 | <i>Immunohistochemistry</i> | 146 |
| 6.1.4 | <i>Stereotactic injection of RV into postnatal mice</i> | 148 |
| 6.1.5 | <i>Quantification of transduced mice</i> | 148 |
| 6.1.6 | <i>Maintenance of cell culture lines (N2A, NIH3T3, HEK293 and Platinum-E HEK293 cells)</i> | 149 |
| 6.1.7 | <i>Transfection of cell culture lines by Calcium Phosphate</i> | 150 |
| 6.1.8 | <i>Transfection of Cell culture lines by TransFectin (BioRad)</i> | 150 |
| 6.1.9 | <i>Subcellular fractionation of N2A cells</i> | 150 |
| 6.1.10 | <i>Cloning of retroviral and AAV and retroviral constructs</i> | 151 |
| 6.1.11 | <i>Purification of AAV via iodixanol centrifugation</i> | 151 |
| 6.1.12 | <i>Purification of RV with Retro-X concentrator (ClonTech)</i> | 152 |
| 6.1.13 | <i>Isolation of NSCs and maintenance of Neurospheres</i> | 153 |
| 6.1.14 | <i>Transduction of NSC cultures</i> | 154 |
| 6.1.15 | <i>FACS sorting of transduced NSCs</i> | 154 |
| 6.1.16 | <i>Differentiation of transduced NSCs</i> | 154 |
| 6.1.17 | <i>Thymidine pulse chase assay of transduced NSCs</i> | 155 |
| 6.1.18 | <i>RNA Isolation</i> | 155 |
| 6.1.19 | <i>RNA-Sequencing of NSCs</i> | 155 |
| 6.1.20 | <i>cDNA synthesis and quantitative reverse transcriptase PCR (qRT-PCR) analysis</i> | 156 |
| 6.1.21 | <i>Production of endotoxin free plasmid DNA</i> | 157 |
| 6.1.22 | <i>In Utero Electroporation</i> | 157 |
| 6.1.23 | <i>IUE tissue preparation and quantification</i> | 158 |

| | | |
|----------|---|------------|
| 6.1.24 | <i>SDS-Page Western Blot</i> | 158 |
| 6.1.25 | <i>Yeast-2-Hybrid and TAP-tag proteomics screen screening</i> | 159 |
| 6.1.26 | <i>Luciferase reporter assays</i> | 160 |
| 6.1.27 | <i>Chromatin immunoprecipitation (ChIP) and ChIP-Sequencing</i> | 160 |
| 6.2 | MATERIALS | 162 |
| 7 | REFERENCES | 167 |
| 8 | APPENDIX..... | 186 |
| 8.1 | PUBLISHED ARTICLE | 186 |
| 8.1.1 | <i>Background for Published Article</i> | 186 |
| 8.1.2 | <i>Statement of Contribution</i> | 186 |
| 8.1.3 | <i>Key Findings</i> | 186 |
| 8.2 | CURRICULUM VITAE | 202 |

Acknowledgements

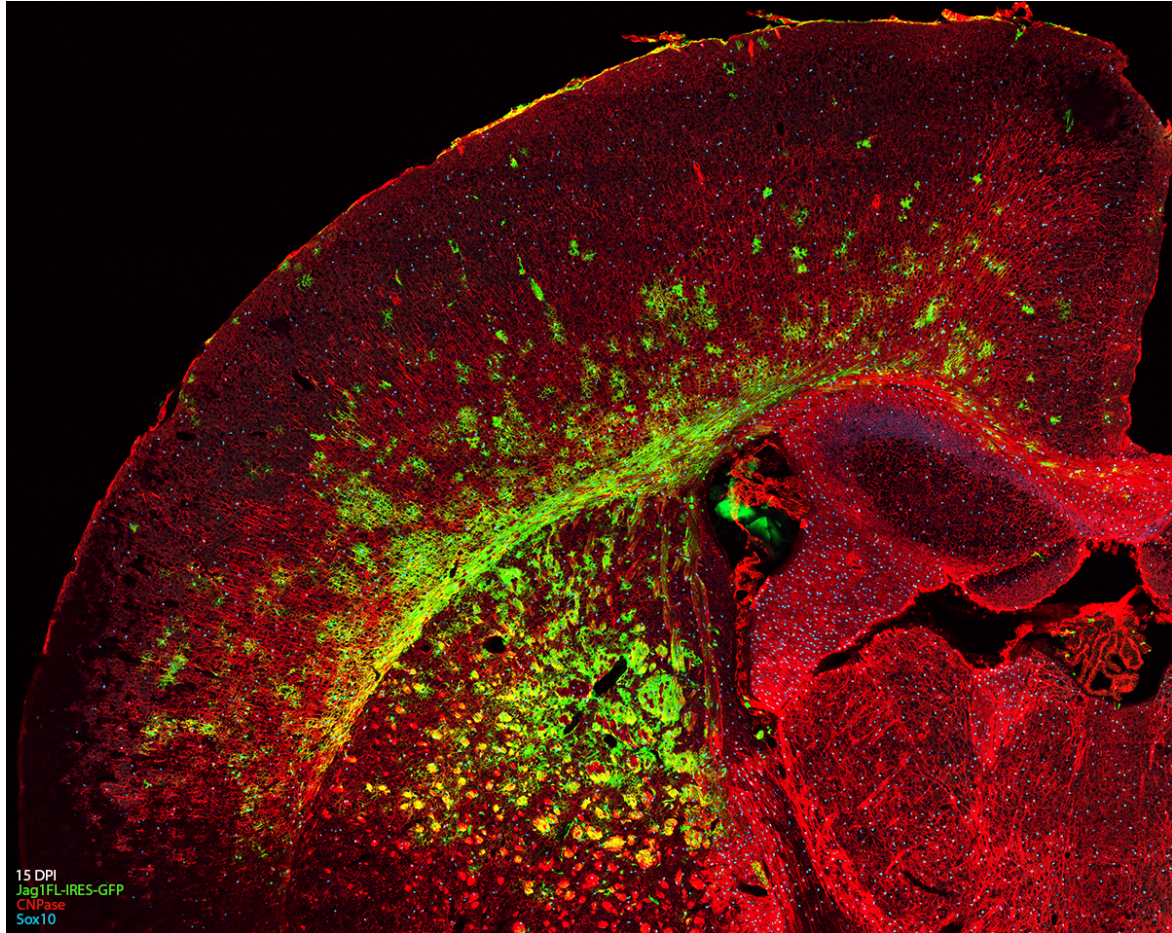
First and foremost, I would like to thank **my parents** and loving girlfriend **Maria Cristina Travaglio** for being there for me and providing support over the years. None of this would have been possible without them.

Due to unique circumstances, I was fortunate enough to study in three world-class universities over the course of my PhD. I made many friends and collaborated with brilliant scientists in all three locations. I would like to thank all those at the Max Planck Institute of Freiburg, The University of Sheffield, and the University of Basel to have had the fortune to observe and learn from them.

I extend my gratitude to all members of the Taylor lab, past and present. Particularly I would like to thank former lab members **Onur Basak**, **Sebastian Lugert**, **Dominik Herzog**, **Antje Grabosh**, **Marion Rutavinik** who were particularly influencing in my development as a student and helped me through the early months of my PhD. To current members, a special thanks to **Claudio Giachino**, **Chiara Rolando**, and **Frank Sager**, all of whom spent many hours and shared their expertise with me when I needed it most. Additionally, thank you to **Tanzila Mukhtar**, who during her Masters, contributed significantly to establishing the ChIP experiments. Most importantly, thank you to **Verdon Taylor**, whose guidance, patience, and belief in me as a student has allowed me to participate and learn science in a world-class laboratory in the field of developmental neuroscience, and for that I am forever in gratitude.

Thank you to **Annalisa Buffo** and **Enrica Boda** for their extensive knowledge of oligodendrogenesis and performing the ongoing NSC grafting experiments. Thank you to **Antonious Rolink** for your help with FACS sorting and **Pascal Lorentz** for introducing me to the world of microscopy. Thank you to **Marco Osterwalder** for help in setting up my ChIP experiments in Basel. Thank you to **Christian Biesel** at the DBSS-E for your crucial help with deep sequencing both my ChIP-seq and RNA-seq samples, and **Robert Ivanek** for not only analyzing the data but for also teaching me the basics of bioinformatics. Thank you to **Joelle Desmarais**, who taught me the cell fractionation technique, and **Christian Unger** who helped with viral purification protocols. Thank you to **Jan Herb** for purifying the AAV particles. Thank you to the labs of **Placzek**, **Rivolta**, **Kemler** and **Zeller** for both interesting scientific discussion and lending of reagents from time to time. Thank you in particular to my two scientific advisors, **Marysia Placzek** and **Marcelo Rivolta** who gave me excellent scientific guidance, even from half a continent away.

Finally, thank you to **Claudio**, **Chiara**, and **Orion Penner** for taking the time to help with proofreading of the manuscript.



For my loving parents, who without their support over the years,
none of this would have been possible.

1 Summary

During formation of the brain in mammals, neural stem cells (NSCs) transit through sequential periods of expansion, neurogenesis and gliogenesis. Notch signaling maintains NSCs and blocks transcription of pro-neurogenic factors. Notch ligands are expressed by differentiating progenitors and activate lateral inhibition signals through Notch. It has long been proposed that Notch signaling occurs bi-directionally through ligands such as Jagged1 (Jag1), which are also type I membrane proteins. However, the molecular mechanisms controlling the transition from stem cell division, where Notch plays a maintenance role, to daughter cell differentiation are poorly understood.

To study the role of Jag1, in niche maintenance I began by transducing NSCs lining the subventricular zone (SVZ) with full length Jag1 (Jag1FL). Surprisingly, Jag1 induced a fate switch to Sox10⁺ oligodendrocyte precursors. NSCs grown under differentiating conditions *in vitro* recapitulated this phenotype to some degree. RNA-Sequencing analysis was performed to study the transcriptome changes of Jag1FL-IRES-GFP transduced NSCs. This screen revealed an upregulation (induction) of key genes involved in oligodendrocyte maturation and myelination, which were further confirmed by qRT-PCR. Ongoing NSC grafting experiments are being performed to analyze the effects of Jag1FL-IRES-GFP⁺ NSCs on mice exhibiting focal myelin lesions. These proof of concept experiments hold promise for elucidating an, as of yet unknown role of Jag1 in remyelination. Through biochemical analyses, we have demonstrated that the Jag1 intracellular domain (JICD) can act as a transcription factor signaling in a cell autonomous fashion upon activation. Through chromatin immunoprecipitation, I have identified potential genomic regions and Wnt signaling target genes, directly bound by nuclear JICD. Taken together with the *in vivo* data, this proposes a new role for Jag1 in NSCs maintenance, and displays its potential for regulating fate switch to an oligodendrocytic lineage.

2 Introduction

2.1 Development of the mammalian central nervous system

Our understanding of the complexity of the human brain has advanced a great deal in the last 25 years. We have made major inroads into understanding how the brain transfers, stores, and retrieves information. However, our understanding of the processes governing brain development has lagged behind to some degree. Developmental neurobiology has made advances, including the discovery of NSCs and NSC niches that remain into adulthood. Hence, it is now clear that diverse progenitor cell types give rise to all cell lineages of the brain. These advances in knowledge have benefited from novel approaches to lineage trace cell populations, advances in high-resolution microscopy, increased cell specific markers and transgenic alleles, and genome-wide analysis of gene expression down to the cellular level. With the advent of cellular reprogramming and programming of human induced pluripotent cells (iPS), we are now entering an age in which functional human neurons can be generated and studied *in vitro* to obtain a greater understanding of gene function and dysfunction. These advances open up avenues that were previously impossible, where patient-derived iPS cells could potentially be used therapeutically for the treatment of neural degenerative diseases. As technologies and our understanding of neuron differentiation continue to advance the field of neurobiology and its potential biomedical applications will expand greatly.

2.1.1 Neurulation: formation of the central nervous system anlage

During early stages of postgastrulation embryonic development the ectoderm differentiates to form the epidermis and the neural ectoderm, the primordium of the nervous system (for review see (Tam and Loebel 2007)). In vertebrates, the central nervous system (CNS) begins as the neural plate, an ectodermal-derived structure which folds dorsally to form the neural tube through a process called neurulation. Neurulation is divided into the sequential phases of primary and secondary neurulation initiated through a combination of growth factors and inhibitory signals secreted by the

underlying axial mesoderm (notochord), dorsal ectoderm, and Spemann organizer, respectively. The neural tube then differentiates rostrally into the future brain and caudally to form the spinal cord and most of the peripheral nervous system, which will not be covered here. The rostral part of the neural tube segregates into three swellings, establishing the forebrain, midbrain and hindbrain. In parallel, the rostrocaudal tube segments into modules called neuromeres (Copp, Greene et al. 2003).

2.1.2 Neurulation and the formation of the neural tube

The mammalian brain and most of the spinal cord are formed during the first phase of neurulation, which is commonly divided into 4 phases. In mice neurulation begins at around embryonic day (E) 8 with the induction of the neural plate when the inhibitory signals Chordin, Noggin and Follistatin are secreted by the Spemann organizer (Smart 1973). These factors block bone morphogenic protein 4 (Bmp4) signaling, inducing dorsal epiblast cells and allowing the anteroposterior midline of the ectoderm to adopt a neuroectodermal fate. These neuroectodermal cells undergo an apicobasal thickening and generate the neural plate along the dorsal midline of the embryo. Once committed, neuroectodermal cells no longer require inhibitory signals for neural plate formation to proceed (Fig. 1) (Copp, Greene et al. 2003, Copp 2005).

The neural plate undergoes a remodeling phase, whereby convergent-extension increases the length (rostrocaudally) while simultaneously narrowing the width (transversely). During these processes, the neural plate continues to thicken apicobasally generating cellular forces that begin to bend the neural plate and induce neural tube formation. As the lateral folds of the neural plate converge to the midline, the ectoderm of the future epidermis delaminates from the neuroepithelium of the neural plate and fusion of both the ectoderm and dorsal neural tube proceeds (Copp, Greene et al. 2003, Copp 2005). The neural tube zips closed posteriorly from the hindbrain and anteriorly from the mid-hindbrain junction, while remaining open over the future 4th ventricle posterior to the cerebellum. By E9 in the mouse, fusion is complete and the neural tube is closed forming the primitive ventricles of the future brain regions (Tong and Alvarez-Buylla 2014).

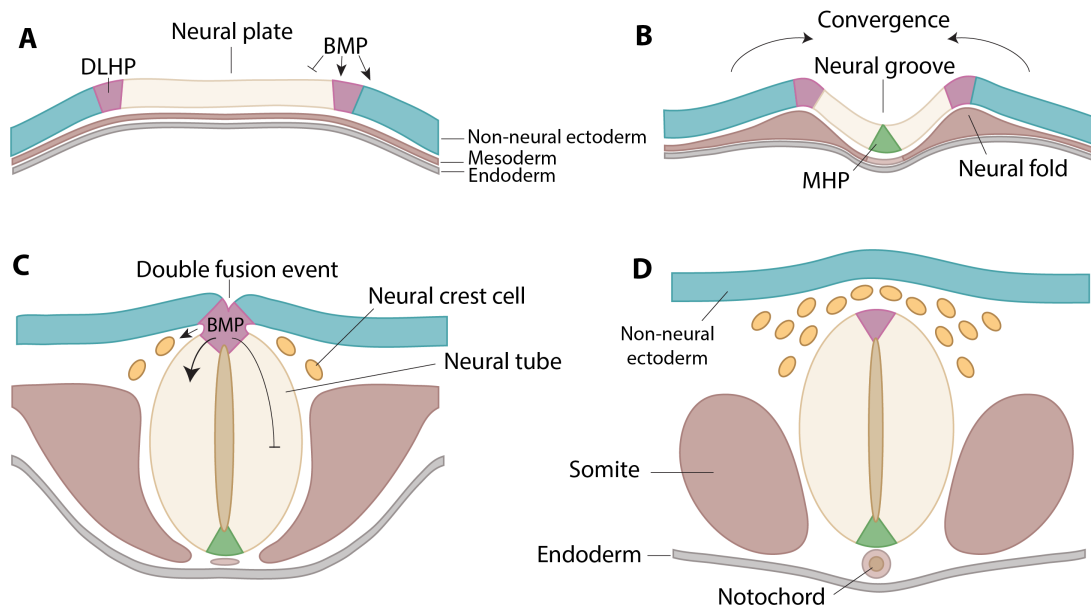


Figure 1. Stages of central nervous system development.

The brain and most of the spinal cord are formed during primary neurulation, which is commonly divided into 4 phases. a) Epiblast cells are induced to a neuroectoderm fate, generating the neural plate. b) The remodeling phase in which the neural plate undergoes convergent-extension and begins to fold along the median hinge point (MHP) and dorsolateral hinge points (DLHPs). c) The two neural folds converge at the midpoint and then proceed to fuse, leading to the dorsal closure of the neural tube. d) By embryonic day 9 in the mouse, fusion is complete. BMP – Bone morphogenetic protein (adapted from (Jessell and Sanes 2000, Liu and Niswander 2005)).

Far less is known about secondary neurulation, which is the formation of the posterior region of the neural tube and caudal-most portion of the spinal cord. Secondary neurulation begins from a solid mass of cells forming from the tail bud. These cells form the medullary cord, which then cavitates to form multiple lumina. Finally, these lumina fuse into a single lumen continuing the central canal of the neural tube in the most rostral aspects. Contrary to primary neurulation, here the process is more a hollowing out of a mass of cells rather than tube formation from an ectodermal plate of cells (Shimokita and Takahashi 2011).

2.1.3 Molecular basis of regionalization of the mammalian neural tube

The neuroepithelium of the neural tube follows a sequential series of overlapping, and competing patterning steps during brain development.

Timing is critical, particularly in structures such as the cerebral cortex where even moderate changes in gene expression pattern can lead to serious developmental, motor, behavioral, psychological and cognitive disorders (Geschwind and Rakic 2013). The best characterized morphogens and signaling pathways involved in regional identity include Sonic hedgehog (Shh), retinoic acid (RA), fibroblast growth factor (FGF), Wingless (Wnt), and BMP signaling (Fig. 2) (Rallu, Corbin et al. 2002, Lupo, Harris et al. 2006). Shh is secreted by the notochord (axial mesoderm) beneath the floor plate of the neural tube and controls neuronal cell fate in a concentration-dependent manner (Cohen, Briscoe et al. 2013). RA is secreted from the mesoderm and defines the posterior CNS, including the hindbrain and spinal cord. RA contributes to segmentation of the hindbrain into eight distinct compartments called rhombomeres, which later give rise to the medulla, pons and cerebellum (Maden 2007). FGF activity along with RA and Wnts leads to the caudalization of the neural tissue (Sansom and Livesey 2009, Tiberi, Vanderhaeghen et al. 2012). Wnt signaling is crucial in development of the neural tube, particularly in establishing anteroposterior polarity. Several Wnt antagonists including Cerberus, Dickkopf and Tlc are important in patterning the dorsal telencephalon (Piccolo, Agius et al. 1999, Bafico, Liu et al. 2001, Houart, Caneparo et al. 2002, Ciani and Salinas 2005, Hebert and Fishell 2008). Diffusion of BMPs and their antagonists along the neural plate creates a gradient of high BMP activity dorsally to low activity ventrally. This leads to the specification of distinct pools of progenitors in the dorsal spinal cord (Liu and Niswander 2005, Lupo, Harris et al. 2006).

2.1.4 Structural organization and function of the developing neural tube

As the neural tube progressively becomes more regionalized the organization of distinct structural domains arises. Segmentation of the neural tube in the mouse begins initially by assigning anterior-posterior identity along the neuraxis dividing into the spinal cord, hindbrain, midbrain and forebrain. The hindbrain (or rhombencephalon) is further divided into rhombomeres which give rise to the metencephalon (the pons and the cerebellum) as well as the myelencephalon (the medulla oblongata). The midbrain (or mesencephalon) is located caudal to the hindbrain and rostral to the forebrain.

The forebrain (prosencephalon) divides into the diencephalon (prethalamus, thalamus, hypothalamus, subthalamus, epithalamus, and pretectum) and the telencephalon (cerebrum). Further divisions of the cerebrum segregate it into the cerebral cortex, the basal ganglia, and the limbic system (Fig. 2). For a full review of the cellular compartments and boundaries in vertebrate brain development, please see Kiecker and Lumsden, 2005 (Kiecker and Lumsden 2005).

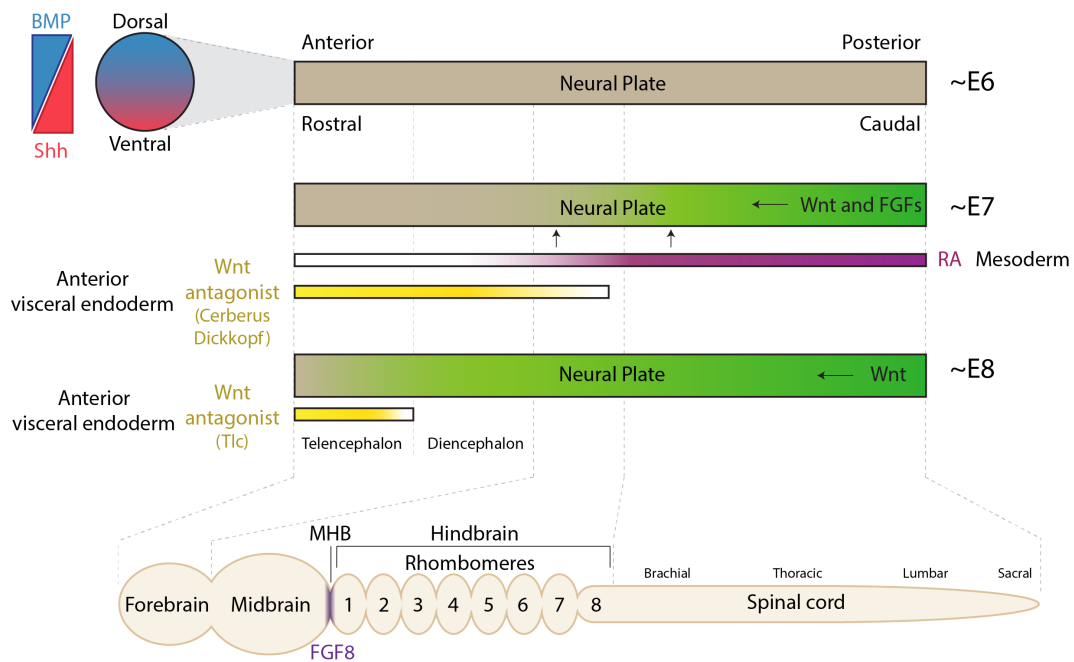


Figure 2. Regionalization during neural tube formation is dependent on overlapping agonistic and antagonistic morphogen gradients.

Dorsoventral patterning of the neural tube is largely dependent on bone morphogenic protein (BMP) and Sonic hedgehog (Shh) signaling. Some of the key factors involved in patterning the anteroposterior axis include wingless (Wnt) and its antagonists (Cerberus, Dickkopf, Tlc), fibroblast growth factor (FGF), and retinoic acid (RA). Distribution of these factors leads to the eventual segmentation of the neural tube into the forebrain, midbrain, hindbrain and spinal cord. FGF8 expression delineates the midbrain-hindbrain boundary (MHB). (Adapted from (Rallu, Corbin et al. 2002, Kiecker and Lumsden 2005))

2.2 Embryonic Neurogenesis

2.2.1 Onset of Neurogenesis in the Telencephalon

The mammalian neocortex modulates processing of sensory information, motor activity, and mediates cognition. The cerebral cortex develops in an inside-out temporal fashion and is comprised of six histologically distinct neuronal layers, forming the isocortex. These layers differ in neuronal composition, connectivity, and density. The earliest born neurons populate the deep layers of the cortex (VI and V), and the later born neurons migrate past the deep layer neurons to form the upper layers (IV, III and II) (Franco and Muller 2013). Diverse neuronal subtypes that contribute to the complex neural circuitry are specified by a multitude of factors. In recent years, much progress has been made towards understanding the molecular pathways and mechanisms controlling neuronal cell-type diversity in the cortex. However, detailed mechanistic knowledge of the interplay between the transcriptional networks and upstream factors has yet to be elucidated (Molyneaux, Arlotta et al. 2007).

2.2.2 The transition of the neuroepithelium to NSCs

Neurogenesis involves multiple processes that include proliferation, fate commitment, differentiation, maturation, expansion, migration and functional integration of newborn neurons into neuronal circuits. In the developing mouse CNS there are at least two distinct classes of progenitor cells, the apical progenitors (APs) and the basal progenitors (BPs; also termed intermediate progenitors). The APs include neuroepithelial progenitors (NEPs) which generate radial glia cells (RGCs) and short neural precursors, all of which have stem cell character (Fishell and Kriegstein 2003, Kriegstein and Gotz 2003, Gotz and Huttner 2005, Gal, Morozov et al. 2006). By E9, the neuroepithelium is a single layer of NEPs that form the pseudostratified neuroepithelium. Due to the displacement of the cell body (karyon) of the NEPs during cell division, the ventricular zone resembles a multicellular structure. The migration of the nucleus (karyon) during cell cycle is referred to as interkinetic nuclear migration, and is cell cycle dependent (Fig. 3) (Takahashi, Nowakowski et al. 1993). Mitosis occurs at the apical side of the

cell at the lumen of the neural tube while S phase takes place at the basal boundary of the ventricular zone, and G1 and G2 occur during directed migration of the nucleus (Fig. 4) (Taverna and Huttner 2010, Lui, Hansen et al. 2011). As NEPs and RGCs transition from symmetric proliferation to asymmetric neurogenic divisions during neurogenesis their cell cycle lengthens almost entirely due to a lengthening of the G1 phase (Takahashi, Nowakowski et al. 1995).

NSCs in the ventricular zone (VZ) of the neural tube connect with each other through tight and adherens junctions at their apical ends. The maintenance of cell polarity is dependent upon the adherens junctions and polarity is critical for NSC function (Gotz and Huttner 2005, Fish, Dehay et al. 2008, Franco and Muller 2013). Between E9 and E10 (before the onset of neurogenesis) NEPs maintain their radial morphology, but begin to exhibit astroglia hallmarks and downregulate tight junctions and other epithelial markers, ultimately transforming into a more restricted distinct cell type called RGCs (Huttner and Brand 1997, Malatesta, Hartfuss et al. 2000, Kriegstein and Gotz 2003). The nuclei of RGCs continue to migrate along the apical-basal axis during cell cycle, but interkinetic nuclear movement becomes continually more restricted to the apical end of the extending basal process. By the time neurogenesis begins in the forebrain, between E10 and E11 in the mouse, RGCs start to upregulate markers characteristic of astroglia such as glutamate transporter (GLAST), brain-lipid-binding protein (BLBP), glial fibrillary acidic protein (GFAP), and vimentin (Gotz and Huttner 2005). Apical end feet of the RGCs remain anchored to each other through adherens junctions. Deletion of essential endocytic genes, *Numb* and *Numb1*, from RGCs results in the disorganization of adherens junctions and loss of cellular polarity (Kuo, Mirzadeh et al. 2006, Rasin, Gazula et al. 2007).

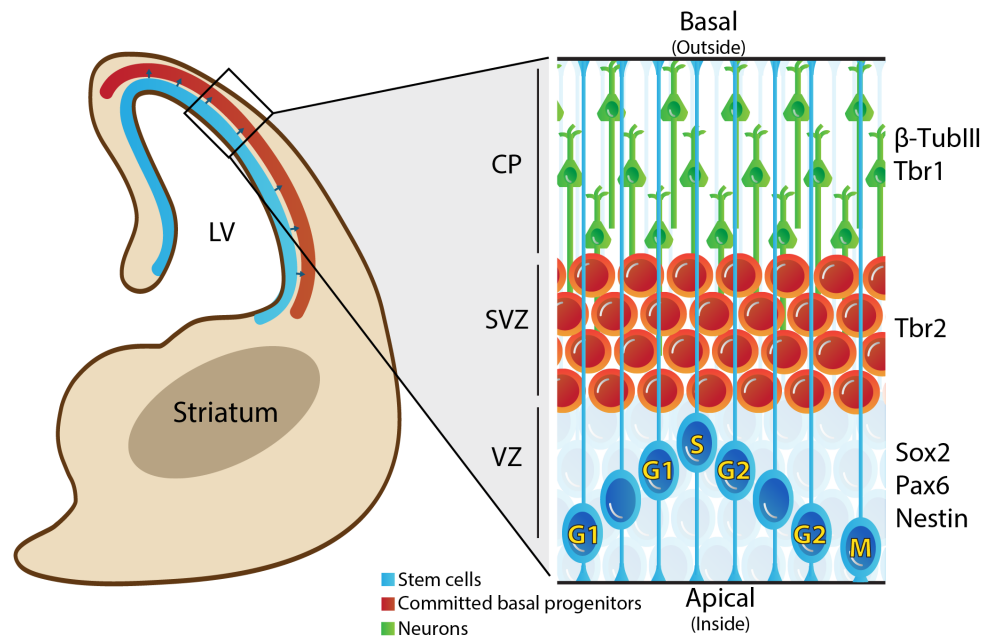


Figure 3. Scheme of a coronal hemisection of the developing mouse telencephalon and the stem and progenitor populations.

As neurogenesis continues, neural stem cells (NSCs) retain contact with the outside of the neural tube and their apical end feet line the tube resulting in long polarized processes. NSCs undergo interkinetic nuclear migration during cell cycle. DNA replication (S-phase) always takes place when the cell body reaches the ventricular (VZ)-subventricular zone (SVZ) boundary, mitosis (M) and karyokinesis take place at the luminal surface (apical) of the neural tube. Committed progeny of the NSCs, basal progenitors migrate to the SVZ where they may divide before differentiating into immature neurons that migrate to the superficial layers of the forming cortical plate (CP) and future cerebral cortex.

As development continues, a class of intermediate progenitors called basal progenitors (BPs) is formed. Unlike NEPs and RGCs, BPs do not have apical connections to the lumen of the neural tube but instead undergo a limited number of cell divisions in the subventricular zone (SVZ), a region basal and adjacent to the VZ (Fig. 4) (Haubensak, Attardo et al. 2004, Noctor, Martinez-Cerdeno et al. 2004). BPs in the SVZ upregulate the transcription factors Cux1, Cux2 and Tbr2 and although limited self-renewing divisions have been shown, they subsequently undergo symmetric differentiating cell divisions to generate two neurons (Nieto, Monuki et al. 2004, Englund, Fink et al. 2005, Cubelos, Sebastian-Serrano et al. 2008).

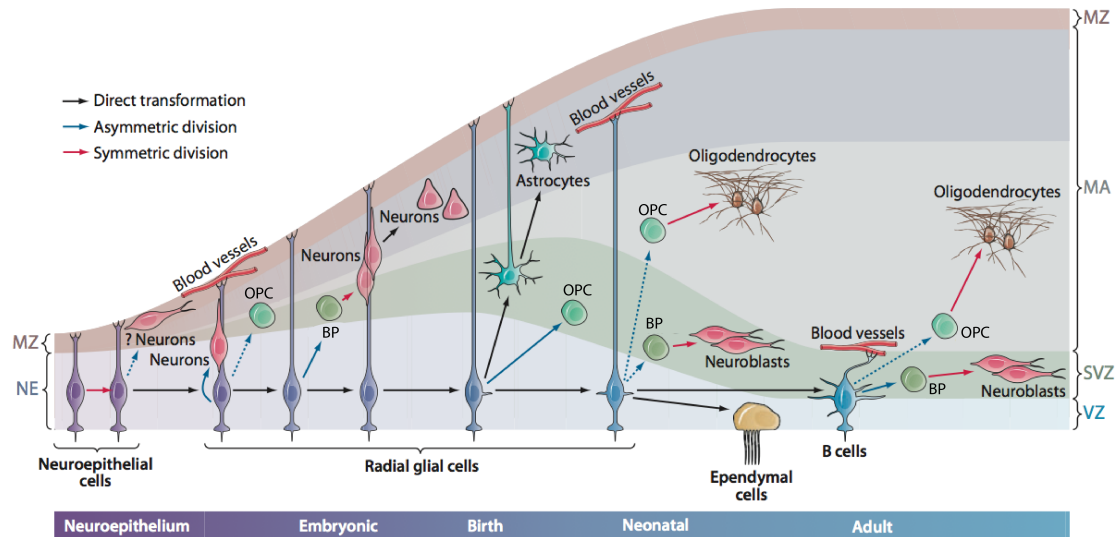


Figure 4. Neurogenesis and migration of neurons in the mouse cortex.

Neural epithelial progenitors (NEPs) in the ventricular zone (VZ) of the developing telencephalon generate the many neuronal subtypes of the six-layered cerebral cortex (see 2.2.6). Before neurogenesis commences, NEPs undergo a series of symmetric divisions in the VZ expanding the stem cell pool. As neurogenesis proceeds, the VZ NEPs transform into radial glial cells (RGCs) and generate basal progenitors (BPs), which populate the subventricular zone (SVZ). Newly formed neurons either derived directly from NSCs or from the BPs migrate radially outwards forming the different cortical layers in an inside out fashion. Each layer of the cerebral cortex is composed of different neuronal subtypes, which are generated sequentially throughout neurogenesis. RGCs can also give rise to oligodendrocyte precursor cells (OPCs), which eventually differentiate into oligodendrocytes. Towards the end of neurogenesis the radial scaffolding of the RGCs is dismantled and RGCs become gliogenic, generating cortical and subventricular zone (SVZ) astrocytes and a sheet of ependymal cells lining the ventricles. (Directly from (Kriegstein and Alvarez-Buylla 2009))

2.2.3 Asymmetric versus symmetric cell divisions

During cortical development, neural progenitors can undergo three modes of cell division. Before neurogenesis begins NEPs divide symmetrically giving-rise to two NEP daughter cells, allowing for rapid expansion of the progenitor pool. Later NSCs can undergo asymmetric divisions, allowing for both self-renewal of the NSC and generation of a differentiated daughter cell (Miyata, Kawaguchi et al. 2001, Noctor, Flint et al. 2001). The committed daughter cells are either a single neuron or a BP, which can undergo further cell divisions. RGCs act as a framework for the newborn neurons to migrate into the cerebral cortex. The third mode of cell division involves an

amplification step at the BP stage, increasing the BP pool before finally differentiating into neurons. Since a single RGC can give rise to multiple BPs, and a single BP can give rise to two or more neurons, the SVZ is generally recognized as one of the main sites of amplification during neurogenesis (Fishell and Kriegstein 2003, Knoblich 2008, Kriegstein and Alvarez-Buylla 2009).

Regulation of RGC numbers as they divide to give rise directly to neurons or BPs is crucial in controlling neurogenesis. Too many daughter cells dividing directly into neurons results in overall neurogenesis being severely reduced due to a lack of BP amplification. Although mitotic spindle orientation is not the only determinant, it has been shown to play a direct role in RGC daughter cell fate (Knoblich 2008).

Asymmetric segregation of cytoplasmic determinants has also been shown to be key in regulating asymmetric cell divisions. Some well-characterized players include EGFR, MALS-3, Dyrk1a, Trim32, Stau32, and polarity protein Par3, but it is predicted many more determinants are actually involved (Sun, Goderie et al. 2005, Srinivasan, Roosa et al. 2008, Schwamborn, Berezikov et al. 2009, Ferron, Pozo et al. 2010, Kusek, Campbell et al. 2012). Time-lapse imaging of embryonic neocortical slice culture and adult SVZ cultures showed asymmetric inheritance of the Notch ligand, Delta-like 1 (Dll1), the E3 ubiquitin ligase Mind bomb-1 (Mib1), and the Notch agonist Numb (Fig. 5d) (Bultje, Castaneda-Castellanos et al. 2009, Dong, Yang et al. 2012, Kawaguchi, Furutachi et al. 2013). Cells inheriting these factors undergo differentiation while the Notch presenting cell remains in an undifferentiated state (Paridaen and Huttner 2014). Whether this asymmetric inheritance is unique to Dll1, or is common amongst other Notch ligands, has yet to be shown. Interestingly the outcome for cells inheriting asymmetrically segregated factors varies amongst vertebrates (Fig. 5b,c). Although the mechanism has yet to be elucidated it seems Par3 in mice remains with the future RGC, while in zebrafish this is segregated with the Notch inhibitor Mib1, resulting in differentiation (Paridaen and Huttner 2014).

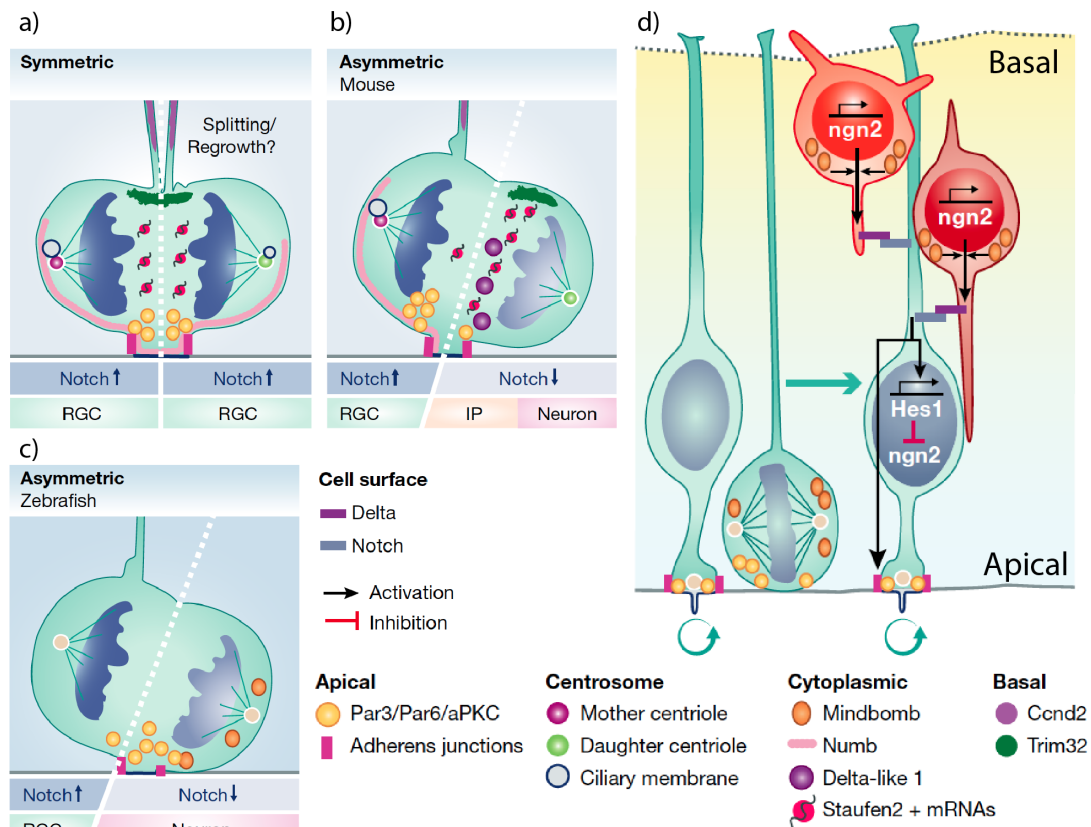


Figure 5. Asymmetric segregation of molecular determinants in asymmetric cell divisions of RGCs.

Segregation of cytoplasmic determinants is believed to be one of the key factors in regulating asymmetric cell divisions. a) Symmetric segregation of fate determinants is thought to occur during symmetric divisions of RGCs. b) However asymmetries, in particular the Par3 complex in vertebrates appears to lead to different fates for the daughter cells. c) The segregation of cell determinants varies amongst vertebrates, with daughter cells fated to become neurons in Zebrafish accumulating higher levels of Par3, opposite to that of mice. d) Additionally, asymmetric distribution of Notch components is believed to lead to differential levels of Notch signaling in daughter cells. (Directly from (Paridaen and Huttner 2014))

2.2.4 Post-transcriptional Control of Neurogenesis in RGCs

How neural progenitors control the transition from stem cell maintenance and expansion to fate restriction is not fully understood, particularly in the developing cerebral cortex. MicroRNAs (miRNA) are endogenous 20-24 nucleotide RNAs that, through complimentary base-pairing, bind and regulate target mRNAs of protein-coding genes. Regulation is controlled by the miRNA-induced silencing complex (miRISC) which directs post-transcriptional silencing by mediating degradation or transcriptional repression of the mRNA transcript (Pasquinelli 2012). Using techniques such as miRNA microarrays

and small RNA deep-sequencing it has been revealed that there is a distinct profile of miRNA expression in the developing mammalian brain (Lagos-Quintana, Rauhut et al. 2002, Landgraf, Rusu et al. 2007, Bak, Silahtaroglu et al. 2008, He, Liu et al. 2012). Links between neurodegeneration and relative levels of miRNAs has been shown to exist through experiments globally disrupting miRNA biogenesis during neural development (Kosik 2006). The role of the miRNA microprocessor in neurogenesis was also recently identified. In the absence of Hes protein repression NSCs in the dorsal forebrain accumulate Ngn2 resulting in the upregulation of NeuroD1 and a commitment to neuronal differentiation (Guillemot 2005, Heng, Nguyen et al. 2008). However, levels of both *Neurog2* mRNA and Ngn2 protein are directly regulated through the protein Drosha, a key component of the microprocessor (Knuckles, Vogt et al. 2012). Therefore, the microprocessor is required for maintaining NSCs and the timing of neurogenesis (Abe and Bonini 2013).

miRNAs have been shown to directly regulate key components of the Notch signaling pathway. For example, miRNA-184 promotes adult NSC proliferation and inhibits neuronal differentiation by directly silencing *Numbl* (*Numbl*), a known regulator of brain development (Liu, Teng et al. 2010). miRNA silencing of Notch ligands has been shown, in particular targeting of Jag1 transcripts by miRNA-124, miRNA-21, -34a, -124a, and -200 (Hashimi, Fulcher et al. 2009, Brabletz, Bajdak et al. 2011, Liu, Chopp et al. 2011, Vallejo, Caparros et al. 2011, Bhalala, Srikanth et al. 2013). So far, only a small number of miRNAs have been identified and characterized in the CNS. Identifying additional miRNAs and elucidating their functional role in regulating and maintaining NSCs will be important for our understanding of neurogenesis and neurodegenerative diseases.

2.2.5 Pathways and transcription Factors involved in embryonic neurogenesis

Numerous pathways, transcription factors, and signaling molecules converge in agonistic and antagonistic crosstalk during neurogenesis. Some key pathways include the well-studied Wnt, Notch, FGF and Shh signaling. Many have a direct role in fate determination of RGCs, and act in harmony with transcription factors such as the family of basic-helix-loop-helix (bHLH) factors which exert both proneural and pro-NSC maintenance effects

(Paridaen and Huttner 2014). Additionally, spatial temporal timing of transcription factors is key in fate determination, especially in developing structures such as the cortex (Greig, Woodworth et al. 2013).

2.2.6 Progenitor fate commitment and restriction through sequential expression of transcription factors during cortical neurogenesis

Currently there is evidence to support two alternative models of temporal expansion and differentiation in the cortex. The 'common progenitor' model proposes that NSCs restrict their fate temporally as neurogenesis progresses, sequentially generating neurons unique to each layer of the isocortex. Alternatively, the 'multiple progenitor' model proposes that NSCs could begin as a heterogeneous pool, in which each NSC subtype would be guided by intrinsic and extrinsic signals to generate specific neuronal subtypes or astrocytes (Greig, Woodworth et al. 2013).

Heterochronic transplantation experiments performed in ferrets by McConnell and colleagues revealed that the potential of NSCs is restricted over time (McConnell 1988). With age NSCs become more defined in their fate, eventually losing the ability to generate deep layer neurons (Desai and McConnell 2000, Han and Sestan 2013). Supporting the common progenitor model clonal analyses showed that neocortical NSCs generate deep and upper layer neurons *in vitro* in a sequential and temporal manner (Shen, Wang et al. 2006). *Fezf2*, a transcription factor enriched in cortical layer 5 and important in fate specification, was shown to exist throughout cortical neurogenesis in NSCs (Chen, Schaevez et al. 2005, Molyneaux, Arlotta et al. 2007, Guo, Eckler et al. 2013). It was demonstrated that *Fezf2*⁺ NSCs could sequentially generate both deeper and upper layer neurons while becoming fate restricted over time (Guo, Eckler et al. 2013). Moreover, *Fezf2* is expressed by NSCs as early as E8.5 in the pallial neuroepithelium, suggesting its impact on fate determination (Leone, Srinivasan et al. 2008, Kwan, Sestan et al. 2012, Greig, Woodworth et al. 2013).

The multiple progenitor model proposes different subsets of progenitors, which are pre-determined and committed to generate specific neuronal subtypes (Greig, Woodworth et al. 2013). These fate restricted NSCs express the transcription factors *Cux1* and *Cux2* in the VZ and SVZ abundantly during

upper-layer neurogenesis, specifying them to become callosal projection neurons (Franco, Gil-Sanz et al. 2012). However, it was shown that during early development $Cux2^+$ NSCs proliferate and expand without differentiating. Later when neurons of the superficial cortical layers are being generated, these NSCs and progenitors switch to a neurogenic mode and generate $Cux2^+$ upper-layer neurons (Franco and Muller 2013). These findings challenged the existing 'common progenitor model' but left many questions unanswered. Subsequent lineage tracing experiments confirmed the presence of $Cux2^+$ NSCs but suggested they generate both upper and deep-layer neurons as well as interneurons derived from the ventral telencephalon (Guo, Eckler et al. 2013). The presence of multi-potent $Fezf2^+Cux2^+$ NSCs does not negate the possibility of the existence of fate-restricted progenitors. Further investigations at the single cell level are crucial in understanding the mechanisms underlying NSC regulation (Guo, Eckler et al. 2013, Han and Sestan 2013).

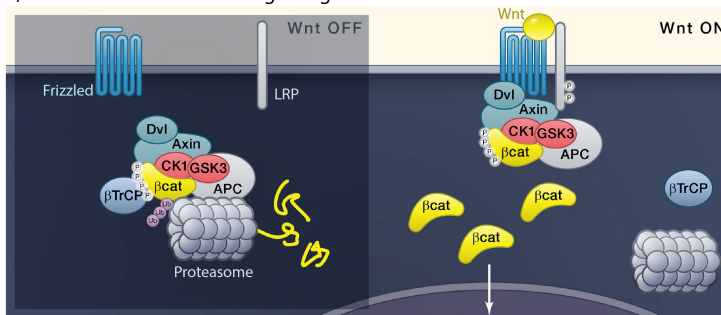
Other models in the field emphasize the presence of stem cells that are multipotent and switch their fate over the course of sequential rounds of cortical neurogenesis. This suggests that NSCs would be initially committed to one fate during development and then switch to an alternate fate as corticogenesis proceeds. Multipotent NSCs could then generate multiple neuronal subtypes while still restricting their potential and eventually becoming unipotent. Further investigation of the mechanisms driving neurogenesis is crucial to understand NSC cell regulation (Greig, Woodworth et al. 2013).

2.2.7 The role of Wnt Signalling in embryonic neurogenesis and NSC proliferation

The Wnt family consists of secreted ligand glycoprotein signaling molecules that regulate cell proliferation, specification, differentiation, and migration throughout development (Clevers and Nusse 2012). There are three characterized pathways of Wnt signaling; canonical Wnt signaling, non-canonical Wnt planar cell polarity pathway, and the non-canonical Wnt/calcium signaling pathway (Fig. 6a) (Clevers and Nusse 2012). In all three pathways signaling is activated when a Frizzled family receptor is bound by secreted Wnt. In canonical Wnt signaling activation of Frizzled recruits the

co-receptor LRP5/6 leading to the phosphorylation and activation of disheveled (Dvl) (Clevers and Nusse 2012). This results in the phosphorylation of LRP6 by GSK-3 β kinase permitting the recruitment of Axin. Axin is part of the destruction complex responsible for sequentially binding, phosphorylating and ubiquinating β -catenin (Ctnnb1), eventually resulting its degradation by the proteasome (Clevers and Nusse 2012). However, when the Axin complex is bound to an activated LRP6 co-receptor it loses its ability to ubiquinate β -catenin and therefore can only bind and phosphorylate (Li, Ng et al. 2012). Eventually there is a saturation of phosphorylated β -catenin and any newly generated β -catenin accumulates in the cytoplasm, eventually translocating to the nucleus (Li, Ng et al. 2012). Nuclear β -catenin can displace the transcriptional repressor Groucho and interact with the transcription factors TCF and LEF (Behrens, von Kries et al. 1996). Further transcriptional coactivators and histone modifiers such as Brg1, CBP, Cdc47, Bcl9 are recruited, driving the transcription of target genes (Fig. 6b) (Clevers and Nusse 2012). When the Frizzled receptor is inactive the β -catenin destruction complex is activated and β -catenin does not accumulate in the cytoplasm, and evidently does not activate target genes (Clevers and Nusse 2012).

a) Model of canonical Wnt Signaling



b) β -catenin in the nucleus

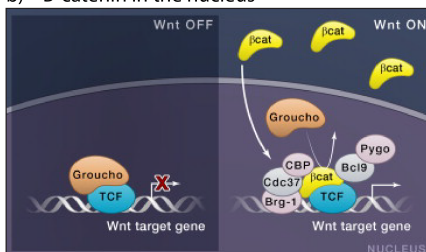


Figure 6. Canonical Wnt signaling.

a) The recently revised model of canonical Wnt signaling where, upon activation of the frizzled receptor by Wnt, the coreceptor LRP becomes phosphorylated. Although β -catenin can still be phosphorylated, it can no longer be ubiquinated, and therefore it begins to

accumulate in the cytoplasm. Eventually β -catenin is transported to the nucleus, where b) it interacts with and displaces the repressor Grocho. Continued on next page.

Figure 6: Continued from previous page. It can then bind and interact with the transcription factors TCF and LEF to modulate target gene expression. (Directly from (Clevers and Nusse 2012))

2.2.8 The direct regulation of target genes by Wnt signaling in Neurogenesis

In neural tube formation Wnt gradients are important in establishing anteroposterior polarity. Additionally, during embryonic neurogenesis, Wnts play a crucial role in controlling the switch between proliferation and differentiation in RGCs. By expressing a stabilized form of β -catenin Chenn and Walsh demonstrated that cortical progenitors proliferate, expanding the cortical neuroepithelium (Chenn and Walsh 2002). Conversely, in loss-of-function experiments there was a measurable increase in RGC differentiation into both BPs and neurons (Woodhead, Mutch et al. 2006, Mutch, Schulte et al. 2010). Interestingly, the downstream target of canonical Wnt signaling, N-myc, can direct APs into BPs, as well as promote neocortical neuronal differentiation (Kuwahara, Hirabayashi et al. 2010). Therefore, Wnt signaling through the activation of N-myc may be crucial in controlling the neuronal number in the developing neocortex. In chick studies N-myc was also shown to influence non-vertical cleavage planes and suppress Notch signaling, both of which were shown to lead to neuronal differentiation (Zinin, Adameyko et al. 2014). Other known targets of the β -catenin/TCF complex include the bHLH gene *neurogenin 1* (*Ngn1*), *Ngn1* together with *Ngn2* is a key determinant in neuronal differentiation (Hirabayashi, Itoh et al. 2004).

In line with previous studies Hirabayashi and colleagues showed that expression of Axin suppressed neuronal differentiation (Hirabayashi, Itoh et al. 2004). More recent reports present data for Axin having an opposing role in the nucleus, instead promoting neuronal differentiation. Fang and coworkers demonstrated that Axin can bind specifically to nuclear β -catenin, directly regulating BP neurogenic induction through modulation of downstream Wnt targets (Fang, Chen et al. 2013).

Although not demonstrated in the developing neocortex, there is evidence for direct regulation of the Notch ligand *Jag1* by Wnt signaling in other mammalian systems (Rodilla, Villanueva et al. 2009, Chen, Stoeck et al. 2010, Jacques, Puligilla et al. 2012). This regulation is mediated through the binding of the β -catenin/TCF complex to two known TCF sites in the promoter

region of *Jag1* and was confirmed through chromatin immunoprecipitation (ChIP) (Rodilla, Villanueva et al. 2009, Chen, Stoeck et al. 2010). In future studies it would be interesting to determine if this link between the Wnt and Notch signaling pathways is conserved in NSCs of the developing embryo.

2.2.9 The dual role of bHLH transcription factors in maintenance of NSCs and neuronal differentiation

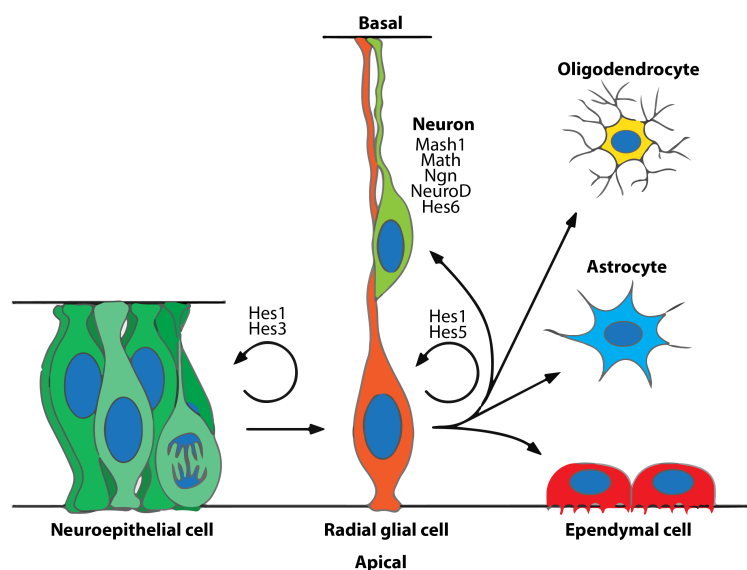
bHLH transcription factors play key roles in maintenance of NSCs and differentiation. There are two main types of bHLH genes in neurogenesis; those involved in gene repression and those involved in gene activation. The repressor genes include the orthologues of Hairy/Enhancer of Split (HES/HEY), while the proneural bHLH activator genes are defined by homologues of the *Drosophila achaete-scute* complex (*Mash*) and *atonal* (*Math, Ngn, NeuroD*) (Ohtsuka and Kageyama 2010).

Hes genes are critical for neural development and maintenance of NSCs including NEPs and RGCs (Fig. 7). Hes1 and Hes3 are mostly required for maintenance of NEPs, while Hes1 and Hes5 are more prominent in RGCs (Ohtsuka and Kageyama 2010). Hes genes are defined by their bHLH domain, an orange domain (helix 3-helix 4 domain), and a WRPW (Trp-Arg-Pro-Trp) domain, which is critical for regulating transcriptional activity of target genes (Grbavec and Stifani 1996). The WRPW repression domain can interact directly with the co-repressor TLE/Grg, which is a homolog of *Drosophila* Groucho. This leads to a modification of the chromatin structure through recruitment of histone deacetylase Rpd3 resulting in target gene inactivation (Grbavec and Stifani 1996). The Hes genes show varying binding affinities for different DNA sequences called the N Box (CACNAG), E box (CANNTG) or class C sites (CACGCG), with Hes1 preferentially binding N box (Sasai, Kageyama et al. 1992). In order for binding to occur they must first form homo- or heterodimers through the helix-loop-helix domain (Sasai, Kageyama et al. 1992). Hes1 and Hes5 directly repress transcription of proneural genes including Achaete-scute homolog 1 (*Ascl1* or *Mash1*), Atonal Homolog 1 (*Atoh1* or *Math1*) and Neurogenin2 (*Neurog2* or *Ngn2*) thereby maintaining NSCs in a progenitor state (Hatakeyama, Bessho et al. 2004, Louvi and Artavanis-Tsakonas 2006).

The activator bHLH genes, including *Mash1*, *Math*, *Ngn1/2* and *NeuroD*, are responsible for regulating neurogenesis and specifically defining neuronal subtype identity (Chien, Hsiao et al. 1996). Activator bHLH factors not only induce neuronal-specific gene expression but, in parallel, inhibit other cell fates such as glia by blocking lineage specific gene expression (Sun, Nadal-Vicens et al. 2001). *Glial fibrillary acidic protein (GFAP)*, a gene involved in astroglia cell fate, is inhibited by a sequestering of co-activators Stat1/3 and Smad1 by Ngn1 (Sun, Nadal-Vicens et al. 2001). This reinforces the role of bHLHs genes as activators in neuronal state specification.

Figure 7. Role of the bHLH Hes factors in fate commitment of NSCs.

Hes1 and Hes3 genes are important in the maintenance of neuroepithelial cells (NEPs), while Hes1 and Hes5 are required to maintain radial glial cells (RGCs). Activating bHLHs such as Mash1, Math1, Ngn, NeuroD and Hes6 are responsible for promoting neurogenesis. (Adapted from (Ohtsuka and Kageyama 2010))



2.2.10 Notch Signaling as a critical regulator in maintenance of NSCs

In order to maintain neurogenesis from embryonic development through to adulthood NSCs must be able to self-renew. One of the best-studied signaling pathways shown to be involved in NSC maintenance, proliferation, quiescence, and survival is the Notch pathway (Ohtsuka, Ishibashi et al. 1999, Hitoshi, Alexson et al. 2002, Androutsellis-Theotokis, Leker et al. 2006, Louvi and Artavanis-Tsakonas 2006, Basak and Taylor 2007, Mizutani, Yoon et al. 2007, Imayoshi, Sakamoto et al. 2010). Notch receptors are type-1, transmembrane proteins that can be activated through extracellular protein-protein interactions with either Delta or Serrate (Delta-like and Jagged respectively in mammals) ligands on adjacent cells. Upon activation

receptors undergo sequential cleavage, first by a disintegrin and metalloprotease (ADAM10 or 17) and then Presenilin (PS) containing γ -secretases, releasing the intracellular domain of Notch (NICD) (Fig. 8) (Brou, Logeat et al. 2000, Mumm, Schroeter et al. 2000). Throughout the animal kingdom the number of Notch receptors varies but in mammals there are four (Notch1-4) (Kopan and Ilagan 2009).

2.2.10.1 Spatiotemporal expression domains of Notch1, 2 and 3 in the developing CNS

During embryonic development components of the Notch signaling pathway, including its receptors and ligands, are expressed in regions where neurogenesis occurs rapidly (Hatakeyama and Kageyama 2006). By *in situ* hybridization, it was first demonstrated that Notch1 expression correlates with neurogenesis in the developing brain, spinal cord and dorsal root ganglia (DRG) in E10 mice (Weinmaster, Roberts et al. 1991). The highest Notch1 expression levels occur between E12 - E14, mostly localized to the developing brain and the DRG, with levels decreasing rapidly thereafter (Weinmaster, Roberts et al. 1991). By postnatal day 4 (P4) in the mouse Notch1 expression is prominent within the ventricular zone (VZ) and the SVZ of the lateral ventricle as well as in the lateral ventricles over the hippocampus (Stump, Durrer et al. 2002). Additionally Notch1 transcripts were detected in the internal granule cell layer (IGL) and Purkinje cells (PC) of the cerebellum, albeit at lower levels (Stump, Durrer et al. 2002). In adults this expression is largely restricted to the SVZ and dentate gyrus (DG) germinal zones, with some scattered expression outside the SVZ and in the rostral migratory stream (RMS), (Stump, Durrer et al. 2002).

The notch receptors Notch2 and Notch3 are expressed in distinct, overlapping domains during brain development where active neurogenesis is occurring. Disruption or ablation of Notch2 results in embryonic lethality, with mice phenotypically different than Notch1 ablated mice (Lindsell, Boulter et al. 1996, Hamada, Kadokawa et al. 1999, Irvin, Zurcher et al. 2001, McCright, Gao et al. 2001). This implies that while Notch receptor expression domains may overlap, receptors are not functionally redundant and expression is carefully regulated spatially and temporally. Differing from Notch1 and

Notch3, Notch2 is expressed in the forebrain germinal zones, is localized to the ventricular zone of the lateral ventricle and not present in the SVZ (Irvin, Zurcher et al. 2001). Additionally, unlike other Notch receptors, Notch2 is expressed in the granule cells of the DG, the choroid plexus epithelium and the external granule cell layer of the cerebellum (Irvin, Zurcher et al. 2001).

During development Notch3 is expressed in a similar pattern to Notch1, albeit at lower levels (Lindsell, Boulter et al. 1996, Irvin, Zurcher et al. 2001). It is present in the ventricular zones of the lateral ventricle but lowly expressed in the SVZ where Notch1 is more prevalent. In the postnatal and adult brain, Notch3 almost exclusively localizes to blood vessels, which lacks Notch1 or Notch2 expression (Lindsell, Boulter et al. 1996, Irvin, Zurcher et al. 2001).

The reason for these distinct expression patterns of Notch ligands is not clear. Notch receptors have a known role in regulating stem cell maintenance, as well as regulating cell fate ((Kopan and Ilagan 2009)). Potentially differences in downstream effectors regulated by activation and processing of the Notch receptors results in different commitment of cell fate. Notch1 and Notch3 activation were shown to induce neural progenitor cells to an astroglial fate (Tanigaki, Nogaki et al. 2001). A loss of Notch signaling through conditional deletion of *Rbpj* results in NSCs differentiating into neurons in both the SVZ and SGZ of the hippocampal DG, underlying the importance of Notch signaling in both maintenance and regulating cell fate (Imayoshi, Sakamoto et al. 2010).

Furthermore, receptors may be differentially activated through distinct Notch ligands (Lindsell, Boulter et al. 1996). Proteins such as Lunatic fringe (Lfng) can modulate Jag1 and Deltalike-1 (Dll-1) signaling by directly binding each ligand, resulting in differential activation of Notch1 and Notch2 (Hicks, Johnston et al. 2000). Domains expressing Dll1 and Jag1 ligands are clearly defined with many cells in the germinal regions specific for only one Notch ligand (Lindsell, Boulter et al. 1996) and see 2.2.11.3). Additionally, variations in Notch ligand glycosylation fine tunes its binding affinity and ability to activate Notch receptors and may be key to regulating differences in cell fate commitment (Kopan and Ilagan 2009).

Another plausible explanation for multiple receptors is that they negatively regulate the cell autonomous signal of other Notch receptors (Irvin, Zurcher et

al. 2001). Notch1 and Notch3 both share overlapping domains and are co-expressed by some cells in the SVZ germinal niche. One hypothesis is that Notch3 activation leads to an inhibition of the NICD, resulting in diminished Notch1 signaling (Irvin, Zurcher et al. 2001).

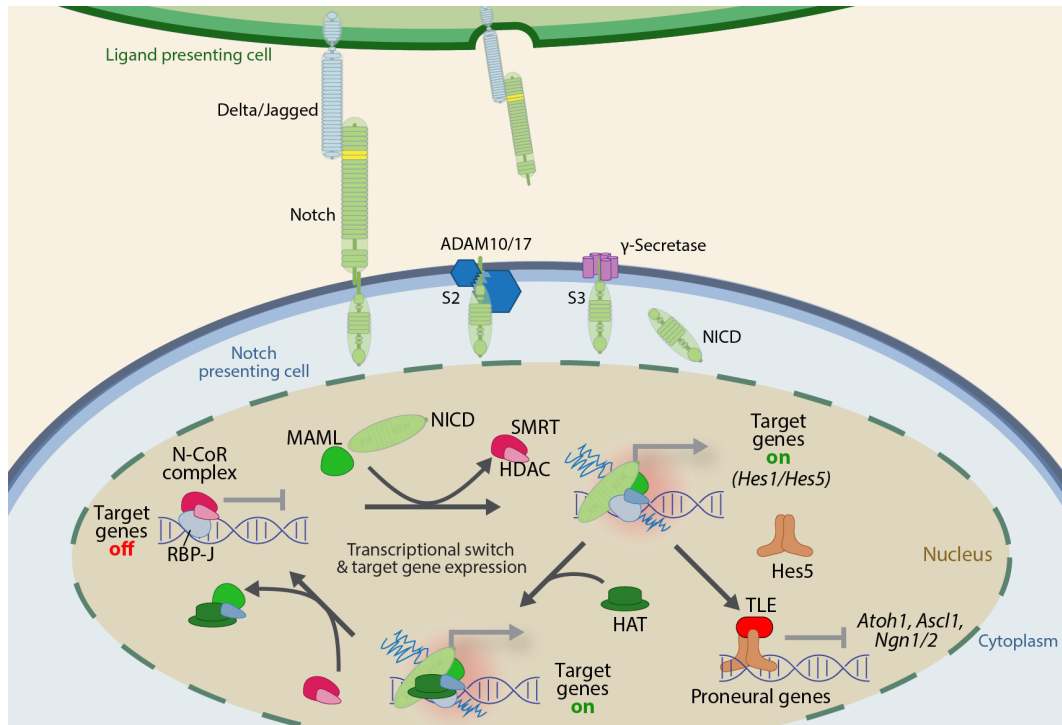


Figure 8. Canonical Notch receptor signaling in the control of neurogenesis.

Notch receptor activation is triggered when either Dll or Jag presented by neighboring cells binds to the ectodomain resulting in regulated intramembrane proteolysis (RIP) in which first a disintegrin and metalloprotease (ADAM10 or 17), and then Presenilin containing gamma secretase (γ -secretase) cleave the receptor releasing a soluble intracellular domain (NICD). The NICD translocates to the nucleus where it interacts with the CSL (CBF1, Su(H), and Lag1 – RBP-J in mice) protein complex including the DNA binding protein recombining binding protein suppressor of hairless (RBP-J). The binding of NICD releases the nuclear receptor co-repressor complex (N-CoR), which includes silencing mediator of retinoid and thyroid receptors (SMRT) and histone deacetylases (HDACs). The NICD-bound CSL complex is a positive regulator of Notch target genes including *Hes1* and *Hes5*. *Hes5* is a bHLH transcription factor that, together with a zinc finger protein of the transducing-like enhancer of split (TLE) family, represses the proneural genes (*Atoh1*, *Ascl1* and *Ngn1/2*) in NSCs and thereby inhibits neuronal differentiation. The NICD complex also interacts with histone acetyltransferase (HATs) leading to epigenetic marking of target genes and transcriptional activation.

2.2.10.2 Notch acts through the CSL transcriptional complex to directly regulate effector genes in the CNS

Canonical Notch signaling is mediated by the interaction of nuclear translocated NICD with the CSL (CBF1/RBP-J/Su(H)/Lag-1) transcriptional complex (RBP-J in mice) (Fig. 8). This interaction occurs through a conserved WxP motif in its RAM domain, disrupting the preformed repressor complex, and subsequently converting it to an activator complex. Factors such as the co-activator Mastermind (Maml1), histone acetyltransferases (HATs), chromatin remodeling factors, and the Mediator complex are recruited by the activator complex to mediate target gene expression (Dou, Zeng et al. 1994, Hsieh and Hayward 1995, Tamura, Taniguchi et al. 1995, Kato, Taniguchi et al. 1997, Kurooka, Kuroda et al. 1998, Fiuza and Arias 2007). When NICD levels decrease in the nucleus the repressor complex is eventually reformed. RBP-J recruits the transcriptional co-repressor proteins SKIP, hairless/CtBP, and Groucho/TLE and the histone chaperone Asf1 (Kopan and Ilagan 2009). Asf1 specifically suppresses the Notch signaling pathway, remaining associated with the promoters of target genes. Additionally, RBP-J can bind with numerous co-repressor proteins including the NCoR/SMRT complex and SHARP/MINT/SPEN complex which now is recognized as the key repressor of Notch genes (Oswald, Winkler et al. 2005, Tsuji, Shinkura et al. 2007, Kopan and Ilagan 2009).

The best-studied targets of the Notch pathway in mammals are the HES/HEY family of bHLH (see 2.2.9), in particular *Hes1* and *Hes5*. Activation of Notch results in maintenance of the cell in a progenitor state, while conversely, inactivation of Notch results in upregulation of the proneural genes and neural progenitor differentiation (Pompa de la, Wakeham et al. 1997, Gaiano, Nye et al. 2000, Lütolf, Radtke et al. 2002, Imayoshi, Sakamoto et al. 2010). Manipulating the Notch signaling pathway using either PS/γ-secretase inhibitors, by ablating *RBP-J*, knocking-out individual members of the Notch family or expressing an activated NICD showed that Notch is key in modulating progenitor cell proliferation and neurogenesis during embryonic development (Pompa de la, Wakeham et al. 1997, Gaiano, Nye et al. 2000, Lütolf, Radtke et al. 2002, Imayoshi, Sakamoto et al. 2010).

Interestingly Notch can interact with other pathways through parallel crosstalk with its effector proteins. For example, Hes1 and Hes5 can both physically interact with and modulate the JAK2-STAT3 signaling pathway by mediating the phosphorylation of STAT3 by JAK2 (Kamakura, Oishi et al. 2004).

2.2.10.3 Oscillatory expression of downstream Notch target genes leads to fate determination of neighboring cells

The classic “lateral inhibition” model of Notch signaling in NSCs proposes that all early progenitors express similar levels of pro-neural genes and Notch ligands. Stochastic variations in the levels of receptors, ligands and pro-neural genes between adjacent cells results in a “salt-and-pepper” pattern of Notch component gene expression. Cells with slightly higher ligand levels activate receptors in neighboring cells causing an inhibition of pro-neural genes in those cells. The differences between neighboring cell gene expression levels continues to be exacerbated by positive and negative feedback loops resulting in exaggerated differences, and eventually leading to the lineage commitment of the high pro-neural gene expressing cells (Fig. 9). Real-time imaging in Hes-reporter mice showed that negative feed-forward and feedback loops exist, resulting in oscillatory expression of downstream Notch signaling components and their targets over time (Shimojo, Ohtsuka et al. , Basak and Taylor 2007, Kageyama, Ohtsuka et al. 2007). Therefore, a cell with high pro-neural gene expression at one time point may revert to a low pro-neural gene expressing state shortly thereafter. These oscillations of Notch signaling in progenitors of the CNS is analogous but not identical to the waves of Notch activity seen during somite formation (Dequéant, Glynn et al. 2006). Oscillations in Notch components may further alter the ability of NSCs to respond to external differentiation cues and be critical for regulating NSC potential (Kageyama, Ohtsuka et al. 2008).

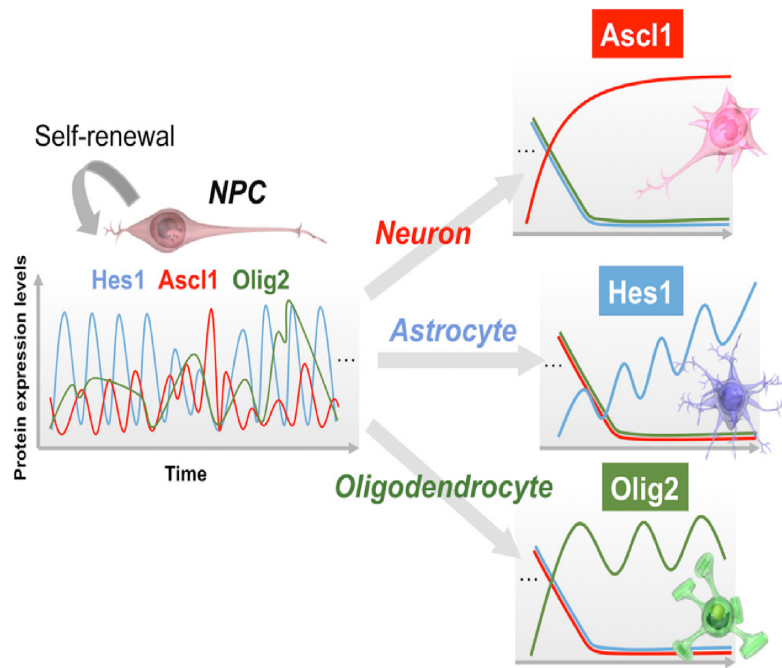


Figure 9. Oscillations of proteins leads to altered NSC potential.

Hes1 and Ascl1 proteins in neural progenitor cells (NPCs) oscillate at a frequency of approximately 2 to 3 hours and are likely dependent upon each other's expression, while Olig2 has a frequency of 5 to 8 hours and is likely independent of Hes1 and Ascl1. Together

their relative expression levels are important determinants in the fate of NPCs. (Directly from (Imayoshi and Kageyama 2014)).

2.2.11 The essential role of canonical DSL Notch ligands in the CNS

Canonical DSL (Delta, Serrate, Lag2) Notch ligands are largely responsible for activating the Notch receptors in the CNS, resulting in the receptors downstream processing by ADAM and PS/ γ -secretase. DSL ligands can therefore regulate cell type specification and progenitor cell maintenance through Notch. In mammals, the canonical DSL ligand family is comprised of 5 members; Jag1, Jag2, Dll-1, Dll-3, Dll-4 (Kopan and Ilagan 2009).

2.2.11.1 The Jag1 ligand structure and functional role in the CNS

The DSL domain characterizes canonical Notch ligands and is required for ligand-receptor interaction. Additionally, receptor binding is mediated by two unique epidermal growth factor (EGF) repeats directly adjacent to the DSL domain termed DOS (Delta and OSM-11-like proteins) (Fig. 10) (Shimizu, Chiba et al. 1999, Kopan and Ilagan 2009). Similar to Notch receptors all DSL ligands have extracellular domains consisting of EGF repeats (D'Souza, Miyamoto et al. 2008). In vertebrates Jag1 and Jag2 have almost twice as many EGF repeats as Dll ligands. Further, Jag1/2 ligands contain cysteine-rich regions inserted close to the membrane that are absent in Dll ligands (Fiuza and Arias 2007). The intracellular domains (ICD) of the Notch ligands

are highly conserved within each subfamily of ligand but lack sequence homology between subfamilies (D'Souza, Miyamoto et al. 2008). It has been suggested that this is because the cytoplasmic tails of the ligands may be required for specific post-translational modifications and for specific protein-protein interactions to occur (Pintar, De Biasio et al. 2007). The cytoplasmic tails of the ligands also contain a PDZ (PSD-95/DI/ZO-1) ligand motif that allows for direct interaction with PDZ domain containing proteins (Pintar, De Biasio et al. 2007). Additionally, Jag1 contains both ADAM and PS/γ-secretase cleavage sites directly juxtaposed to the transmembrane region (TM). Interestingly, Jag1 contains a nuclear localization signal on the N-terminus of the Jag1 intracellular domain (JICD), implying that, if processed through regulated intramembrane proteolysis (RIP), the JICD could translocate and signal to the nucleus of the ligand-presenting cell.

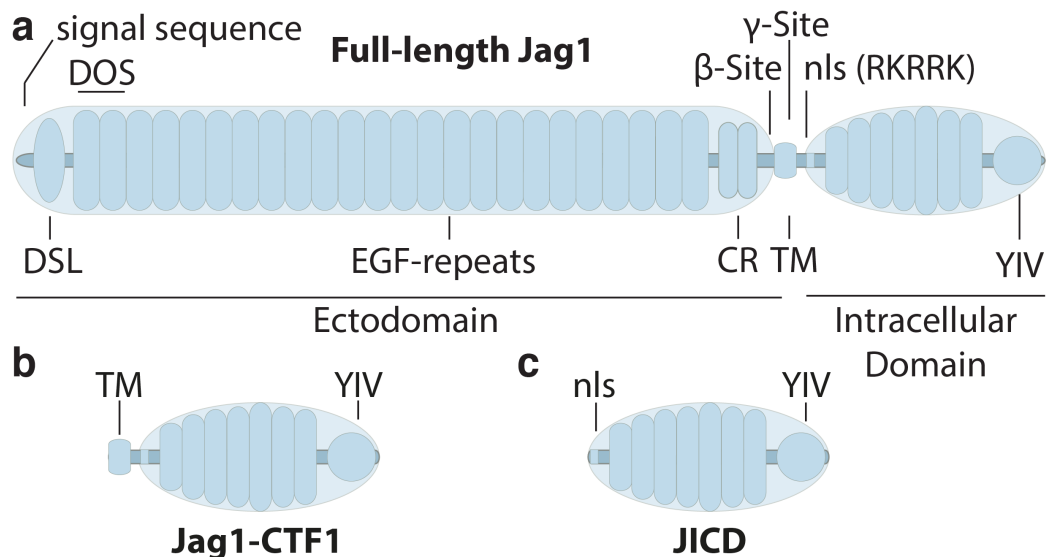


Figure 10. Protein structure of the Notch ligand Jag1.

a) Structure of full length Jag1 ligand. The extracellular domain is composed of a Delta/Serrate/Lag-2 (DSL) and a DOS (Delta and OSM-11-like proteins) domain, which is responsible for interacting with the epidermal growth factor (EGF) repeats on Notch resulting in its activation. Jag1 also contains EGF repeats similar to those found in Notch. In contrast to Dll ligands Jag1 contains a cysteine rich (CR) region close to the transmembrane (TM) domain. There are proteolytic cleavage sites that can be recognized and processed by ADAM17 and PS/γ-secretase directly adjacent to the TM domain. The intracellular domain (ICD) contains a nuclear localization sequence, as well as a C-terminal PDZ ligand (amino acid sequence YIV) which can interact with PDZ domains. b) Jag1-C-terminal fragment (Jag1-CTF1) c) Jag1-intracellular domain (JICD).

2.2.11.2 The putative role of the PDZ-ligand domain in Jag1

Jag1, Dll-1 and Dll-4 all have PDZ ligands at the C-termini of their ICD that are essential for mediating interactions with PDZ-containing scaffold/adaptor proteins (Ascano, Beverly et al. 2003, D'Souza, Miyamoto et al. 2008). Experiments where Jag1 and Dll PDZ domains were abolished demonstrated that they are required for ligands to exert an effect on cell adhesion, migration and oncogenic transformation (Ascano, Beverly et al. 2003, Wright, Leslie et al. 2004, Mizuhara, Nakatani et al. 2005, Estrach, Legg et al. 2007). It was demonstrated through yeast two hybrid (Y2H) experiments that the JICD-PDZ motif (MEYIV) could directly bind the PDZ domain protein afadin/AF6 (Pintar, De Biasio et al. 2007). Downstream effectors of AF6 includes the superfamily of RAS signaling proteins, suggesting a potential mediation by Jag1 through AF6 (Ascano, Beverly et al. 2003). Other proteins directly interacting with JICD-PDZ have yet to be elucidated.

2.2.11.3 Domains expressing Jag1 in the mammalian CNS

Jag1 is widely expressed in the developing mammalian CNS (Lindsell, Boulter et al. 1996, Stump, Durrer et al. 2002, Irvin, Nakano et al. 2004) and Fig. 20a,b). At E13.5 mRNA transcripts are found in the telencephalon, diencephalon, metencephalon, myelencephalon and the spinal cord VZ (Irvin, Nakano et al. 2004). Interestingly it appears that the expression of the DSL ligands Jag1 and Dll-1 are complimentary, forming sharply demarcated boundaries within the hindbrain and spinal cord (Lindsell, Boulter et al. 1996). This may reflect the differing roles these ligands play in cell fate specification of the CNS. By E17, Jag1 transcripts can be detected in the VZ of the developing forebrain although expression is more prominent in the hindbrain VZ (Irvin, Nakano et al. 2004). Jag1 expressing cells reside directly adjacent to Notch1, Notch2 and Notch3 cells in the VZ and can functionally bind and activate all 3 Notch receptors. This results in their processing through regulated intramembrane proteolysis (RIP) and the downstream Notch signaling cascade being activated (Shimizu, Chiba et al. 1999, Shimizu, Chiba et al. 2000). Unlike Jag1, Jag2 does not localize specifically to the neurogenic regions (Irvin, Nakano et al. 2004). Additionally, unlike Dll, Jag1 is found in the choroid plexus and meninges (Irvin, Nakano et al. 2004).

In perinatal mice (P4), Jag1 is highly associated with the developing forebrain and cerebellum, and most notably unlike other DSL ligands, is found expressed by cells lining the SVZ and by the granule cells of the DG (Stump, Durrer et al. 2002). In the SVZ Jag1 mRNA expression is not evenly distributed, but instead there are a number of cells expressing Jag1 transcripts in the dorsolateral corner and most rostral part of the SVZ (Irvin, Nakano et al. 2004). At this time point, Jag1 is present on ependymal cells, Type B progenitors and some blood vessels in the SVZ in a salt and pepper pattern (Fig. 13) (Stump, Durrer et al. 2002, Nyfeler, Kirch et al. 2005).

Jag1 is expressed throughout the cerebellum and has been demonstrated to be critical for maintaining Bergmann glia in the early postnatal cerebellum (Weller, Krautler et al. 2006). A loss of Jag1 leads to ectopic differentiation in the external germinal and molecular layers, with granule cell precursors undergoing apoptosis and an overall reduction in Bergmann glia numbers. Additionally, it was demonstrated that a loss of Jag1 results in defects in the migration of immature granule cells into the internal granule cell layer (Weller, Krautler et al. 2006).

2.2.11.4 The putative mechanisms of cell-autonomous Jag1 signaling

The work by LaVoie and Selkoe on Jag1 and Dll ligand processing demonstrated that both ligands can be proteolytically cleaved in a similar manner to the Notch receptors. Moreover, both Jag1 and Dll can release putative signaling ICD fragments into the cytoplasm, potentially implying bi-directional signaling between neighboring cells (LaVoie and Selkoe 2003). Both ligands undergo RIP when they bind to the Notch receptor on adjacent cells in trans. ADAM17 first processes Jag1 in a similar fashion to the Notch receptor, releasing its ectodomain fragment. This finding was recently supported by the demonstration that the ADAM17 cleavage occurs in a lipid-raft-independent manner (Parr-Sturgess, Rushton et al. 2010). After processing by ADAM17 the remaining membrane-anchored fragment, Jag1-CTF1, competes with Notch for PS/ γ -secretase cleavage causing a decrease in Notch signaling. This is due to the release of the ligand ectodomain resulting in a conformational change in the ligand CTF, allowing PS/ γ -secretase to cleave. It was also shown that Jag1 and Dll CTF's

coimmunoprecipitate with PS/ γ -secretase, adding more strength to this hypothesis that PS/ γ -secretase is involved in cleavage and release of the ligand ICD (LaVoie and Selkoe 2003).

An intriguing finding was that after cleavage and release of the ligand ICD, the ICD is not only in the cytoplasm, but also nuclear. This was previously shown for NICDs, but not for Notch ligands. Using an AP1-mediated reporter system they demonstrated that the JICD was able to stimulate gene expression. However, it may not be necessary for JICD to enter the nucleus to activate AP1 since a construct lacking the putative nuclear localization signal (NLS) was still able to increase activity, but this still raises the question of whether the JICD could play a role in transcriptional regulation. Other evidence supporting this data showed that Jag1 expression causes an increase in Jag1, Dll-1 and Notch3 mRNA levels but not Notch1, -2, or -4 (Ascano, Beverly et al. 2003). Induction of specific genes shows that the JICD can have an effect on gene expression. Furthermore, there is no published evidence that ligand ICD's can bind DNA directly since they do not contain a recognizable DNA binding motif, but they may be involved in recruitment of other TFs (LaVoie and Selkoe 2003).

Recently Duryagina, et al. 2013, confirmed that Jag1 in human mesenchymal stromal cells (MSCs), can undergo cleavage to release an intracellular domain that can translocate to the nucleus (Duryagina, Thieme et al. 2013). They further showed through reporter assays that recombinant JICD could stimulate target gene stromal cell-derived factor-1 (*SDF-1*) but endogenous expression of JICD while overexpressing full-length Jag1 did not stimulate its expression. They explain this contradictory role by showing that full-length Jag1 (Jag1FL) can actually block SDF-1 and inhibit its expression, negating the enhancing effects of the JICD (Duryagina, Thieme et al. 2013).

2.2.11.5 Alternative regulation mechanisms of Jag1 in Notch signaling

For correct activation of canonical Notch signaling to occur, ligand and receptor must interact with each other in trans (opposing cells). If this interaction occurs in cis (same cell), Jag1 functions as a dominant negative repressor of the Notch receptor preventing activation (Fig. 11) (Celis de and Bray 1997, Klein, Brennan et al. 1997, Micchelli, Rulifson et al. 1997,

Sakamoto, Ohara et al. 2002, Li and Baker 2004, Cordle, Johnson et al. 2008). This model for cis-inhibition was clearly demonstrated in the *Drosophila* wing when Serrate (Jag1) was overexpressed, leading to a downregulation of Notch target genes (Micchelli, Rulifson et al. 1997). The mechanism of how this inhibition occurs is unclear but it has been proposed that the interaction between DSL ligands and Notch receptor may be able to exist in a parallel and antiparallel binding formation (Cordle, Johnson et al. 2008). Binding of Notch in parallel (cis) would form a heterodimer complex preventing the receptor from transitioning to an active state. This inactivation through titration model has recently gained support with studies using Dll to observe the effects of cis- versus trans- activation thresholds (Sprinzak, Lakhanpal et al. 2010). The domains responsible for Jag1 cis-inhibition were recently identified as EGF repeats 4-6 (Fleming, Hori et al. 2013). This would fit with the parallel/antiparallel binding hypothesis since EGF repeats 4-6 are dispensable for Notch transactivation, while EGF repeats 1-2 are required (Shimizu, Chiba et al. 1999, Fleming, Hori et al. 2013).

Notch signaling also plays a pivotal role in the development of the inner ear and commitment of otic progenitors to a prosensory fate (Neves, Parada et al. 2011). Recently the competition of Jag1 and Dll in the inner ear hair cell development was modeled (Petrovic, Formosa-Jordan et al. 2014). From that model Jag1 was predicted, and then confirmed, to induce a weaker Notch response than Dll in the opposing cell. Additionally, they measured a competitive response between the two ligands, with Jag1 inhibiting Dll/Notch signaling. This results in inhibition of Jag1 expression in the neighboring cell, and consequently hair cell patterning through lateral inhibition (Petrovic, Formosa-Jordan et al. 2014). Potentially this mechanism of ligand competition is conserved and exists in other developmental systems where Notch signaling is a driving factor in fate commitment.

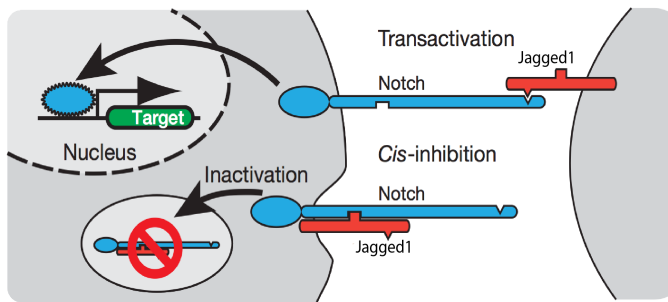


Figure 11. Cis inhibition of Notch. Jag1 can interact with the Notch receptor through either trans- or cis-presentation, resulting in Notch activation or inhibition respectively. (Adapted from (Sprinzak, Lakhonpal et al. 2010))

2.2.11.6 *Jag1* in human disease: Tetralogy of Fallot and Alagille syndrome

Mutations in the *JAG1* gene, which is located on human chromosome 20, are associated with two human diseases (Fig. 12). The first, Tetralogy of Fallot (ToF), is the most common congenital heart defect occurring in approximately 1 in 3,000 live births (Eldadah, Hamosh et al. 2001). Mutations directly result in ventricular septal defects that obstruct the right ventricular outflow and ultimately cause ventricular hypertrophy. Missense mutations in ToF have been correlated with the 2 DOS domains that are responsible for aiding the interaction with Notch receptor (Eldadah, Hamosh et al. 2001, Kopan and Ilagan 2009).

Alagille syndrome (AGS) is caused by heterozygous *JAG1* mutations resulting in multi-system congenital defects affecting the heart, liver and kidneys (Li, Krantz et al. 1997, Oda, Elkahloun et al. 1997, Yuan, Kohsaka et al. 1998, Spinner, Colliton et al. 2001, Yuan, Kobayashi et al. 2006, Guegan, Stals et al. 2012). Reflecting the multi-system nature of this disease, symptoms of AGS include mental retardation, spontaneous intracranial bleeding and stroke, the last being the main cause of lethality (Piccoli and Spinner 2001). Missense mutations in *JAG1* are associated with the disulfide bonds in the DOS Notch-binding domain. A loss of DOS disulfide bonds may interfere with the overall structural integrity of this domain and therefore decrease its efficiency to activate the Notch receptor (Kopan and Ilagan 2009). Additionally, *JAG1* haploinsufficiency due to null mutations are commonly found in patients (Yuan, Kohsaka et al. 1998, Spinner, Colliton et al. 2001).

Xue and colleagues studied the *in vivo* function of Jag1 by creating Jag1-null mice (Xue, Gao et al. 1999). They removed a 5kb segment from the 5'

end of the Jag1 gene, encoding the DSL and DOS domain responsible for interacting with the Notch receptor. Mice heterozygous for the deletion could be identified through an eye dysmorphology. Homozygous mutants however die at day E11.5 due to vascular defects. This was the first direct evidence of Jag1s essential role in vascular development (Xue, Gao et al. 1999). Additionally, due to the lethality of Jag1 null embryos, future studies incorporated conditional deletion alleles with LoxP sequences flanking the first and second exons (Nyfeler, Kirch et al. 2005).

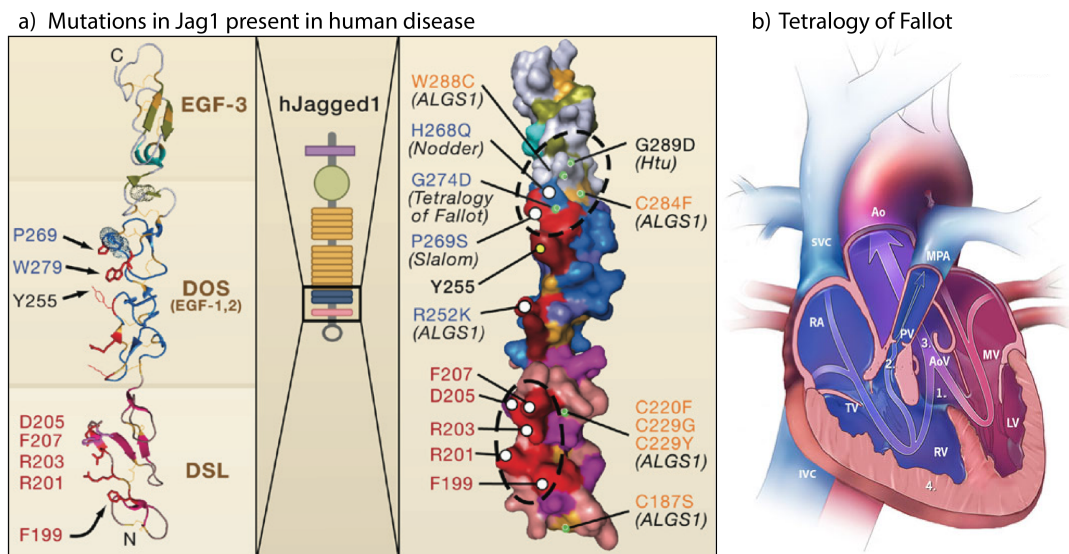


Figure 12. Human diseases directly correlated with Jag1 missense mutations.

Jag1 mutations are responsible for the human diseases Tetralogy of Fallot and Alagille syndrome (ALGS1). a) Missense mutations for both diseases have been associated with the extracellular DSL and DOS domains of Jag1, which are responsible for binding to and activating the Notch receptor. b) Tetralogy of Fallot is the most common congenital heart birth defect, which causes a right ventricular hypertrophy. (Adapted from CDC and Prevention and (Kopan and Ilagan 2009)).

2.3 Adult Neurogenesis

2.3.1 The Neurogenic Regions in the Adult

Two germinal zones have been identified that continue to produce new neurons into adulthood in mice. The first is the subgranular zone (SGZ) of the hippocampal DG and the second is the SVZ lining the lateral ventricle walls (Fig. 13) (reviewed in (Kriegstein and Alvarez-Buylla 2009)). Continued neurogenesis has been shown to be key in brain homeostasis and reductions are associated with impaired learning, memory, and major depression (Zhao, Deng et al. 2008, Braun and Jessberger 2014). Regulation of adult neurogenesis occurs through a complex network of extrinsic and intrinsic factors that modulate numerous signaling pathways and transcription factors (Basak and Taylor 2009, Faigle and Song 2013, Rolando and Taylor 2014). In both germinal niches, extrinsic factors such as cell-to-cell interactions, secreted factors, and neurotransmitters maintain the NSCs (Faigle and Song 2013). Further, both physiological and pathological activities including seizures, aging and exercise can influence stem cell proliferation and govern neurogenesis (Kuhn, Dickinson-Anson et al. 1996, Van Praag, Shubert et al. 2005, Lugert, Basak et al. 2010).

Neurons born in both adult germinal niches first migrate to their final destination before integrating and fully differentiating. New born SGZ neurons, migrate to the granule cell layer and differentiate to become dentate granule cells (Zhao, Deng et al. 2008). SVZ neurons migrate first along the rostral migratory stream (RMS), changing their migratory direction once they reach the olfactory bulb (OB). In the OB they migrate radially, differentiating into granule cells or periglomerular neurons (Zhao, Deng et al. 2008). The Notch ligand, Jag1 has been shown to be crucial in the maintenance of NSCs in both the SGZ and the SVZ (Nyfeler, Kirch et al. 2005, Lugert, Basak et al. 2010, Imayoshi 2012, Giachino, Basak et al. 2014, Lavado and Oliver 2014).

In recent years, other neurogenic regions have been identified including the α -Tanyctes of the adult hypothalamic third ventricle (Robins, Stewart et al. 2013). Further research will need to be done to determine whether additional neurogenic regions can be discovered in the adult mammalian brain.

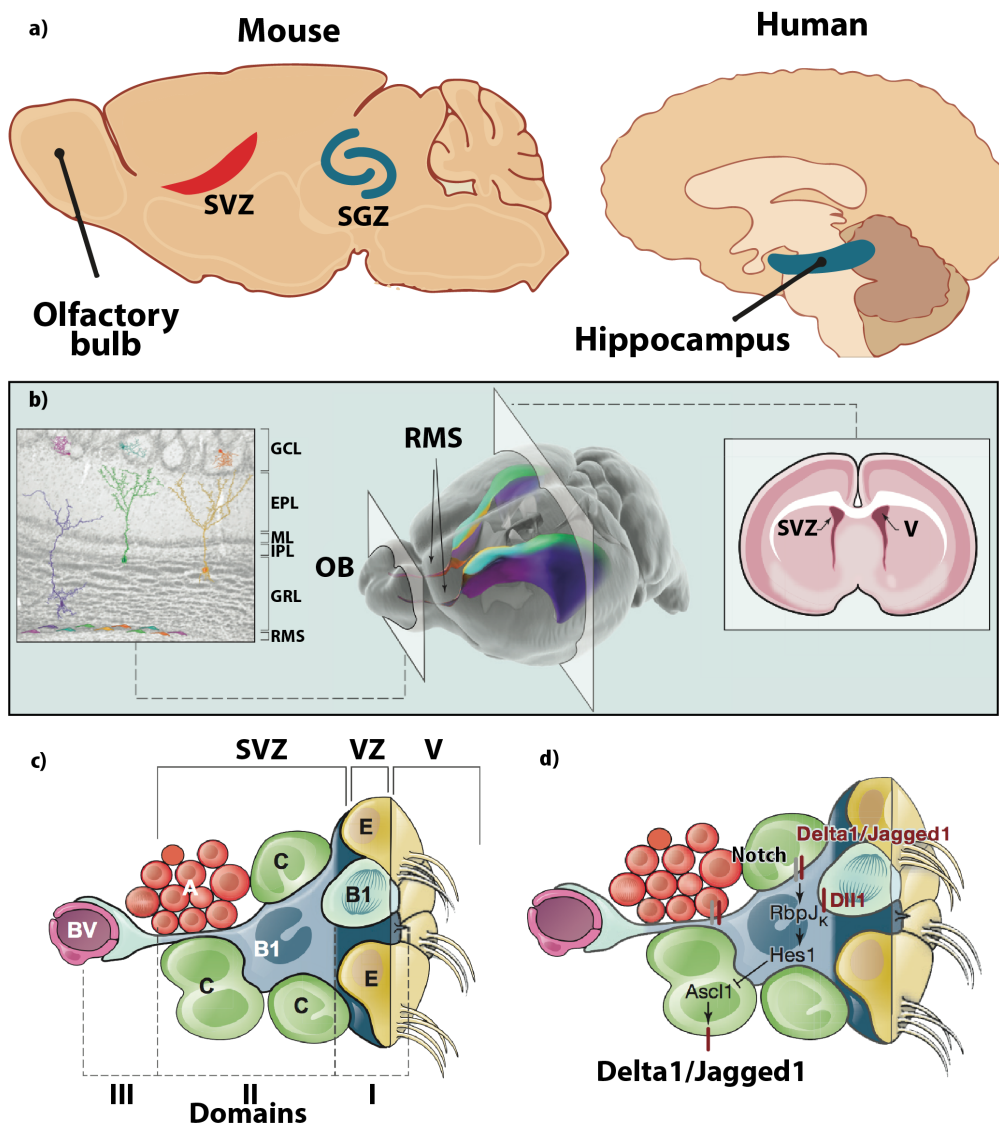


Figure 13. Stem cell niches in adult mammals.

a) Adult neurogenesis in the subventricular zone (SVZ) and the subgranular zone (SGZ) of the hippocampal dentate gyrus (DG). b) Neurons born in the SVZ, migrate along the rostral migratory stream (RMS) until they reach their final destination in the olfactory bulb (OB). Here they migrate radially, differentiating into periglomerular neurons. c) The SVZ is composed of 4 main cell types. Type B cells are the primary progenitors of the niche and give rise to the quickly dividing type C cells. Type B cells are further classified into type B1 and B2, with B1 cells remaining in contact with both the ventricle and niche blood vessels (BV). Type C cells can divide asymmetrically to give rise to the migrating type A cells. The ependymal (E) cells lining the ventricle are ciliated and can direct the flow of cerebral spinal fluid in the ventricle, which contains inductive cues for the niche. d) Key determinants of the Notch signaling pathway are highly active in the SVZ niche, directly influencing cell maintenance, proliferation and fate. *Ascl1* (*Mash1*), which is high in type C cells, is inhibited through the Notch effector bHLH gene *Hes1*. *Jag1* is expressed by ependymal cells, type B cells and blood vessels of the SVZ niche. (Adapted from (Tong and Alvarez-Buylla 2014, Vadodaria and Gage 2014))

2.3.2 The SVZ neurogenic niche

The neurogenic ventricular-SVZ (V-SVZ) is composed of four cell-types, which are defined by their morphology, antigen expression, activity, and location in the neurogenic niche (Fig. 13b-d). Each influences the local environment through direct cell-cell interactions and excreting extracellular signaling molecules. Additionally, they can be defined by their marker expression pattern and location with respect to the ventricle and blood vessels. The proliferative cells of the niche include the slowly dividing type B cells (primary progenitors) and the rapidly multiplying type C cells (intermediate progenitors). Type B cells are believed to retain characteristics of both RGCs and astrocytes, and can be defined by marker expression of Nestin, Sox2, GFAP, GLAST, Lewis X (LeX) and CD133 (reviewed by (Ihrie and Alvarez-Buylla 2011)). The multiciliated ependymal cells line the ventricle, forming pinwheel structures called rosettes (Ihrie and Alvarez-Buylla 2011). Type C cells proliferate rapidly to give rise to the fourth niche cell, type A, which are the immature neuroblasts that express Doublecortin (Dcx) and PSA-NCAM. Type A cells are highly migratory and transverse along the RMS towards the OB (Ihrie and Alvarez-Buylla 2011). There is a small number of a second type C cell in the V-SVZ which express the oligodendrocyte lineage transcription factor Olig2 and can give rise to immature oligodendrocyte precursors (OPC) and mature myelinating oligodendrocytes (Menn, Garcia-Verdugo et al. 2006).

The type B cells can be further categorized based on their morphology and location relative to the ventricle (type B1, B2, B3) (Doetsch, Garcia-Verdugo et al. 1997, Giachino, Basak et al. 2014). The slowly dividing type B1 cells extend their primary cilium through the center of the ependymal rosette structures, allowing them direct access to the ventricular lumen (Mirzadeh, Merkle et al. 2008). Additionally, the process forms symmetric adherens junctions joining type B1 cells with the surrounding ependymal cells. Increasing evidence suggests that this direct contact with the ventricle and the ependymal cells allows for signaling molecules in the cerebral spinal fluid or ependymal cells to influence the fate of type B1 cells directly (Mirzadeh, Merkle et al. 2008). Type B1 cells share some familiar characteristics with

RGCs in the developing embryo. They have an apical process contacting the ventricle, a basal process associated with blood vessels and proposed karyon movements that are reminiscent of interkinetic nuclear migration in the developing embryo (Ihrie and Alvarez-Buylla 2011).

Careful lineage analysis of type B cells has identified mitotically active BLBP⁺ NSCs in the adult mouse V-SVZ (Giachino, Basak et al. 2014). With age, active BLBP⁺ type B cells are lost, correlating with a decrease in active neurogenesis (Giachino, Basak et al. 2014). Interestingly, BLBP expression also correlates mitotic activity in the adult human V-SVZ. In contrast BLBP⁻ type B cells are relatively quiescent and therefore it is thought that BLBP⁺ cells are the key drivers of neurogenesis during homeostasis. It will be a matter of future experiments to analyze these populations in detail to determine the mechanisms involved in converting BLBP⁻ type B cells to an active BLBP⁺ state, and potentially recapitulate a loss of neurogenesis in aged mammals (Giachino, Basak et al. 2014).

Jag1 is an essential component of the SVZ niche (Nyfeler, Kirch et al. 2005). Jag1 is found on both ependymal and B cells in the niche as well as on endothelial cells of the blood vessels (Fig. 13d). Understanding the dual role of Jag1 as a regulator of neural progenitor maintenance as well as a neural determinant factor in the ligand-presenting cell is crucial for discerning niche maintenance.

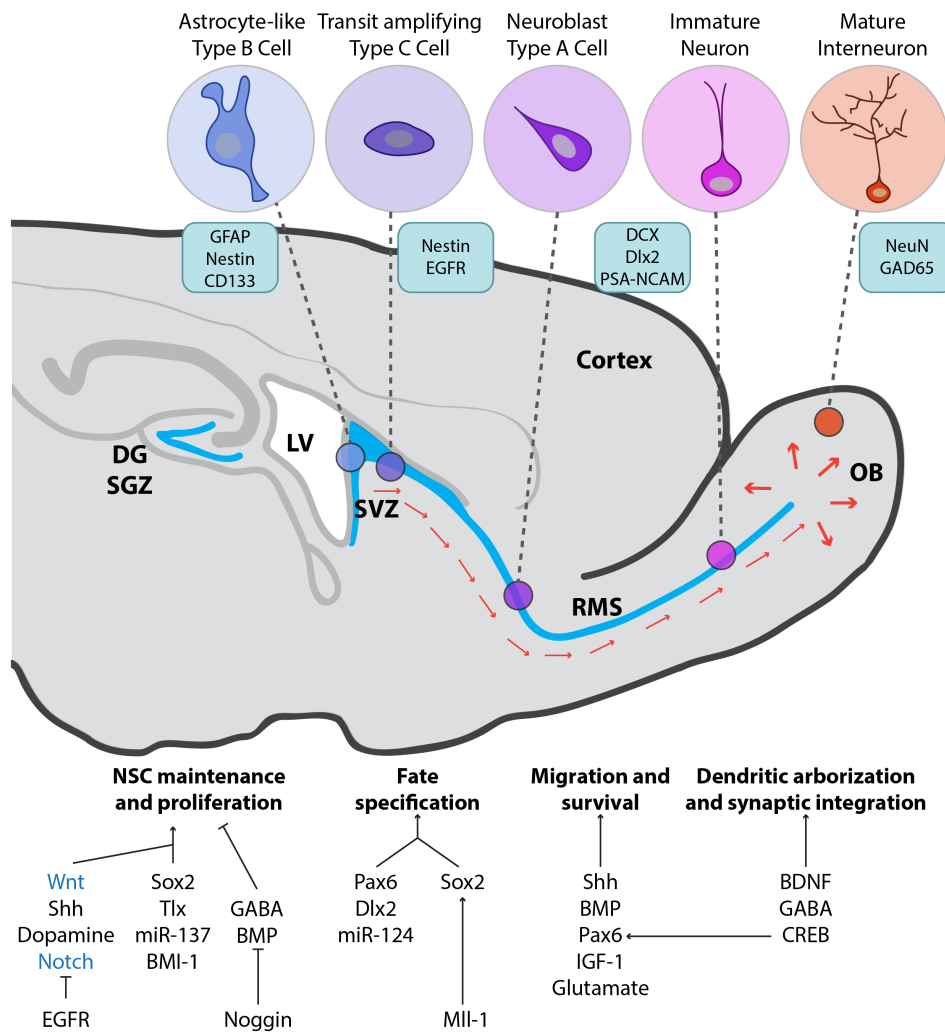


Figure 14. Pathways and molecular factors involved in maintenance of the adult SVZ niche.

The adult SVZ niche is maintained through a complicated network of signaling pathways, morphogens and growth factors. As type B cells sequentially progress to type C, and eventually type A cells, they require signals to coordinate fate specification, migration, and eventually differentiation to develop into mature OB interneurons. Marker expression profiles differ amongst type B, C and A cells. A few of the markers that B cells express include GFAP, Nestin and CD133. Type A cells however express Dcx, Dlx2 and PSA-NCAM. (Adapted from (Faigle and Song 2013)).

2.3.3 Molecular factors and signaling pathways involved in maintenance of the adult neurogenic niche

In recent decades an explosion of new technologies have allowed us to probe and study adult neurogenesis in ways that were not previously possible. Through these studies numerous novel growth factors and signaling pathways have been identified that directly control and maintain the adult germinal niches. Some of these include the growth factors VEGF, EGF, FGF and BDNF, the Wnt, Shh, Notch signaling pathways, BMPs, neurotrophins and neurotransmitters (Fig. 14). For a concise review of the role of these pathways and factors in the adult neurogenic niches please see (Faigle and Song 2013).

2.3.3.1 *Role of Wnt signaling in adult neurogenesis*

While Wnt signaling plays an important role in the initial patterning and segmentation of the developing neural tube, it also appears to be crucial for adult neurogenesis (Faigle and Song 2013). Of all the members in the Wnt family of signaling molecules, Wnt3 expressed in the DG hilar cells is the best studied in the context of adult neurogenesis (Faigle and Song 2013). Kuwabara and colleagues, demonstrated that positive regulation of NeuroD1 through Wnt3a-activated canonical Wnt signaling was sufficient for neuronal differentiation in adult hippocampal neural progenitors (Kuwabara, Hsieh et al. 2009). Wnt signaling can increase adult neurogenesis by first expanding the progenitor pool, before they eventually differentiate, producing a greater number of neurons (Wexler, Paucer et al. 2009).

Aging and neuronal activity has been shown to negatively and positively regulate adult neurogenesis in the DG, respectively (Zhao, Deng et al. 2008). Furthermore, two studies demonstrate that relative levels of Wnt signaling are at least partially responsible for this regulation (Jang, Bonaguidi et al. 2013, Seib, Corsini et al. 2013). Exercise was shown to decrease the levels of secreted frizzled-related protein 3 (sFRP3). sFRP3 is responsible for binding and sequestering Wnt proteins, resulting in a decrease of Wnt signaling. Therefore, by inhibiting sFRP3 through exercise, an increase in Wnt signaling occurs, resulting in an overall escalation of neurogenesis (Jang, Bonaguidi et al. 2013). Conversely, with age there is a gradual accumulation of the

secreted glycoprotein Dickkopf 1 (Dkk1), which blocks neurogenesis at least in part by decreasing levels of Wnt signaling. Upon deletion of Dkk1 adult mice exhibit expanded populations of neurons and increased levels of Wnt signaling (Seib, Corsini et al. 2013). Interestingly, deletion of Dkk1 only resulted in expansion of neuronal populations, whereas in sFRP3 knockout (KO) expanded, neurons and glia, suggesting differing roles of Wnt dependent signaling regulation (Jang, Bonaguidi et al. 2013, Seib, Corsini et al. 2013).

2.3.3.2 Role of Notch signaling in adult neurogenesis

It has been proposed that Notch1 plays a role in maintenance of the actively dividing NSCs in the adult niche (Nyfeler, Kirch et al. 2005, Androutsellis-Theotokis, Leker et al. 2006, Breunig, Silbereis et al. 2007, Ables, Decarolis et al. 2010, Aguirre, Rubio et al. 2010, Basak, Giachino et al. 2012). In the DG and SVZ Notch activity promotes NSC survival, maintenance, and stem cell self-renewal (Stump, Durrer et al. 2002, Nyfeler, Kirch et al. 2005, Breunig, Silbereis et al. 2007, Basak and Taylor 2009, Ables, Decarolis et al. 2010, Aguirre, Rubio et al. 2010, Chapouton, Skupien et al. 2010, Ehm, Goritz et al. 2010, Lugert, Basak et al. 2010). However, both the preservation of, and the transition from a quiescent NSC state to, an activated one appear to be RBP-J dependent (Carlén, Meletis et al. 2009, Ehm, Goritz et al. 2010, Imayoshi, Sakamoto et al. 2010, Lugert, Basak et al. 2010, Basak, Giachino et al. 2012). Hence Notch1 may play a role in maintaining active NSCs, but not in switching from inactive to active states (Lugert, Basak et al. 2010, Basak, Giachino et al. 2012, Giachino, Basak et al. 2014).

Great efforts have been made over the years to identify molecular markers that discriminate populations of niche astrocytes from quiescent and activated NSCs (Pastrana, Cheng et al. 2009, Beckervordersandforth, Tripathi et al. 2010, Mira, Andreu et al. 2010, Ferron, Charalambous et al. 2011, Codega, Silva-Vargas et al. 2014). EGF receptors have been associated with active SVZ NSCs that maintain astrocytic (BLBP) and glial (GFAP) markers (Pastrana, Cheng et al. 2009, Giachino, Basak et al. 2014). Horizontal, non-radial cell morphology identifies a population of actively dividing progenitors in the adult DG (Lugert, Basak et al. 2010). However, there is also a population

of quiescent horizontal cells that currently cannot be discerned based on molecular marker alone (Suh, Consiglio et al. 2007, Lugert, Basak et al. 2010). New genetic tools are needed and markers identified that allow for independent and simultaneous lineage tracing of these two NSC populations. For an in depth analysis of the role of Notch in quiescence and active NSC populations see Giachino and Taylor, 2014 (Giachino and Taylor 2014).

In the SVZ niche NSCs receive inductive cues directing them to specific fates, as well as restrictive signals which limit their potential and prevent differentiation (Doetsch 2003). Some of these inductive cues most likely work in tandem with Notch (Shen, Goderie et al. 2004). Non-canonical activation of Notch through pigment epithelium–derived factor (PEDF), secreted by vascular endothelial cells within the SVZ, can bias cell fates towards radial glia. By activating NF- κ B PEDF exports nuclear receptor co-repressor (NCoR), which acts as a transcriptional inhibitor of the Notch target genes *Hes1* and *Egfr*, allowing NSCs to undergo asymmetric, self-renewing divisions (Andreu-Agulló, Morante-Redolat et al. 2009). Other inductive cues include hypoxia-inducible factor 1 α (HIF1 α), that under hypoxic conditions is stabilized and cooperates with Notch signaling to promote expression of target genes in NSCs (Gustafsson, Zheng et al. 2005, Bar, Lin et al. 2010).

To date, much of our knowledge about the Notch signaling pathway is derived from its role in NSC maintenance in the niche as a whole. However, the role of Notch has not yet been addressed in detail at the single cell level, where levels of Notch signaling activity in NSCs may modulate response sensitivity to extrinsic signals. New technologies allowing for precise single cell analysis may one day allow for identification and discrimination of NSC populations at the transcriptional level.

2.4 Oligodendrogenesis in mammals

2.4.1 Signaling pathways involved in oligodendrocyte maturation

Glia cells carry out a diverse range of critical functions in the brain including ensuring adequate nutrient supplies to neurons, providing scaffolding and support, insulation of axons, removal of cellular debris and destruction of pathogens. Oligodendrocytes are one of the major types of glia cells and

have the ability to not only provide support, but when mature also myelinate and insulate, axons thereby ensuring proper signal transduction (reviewed in (Pfeiffer, Warrington et al. 1993)). Differentiation of oligodendrocytes from early oligodendrocytic precursor cells (OPCs) into mature myelinating cells is a process termed oligodendrogenesis. Much like neurogenesis, oligodendrogenesis requires a complex network of morphogens, transcription factors, and signaling pathway crosstalk in order for maturation to occur correctly. Some of the key signaling pathways involved include Wnt, Shh, BMP and Notch (Li, He et al. 2009).

2.4.2 Origin of Oligodendrocytes in the SVZ

Oligodendrocytes in the developing forebrain are produced in three sequential and competitive phases beginning in the embryo and continuing into early postnatal development (Fig. 15) (Kessaris, Fogarty et al. 2006). The first wave begins ventrally at E11.5 in the Medial Ganglionic Eminence (MGE) - anterior entopeduncular region (AEP) and then moves more dorsally to the Lateral Ganglionic Eminence (LGE) - Caudal Ganglionic Eminence (CGE) from E15.5 onwards. The third and final wave occurs even more dorsally in the postnatal cortex (Kessaris, Fogarty et al. 2006). Interestingly, oligodendrocytes from the first wave of oligodendrogenesis in the forebrain are almost completely absent in the postnatal brain, potentially eliminated or are out competed by later waves (Kessaris, Fogarty et al. 2006). Oligodendrocytes begin in the developing neural tube as multipotent NEPs. Through sequential rounds of asymmetric cell divisions morphogen gradients of BMP and Shh restrict NEPs first to RGCs and then to OPCs (Fig. 4) (Li, He et al. 2009). OPCs then proceed to receive chemo-attractant and mitogen signals, instructing them to proliferate and migrate from the SVZ into the developing forebrain (Li, He et al. 2009). Once OPCs reach their destination, they proceed to integrate, differentiate, ensheath axons and form myelin.

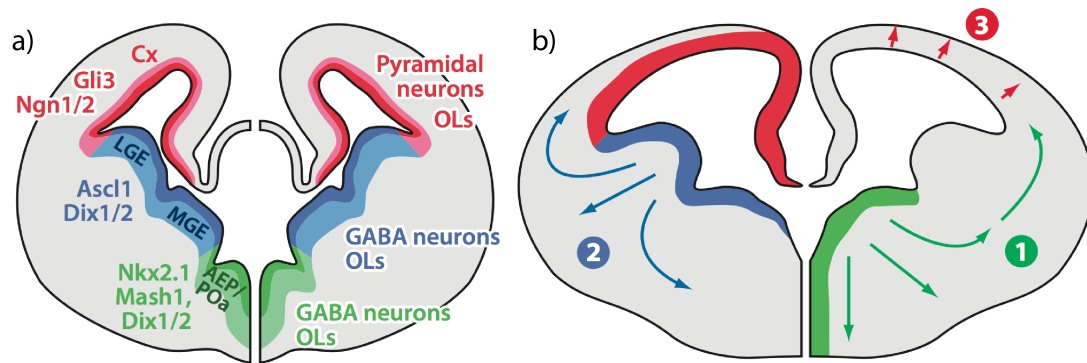


Figure 15. Waves of oligodendrogenesis in the developing forebrain

a) As the forebrain develops the region of active oligodendrogenesis gradually moves more dorsally. b) Oligodendrogenesis happens in three distinct waves, with the first two occurring during embryogenesis and the third postnatally. The first wave (green) begins at approximately E11.5 in the Medial Ganglionic Eminence (MGE) - anterior entopeduncular region (AEP). The second wave (blue) occurs after E15.5 in Lateral Ganglionic Eminence (LGE) - Caudal Ganglionic Eminence (CGE). The third wave (red) takes place in the postnatal cortex, with OPCs able to distribute to all parts of the brain. (Directly from (Fancy, Chan et al. 2011)).

2.4.3 Oligodendrocyte maturation in the developing forebrain

Oligodendrocyte maturation is a process requiring precise spatiotemporal coordination of both intrinsic factors, as well as direct contact with extrinsic factors such as active axons (Zuchero and Barres 2013). During this process, oligodendrocytes undergo extensive chromatin reorganization resulting in transcriptional upregulation of maturation genes (Nielsen, Hudson et al. 2002, Yu, Chen et al. 2013). One of the key transcription factors believed to regulate this remodeling is Olig2, and has been demonstrated to be critical in fate commitment to the oligodendrocyte lineage (Meijer, Kane et al. 2012, Zhu, Zuo et al. 2012). Olig2 can act as a pre patterning factor by binding to the promoter of oligodendrocyte specific genes (Yu, Chen et al. 2013). Olig2 is then recognized by the ATP-dependent SWI/SNF chromatin-remodeling enzyme Smarca4/Brg1, resulting in it also localizing to these promoters. Smarca4/Brg1 then alters the chromatin structure and recruits additional proteins that actively transcribe target oligodendrocyte genes (Yu, Chen et al. 2013).

In recent years Sox10 has emerged as a key fate determinant of early oligodendrocyte precursor specification (Fig. 16) (Kuhlbrodt, Herbarth et al. 1998, Stolt, Rehberg et al. 2002, Li, Lu et al. 2007, Finzsch, Stolt et al. 2008, Rivers, Young et al. 2008). In precursor specification Olig2 binds through an evolutionary conserved distal enhancer to directly control the expression of Sox10 (Fig. 17) (Küspert, Hammer et al. 2011). Sox10 is specifically expressed through the entire process of oligodendrogenesis, from OPCs to myelinating oligodendrocytes (Fancy, Chan et al. 2011). Conditional genetic ablation studies have shown that Sox10 is essential for OPCs (Finzsch, Stolt et al. 2008). Following the ablation of both Sox10 and Sox9, expression of platelet-derived growth factor receptor alpha (PDGFR α), which serves as both an important cue for migration and a survival factor for OPCs is lost (Finzsch, Stolt et al. 2008). In the peripheral nervous system (PNS) Sox10 has been shown to interact with the transcription factor Krox20 (Egr2) (Ghislain and Charnay 2006). Together, they bind to the promoters and directly regulate a cascade of genes involved in myelination (LeBlanc, Jang et al. 2006, Srinivasan, Sun et al. 2012). Although Krox20 is not expressed in oligodendrocytes of the CNS a functionally similar protein called myelin regulatory factor (Myrf; also referred to as Mrf in the literature) has been identified. Similar to what is seen with Krox20 expression in Schwann cells, Myrf is upregulated in myelinating oligodendrocytes of the CNS (Emery, Agalliu et al. 2009).

Upregulation of Sox10 does not immediately result in the expression of Myrf. Data suggests that Sox10 binding sequences in the promoter of Myrf require chromatin remodeling from Smarca4/Brg1 and Olig2 before Sox10 can bind (Hornig, Frob et al. 2013, Yu, Chen et al. 2013). Interestingly, both Sox10 and Myrf can bind and act as a functional transcriptional complex (Hornig, Frob et al. 2013). ChIP data also suggests that Myrf shares similar binding sites to Sox10, and can be found on the promoters of myelin specific genes including MBP (Bujalka, Koenning et al. 2013).

Depending on the stage of oligodendrocyte maturation, oligodendrocytes express a range of unique markers (Fig. 16). Key markers displayed by OPCs include PDGFR α , Nkx2.2, NG2, as well as the transcription factors Olig2 and Sox10 (Fancy, Chan et al. 2011). However a variety of OPC

populations exist, with some having limited or no expression of PDGFR α (Spassky, Goujet-Zalc et al. 1998, Spassky, Heydon et al. 2001).

Newly derived premyelinating oligodendrocytes have a distinct morphology that contains multiple processes extending both radially and symmetrically. They express the markers myelin-associated glycoprotein (MAG), 2',3'-cyclic nucleotide 3'-phosphodiesterase (CNPase) and myelin basic protein (MBP) (Fig. 16) (Fancy, Chan et al. 2011). Premyelinating oligodendrocytes can then either undergo apoptosis and be removed, or continue to mature and become myelinating oligodendrocytes (Barres, Hart et al. 1992, Barres, Hart et al. 1992).

Similar to premyelinating oligodendrocytes, maturing oligodendrocytes express the markers MBP, CNPase and MAG however additional markers including proteolipid protein (PLP), myelin oligodendrocyte glycoprotein (MOG), peripheral myelin protein 22 (PMP22), myelin protein zero (P0) are also used to identify these cells (Fancy, Chan et al. 2011). During maturation, these proteins are transported to the cell membrane with MAG targeted to the periaxonal membranes, CNPase to noncompact and PLP to compact myelin regions of the myelin internode (Martini and Schachner 1986, Sorg, Smith et al. 1987, Braun, Sandillon et al. 1988, Trapp, Bernier et al. 1988, Trapp, Andrews et al. 1989). Additionally, contactin-associated protein (Caspr) can identify fully mature oligodendrocytes which have formed multiple ensheathing wraps of myelin around axons (Einheber, Zanazzi et al. 1997). This is denoted by punctate Caspr expression at the paranodal junctions on myelinated axons (Rios, Melendez-Vasquez et al. 2000). Interestingly the individual role of each protein seems to be quite complicated, with mutations resulting in a large range of phenotypes. MBP ablated mice (shiverer mouse) are dysmyelinated but still form axons that are functional and intact (Readhead, Popko et al. 1987). Conversely, PLP null mutations results in mature myelination but non-functional axons (Griffiths, Klugmann et al. 1998).

While axons are not essential for oligodendrocyte production, they do act extrinsically on neighboring oligodendrocytes and regulate oligodendrocyte maturation and number (Nave and Trapp 2008). Neuregulin-1 (Nrg1) is expressed by axons and can bind to ErbB receptor tyrosine kinases on oligodendrocytes and promote their development (Vartanian, Goodearl et al.

1997, Esper, Pankonin et al. 2006). Nrg1 can also act as a chemoattractant for OPCs and direct their migration through embryonic development (Ortega, Bribián et al. 2012). Furthermore, in spinal cord neural precursor cells, exogenous Nrg1 can enhance proliferation and differentiation into oligodendrocytes at the expense of astrocytes (Gauthier, Kosciuczyk et al. 2013).

As axons and oligodendrocytes mature, they signal to each other regulating their maturation spatially and temporally (Nave and Trapp 2008). Oligodendrocytes synthesize and release known neurotrophic factors such as Prostaglandin D that can act as a neuroprotective molecules for adjacent neurons, however the mechanism is not fully understood (Taniike, Mohri et al. 2002, Nave and Trapp 2008). Laminin- α 2 and β 1-integrin mediated signaling is also essential for correct axon selection and myelin thickness (Mitew, Hay et al. 2014). Ablation of β 1-integrin does not disrupt normal oligodendrocyte development however cells are unable to extend and form myelin sheaths or activate AKT, which is critical for axonal ensheathment (Lee, De Repentigny et al. 2006, Barros, Nguyen et al. 2009).

It has long been known that axon diameter increases with the maturation and myelin expression of oligodendrocytes (Foster, Connors et al. 1982, Brady, Witt et al. 1999). Oligodendrocytes that ensheath axons after a demyelinating injury form thinner myelin wraps than those during normal development, implying that axons and oligodendrocytes are providing feedback cues to each other (Lasiene, Shupe et al. 2008). The biophysical properties of axonal diameter on oligodendrocyte maturation was addressed through studying engineered nanofibers in vitro (Lee, Leach et al. 2012). Oligodendrocytes not only show preference for axons of 0.5 μ m in diameter or larger, but also initiate membrane ensheathment before they have begun to differentiate (Lee, Leach et al. 2012).

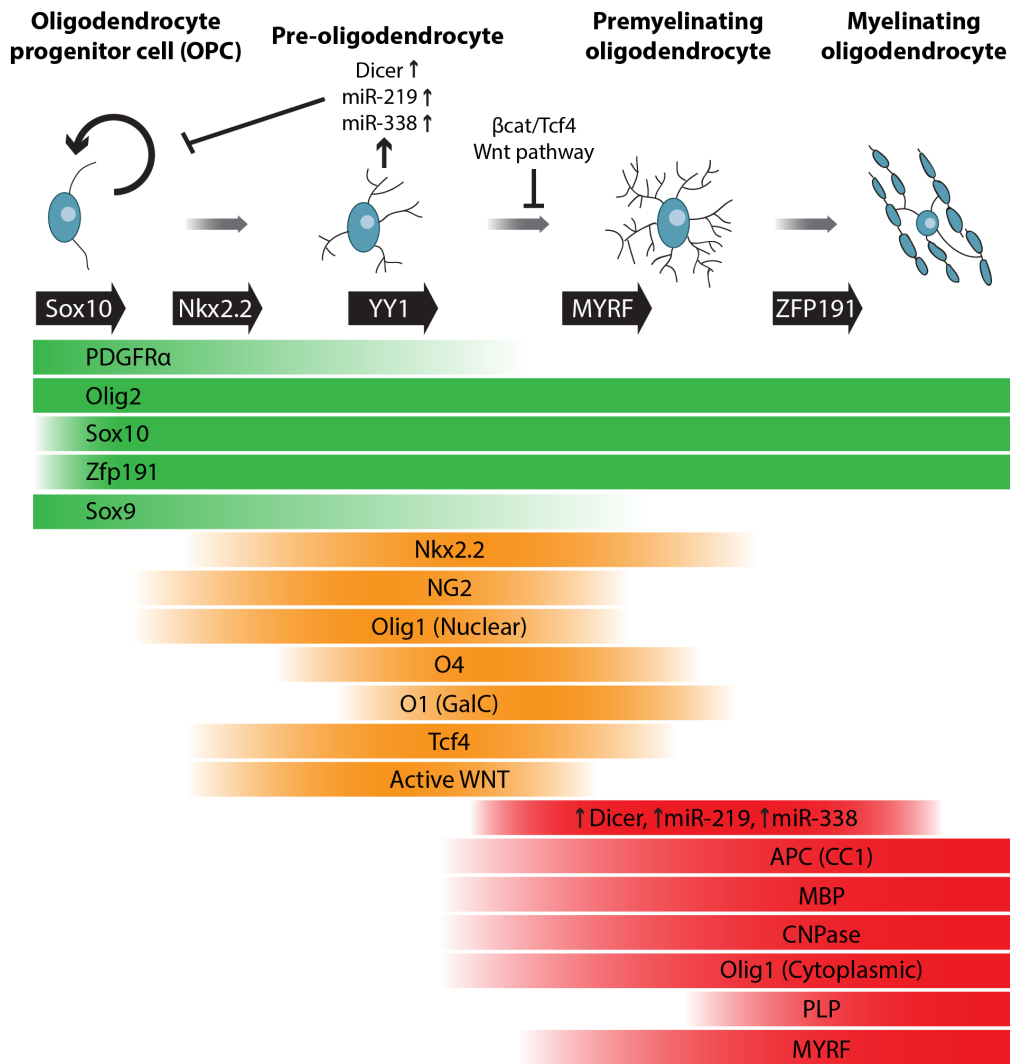


Figure 16. Marker expression during lineage restriction of oligodendrocytes

As oligodendrocytes progress from OPCs through to mature myelinating oligodendrocytes, they express a cascade of molecular markers and genes. Transcriptional factors, Sox10, Nkx2.2, YY1, Myrf, and Zfp191 are delineated with solid black arrows and are essential for each stage of oligodendrogenesis to proceed. Gradient bars define temporal expression of each factor, with green bars representing generally early expressed genes, orange being expressed by pre-myelinating oligodendrocytes, and red expressed in myelinating oligodendrocytes. Other mechanisms including Wnt signaling and miRNA regulation play a role in both inhibiting and promoting maturation. (Adapted from (Back, Riddle et al. 2007, Silbereis, Huang et al. 2010, Fancy, Chan et al. 2011)).

2.4.4 The role of Wnt signaling in maturation of oligodendrocytes

Both Wnt and Notch signaling pathways act as repressors of oligodendrocyte maturation. However, Wnt signaling has been shown to enhance proliferation of less fate restricted OPCs and careful regulation is required for myelinating oligodendrocytes to occur (Fancy, Baranzini et al. 2009). In line with this evidence, canonical Wnt negative regulators Axin2 and Adenomatous polyposis coli (APC) have been shown to be essential in ensuring correct OPC maturation (Fancy, Baranzini et al. 2009, Fancy, Harrington et al. 2011). The negative role of Wnt in maturation is due in part to the Wnt downstream effector TCF4, which can bind to an activated form of β -catenin (Leung, Kolligs et al. 2002). The β -catenin/TCF4 complex to the promoter region of MBP results in its expression being repressed, and consequently, a block in myelination (He, Dupree et al. 2007). Disruption of TCF4 repression through HDAC1 and HDAC2 was found to alleviate some of these inhibitory effects by allowing expression of late stage maturation genes (Ye, Chen et al. 2009). Other regulators of canonical Wnt signaling, including homeodomain interacting protein kinase 2 (HipK2) which phosphorylates TCF4 preventing it from binding to DNA, and therefore may play a role in modulating oligodendrogenesis (Gao, Xiao et al. 2014).

Precise regulation and fine tuning of oligodendrogenesis by Wnt signaling is crucial, resulting in it being both required for early development and repressed in later development. In the adult dorsal SVZ, Wnt3a can induce the nuclear localization of β -catenin (Azim, Rivera et al. 2014). Interestingly, it was shown that nuclear β -catenin accumulation was completely abolished through overexpression of BMP4, highlighting its potential role as an inhibitor of OPC development (Azim, Rivera et al. 2014). However, constitutive expression of an active form of β -catenin results in the inhibition of OPC development and a loss of re-myelination *in vivo* (Fancy, Baranzini et al. 2009, Ye, Chen et al. 2009). Moreover, APC must be expressed in order to prevent OPCs from transitioning to high levels of Wnt signaling (Fancy, Harrington et al. 2014). They went on to show that OPCs with high Wnt, do not express APC and could not fully mature or myelinate (Fancy, Harrington et al. 2014). Therefore, the complicated dual role of Wnt signaling appears to

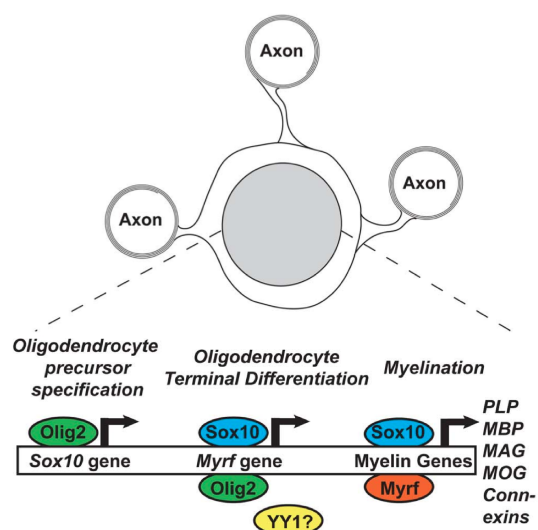
be required for correct spatial temporal timing of events in oligodendrogenesis (Fancy, Chan et al. 2011).

2.4.5 The role of Notch signaling in maturation of oligodendrocytes

Activated Notch signaling is believed to play an inhibitory role in OPC maturation (Wang, Sdrulla et al. 1998, Jurynczyk, Jurewicz et al. 2008, Zhang, Argaw et al. 2009, Aparicio, Mathieu et al. 2013, Hammond, Gadea et al. 2014). However, conflicting reports reveal that it is unclear how Notch may inhibit OPC development (Stidworthy, Genoud et al. 2004, Nakahara, Kanekura et al. 2009). In remyelinating lesions activation of Notch receptor through Jag1 presenting reactive astrocytes leads to an overall decrease in remyelinated axons (Hammond, Gadea et al. 2014). It was proposed that stimulation of Jag1 by endothelin-1 (ET-1) in reactive astrocytes leads to an over-activation of Notch1, and an increase in nuclear translocated NICD. The NICD then potentially acts through Notch effector proteins such as Hes5 to inhibit OPCs (John, Shankar et al. 2002). Conversely, it was demonstrated that active Notch signaling does not result in an inhibition of remyelination (Stidworthy, Genoud et al. 2004). Additionally it was shown that inhibition of remyelination was not due to an activation of Notch but instead an upregulation and accumulation of TAT-interacting protein (Tip30) in OPCs, which inhibits the nuclear translocation of the NICD (Nakahara, Kanekura et al. 2009). Although it is clear that Notch signaling plays a role in OPC maturation, what that role may be is still unclear.

Figure 17. Sox10 and Myrf are essential transcription factors required for oligodendrocyte terminal differentiation in the CNS.

During OPC specification Olig2 positively regulates the expression of Sox10. In order for oligodendrocytes to fully mature and express myelin, Sox10 and Olig2 must act in concert to induce Myrf expression. Once expressed, Sox10 and Myrf can bind to similar sequences in promoters of essential myelin genes including PLP, MBP, MAG and MOG. (Directly from (Emery 2013)).



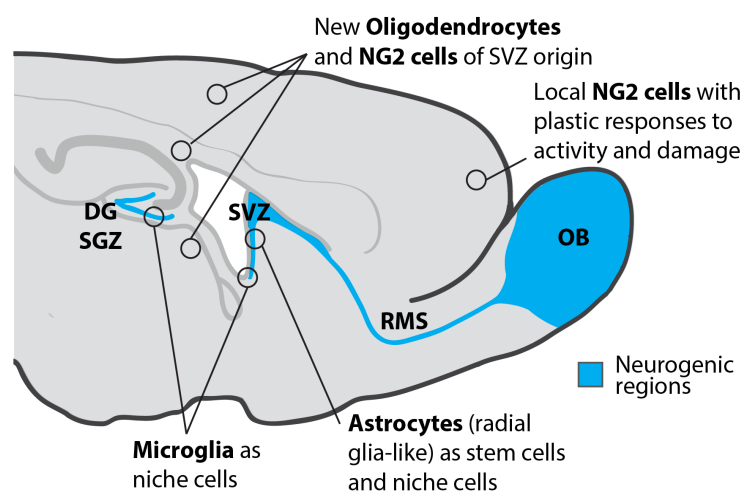
2.4.6 Multiple Sclerosis: The demyelinating disease

2.4.6.1 Fundamentals of MS

Multiple Sclerosis (MS) is a complicated autoimmune inflammatory demyelinating disease where the immune system targets and degrades myelinating oligodendrocytes, ultimately resulting in neuronal degeneration (Franklin, French-Constant et al. 2012). Although the precise mechanisms involved are still unclear, it is believed to be the result of a cascade of cellular malfunctions. Sites where inflammation and demyelination occur are referred to as lesions. Axonal damage is a pathological condition of the disease, which can be contributed to oxidative damage, sodium accumulation and energy deprivation of the cells (for a full review please see (Franklin, French-Constant et al. 2012). Unlike other neurodegenerative diseases, such as Parkinson's or Huntingtons disease, the only cells that are lost in MS are myelinating oligodendrocytes. Luckily the body can naturally regenerate these cells through a process termed "remyelination", in which a natural reserve of OPCs (Fig. 18) can migrate to the site of the lesion, become activated, and undergo differentiation. The precise mechanisms controlling this recruitment and differentiation are still unclear. The key to curing MS lies in understanding why remyelination fails in patients with MS and how to recapitulate a healthy level of remyelination, while in parallel limiting the immune system degradation of newly generated myelin.

Figure 18. Regionalization of glia in the adult mammalian brain

In the adult mouse OPCs expressing the marker NG2 are scattered throughout the brain and can become activated and migrate large distances to the site of lesions. Additionally, microglia, the resident



immune cells of the adult brain, can migrate to the site of lesion and release mitogens to attract and activate OPCs. (Adapted from (Morrens, Van Den Broeck et al. 2012))

2.4.6.2 The process of remyelination in MS lesions

In MS, although remyelination of lesions occurs naturally, relapse and new lesions form due to a continued autoimmune response against myelinating cells. The process of remyelination is composed of three phases (Fig. 19a). The OPCs activation phase, the OPC recruitment phase, and finally the differentiation phase where OPCs mature and remyelinate the axonal processes (for a full review please see (Franklin and ffrench-Constant 2008)). After a lesion has occurred, the first cells to recognize and respond are astrocytes and the resident immune cells of the brain, the astrocytic microglia (Glezer, Lapointe et al. 2006, Rhodes, Raivich et al. 2006). Together they release a cascade of mitogens and chemoattractants including platelet derived growth factor (PDGF) and fibroblast growth factor (FGF) that are involved in recruiting and activating migratory OPCs (Fig. 19b) (Scolding, Franklin et al. 1998, Sim, Zhao et al. 2002, Wilson, Scolding et al. 2006). During the recruitment phase the activated OPCs then proceed to invade the lesion site (Franklin 2002, Larsen, Wells et al. 2003). Once at the site of the lesion they enter their final phase and begin to remyelinate the demyelinated axons. This process is quite complex and not fully understood, but OPCs must begin by making physical contact with the cells it will ensheath. Then the OPCs express myelin specific genes (Fig. 16) permitting them to continue the maturation process. Finally, the processes of the myelinating oligodendrocyte ensheath neighboring axons forming a functional myelin membrane (Franklin and ffrench-Constant 2008).

2.4.6.3 The role of inflammation in remyelination

A key inhibitor of remyelination in the mammalian brain is the T-cell mediated inflammation response. In experimental autoimmune encephalomyelitis (EAE), a mouse model of MS, lesions are associated with elevated levels of Th1 and/or Th17 responsive T-cells (Balashov, Smith et al. 1997, Crawford, Yan et al. 2004, Kebir, Kreymborg et al. 2007, Tzartos, Friese et al. 2008). Even though myelin-specific T-cells exist in healthy individuals they do not become activated and induce MS under normal conditions. Interestingly, both pro-inflammatory cytokines interleukin-1 (IL1) and tumour necrosis factor- α (TNF α) appear to be required in the process of

remyelination (Arnett, Mason et al. 2001, Mason, Suzuki et al. 2001). Contrary to the inflammatory Th1 induced cell response, a Th2 mediated response appears to have anti-inflammatory effects in lesions and promote remyelination (Aharoni, Teitelbaum et al. 1997, Park, Li et al. 2005, Bergamaschi, Villani et al. 2009, Pedotti, Farinotti et al. 2009, Guerau-de-Arellano, Smith et al. 2011). The Notch signaling pathway which plays a role in the remyelination of lesions (see 2.4.5), can differentially regulate either Th1 or Th2 T-cell responses depending on if it is activated by Dll or Jag1 ligands respectively (Amsen, Blander et al. 2004, Amsen, Blander et al. 2004, Rutz, Mordmüller et al. 2005, Elyaman, Bradshaw et al. 2007). Elyaman, et al. showed this by blocking Jag1 *in vivo*, which resulted in a Th2 specific decrease (Elyaman, Bradshaw et al. 2007). When Dll was blocked, this decrease was specific for Th1 T-cell mediated response (Elyaman, Bradshaw et al. 2007). Although it has been demonstrated in endothelial cells that Jag1 can be positively regulated by TNF α it appears that in the CNS it has an inhibitory effect on the ligand (Elyaman, Bradshaw et al. 2007, Sainson, Johnston et al. 2008, Johnston, Dong et al. 2009). Potentially through multiple levels of Jag1 regulation in active lesions, a finely-tuned Th2 T-cell anti-inflammatory response can be mediated through Notch signaling.

2.4.7 Putative role of Jag1 in remyelination

At present there are conflicting reports on the role of Jag1 in remyelination. The lab of Vittorio Gallo has put forth the hypothesis that through stimulation by ET-1, Jag1 is upregulated in reactive astrocytes, which in turn activates Notch signaling in active OPCs of the lesion (Hammond, Gadea et al. 2014). Other labs in recent years have also demonstrated that reactive astrocytes expressing Jag1 resulting in an inhibition of differentiating OPCs and remyelination, implying that activation through the Notch signaling pathway may exhibit an inhibitory role (Stidworthy, Genoud et al. 2004, Zhang, Argaw et al. 2009). This, however, contradicts the findings of other labs that show Jag1 expression to be highest in astrocytes of MS lesions undergoing active remyelination (Elyaman, Bradshaw et al. 2007, Seifert, Bauer et al. 2007). Moreover, multiple studies have shown that astrocytes in remyelinating lesions express high levels of Jag1 and not Dll, implying that it is the key

ligand in regulating remyelination (Stidworthy, Genoud et al. 2004, Elyaman, Bradshaw et al. 2007). Additionally it was shown that even within lesions containing OPCs with high levels of Notch and Jag1, remyelination can still occur (Stidworthy, Genoud et al. 2004). Understanding the functional role of Jag1 at a molecular level is key to determining the potential mechanisms involved in its regulation of remyelination.

Figure 19. Remyelination in the adult mammalian brain (next page)

a) There are three phases in remyelination of the adult mammalian brain. Activation, recruitment and differentiation. These processes must be carefully regulated both temporally and spatially in order for functional remyelination to occur. Key mitogens and signaling pathways have been denoted for each step. b) A depiction of normal adult white matter (i) undergoing a demyelinating lesion (ii), resulting in the loss of oligodendrocytes ensheathing the axons. This activates microglia and astrocytes, which attract and activate OPCs through excretion of mitogens. Once at the lesion site (iii) OPCs begin to express markers for oligodendrocytic differentiation and start to ensheath the demyelinated axons (iv). Careful timing of recruitment and differentiation factors is critical in order for myelination to occur (Adapted from (Franklin and ffrench-Constant 2008, Filipe Palavraa 2014)).

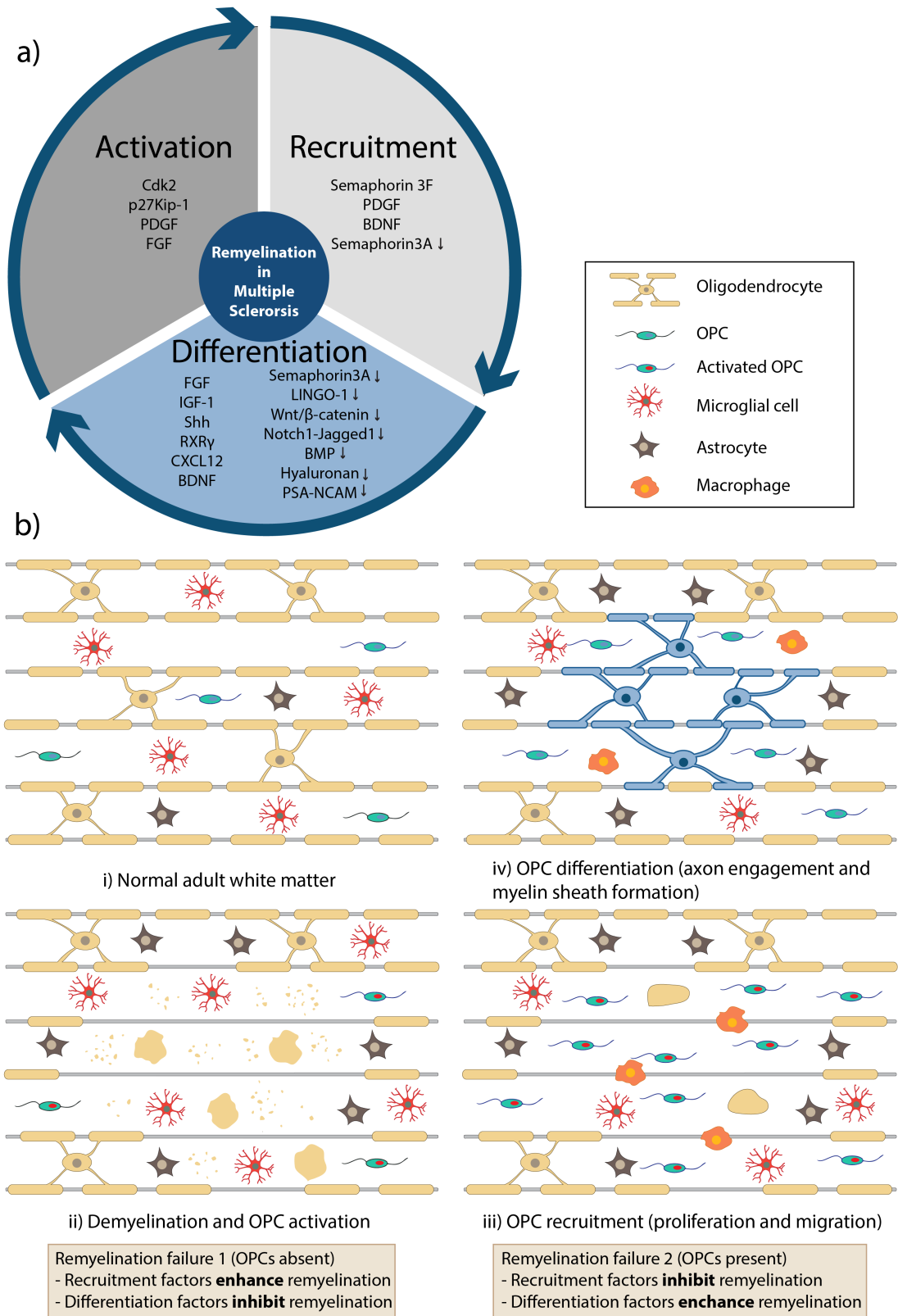


Figure 19. Remyelination in the adult mammalian brain (legend on previous page).

3 Results

3.1 Project 1: The role of Jag1 full length in maintaining the NSC niche

3.1.1 Background

Jag1 plays an important role in lateral activation of Notch, including during brain and ear development, vasculogenesis and cancer, (Xue, Gao et al. 1999, Nyfeler, Kirch et al. 2005, Kiernan, Xu et al. 2006, Roca and Adams 2007). However, the molecular mechanisms controlling the transition from stem cell division, where Notch plays a maintenance role in most systems, to daughter cell differentiation, are not understood. Our lab has previously shown by genetic ablation experiments that Jag1 provides niche signals for NSC maintenance during development of the mouse brain and in controlling adult neurogenesis (Nyfeler, Kirch et al. 2005, Weller, Krautler et al. 2006). An active secreted form of Jag1 was sufficient to compensate for the lost lateral signal in Jag1-ablated stem cell cultures and maintain wild type but not Notch1^{-/-} NSCs *in vitro* (Nyfeler, Kirch et al. 2005).

The developing forebrain is highly organized and cell population identity determined based on topological position and marker expression (Fig. 3). Jag1 is expressed by progenitors in the developing forebrain, where it localizes to the apical domain and we postulate plays a role in lateral signaling *in vivo* (Fig. 20a-d). In the first part of my thesis I will describe the results of experiments designed to address the functions of Jag1 in regulating NSC and progenitor differentiation.

3.1.2 AAV-Jag1FL particles are able to package Jag1FL transcript and transduce cells *in vitro*

In an attempt to address the role of Jag1 in the developing SVZ niche, I adopted a gain-of-function approach, expressing Jag1FL from viral vectors. Type B1 cells of the SVZ can go through long periods of quiescence, and divide infrequently to give rise to intermediate progenitors which differentiate into neurons, astrocytes and oligodendrocytes. To express Jag1 in NSCs of the niche I took two approaches. First, with an adeno-associated virus (AAV) which can transduce mitotically active and inactive cells (Tenenbaum, Chtarto

et al. 2004) and secondly with a retrovirus for transduction of actively dividing cells (see below).

Jag1FL open-reading frame encoding mRNA was cloned between the inverted terminal repeats (ITRs) of the Strategene AAV-2 Helper Free System (Fig. 20e). The total fragment size between the ITRs (red) was 5496 bp, which is near the theoretical maximum encapsulation capacity of AAVs (Wu, Yang et al. 2010). The vector AAV-Jag1FL was sequenced to confirm integrity and shown to express Jag1FL protein *in vitro* (Fig. 20I, g). High transfection efficiency of viral plasmids ensured that co-transfection with pHelper and pAAV-RC plasmids occurred at a high frequency (Fig 20F). AAV particles were purified and titered in collaboration with Jan Herb at the Max-Planck-Institute for Medical Research in Heidelberg, Germany (20K). Viral titers of AAV-Jag1FL were lower than control (3.33×10^9 capsides/ul), but the purified virus was still capable of transducing both HEK293 (Fig. 20J) and wild type (WT) C57BL/6 mouse NSC cultures (Fig. 20K,L). This viral construct is a valuable tool for the expression of Jag1FL protein but has the limitation of relatively low viral titer and no reporter gene to monitor transduction and the fate of infected cells. Therefore, in parallel I generated an additional viral construct based on the mouse Moloney leukemia virus (MMLV) retrovirus (RV).

3.1.3 Retro-Jag1FL particles are highly efficient at transducing cells *in vitro*

The Jag1FL open-reading frame cDNA sequence was cloned into the pMIG RV expression vector (Fig. 21a). pMIG contains an internal ribosome entry sequence (IRES) driving expression of a GFP reporter and due to the larger capacity of the RV, more sequence information can be packaged in each viral particle. Expression of Jag1 from the pMIG vector was confirmed through transfection of HEK293 cells with the viral backbone plasmid and Jag1-specific qRT-PCR and western blot analysis (Fig. 21b,c). Viral particles were confirmed to be capable of transducing cells *in vitro* using a NIH3T3 fibroblast cell line (Fig. 21d-f). Both control (IRES-GFP only) and Jag1FL-IRES-GFP RVs transduced NIH3T3 cells with a similar efficiency. Notably, by immunohistochemistry (IHC) Jag1FL protein was detectable at the cell

membrane at higher levels in the Jag1FL-IRES-GFP expressing cells than the endogenous levels detected in the IRES-GFP transduced cells. Jag1FL-IRES-GFP NSCs were also confirmed to express elevated levels of Jag1 protein (Fig. 21g,h).

3.1.4 Jag1FL-IRES-GFP transduction into the postnatal SVZ niche results in a fate shift to Sox10⁺ oligodendrocytes

To address the role of Jag1 in the SVZ niche, RV was injected into the right lateral hemisphere of postnatal day (P) 2 wildtype C57BL/6 mice using predefined stereotactic coordinates (experimental outline Fig. 22a). Since RV can only incorporate their genome into mitotically dividing cells, transduction in the SVZ likely targets actively dividing type B1 NSCs, and the proliferating type C (transient amplifying) cells. Mice were analyzed at 3, 7, 15 and 30 days post-infection (DPI) (Fig. 22a). Jag1 was detectable by IHC in cells expressing the GFP reporter from the Jag1FL-IRES-GFP RV (Fig. 22b). Initial analysis of Jag1FL-IRES-GFP⁺ cells in 30 DPI animals, revealed a disproportionate number of Jag1FL-IRES-GFP⁺Sox10⁺ cells when compared to IRES-GFP⁺ control cells, particularly in the cerebral cortex (Fig. 22c). IHC of 3 DPI mice demonstrated that RV infection occurred in the targeted progenitor cells lining the lateral ventricle (LV) (Fig. 23a). Surprisingly, Jag1FL-IRES-GFP⁺ cells at 30 DPI exhibited an oligodendrocyte-like morphology more obvious than IRES-GFP⁺ cells at the same time-point (Fig. 23a,b,d,e). Analysis of cell migration demonstrated that there was a significant increase in Jag1FL-IRES-GFP⁺ cells in the cerebral cortex by 7 and at 15 DPI compared to IRES-GFP⁺ cells (Fig. 23c).

High migration potential is characteristic of OPCs that are capable of traversing large distances during oligodendrogenesis (Fancy, Chan et al. 2011). Based on the migration data and the oligodendrocyte-like morphology of the Jag1FL-IRES-GFP⁺ cells, I hypothesized that expression of Jag1FL could induce a fate switch of transduced cells to the OPC lineage. To test this, I studied the expression of essential oligodendrocyte transcription factors Olig2 and Sox10 (Fig. 24), both of which are required for OPC commitment (Introduction Fig. 16). In both the corpus callosum and the cerebral cortex of Jag1FL-IRES-GFP transduced animals there was a noticeable increase in

Jag1FL-IRES-GFP⁺Olig2⁺Sox10⁺ expressing cells when compared to control mice. Since most Sox10⁺ cells were also Olig2⁺, future experiments used Sox10⁺ labeling to denote cells in the oligodendrocytic lineage. By 30 DPI, there was a significant difference in the number of Jag1FL-IRES-GFP⁺ cells residing in the corpus callosum and striatum (Fig. 25a). Surprisingly, compared to IRES-GFP⁺ controls there was almost double the number of Jag1FL-IRES-GFP⁺Sox10⁺ cells by 15 DPI, which was maintained through to 30 DPI (Fig. 25b).

I asked if this shift in Sox10 expression amongst Jag1FL-IRES-GFP⁺ cells was brain region specific. While there were slight increases in Sox10⁺ cells in all regions of the forebrain of Jag1FL-IRES-GFP transduced animals examined at 3 DPI, compared to IRES-GFP transduced controls there was only a significant shift in Sox10⁺ in the cerebral cortex (Fig. 25c, 26a,b). However, by 15 DPI there was a significant change in Jag1FL-IRES-GFP⁺Sox10⁺ in all forebrain regions. The most dramatic increase was seen in the cerebral cortex where almost 80% of Jag1FL-IRES-GFP⁺ cells at 15 DPI were Sox10⁺. This trend was maintained in mice at 30 DPI (Illustrated in Fig. 27b).

3.1.5 Jag1FL-IRES-GFP⁺Sox10⁺ cells express the early OPC marker NG2

If Jag1FL causes a fate shift to the oligodendrocyte lineage, one would expect to see differences in early OPC marker expression in Jag1FL-IRES-GFP⁺ cells. To study this I examined the expression of the early OPC marker NG2. NG2 (also known as Chondroitin Sulfate Proteoglycan, Cspg4) is an integral membrane proteoglycan (Nishiyama, Chang et al. 1999). NG2 expression is downregulated at later stages of OPC development and can only identify OPCs in their most primitive stages (Stallcup and Beasley 1987). At 7 DPI almost 40% of Jag1FL-IRES-GFP⁺ cells in the cerebral cortices of infected mice expressed NG2 compared to approximately 10% in IRES-GFP⁺ cells (Fig. 28a-c). Interestingly, at this same time point the percent of total transduced cells that were Sox10⁺NG2⁺ decreased by approximately 15% in Jag1FL-IRES-GFP⁺ mice compared to control (Fig. 28c). The cell-surface receptor PDGFR α , is another widely accepted marker for early OPC

development, although PDGFR α ⁻ OPC populations have been identified (Spassky, Goujet-Zalc et al. 1998, Nishiyama, Chang et al. 1999, Spassky, Heydon et al. 2001). By 30 DPI, no Jag1FL-IRES-GFP⁺ cells had detectable levels of PDGFR α (Fig. 28d).

To confirm that Jag1FL-IRES-GFP⁺ cells progress to later stages of oligodendrocyte development, I addressed whether they expressed the mature myelination markers CNPase (Cnp) and MBP (Boulanger and Messier 2014). Although analysis is ongoing, Jag1FL-IRES-GFP⁺ cells appear to co-express CNPase in the cerebral cortex as early as 15 DPI, which is not a common phenomenon seen for IRES-GFP⁺ cells (Fig. 29a). This increased number of Jag1FL-IRES-GFP⁺CNPase⁺ cells compared to control appears to become more pronounced by 30 DPI (Fig. 29b). Additionally, by 30 DPI Jag1FL-IRES-GFP⁺MBP⁺ cells were present in all forebrain regions (Fig. 29b, 30a-c).

Potentially, the oligodendrocytic phenotype could be explained by a Jag1FL-induced increase in proliferation. Using the active cell proliferation marker Ki67, I examined the cortices of mice 7 DPI (experimental outline Fig. 30D) but observed no significant differences between Jag1FL-IRES-GFP⁺ and IRES-GFP⁺ cells (Fig. 30e).

3.1.6 Jag1FL-IRES-GFP⁺ NSCs lose sphere-forming capacity but do not change rate of proliferation

To study the phenotype of Jag1FL-IRES-GFP⁺ NSCs *in vitro*, I used the neurosphere assay and measured the sphere-forming capacity of NSCs after transduction. Data from Nyfeler and colleagues, demonstrated that Jag1 could act as a stem cell regulator, maintaining sphere formation and differentiation capacity through lateral activation of Notch even in the absence of EGF in the media (Nyfeler, Kirch et al. 2005). However, based on my *in vivo* findings, Jag1FL-IRES-GFP⁺ cells lose their ability to remain as multipotent progenitors and become more fate-restricted over time. NSCs derived from postnatal pups were transduced with either Jag1FL-IRES-GFP or IRES-GFP RVs, sorted by fluorescent activated cell sorting (FACS) and then maintained at clonal densities in 24 well culture plates (experimental outline Fig. 31a,b). After multiple passages, Jag1FL-IRES-GFP⁺ NSCs lost

the capacity to form spheres, suggesting a loss of progenitor cell maintenance (Fig. 31c). This was most pronounced after passaging the NSCs 3-4 times. To examine if a loss of sphere formation was due to a change in the rate of cell proliferation, spheres were dissociated and pulsed with a thymidine analogue (EdU) before staining for the mitotic marker Ph3. No significant differences in EdU incorporation or Ph3 labeling were seen when comparing Jag1FL-IRES-GFP⁺ cells to control (Fig. 31d).

3.1.7 Under differentiating conditions, Jag1FL-IRES-GFP⁺ NSCs can upregulate essential genes involved in oligodendrocyte maturation

NSCs lose their ability to give rise to all neural cell lineages as they become fate restricted. NSC fate commitment was monitored using the neurosphere differentiation assay where spheres were grown on coverslips under differentiating conditions (experimental outline Fig. 32a). Transduced NSCs were sorted for GFP expression by FACS before initiating differentiation. Jag1FL-IRES-GFP⁺ and IRES-GFP⁺ transduced NSCs exhibited viral silencing under differentiating conditions, most notably at the peripheries of the colony (Fig. 32b). qRT-PCR analysis of differentiated cultures showed an increase in relative expression of the oligodendrocyte genes Enpp6, MBP, PDGFRa, Sox10, Myrf and Olig2 in Jag1FL-IRES-GFP⁺ colonies (Fig. 32c). In addition, Jag1FL-IRES-GFP⁺ colonies displayed an upregulation of Olig2 protein (Fig. 32e).

3.1.8 Next generation RNA sequencing of the transcriptome profiles of Jag1FL-IRES-GFP⁺ NSCs

I hypothesized that the Jag1FL-IRES-GFP⁺ NSCs would have a change in transcription profile compared to IRES-GFP⁺ control cells. I anticipated that a genome-wide analysis of Jag1FL-induced gene expression could present a plausible explanation for both the fundamental changes seen in the oligodendrocytic fate shift *in vivo* and the differentiation ability *in vitro*. Hence, transduced spheres were cultured, sorted for GFP expression by FACS and RNA immediately isolated for sequencing (Fig. 33). In parallel, RNA-Seq target genes were confirmed by qRT-PCR to eliminate false positives.

3.1.9 Jag1FL-IRES-GFP⁺ NSCs upregulate genes involved in oligodendrocyte maturation

RNA-Seq was performed in duplicate (referred to as rep1 and rep3) on control and Jag1FL-IRES-GFP⁺ NSCs. Reads per 1 kB transcripts, per 1 mB library (RPKM) were used for normalization of the data, taking into account variances in sample library size. Libraries were analyzed using empirical analysis of digital gene expression data in R (edgeR). FastQC quality reports were generated to verify that sequencing of all samples worked correctly (Fig. 34). Replicates were then cross-analyzed using a 2x2 contingency table and hypergeometric tests and low expressing genes filtered out (Fig. 35). A total of 13 469 expressed genes were observed, with 220 genes exhibiting a significant +/- log₂ fold change of 1 (p<0.05) between Jag1FL-IRES-GFP⁺ NSCs and IRES-GFP⁺ control NSCs. Analysis of differentially expressed genes with the gene ontology (GO) database identified enriched gene categories for central nervous system myelination (Odds ratio: 15.1), axon ensheathment in the CNS (Odds ratio: 15.1), oligodendrocyte development and differentiation (Odds ratio: 8.47 and 6.93 respectively) (Fig. 36a). In depth analysis of gene expression profiles revealed an increase in oligodendrocyte differentiation genes and a slight decrease in Wnt signaling genes (Fig. 36b). Target genes from the screen were confirmed through gene specific qRT-PCR, with 84.2% of the genes analyzed proving to be true positives (Fig. 37a). Interestingly, among the top 15 upregulated genes in the Jag1FL-IRES-GFP⁺ cells were *ErbB4*, *HipK2*, *Tnr*, *Enpp6*, and *Gpr17* all of which have known roles in promoting oligodendrocyte maturation (Fig. 37b) (Pesheva, Gloor et al. 1997, Park, Miller et al. 2001, Roy, Murtie et al. 2007, Czopka, Von Holst et al. 2009, Greiner-Tollersrud, Berg et al. 2013). Additionally, the oligodendrocyte specific genes *Sox10*, *Myrf*, *NG2* and *PDGFR α* were all confirmed to be upregulated in Jag1FL-IRES-GFP⁺ cells compared to the control (Fig. 37a). A list of transcriptome changes in Jag1FL-IRES-GFP⁺ NSCs is shown in supplementary table 1.

3.1.10 Current experiments studying the role of Jag1FL in the NSC Niche

Ongoing experiments performed by our collaborators Annalisa Buffo and Enrica Boda in Torino, Italy, are addressing the ability of Jag1FL-IRES-GFP⁺

cells to remyelinate induced and congenital demyelinated lesions. Transduced cells are being grafted into both lysolecithin-induced focal demyelinating lesion animal models and Citron-kinase knockout (KO) mice (Cit-K KO) (experimental outline Fig. 38a). The cells used in these experiments were transduced with Jag1FL-IRES-GFP or IRES-GFP RVs, sorted for GFP by FACS and delivered to the Buffo lab where the grafting experiments are being performed (Fig. 38b).

Although these are preliminary results, Jag1FL-IRES-GFP cells grafted in the lysolecithin experiments appear to have a better survival rate and migrate further to the site of the lesion based on analysis of transduced cells (Fig. 39a,b). Additionally, in the Jag1FL-IRES-GFP grafts, there are visually many more Sox10⁺ cells, however quantifications for this as well as migration and survival are still on going. Transduced cells are densely grouped in the Jag1FL-IRES-GFP cell grafted animals and their processes overlapping, but there appears to be some CNPase co-localisation (Fig. 39d-e). IHC for NG2 expression is inconclusive and further optimization of stainings for early OPC markers will be needed (Fig. 39f-h).

Interestingly, analysis of the first two brains from Cit-K KO mice show grafted Jag1FL-IRES-GFP cells that are CNPase⁺ (Fig. 40a-c). This has not been seen in control cell (IRES-GFP⁺) grafted mice, and was never observed in OPC grafting experiments from the Buffo lab (Fig. 40f,g). There is still a large heterogeneity of cell populations, with some appearing astrocytic, and others early OPC (Fig. 40 d,e). Some grafted Jag1FL-IRES-GFP cells expressed NG2, but quantifications are currently ongoing (Fig. 40h-k).

3.2 Project 2: Jag1 and the role of the JICD in bi-directional signaling

3.2.1 Background

It has been proposed that Jag1 can signal bi-directionally as a ligand activating Notchs on adjacent cells and as a receptor that can be cleaved by secretases releasing an ICD that signals to the nucleus of the Jag1 presenting cell (see section 2.2.11.4) (LaVoie and Selkoe 2003, Duryagina, Thieme et al. 2013) (unpublished lab data). In my first project where I addressed the role of Jag1FL in the adult SVZ niche, it was not possible to distinguish between the autonomous or non-autonomous roles of Jag1. Therefore, the aim of this project was to address the autonomous effects JICD may have on differentiation.

In previous experiments studying the role of Notch and Jag1 in NSCs, we found that Jag1 is an important ligand in the postnatal neurogenic SVZ for maintaining NSCs. We found that a soluble form of Jag1 could rescue Jag1^{-/-} neurospheres and expand NSCs. In addition, soluble Jag1 not only rescued Jag1^{-/-} NSCs but also increased maintenance of the stem cell state producing more colonies in clonal assays than Jag1-treated wild type stem cells. This suggested that Jag1 has an autonomous signal in NSCs that negatively influences stem cell maintenance. Interestingly, active secreted Jag1 was able to maintain NSCs in culture, even in the absence of EGF, the growth factor usually used as a mitogen in these cultures (Nyfeler, Kirch et al. 2005). Hence, this data suggested that Jag1 induces a signal, potentially in a cell-autonomous fashion, that drives stem cell differentiation. In the next part of my thesis I will describe experiments performed to address the cell autonomous role of Jag1 signaling by studying the JICD and its effect on the Jag1 presenting cell.

3.2.2 JICD induces a cell autonomous loss of progenitor markers and stimulates differentiation genes in a PDZ dependent manner

Jag1-null (Jag1^{-/-}) mice die *in utero* by E11.5 (Xue, Gao et al. 1999). Examination of the forebrain at E10 showed that Sox2⁺ progenitors remain but early neurogenesis is severely reduced in the Jag1 mutants (Fig. 41a), which

is in stark contrast to loss of Notch signaling where neurons differentiate prematurely (Yoon and Gaiano 2005). The Taylor lab previously demonstrated that *in vitro* rescue experiments with an active secreted form of Jag1 ectodomain was sufficient to compensate for the lost lateral signal and maintain wild type but not Notch1^{-/-} NSCs *in vitro* (unpublished data). More importantly, exogenous Jag1 could also rescue the Jag1^{-/-} NSCs increasing the number of sphereogenic stem cells above that seen in controls. Combining the *in vitro* and *in vivo* loss-of-function data, we concluded that a cell-autonomous Jag1 signal mediated through the ICD could explain Jag1 role in promoting differentiation in the forebrain.

Taking a gain-of-function approach I expressed the JICD in forebrain neural progenitors *in vivo* by *in utero* electroporation (IUE) at E13.5 (experimental outline Fig. 41b). JICD expression induced a rapid and maintained exit of cells from the ventricular zone (Fig. 41c) and a cell-autonomous loss of progenitor cell markers compared to control (Sox2, Pax6 and Nestin; Fig. 41f-h). In contrast, JICD stimulated expression of genes associated with differentiation including the basal progenitor marker Tbr2 and the neuronal proteins β -TubulinIII and neurofilament (NF160) within 24 hours (Fig. 41i-j) but did not affect neuronal migration or differentiation in the cortical plate after 48 hours (Fig. 42a-b). The cell cycle in the nervous system is precisely controlled upon onset of differentiation (Gotz and Huttner 2005, Kriegstein and Alvarez-Buylla 2009). JICD significantly reduced cell labeling with the S-phase marker bromodeoxyuridine (Fig. 42c-e). The expression of the cell cycle marker Ki67 was not affected suggesting prolongation of the cell cycle rather than exit consistent with initiation of differentiation (Fig. 42c-e). I conclude from these data that JICD can promote neuronal differentiation *in vivo*.

3.2.3 Molecular components of JICD identified through TAP and Y2H screens

In order to identify molecular components of Jag1 signaling, Antje Grabosch used JICD as bait and performed Tandem Affinity Purification (TAP) followed by mass spectroscopic proteome analysis for interacting proteins in a neuroblastoma cell line (N2A) and a yeast-2-hybrid screen (Y2H)

of a developing brain cDNA library (Fig. 43a). Multiple clones encoding the Protein Interacting with C-Kinase (PICK1) were identified by Y2H and interaction with full-length Jag1 and the JICD was confirmed by co-immunoprecipitation from N2A cells (Fig. 43b,c). PICK1 binds active protein kinase C-alpha (PKC α) recruiting it to target proteins and the intracellular surface of membranes (Staudinger, Lu et al. 1997, Hanley 2008). PKC α co-immunoprecipitated with full-length Jag1 and JICD (Fig. 43b,c). PKCs can activate ADAM metalloproteases such as TACE to stimulate shedding of surface proteins (Merlos-Suarez, Ruiz-Paz et al. 2001). Treatment of Jag1 expressing N2A cells with phorbol ester (PMA) to activate PKC stimulated translocation of PKC α to the plasmamembrane and colocalization with Jag1 (Fig. 43d), RIP of Jag1 and generation of Jag1CTF1 (Fig. 43g,h). Blockage of gamma-secretase with DAPT increased Jag1CTF1 formation ($P < 0.05$) supporting the normal processing of the CTF1 fragment to release the ICD. Activation of PKC with PMA and concomitant DAPT treatment increased Jag1CTF1 levels above PMA or DAPT treatment alone (Fig. 22g,h; $P < 0.001$). Surprisingly, although the ADAM inhibitor GM6001 slightly reduced Jag1CTF1 levels, it did not completely block RIP (Fig. 43g,h). Therefore, RIP of Jag1 is stimulated by PKC activation. We addressed whether PICK1 is required for RIP of Jag1. We knocked-down PICK1 80% ($P < 0.001$) with two independent shRNA vector constructs (Fig. 43i and not shown). In three independent knockdown cultures (shPICK1), PMA failed to induce JagCTF1 accumulation above vehicle-treated cultures (DMSO) (Fig. 43j,k; right graph) and compared to N2A cells expressing a control shRNA (Fig. 43j,k; left graph $P < 0.001$). We conclude that PICK1 regulates PKC-induced RIP of Jag1.

Interestingly, the Y2H screen also identified the binding targets Galectin-3 and PMP2, both of which have been shown to play a role in oligodendrocyte maturation and myelination (Majava, Polverini et al. 2010, Pasquini, Millet et al. 2011). Future co-immunoprecipitation experiments are required to confirm these targets.

Mass spectroscopic analysis of proteins associated with JICD identified the transcriptional regulators TBL1 and TBLR1 as well as core Histones H3, H4 and H2A (Fig. 43a). Antje confirmed association of TBLR1 and core Histones with JICD in co-purification assays (Fig. 43e,f). She was unable to co-purify

TBL1 directly with JICD suggesting that TBL1 may not directly associate with JICD but be in a tertiary complex with other proteins.

TBLR1 is a key component of the Notch and Wnt pathways (Perissi, Aggarwal et al. 2004, Perissi, Scafoglio et al. 2008). Antje performed luciferase reporter assays in HEK293 cells using the TopFlash reporter to measure Wnt/ β -Catenin signaling (Fig. 44a). JICD did not stimulate the Wnt/ β -Catenin TopFlash reporter but synergized with submaximal levels of stabilized β -Catenin to potentiate expression of Wnt/ β -Catenin target genes (Fig. 44b). TBLR1 has been shown previously to be able to potentiate β -Catenin activation of TopFlash (Li and Wang 2008). When both TBLR1 and β -catenin were expressed with JICD, we found that it dramatically enhanced reporter expression in a synergistic fashion (Fig. 44b). We also assessed the effects of JICD on an endogenous Wnt/ β -Catenin target promoter Axin-2. Although JICD and β -Catenin did not synergize in this assay, JICD, β -Catenin and TBLR1 together resulted in a synergistic potentiation of Axin-2 promoter expression (Fig. 44c). To explain the transcriptional modulatory effect we addressed whether JICD interacts with p300 and CBP but were unable to co-immunoprecipitate either with JICD (Fig. 44d). Similarly, we did not observe an interaction of JICD with TLE proteins, other key components in the Notch and Wnt/ β -Catenin pathways (Fig. 44e). Therefore, JICD can modulate transcriptional regulation of the Wnt signaling pathway, which is critical for development, particularly of the nervous system and in some cancers (Radtke and Clevers 2005).

As TBLR1 displayed a synergistic effect on JICD-modulated Wnt/ β -Catenin signaling, we generated mutant proteins to map the interaction domain on the JICD. Sequential truncation of 25 amino acids at the C-terminus of Jag1 (F1-F3) and co-affinity purification revealed reduced interaction when the last 75 amino acids were removed suggesting that this region of TBLR1 is required for binding to JICD (Fig. 45a,b). When tested in reporter assays, these truncated JICDs had all lost their transcriptional co-stimulatory activity (Fig. 45c,d and not shown). In addition, although the JICD-F1 fragment was still able to bind TBLR1, TBLR1 co-expression failed to rescue the function of this mutant (Fig. 45c). Thus, the C-terminal 25 amino acids contain a functionally

important domain that mediates JICD effect in modulating Wnt/ β -Catenin transcription independent of TBLR1 interaction.

We deleted the PDZ-ligand from the C-terminus of the JICD (JICDdelPDZ) to address whether this affected co-stimulatory function. JICDdelPDZ localized to the nucleus (Fig. 46a) but failed to potentiate β -Catenin induced transcription (Fig. 46b) indicating that the synergistic activity of JICD on β -Catenin mediated transcriptional regulation resides in the PDZ-ligand domain. We postulated that PDZ proteins are involved in JICD function. We never observed a direct interaction of JICD with β -Catenin in co-immunoprecipitation assays (not shown). Based on our link between PICK1/PKC α and JICD, we addressed whether the function of JICD in transcriptional modulation requires PKC activity. Inhibiting PKC α with RO 32-0432 in the TopFlash assay dramatically reduced the JICD/TBLR1 potentiated activity of β -Catenin (Fig. 46c). Surprisingly, inhibition of PKC α also reduced β -Catenin signaling, the mechanism of which remains to be elucidated but suggests that PKC α is a key regulator of β -Catenin transcriptional activity and that JICD functions as a co-regulator to increase this activity (Fig. 46c). Thus, PKC promotes RIP of Jag1 but also cooperatively regulates JICD and β -Catenin activity.

Next, I addressed whether the phenotypic effect of JICD to promote differentiation *in vivo* is also dependent on the PDZ-ligand domain. JICDdelPDZ did not induce exit of NSCs from the ventricular zone or differentiation of neural progenitors when expressed *in vivo* (Fig. 46d-g). Therefore, the differentiation effect of JICD and the autonomous Jag1 signal was dependent upon PDZ-mediated protein interaction. This supports previous observations that the transforming effect of Jag1 is PDZ-dependent and suggests that this may be through activation of β -Catenin signaling (Ascano, Beverly et al. 2003). The PDZ adapter protein AF-6 was shown to bind to JICD in a Y2H screen where AF-6 was used as bait (Hock, Bohme et al. 1998). AF-6 binds a number of proteins including Ras in a PDZ-independent manner. We did not identify AF-6 in our Y2H or TAP assays with JICD as bait. However, it is possible that Jag1 could, in addition, signal through AF-6 to regulate other downstream pathways. Further experiments will be required to address potential cross-talk between AF-6 and JICD and TBLR1 in the regulation of β -Catenin.

3.2.4 Basis for ChIP-Seq experiments

Taking together the *in vitro* and *in vivo* data, I proposed that the Jag1 signaling pathway is a hub for the regulation of one or more signal transduction pathways involved in NSC differentiation. I hypothesized that Jag1 is a signal integrator modulating neural progenitor fate and driving the onset of differentiation in the developing brain. Previously we had shown that JICD could interact directly with histones (Fig. 43e,f). As a follow up experiment, I performed a subcellular fractionation of N2A cells expressing either JICD-eGFP or eGFP as a control (experimental outline Fig. 47a) to observe where JICD was localized in the cell. Although JICD was present in the cytoplasm of cells, most of the JICD was in the nucleus due to the basic nuclear localization sequence (Introduction Fig. 10) and the majority of the JICD was bound to chromatin providing direct support that JICD plays a role in transcriptional regulation (Fig. 47b).

Since JICD was chromatin bound, I hypothesized that it may be binding to the promoters of genes, resulting in the regulation of their expression. To address transcriptional targets of the Jag1 signaling pathway *in vitro*, I performed chromatin immunoprecipitation (ChIP) followed by ChIP-Sequencing (ChIP-Seq) (experimental outline Fig. 47c,d). Although JICD has no known DNA binding domain, it may act by forming a transcriptional complex by binding to partners that bind DNA. This would also support our data that shows JICD can bind through PDZ-mediated protein interactions. Due to a lack of JICD specific ChIP grade antibodies, I used a JICD construct with an N-terminal tandem affinity purification (TAP) tag. This allows for efficient purification of bound protein using streptavidin resin. Based on our previous Wnt signaling luciferase reporter data, I was curious to see if the binding affinity for promoter sequences would change or shift when JICD was expressed with either an active form of β -Catenin alone or when β -Catenin and TBLR1 were both present. I established ChIP conditions by optimizing crosslinking, DNA sonication to ensure sheared DNA fragment sizes were 200-300bp and reverse-crosslinking to release the ChIPed DNA fragments (Fig. 47h). ChIPs were performed in parallel from N2A cells under four transfection conditions, empty N-TAP expression vector, JICD-NTAP expression vector alone, JICD-NTAP and an active form of β -Catenin

together, or JICD-NTAP, β -Catenin and TBLR1 transfected simultaneously. Sister plates of N2A cells were transfected in parallel to the ChIP experiments for RNA isolation to assess transcriptional expression profiles by qRT-PCR.

Since our luciferase data demonstrated that JICD in combination with β -Catenin and TBLR1 could potentiate Axin2, transcript levels of Axin2 were verified from sister plates by qRT-PCR before performing JICD-NTAP ChIP (Fig. 47f). When JICD and TBLR1 were expressed with submaximal levels of β -Catenin, Axin2 expression was potentiated in the N2A cells reconfirming the luciferase findings (Fig 44b,c). Interestingly, western blot analysis on sister plate lysates showed an upregulation of Jag1 under both JICD-NTAP, β -Catenin and JICD-NTAP, β -Catenin, TBLR1 conditions, hinting that the JICD may directly or indirectly regulate expression of the endogenous *Jag1* gene (Fig. 47g). In total, three individual ChIPs were sequenced by Illumina next generation sequencing, with samples summarized in Fig. 47i (see Fig 48 for Illumina HiSeq2000 workflow).

3.2.5 Analysis of JICD ChIP experiments

ChIP-Seq was performed at the Quantitative Genomics Facility of the University of Basel, Switzerland. Sequence alignment to the genome and model-based analysis of ChIP-Seq data (MACS) was performed by Robert Ivanek, at the bioinformatics service of the Department of Biomedicine at the University of Basel. Cross-analysis of promoter peak enrichment amongst replicate samples was carried out to compare the similarity of samples (Fig. 49). Additionally, the number of mapped and unique reads per sequencing sample was measured (Fig. 50 and 51). A high variability in the sequences from the samples replicates likely reflected the indirect binding of the JICD with chromatin and that the JICD most likely binds through an interaction partner. Peaks were compiled using a union of peaks, which combines any replicates that have 1 or more base pair (bp) overlapping. Peaks with a \log_2 value of greater than 0.6 (compared to input) were then cross-compared to other ChIP samples, and peaks unique for each treatment were compiled (experimental outline Fig. 52a and summary of peaks supplementary table 2). Genes containing enrichment in their promoters were then screened using the GO database to organize targets by function and pathway significance (Fig.

52b). qRT-PCR primers were designed for these specific gene targets to determine their relative expression levels in each treatment conditions. Finally, peak specific primers were designed and tested by ChIP-PCR on genes that exhibited a positive enrichment in JICD-NTAP/ β -Catenin/TBLR1 treatments (quantitative ChIP PCR).

3.2.6 Confirmed targets identified by the JICD ChIP

Analysis of promoter specific peaks identified enrichment for the GO categories central nervous system myelination and Wnt targets (Fig. 52b). qRT-PCR of Wnt target genes containing peaks in their promoters revealed enrichment for Axin2, Lgr5, Lef1, and Id2 in the JICD-NTAP/ β -Catenin/TBLR1 treatment. I hypothesized that potentially the affinity of DNA binding sites for JICD, shifted when co-expressed with β -Catenin and TBLR1. Therefore I designed JICD treatment peak specific primers for the promoter region of Axin2 as well as peak specific primers for a peak only found in the JICD-NTAP/ β -Catenin/TBLR1 treatment (see Fig 53 and 54a). Primers were tested and validated based on their qRT-PCR melting curves and their specificity for only one PCR product. Peak enrichment was quantified by quantitative ChIP PCR run on ChIP elutes from all four treatments and the input samples. Although the JICD treatment specific peak was not enriched for, the JICD-NTAP/ β -Catenin/TBLR1 treatment peak showed almost 5-fold enrichment over JICD treatment alone. Taken together with the Axin2 potentiation data, this would suggest that when JICD, β -Catenin, TBLR1 are expressed together, JICD can bind to the promoter region of Axin2, and directly upregulate its expression. Similarly, using peak specific primers for the JICD-NTAP/ β -Catenin/TBLR1 treatment, peaks in the promoters of Lgr5, Lef1 and Id2 were all confirmed (Fig. 54b-d). This is clear evidence that together with β -Catenin and TBLR1, JICD can be enriched at the promoter sequences of Wnt target genes, resulting in their direct regulation.

3.2.7 Figures

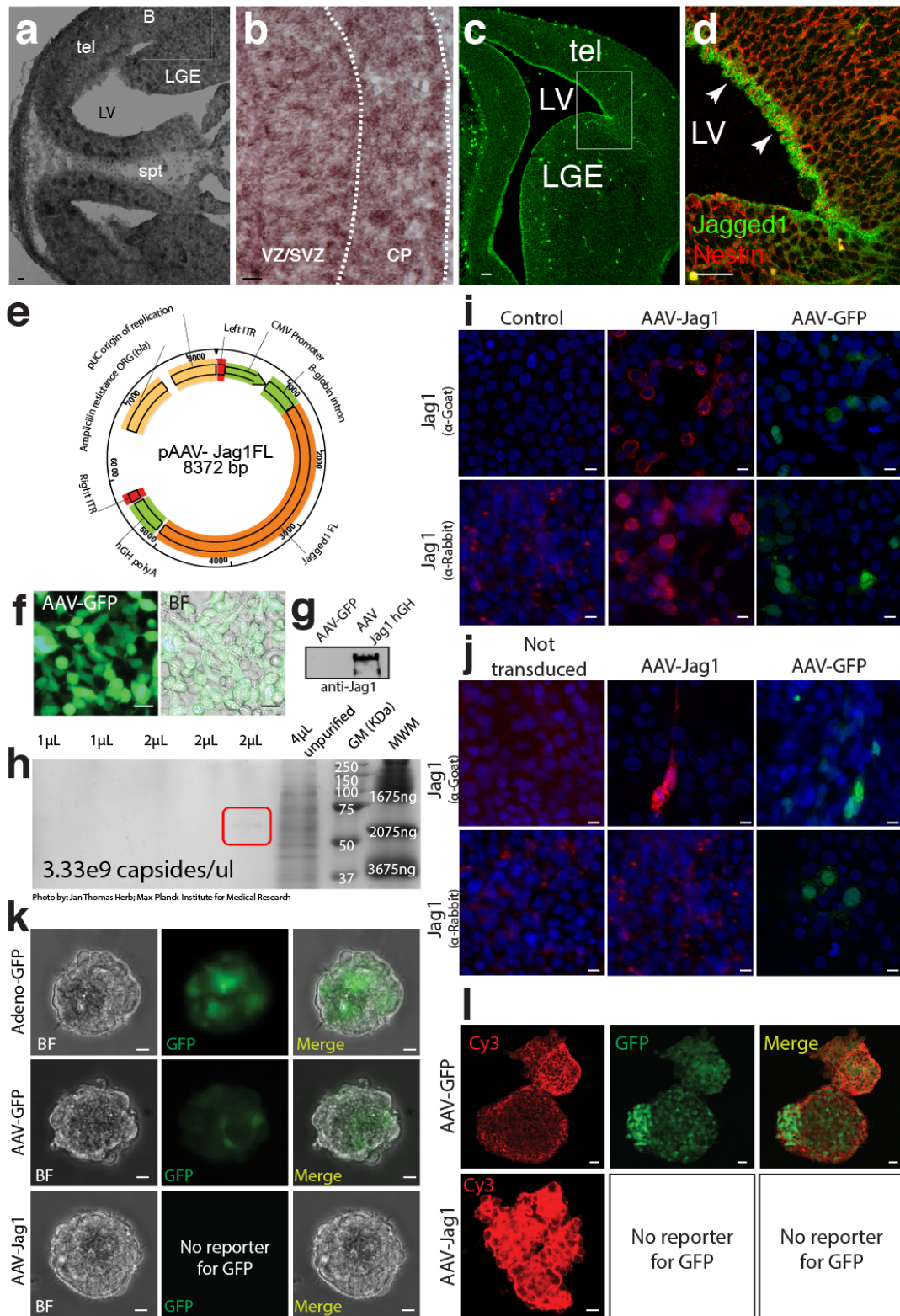


Figure 20

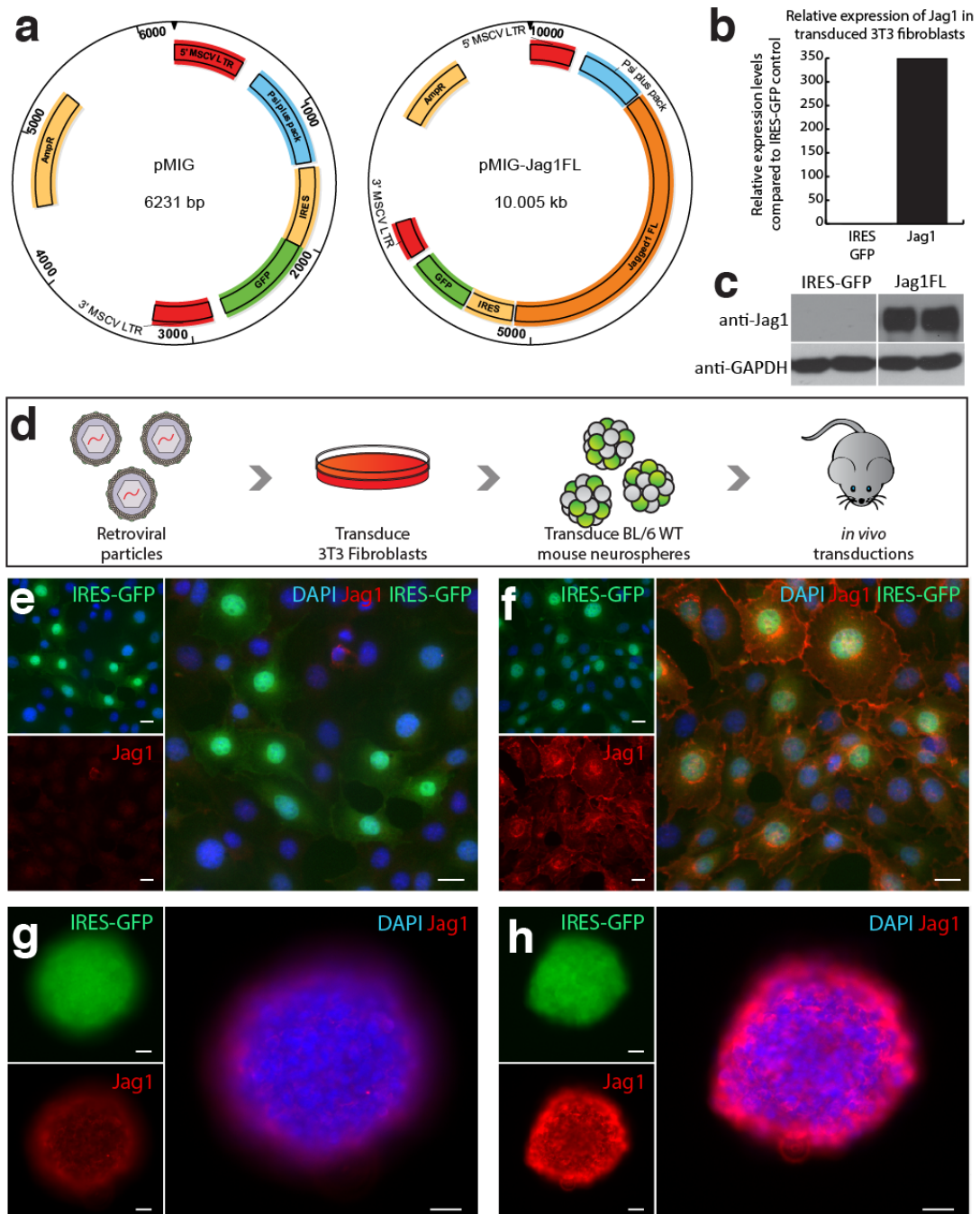


Figure 21

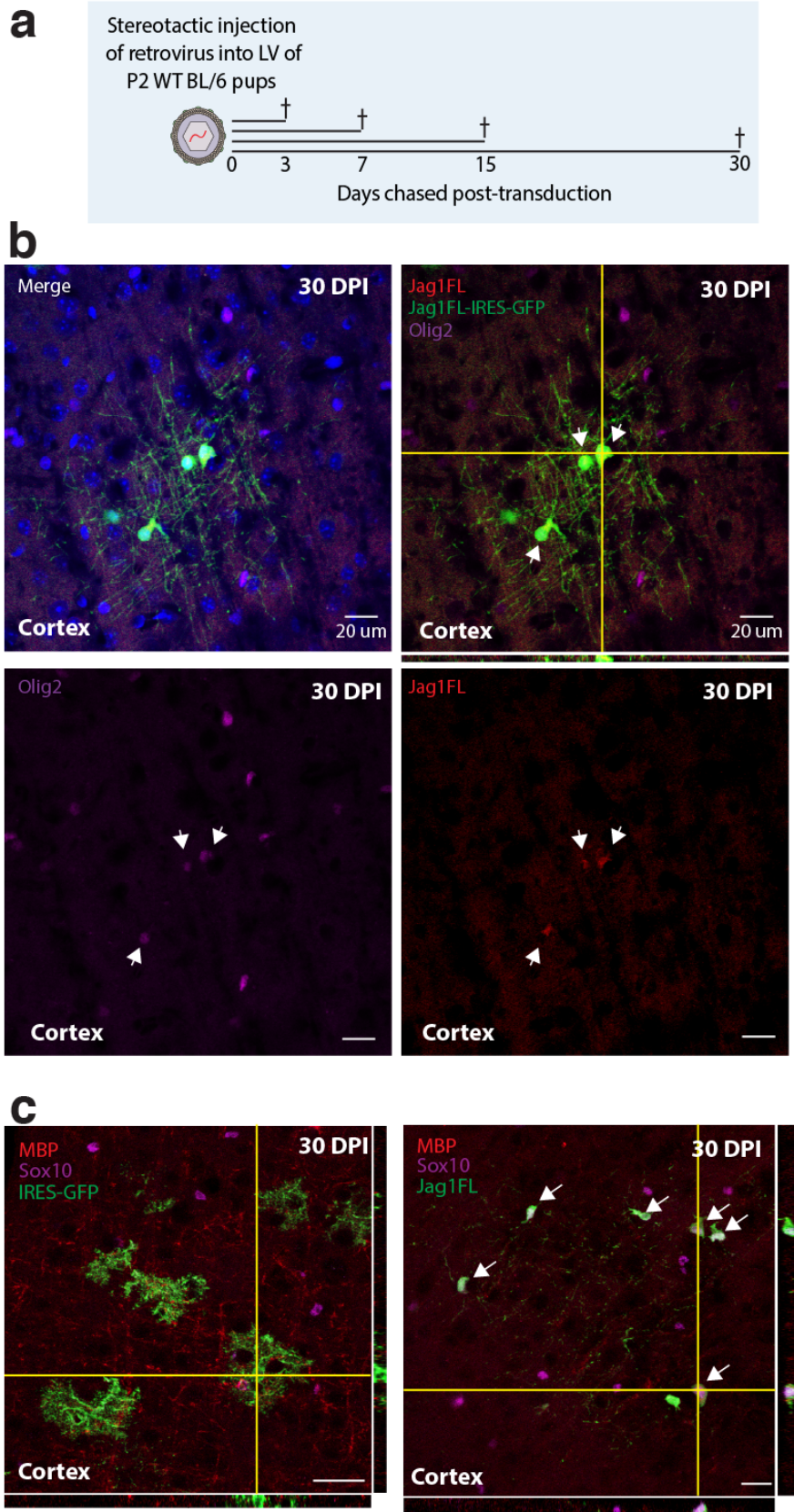
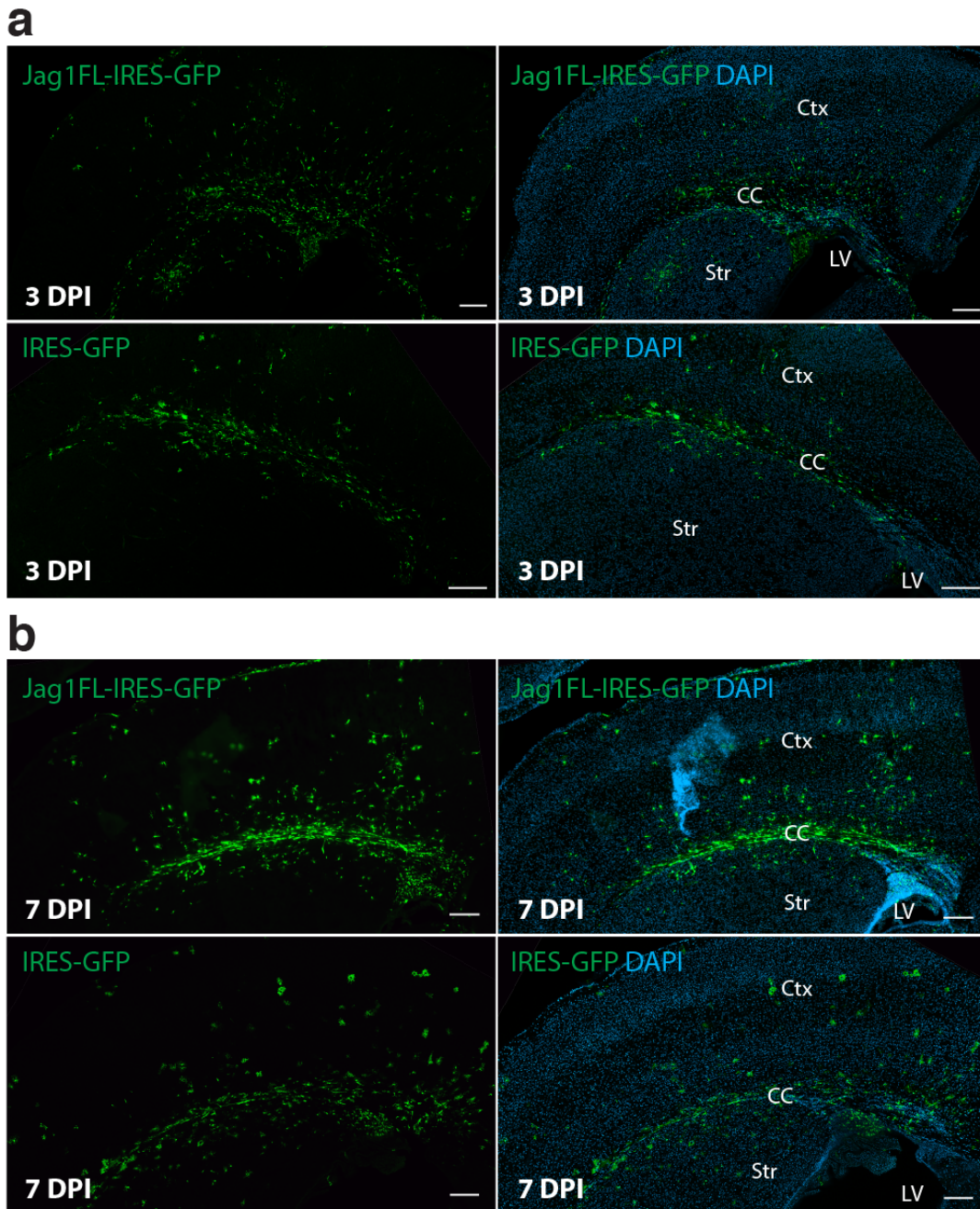


Figure 22



c Average distance Jag1FL transduced cells migrate into the cortex 7 and 15 days post infection

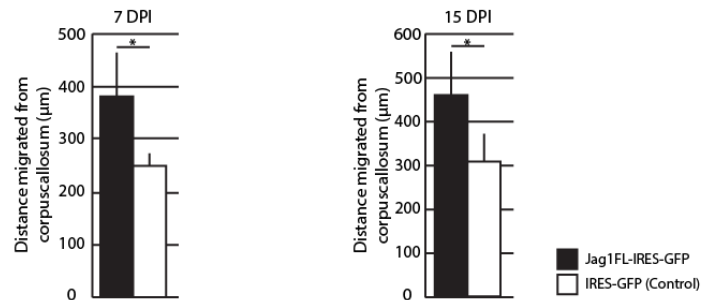


Figure 23

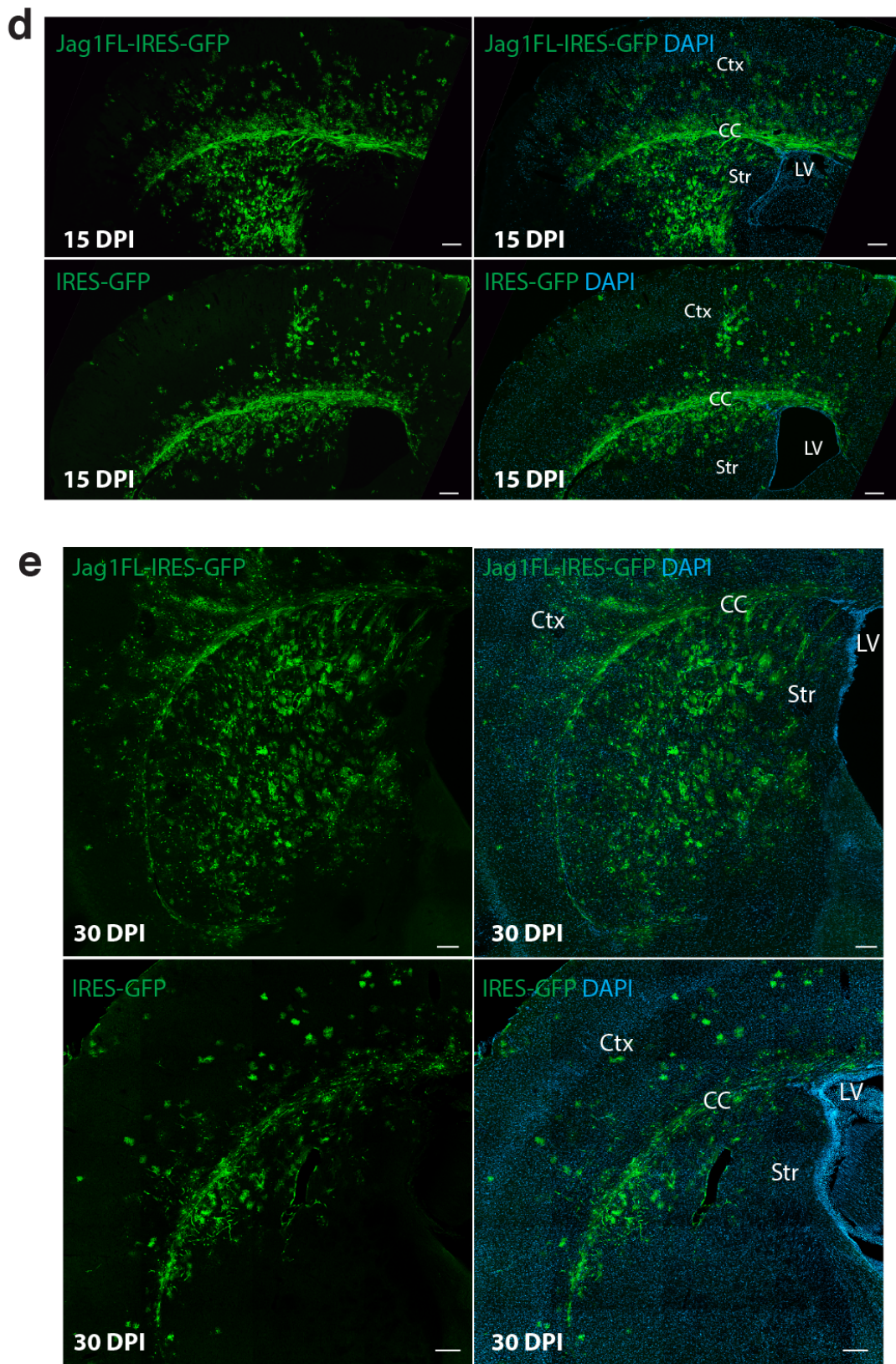


Figure 23 Continued

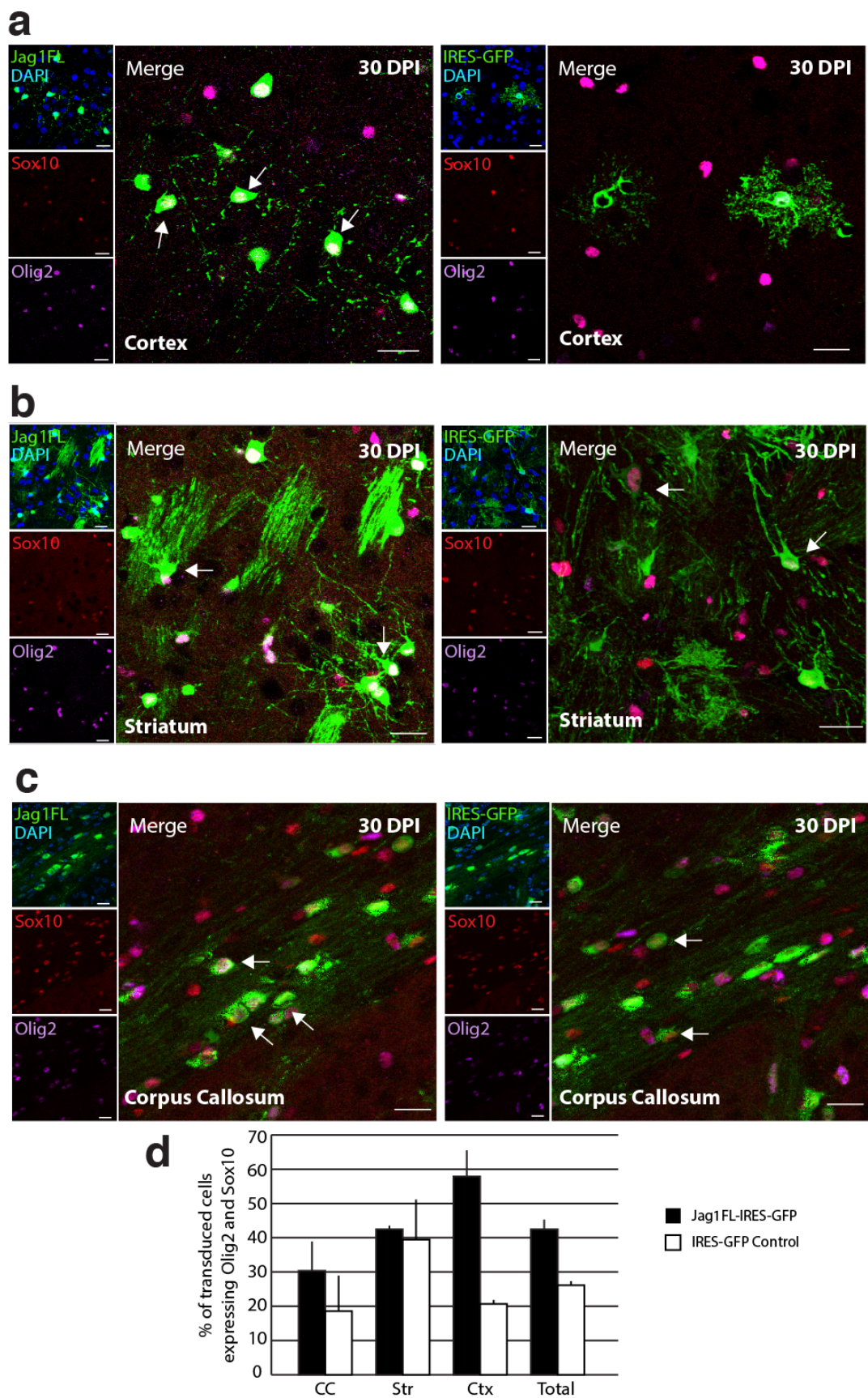


Figure 24

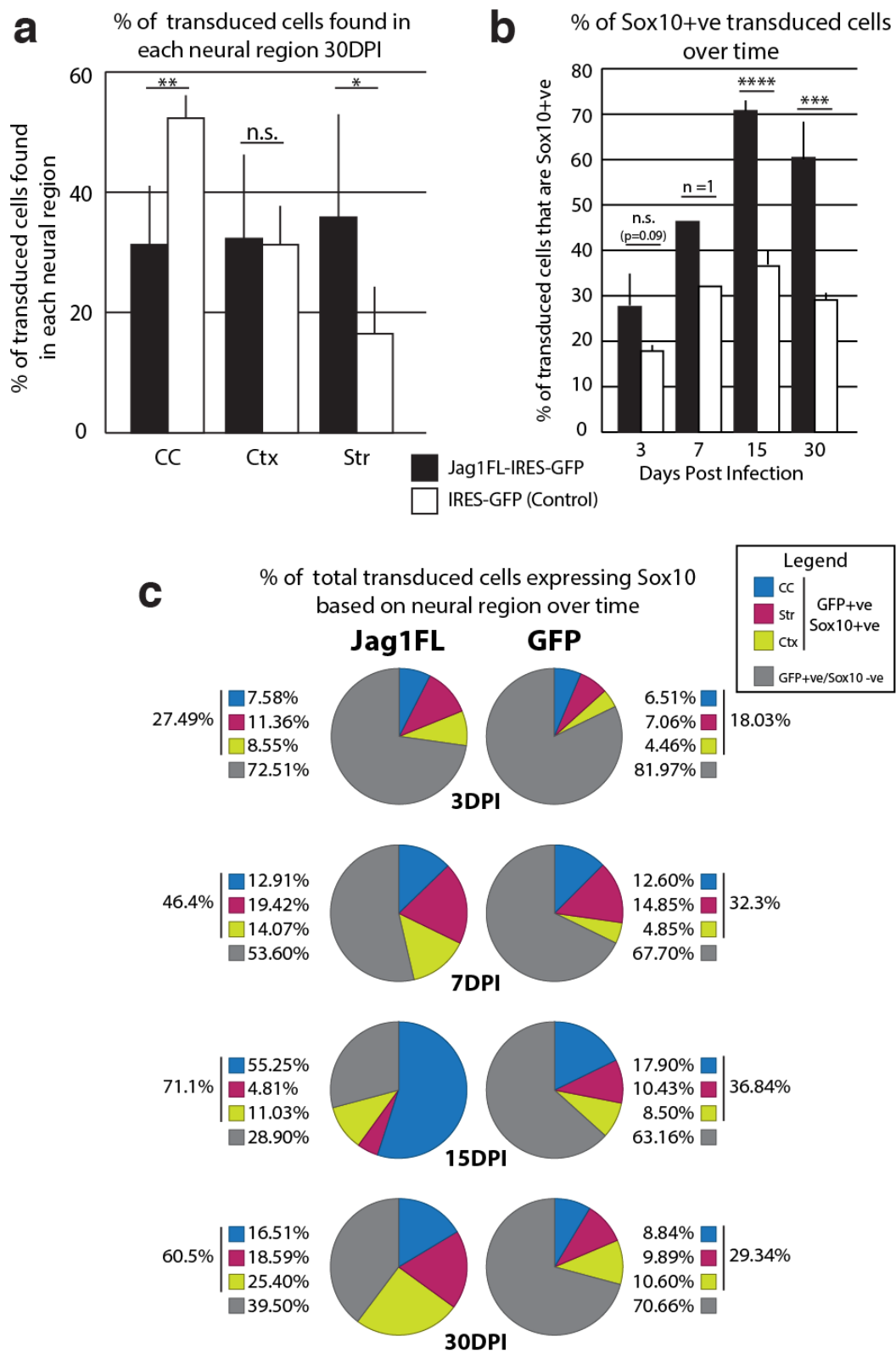


Figure 25

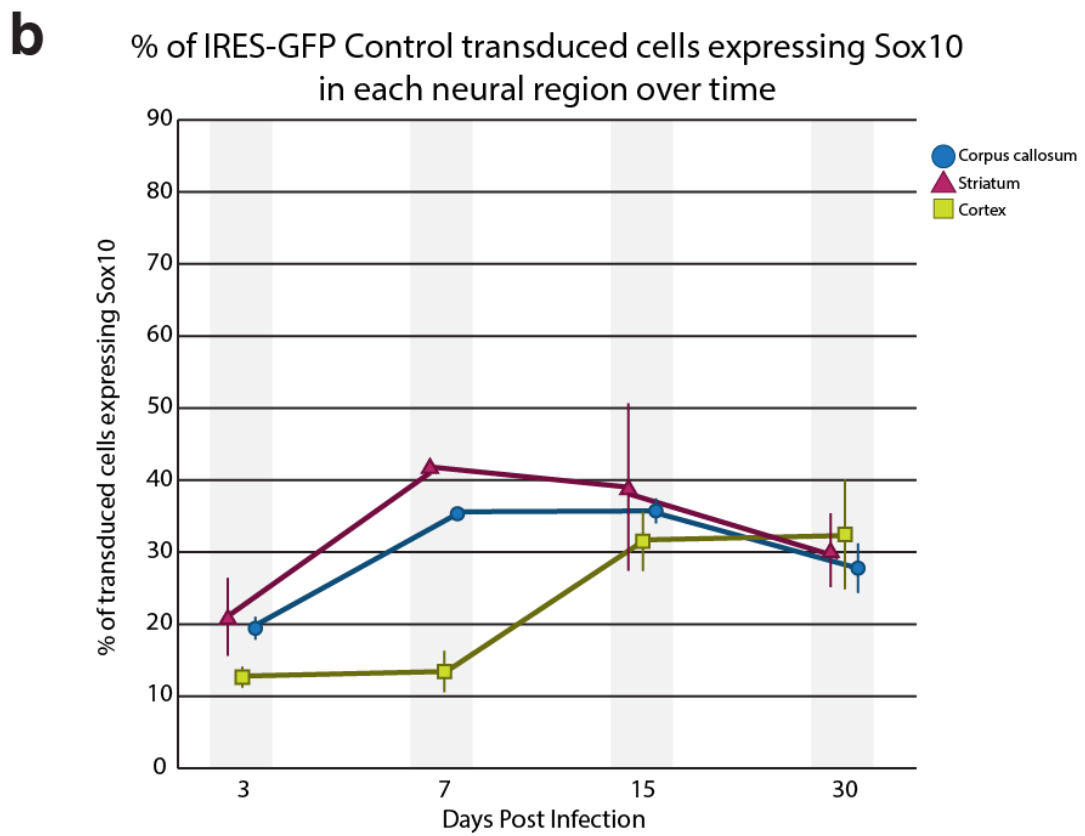
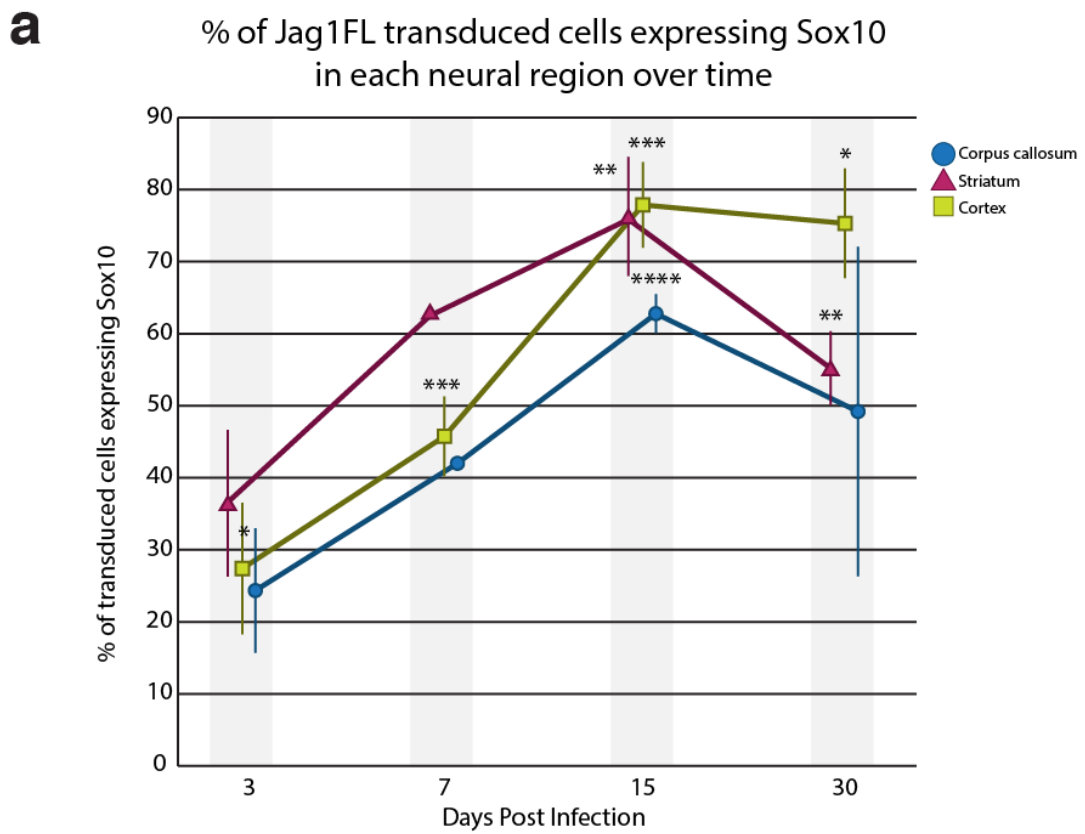


Figure 26

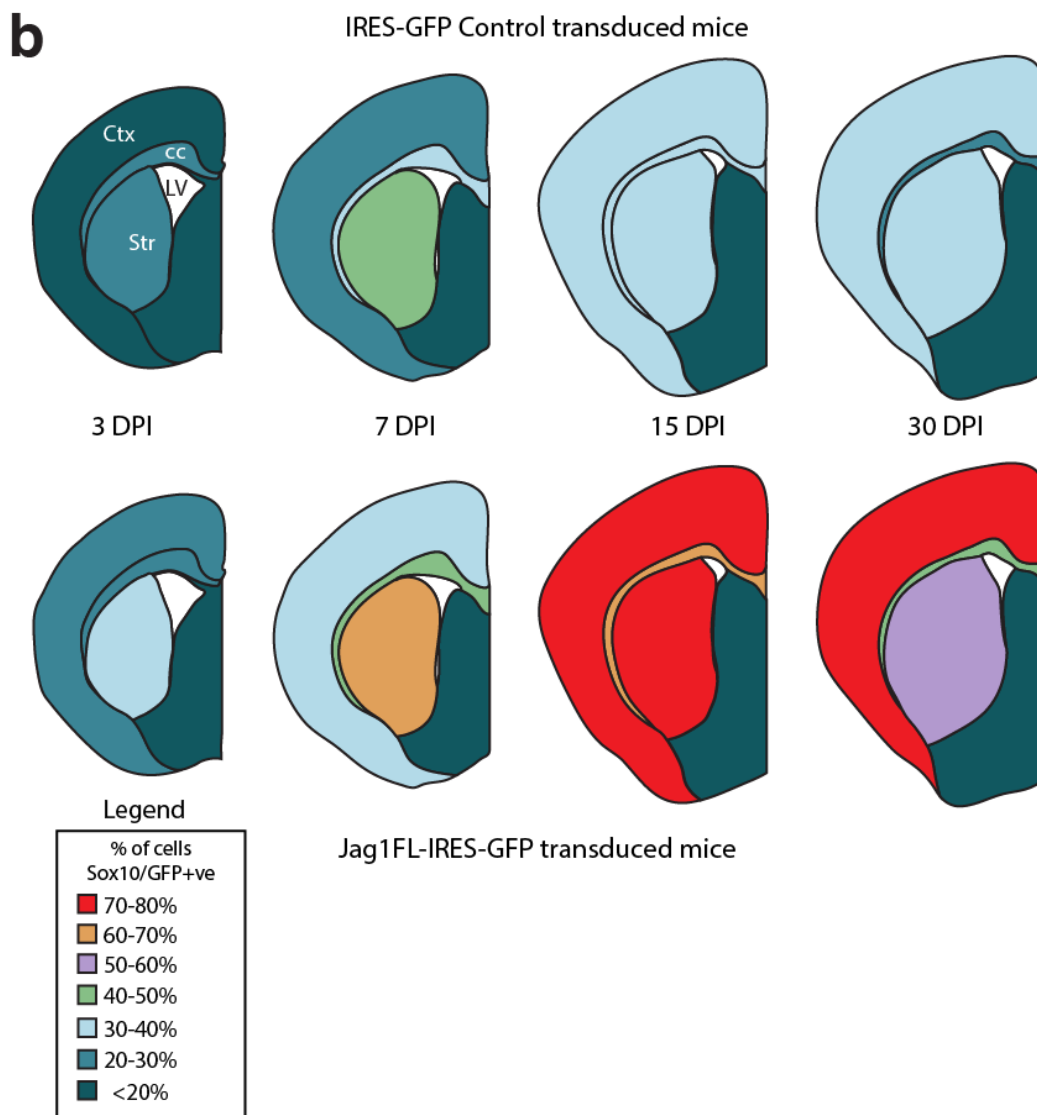
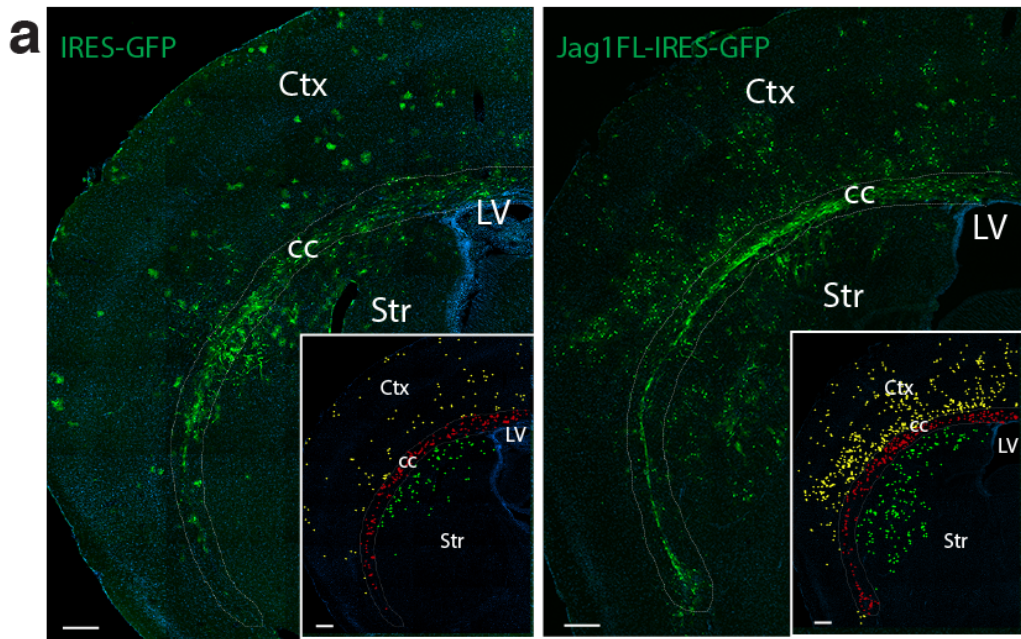


Figure 27

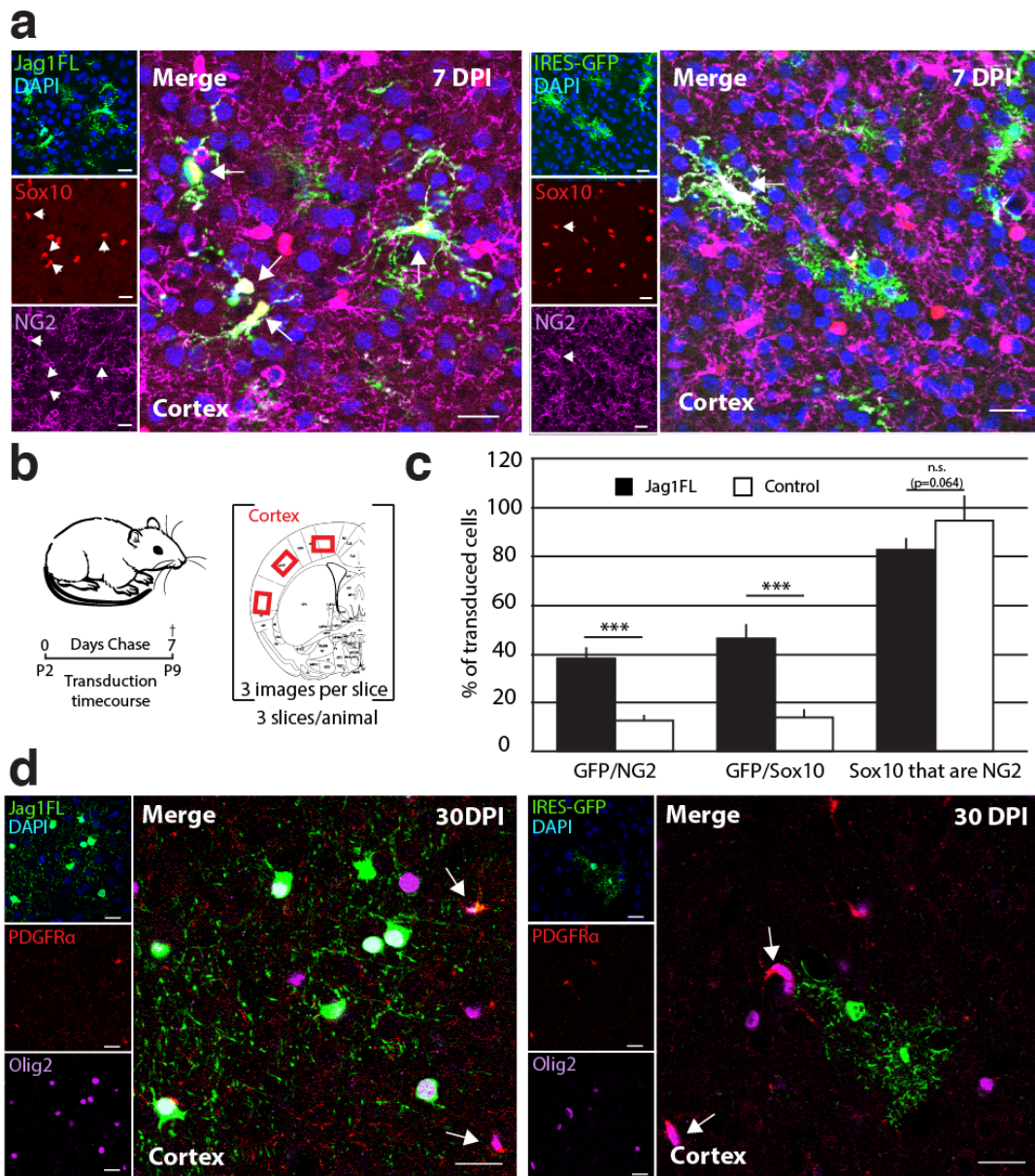


Figure 28

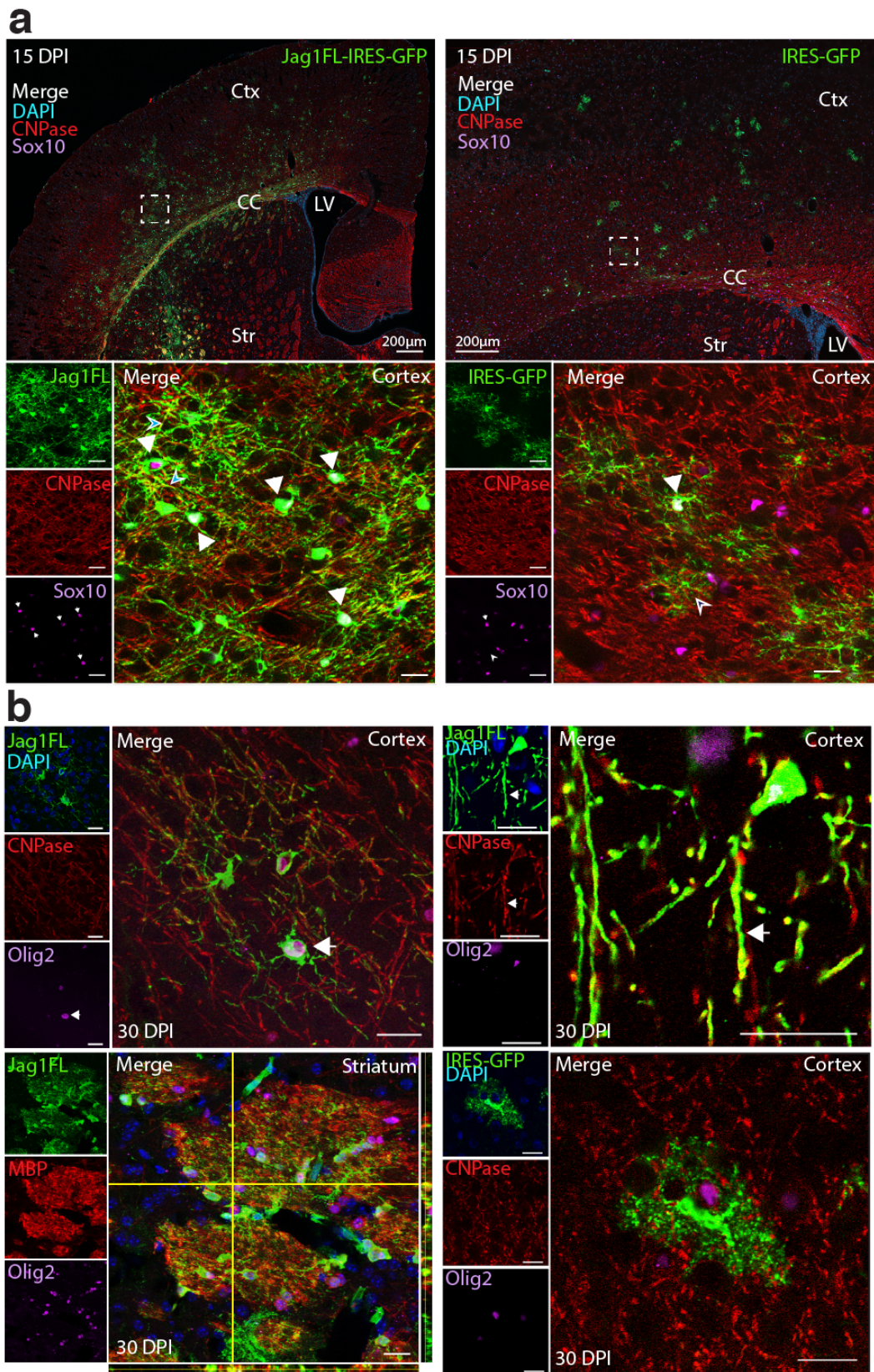


Figure 29

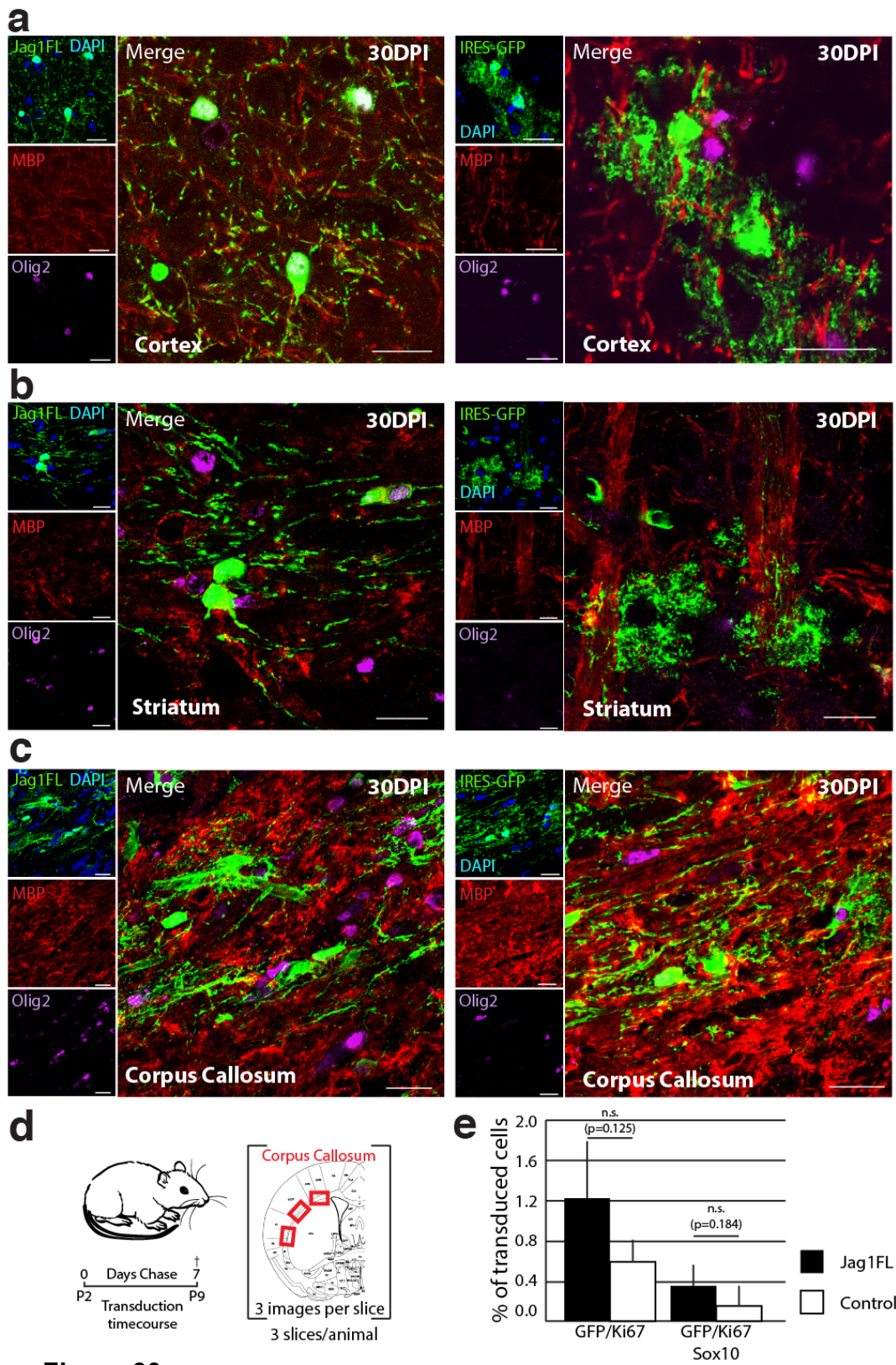
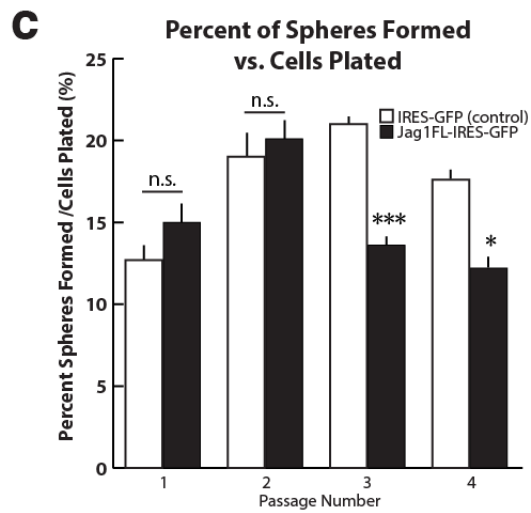
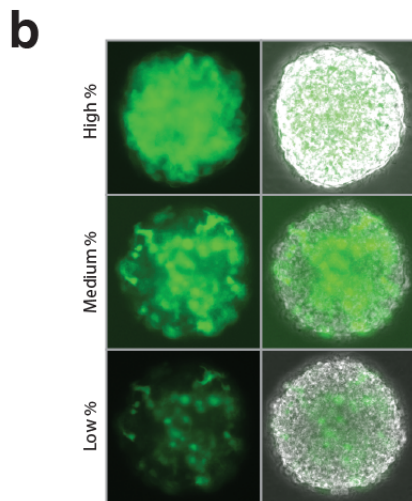
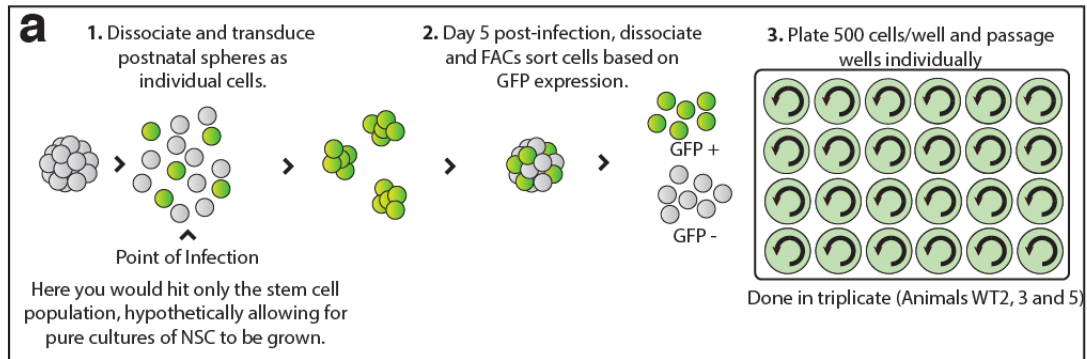


Figure 30



d

Jag1FL transduced neurosphere proliferation assay

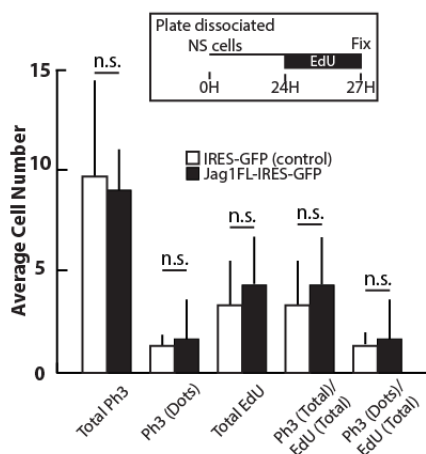


Figure 31

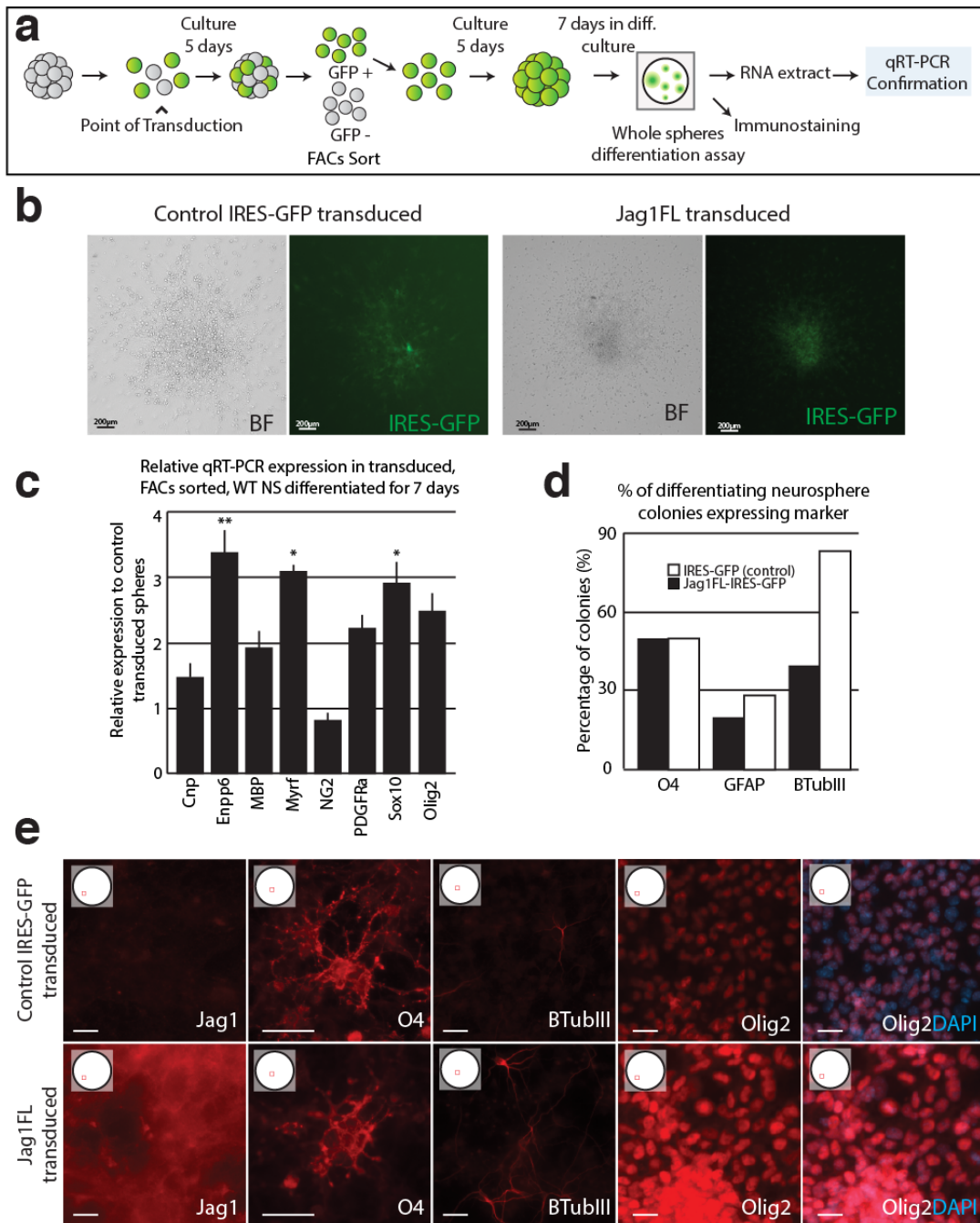
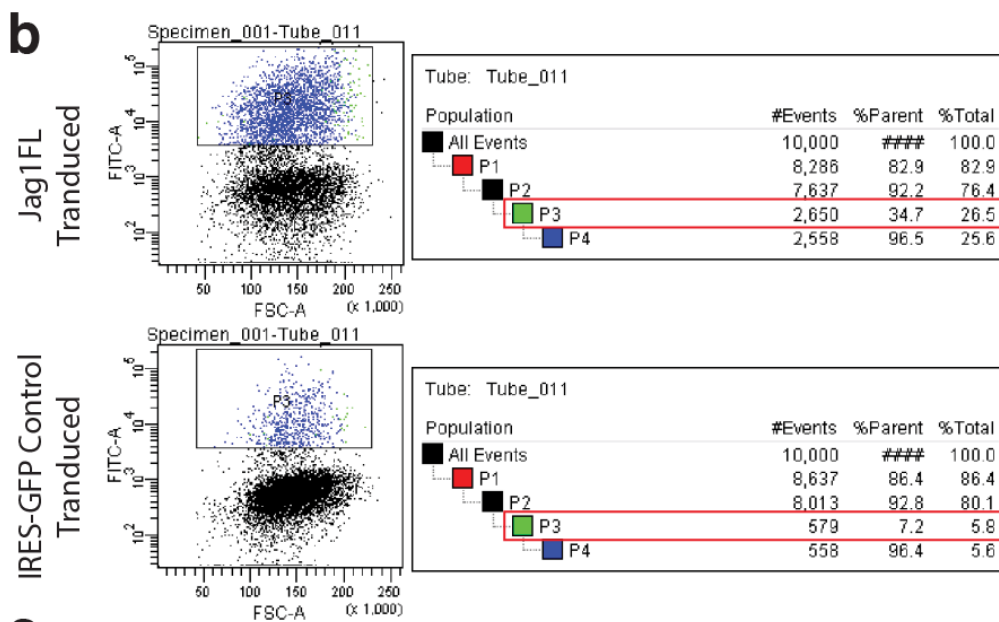
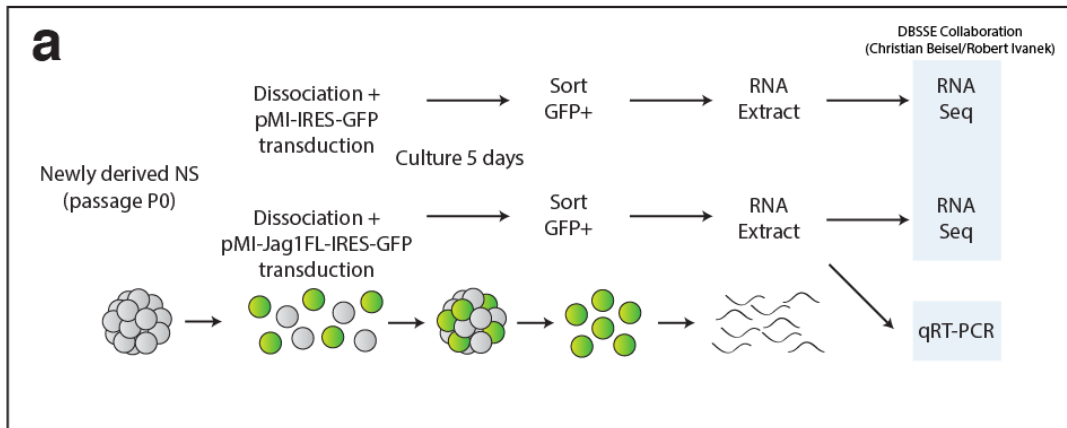


Figure 32

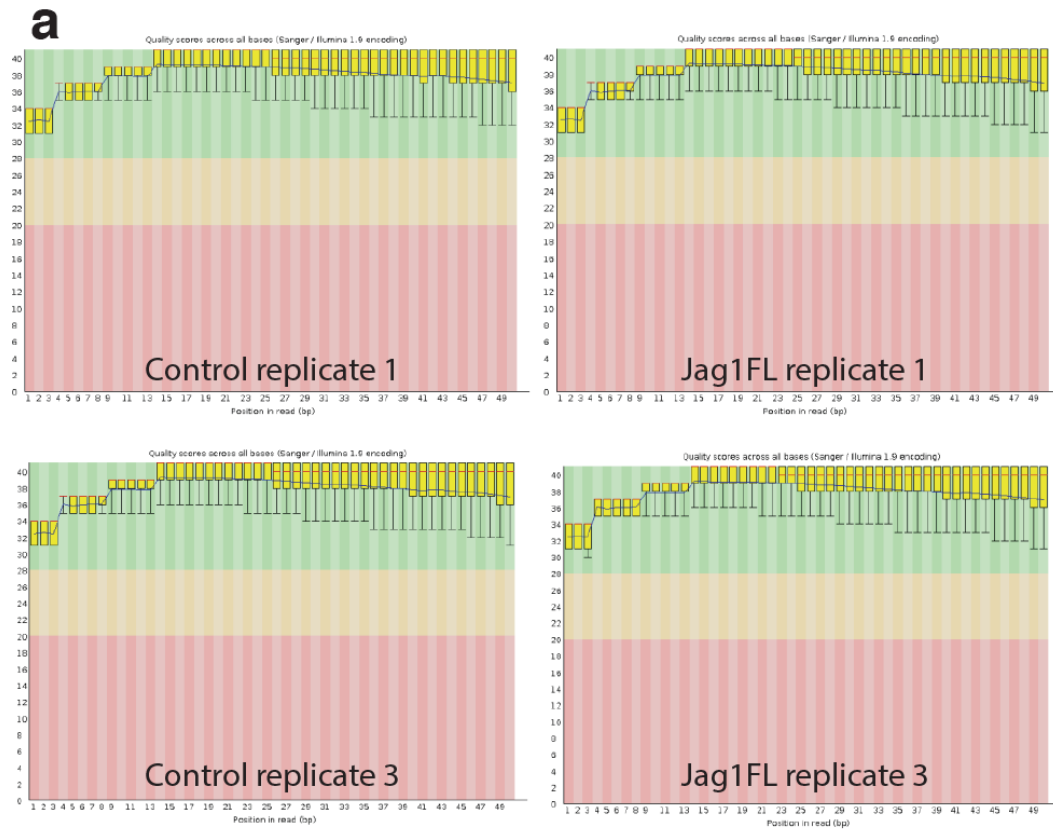


c

| Sample ID | Cells Sorted* | Conc. | unit | A260 | A280 | 260/280 | 260/230 |
|-----------|---------------|-------|-------|--------|-------|---------|---------|
| Jag1-Rep1 | 450 | 238.1 | ng/uL | 5.951 | 3.307 | 1.8 | 1.11 |
| Jag1-Rep2 | 650 | 402.2 | ng/uL | 10.056 | 4.96 | 2.03 | 0.85 |
| Jag1-Rep3 | 500 | 280.5 | ng/uL | 7.012 | 3.662 | 1.91 | 0.93 |
| Jag1-Rep4 | 490 | 217.1 | ng/uL | 5.429 | 2.928 | 1.85 | 1.48 |
| GFP-Rep1 | 90 | 163.7 | ng/uL | 4.092 | 2.303 | 1.78 | 1.83 |
| GFP-Rep2 | 190 | 176 | ng/uL | 4.401 | 2.443 | 1.8 | 1.09 |
| GFP-Rep3 | 125 | 132 | ng/uL | 3.301 | 1.906 | 1.73 | 1.32 |
| GFP-Rep4 | 100 | 92 | ng/uL | 2.292 | 1.381 | 1.66 | 1.53 |

*GFP positive cells (1000's)

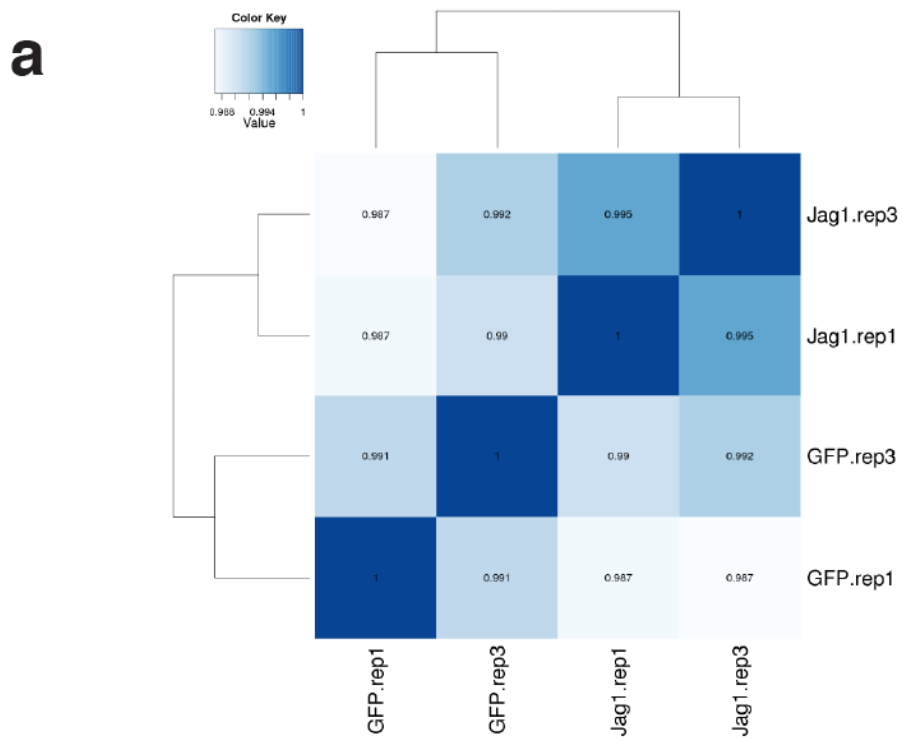
Figure 33



b

| Sample name | Identifier | Total reads (Mio.) | Unique reads (% of total) | Passed filters (% of total) | Aligned (% of passed) | Single hit (% of passed) |
|-------------|----------------------------|--------------------|---------------------------|-----------------------------|-----------------------|--------------------------|
| GFP.rep1 | DBM_VT_Mm_RNAseq_GFP_rep1 | 32.1 | 17.4 (54.2) | 32.1 (99.9) | 27.4 (85.4) | 23.0 (71.6) |
| GFP.rep3 | DBM_VT_Mm_RNAseq_GFP_rep3 | 37.2 | 19.8 (53.2) | 37.1 (99.9) | 31.8 (85.6) | 26.3 (70.9) |
| Jag1.rep1 | DBM_VT_Mm_RNAseq_Jag1.rep1 | 54.0 | 27.4 (50.7) | 54.0 (99.9) | 46.1 (85.4) | 38.8 (71.8) |
| Jag1.rep3 | DBM_VT_Mm_RNAseq_Jag1.rep3 | 59.6 | 29.9 (50.2) | 59.5 (99.9) | 50.8 (85.4) | 42.8 (71.9) |

Figure 34



b

RNASeq: Jag1 vs. GFP
13469 Genes After Filtering For Low Expression

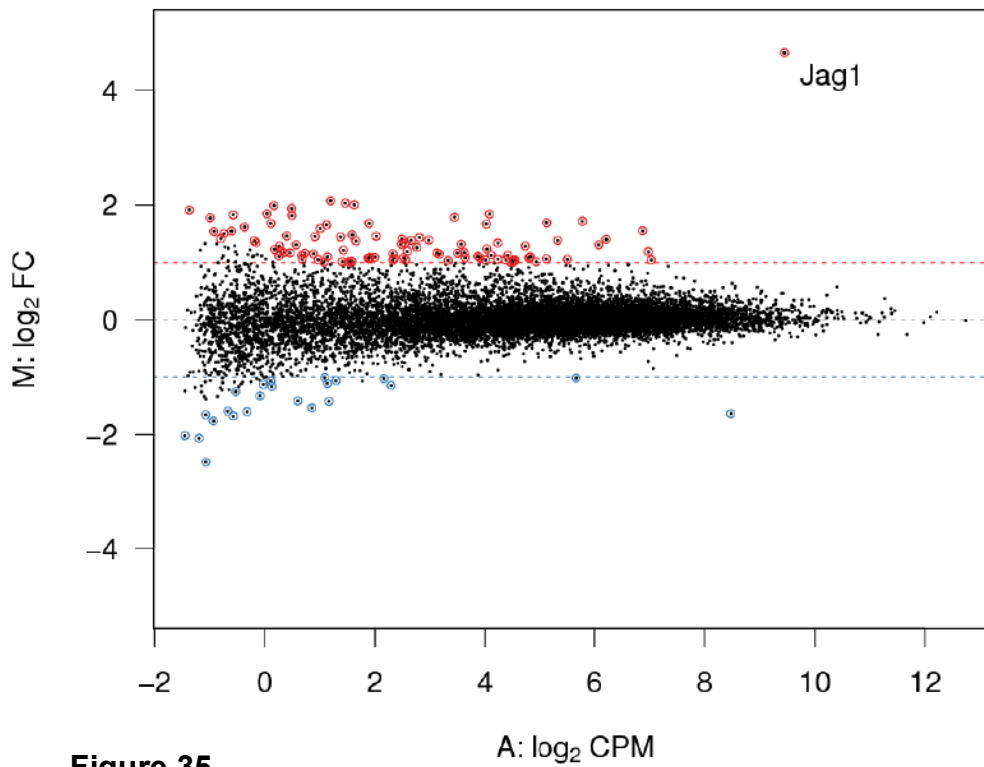


Figure 35

a

Top 10 upregulated GO categories

| GO Accession | Functional name | Genes | Category size | Overlap | Odds Ratio | P-Value |
|--------------|---|-------------------------------|---------------|---------|------------|----------|
| GO:0001840 | Neural plate development* | Htt, Ptch1, Zfp568 | 10 | 3 | 17.20 | 1.54E-03 |
| GO:0060438 | Trachea development | BMP4, Lrp6, Edaradd | 10 | 3 | 17.20 | 1.54E-03 |
| GO:0003209 | Cardiac atrium morphogenesis | Lrp6, Prox1, Sox4 | 11 | 3 | 15.10 | 2.08E-03 |
| GO:0022010 | Central nervous system myelination* | Plp1, Myrf, Fa2h | 11 | 3 | 15.10 | 2.08E-03 |
| GO:0032291 | Axon ensheathment in central nervous system* | Plp1, Myrf, Fa2h | 11 | 3 | 15.10 | 2.08E-03 |
| GO:0061298 | Retina vasculature development in camera-type eye | Acvr2b, Bmpr2, PDGFRa | 11 | 3 | 15.10 | 2.08E-03 |
| GO:0001964 | Startle response | Pcdh15, Ctnna2, Grin1, Grin3a | 16 | 4 | 13.40 | 5.11E-04 |
| GO:0003230 | Cardiac atrium development | Lrp6, Prox1, Sox4 | 13 | 3 | 12.00 | 3.48E-03 |
| GO:0048339 | Paraxial mesoderm development | Dll3, Htt, Tead1 | 13 | 3 | 12.00 | 3.48E-03 |
| GO:0060412 | Ventricular septum morphogenesis | Lrp5, Prox1, Sox4, Rbm15 | 18 | 4 | 11.50 | 8.26E-04 |

Other interesting upregulated GO categories

| GO Accession | Functional name | Genes | Category size | Overlap | Odds Ratio | P-Value |
|--------------|----------------------------------|---|---------------|---------|------------|----------|
| GO:0014003 | Oligodendrocyte development* | Plp1, Myrf, Fa2h, Zfp488 | 23 | 4 | 8.47 | 2.17E-03 |
| GO:0048709 | Oligodendrocyte differentiation* | Plp1, Myrf, Fa2h, Zfp488, BMP4, Sox5, Sox10 | 48 | 7 | 6.93 | 1.55E-04 |

*Category may correlate with *in vivo* phenotype.

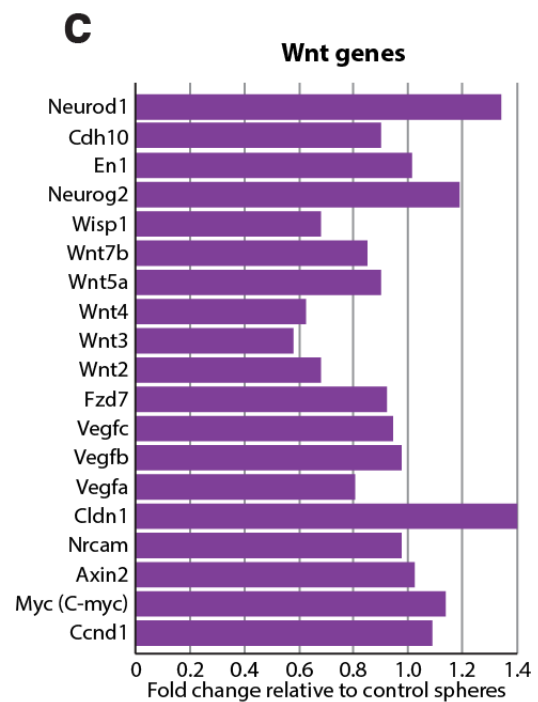
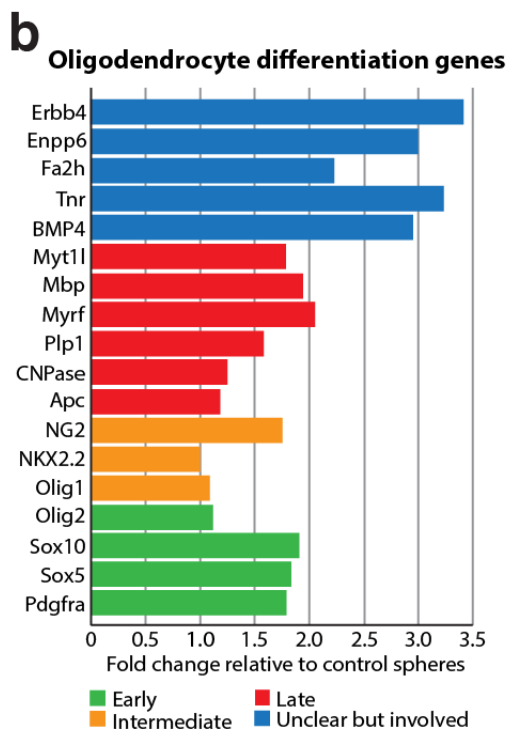
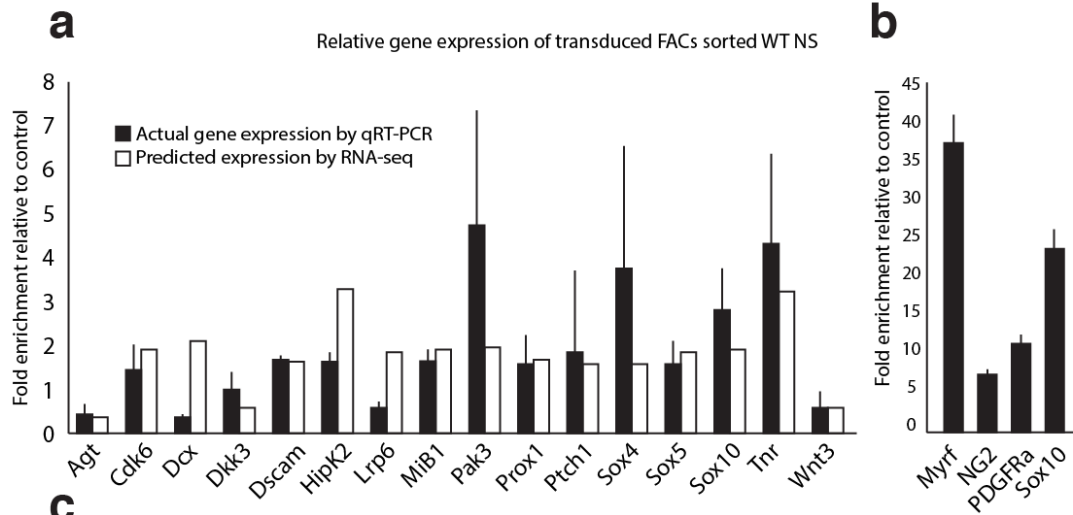


Figure 36



c

| Top 15 | | | | | RNAseq | qRT-PCR | Known role |
|-------------|--|-------|----------|----------|-------------|-------------|--|
| Gene Symbol | Gene Name | logFC | PValue | FDR | Fold change | Fold change | |
| Jag1 | jagged 1 | 4.65 | 0.00E+00 | 0.00E+00 | 25.13 | 62.18 | Ligand for multiple Notch receptors and involved in the mediation of Notch signaling. (UniProtKB) |
| Rnf213 | ring finger protein 213 | 2.07 | 2.91E-08 | 3.53E-06 | 4.21 | - | Probable E3 ubiquitin-protein ligase that may play a role in angiogenesis. May also have an ATPase activity (UniProtKB) |
| Sacs | sacsin | 2.04 | 1.59E-09 | 2.74E-07 | 4.10 | - | Co-chaperone which acts as a regulator of the Hsp70 chaperone machinery and may be involved in the processing of other ataxia-linked proteins. (UniProtKB) |
| Cntnap5b | contactin associated protein-like 5B | 1.99 | 6.71E-07 | 5.33E-05 | 3.97 | - | May play a role in the correct development and proper functioning of the peripheral and central nervous system and be involved in cell adhesion and intercellular communication (UniProtKB) |
| Syt14 | synaptotagmin XIV | 1.84 | 5.06E-06 | 2.85E-04 | 3.59 | - | May be involved in the trafficking and exocytosis of secretory vesicles in non-neuronal tissues. Is Ca(2+)-independent (UniProtKB) |
| Igsf9b | immunoglobulin superfamily, member 9B | 1.84 | 1.26E-28 | 4.25E-25 | 3.58 | - | Functions in dendrite outgrowth and synapse maturation. Paralog of Igsf9 (UniProtKB/GeneCards) |
| Tmem90a | transmembrane protein 90a | 1.83 | 8.37E-05 | 2.86E-03 | 3.55 | - | Multi-pass membrane protein (Potential). Golgi apparatus, cis-Golgi network (UniProtKB). |
| Pabpc5 | poly(A) binding protein, cytoplasmic 5 | 1.82 | 5.07E-07 | 4.13E-05 | 3.52 | - | Binds the poly(A) tail of mRNA. May be involved in cytoplasmic regulatory processes of mRNA metabolism.(UniProtKB) |
| ErbB4* | v-erb-a erythroblastic leukemia viral oncogene homolog 4 (avian) | 1.78 | 3.96E-16 | 2.97E-13 | 3.45 | - | Acts as cell-surface receptor for the neuregulins NRG1, NRG2, NRG3 and NRG4 and the EGF family members (UniProtKB) |
| Hipk2* | homeodomain interacting protein kinase 2 | 1.72 | 8.31E-45 | 3.73E-41 | 3.29 | 1.63 | Negative regulator through phosphorylation and subsequent proteasomal degradation of CTNNB1 and the antiapoptotic factor CTBP1. In the Wnt/beta-catenin signaling pathway acts as an intermediate kinase between MAP3K7/TAK1 and NLK to promote the proteasomal degradation of MYB. (UniProtKB). HIPK2 phosphorylate TCF/LEF factors to inhibit their interaction with DNA (Gao et al 2014, Cell & bioscience) |
| Tnr* | tenascin R | 1.69 | 1.91E-26 | 5.16E-23 | 3.23 | 4.31 | Neural extracellular matrix (ECM) protein involved in interactions with different cells and matrix components. (UniProtKB) |
| Enpp6* | ectonucleotide pyrophosphatase/phosphodiesterase 6 | 1.59 | 9.97E-05 | 3.28E-03 | 3.02 | - | Choline-specific glycerophosphodiester phosphodiesterase. (UniProtKB) |
| Gpr17* | G protein-coupled receptor 17 | 1.55 | 8.43E-13 | 3.44E-10 | 2.93 | - | GPR17 expression peaks at intermediate phases of oligodendrocyte differentiation and is thereafter downregulated to allow terminal maturation. GPR17 activation stimulates OPC migration. Pugliese et al 2013 (Glia) |
| Bmp4 | bone morphogenetic protein 4 | 1.55 | 8.63E-04 | 1.67E-02 | 2.92 | 9.25 | Negative regulator of oligodendrocyte maturation. |

* Gene may correlate with *in vivo* phenotype

Figure 37

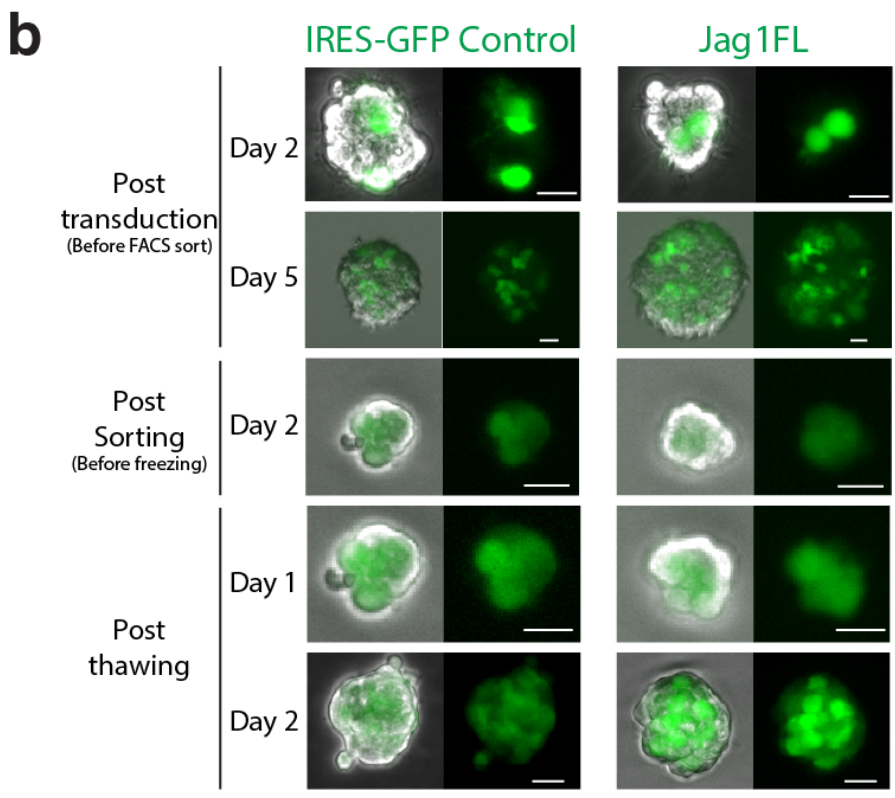
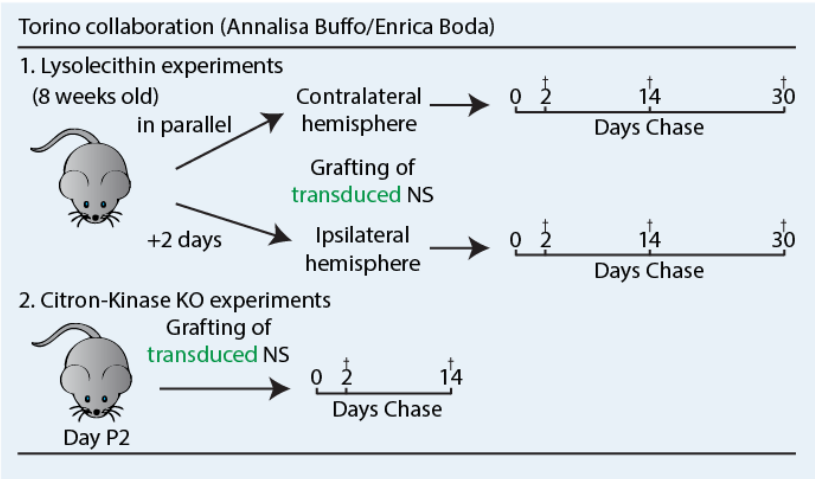
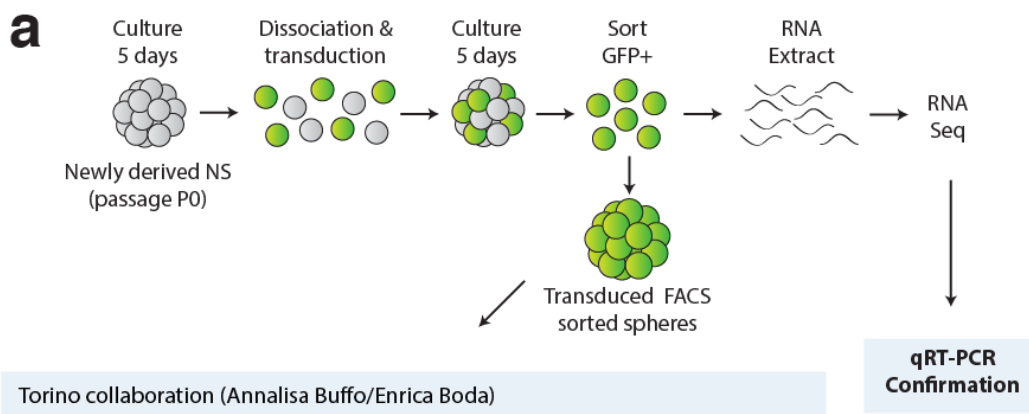


Figure 38

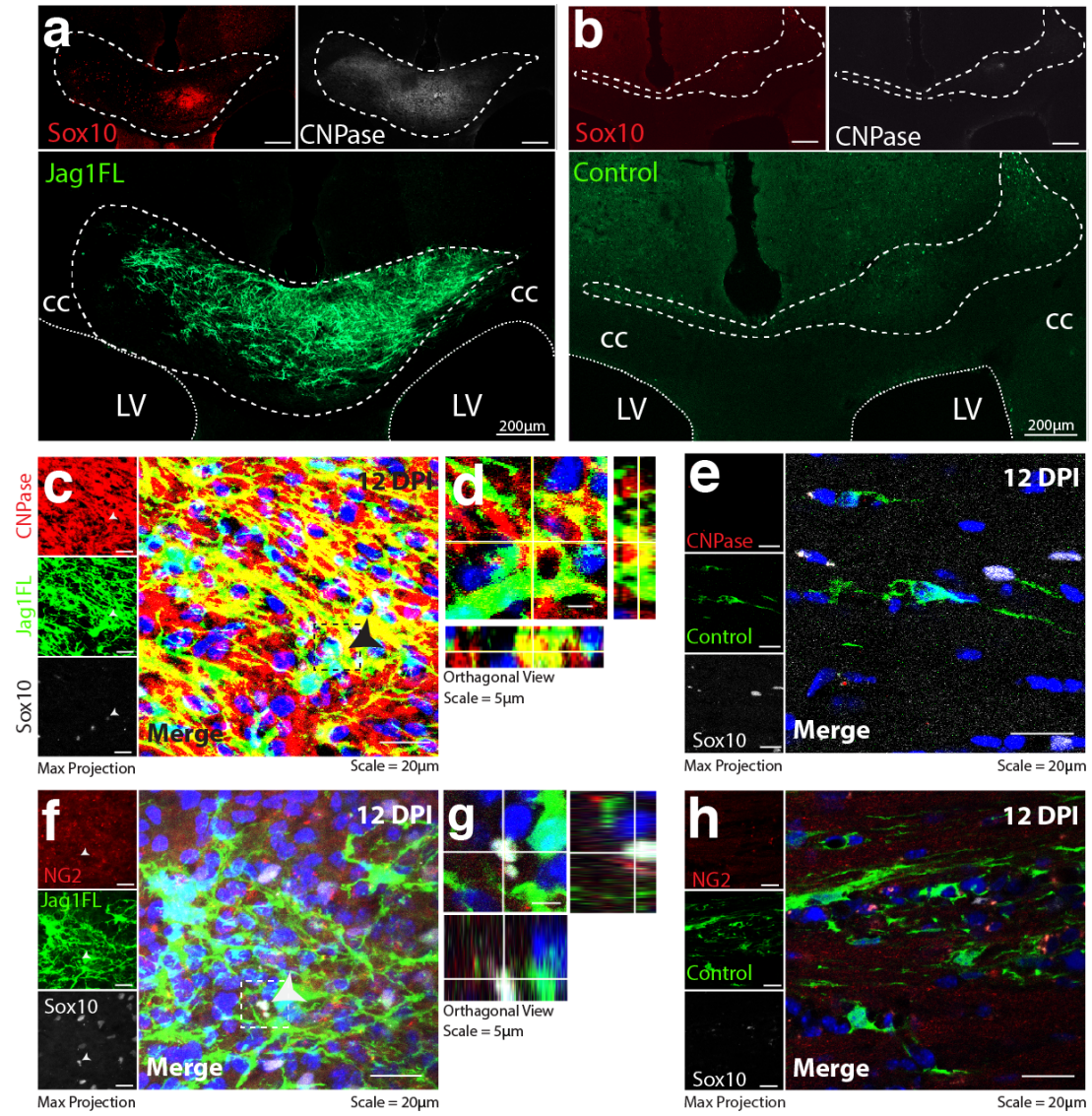


Figure 39

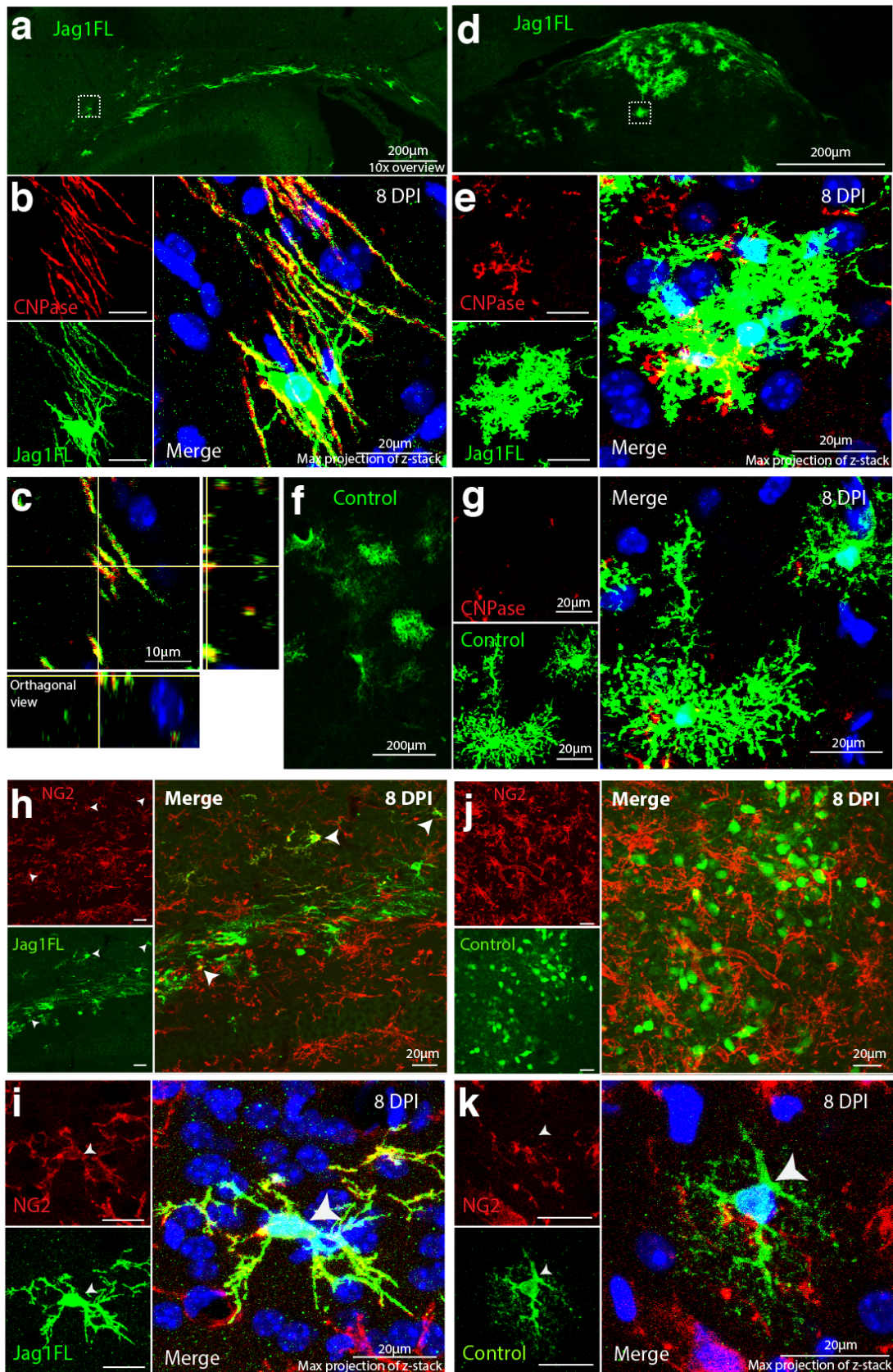


Figure 40

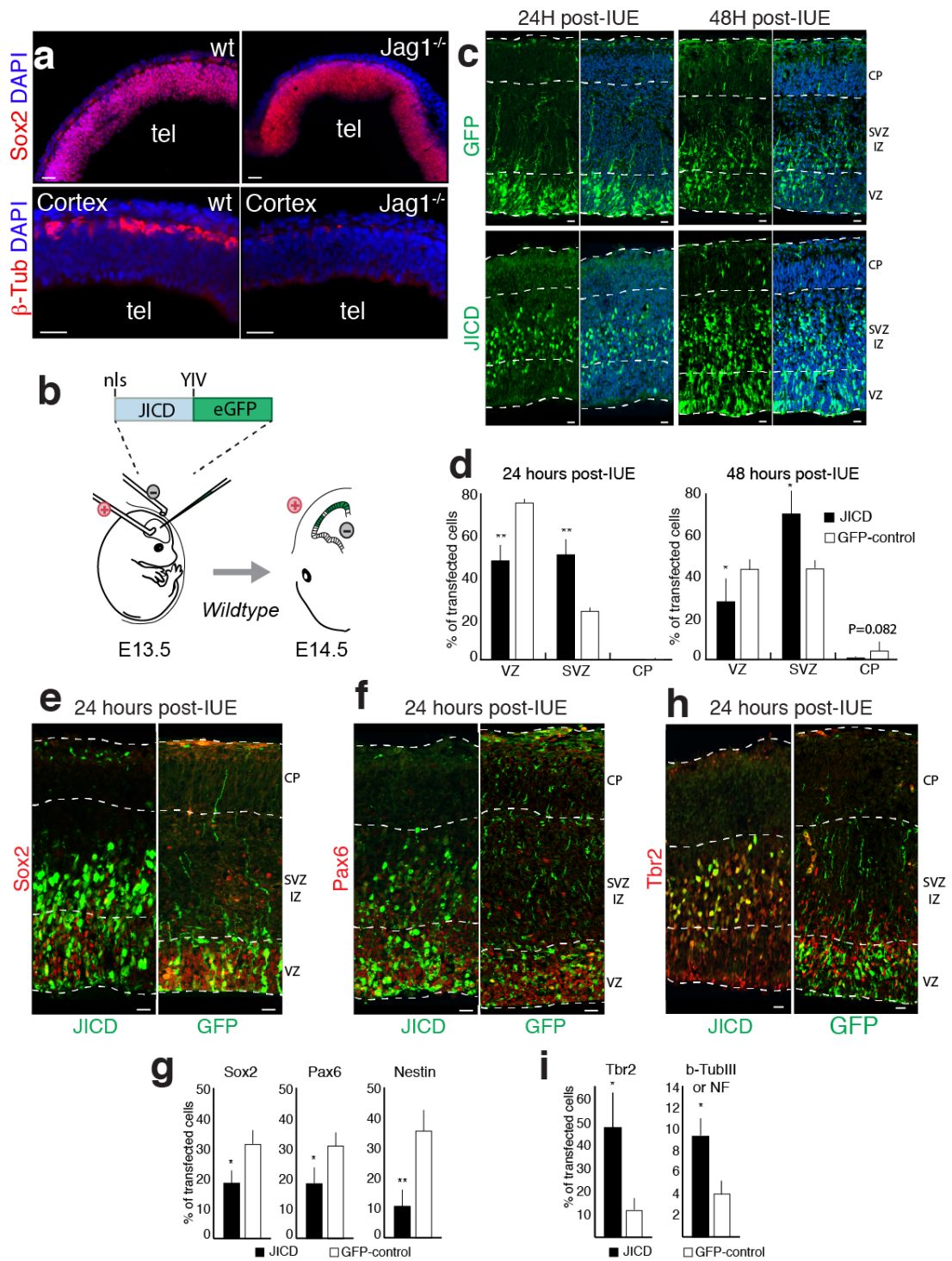


Figure 41

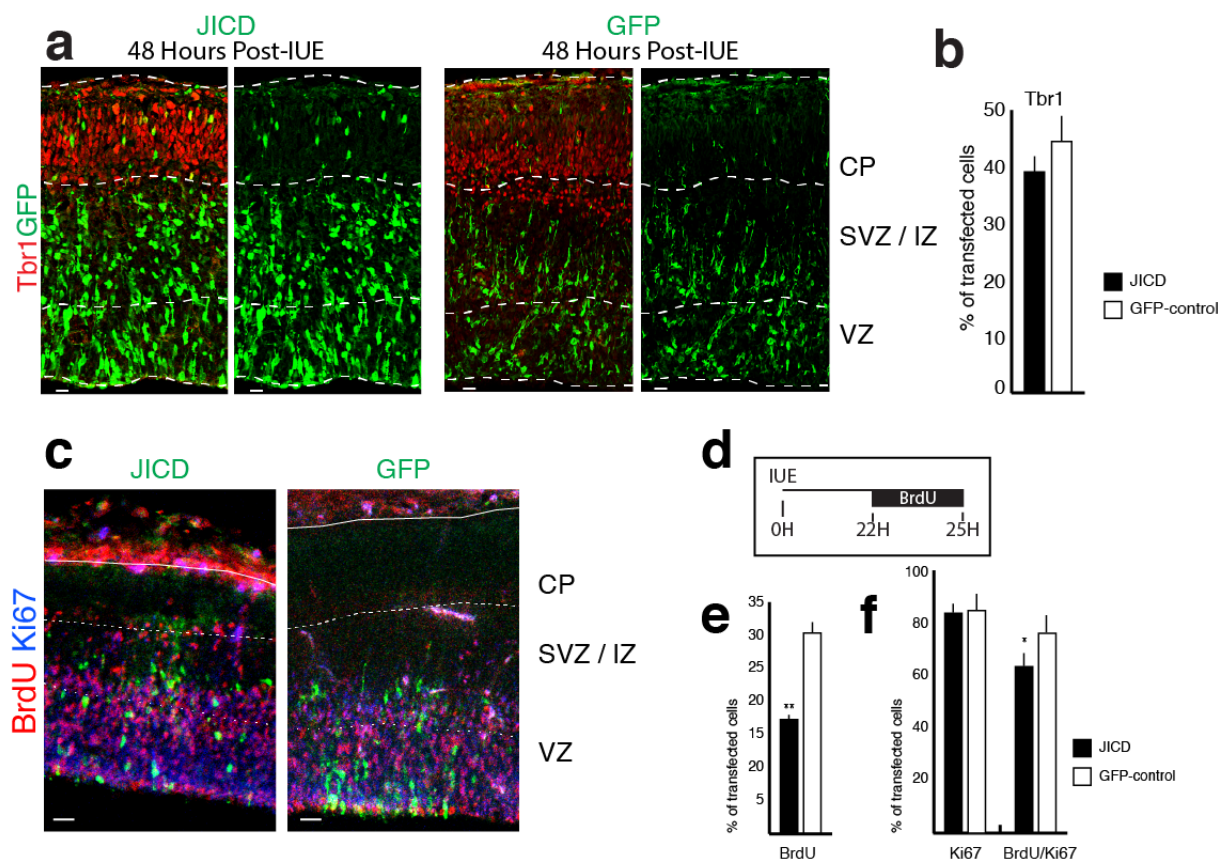


Figure 42

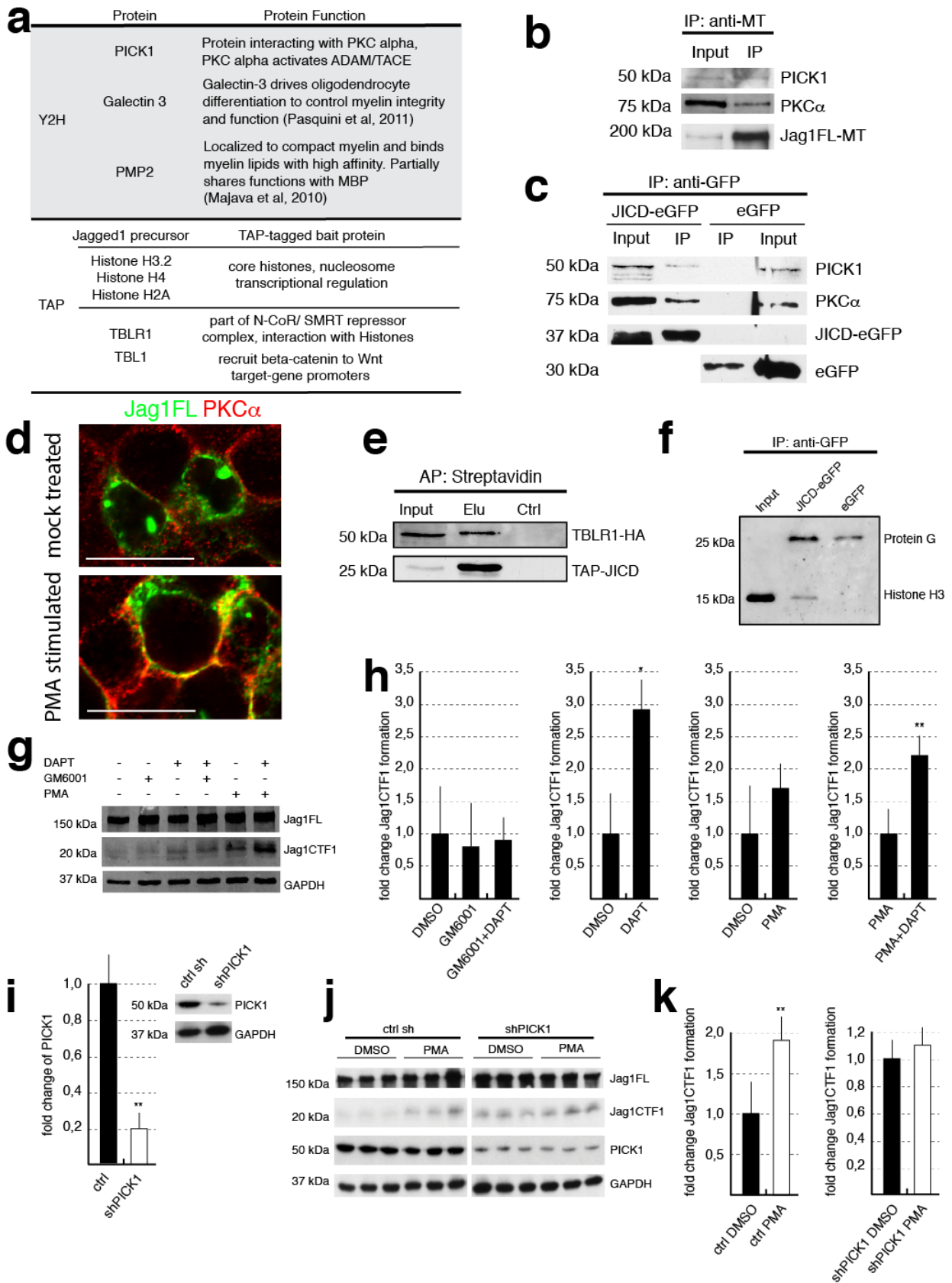


Figure 43

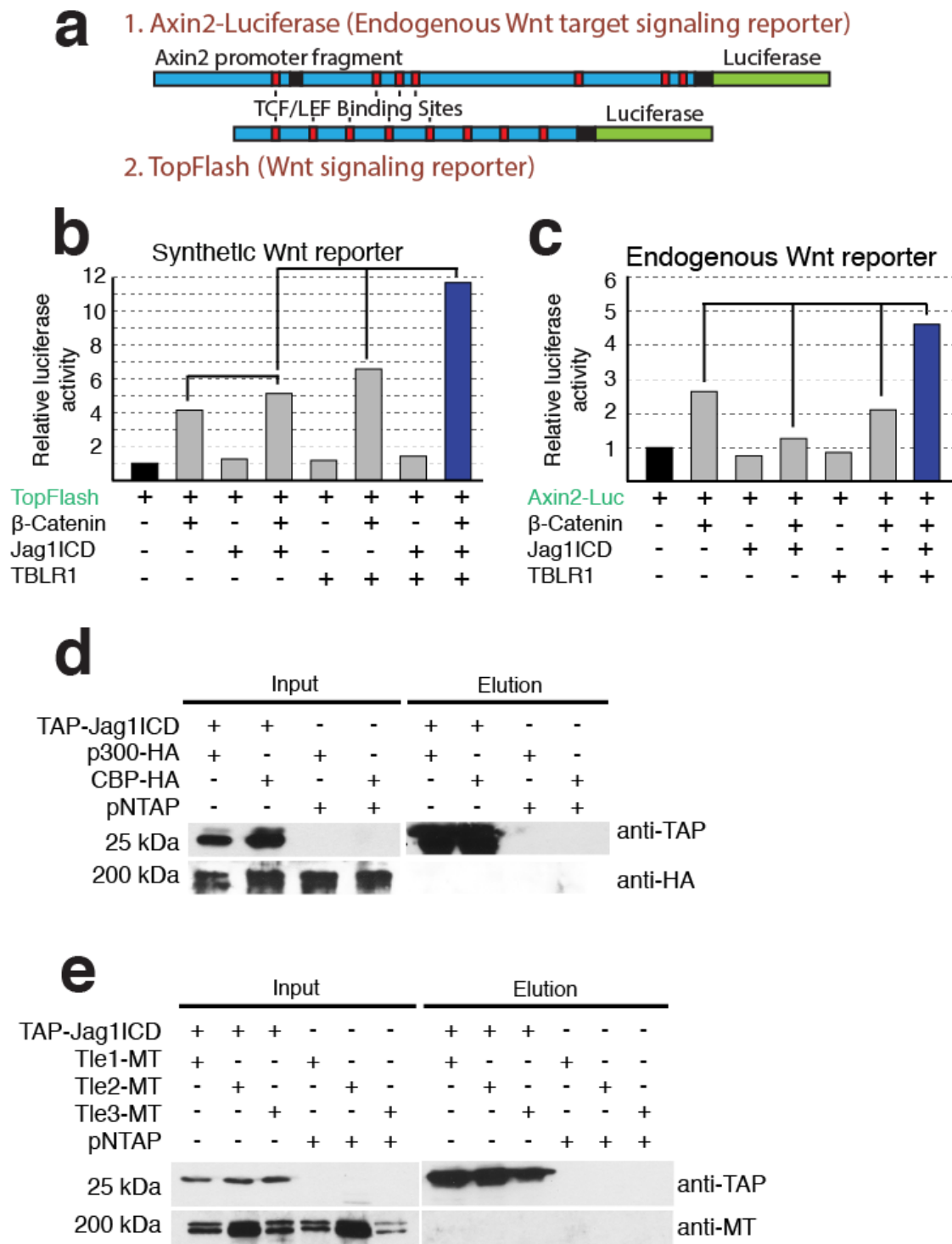


Figure 44

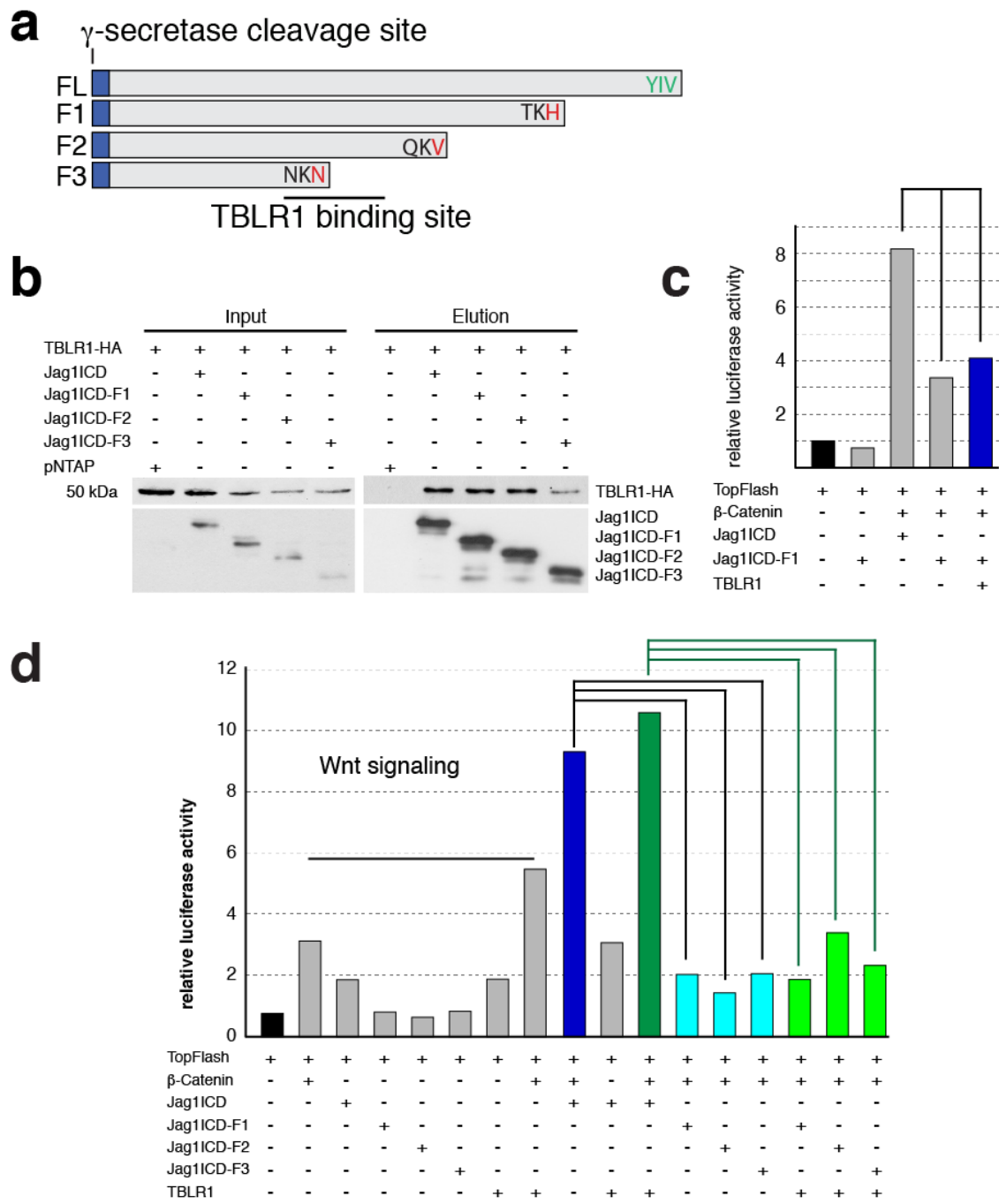


Figure 45

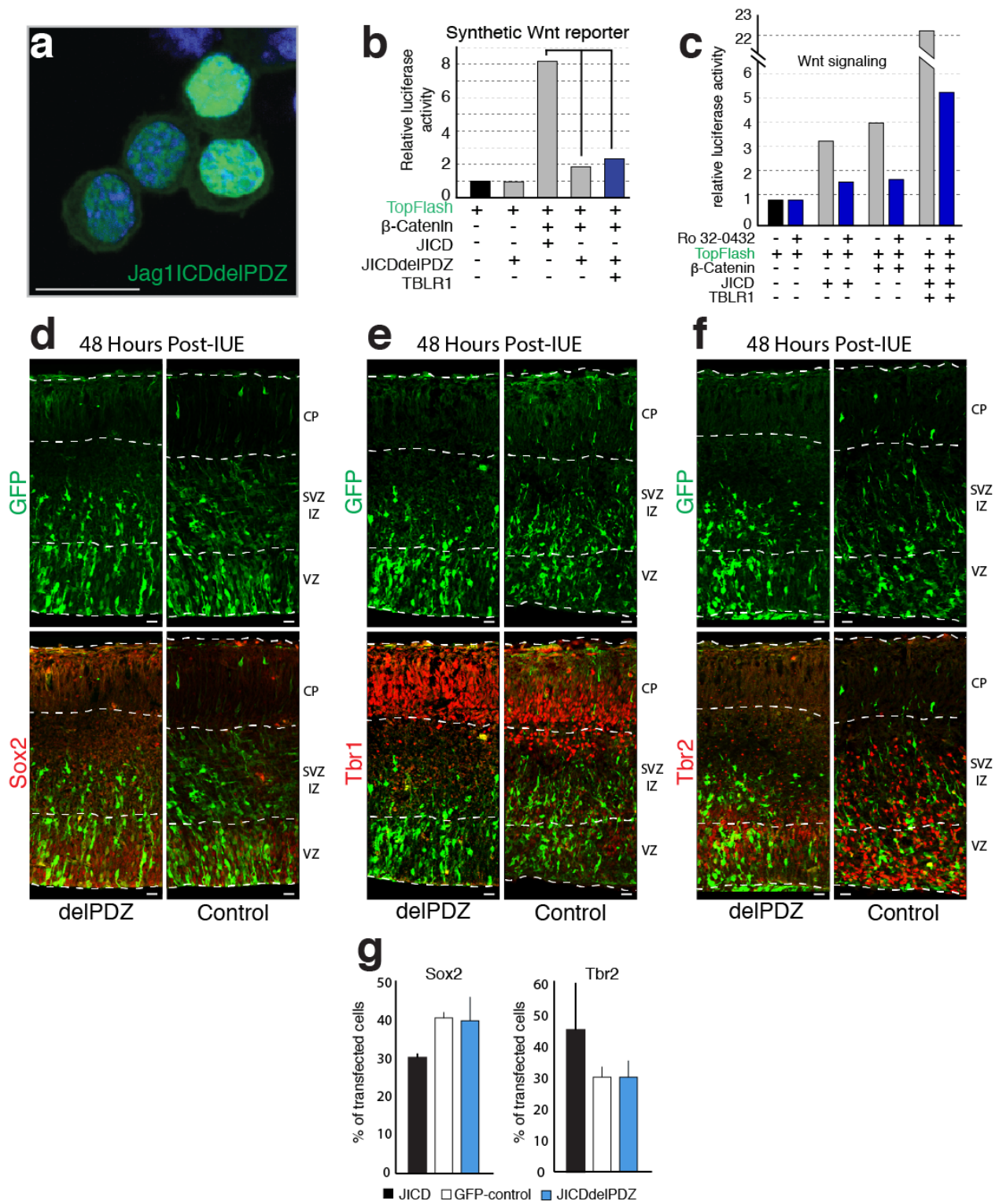


Figure 46

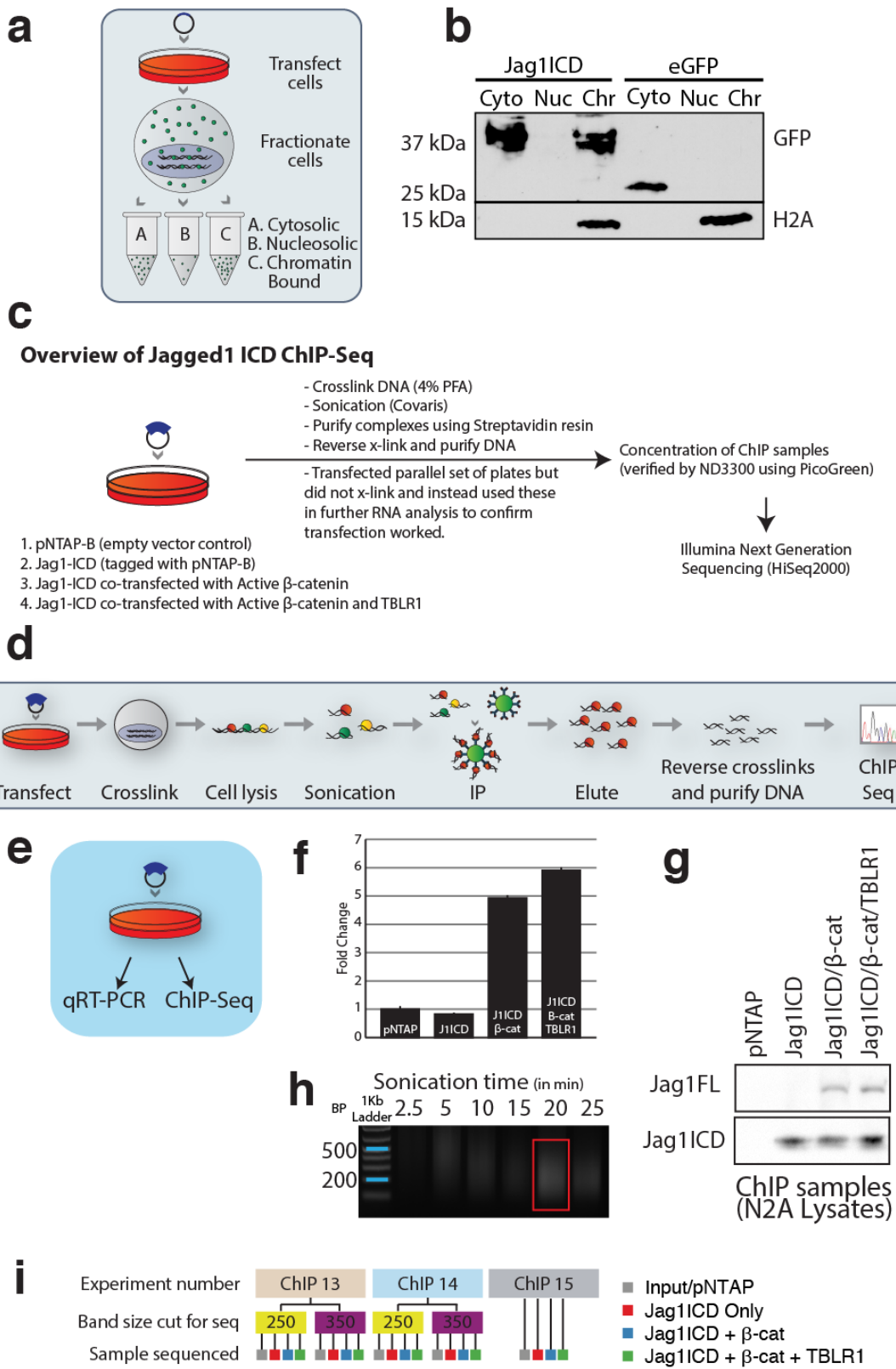


Figure 47

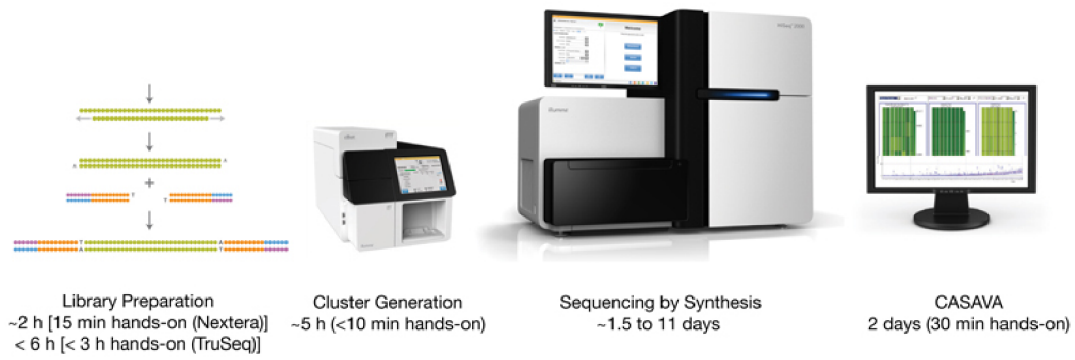


Figure 48

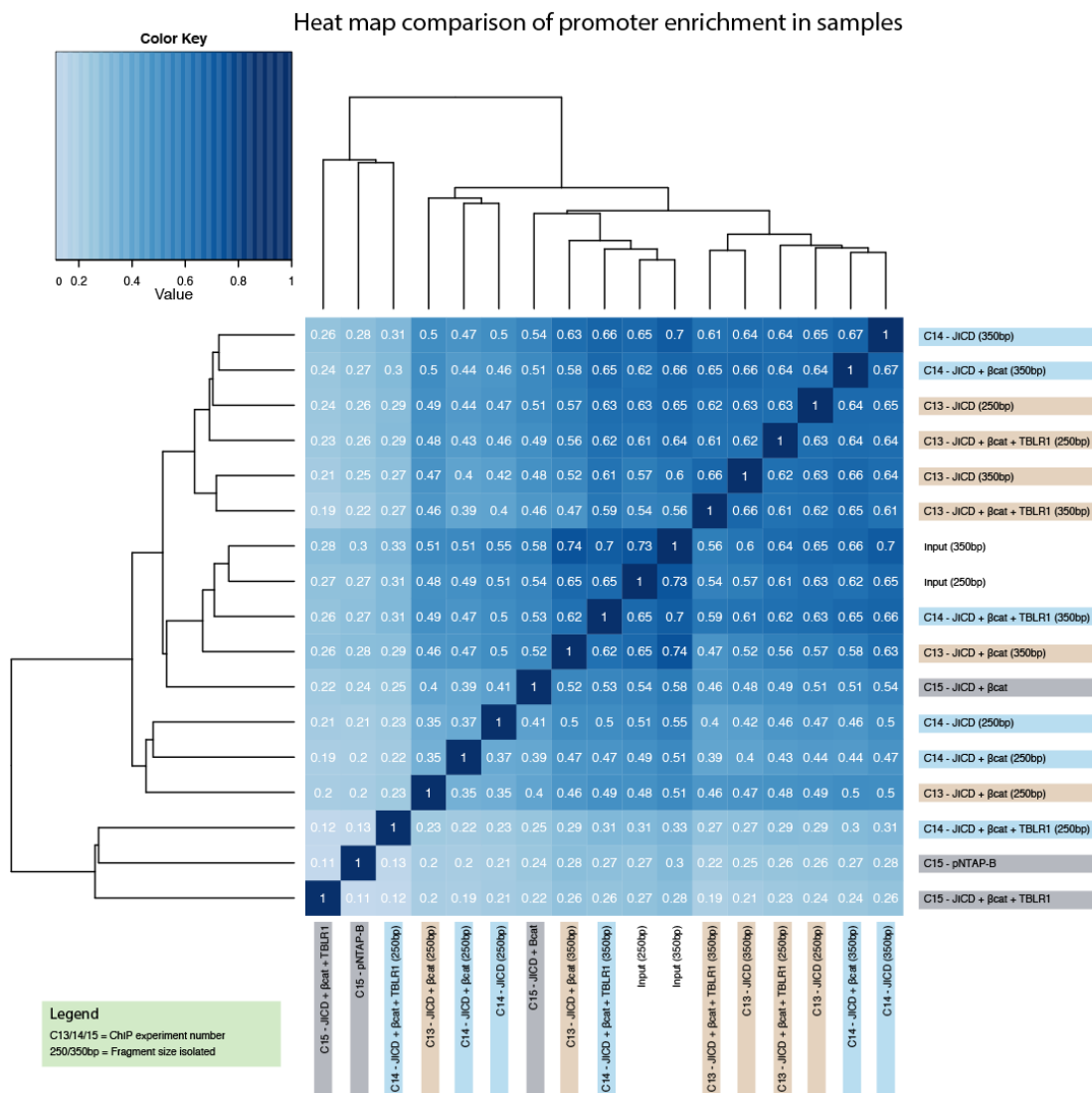


Figure 49

Number of mapped reads per CHIP sample

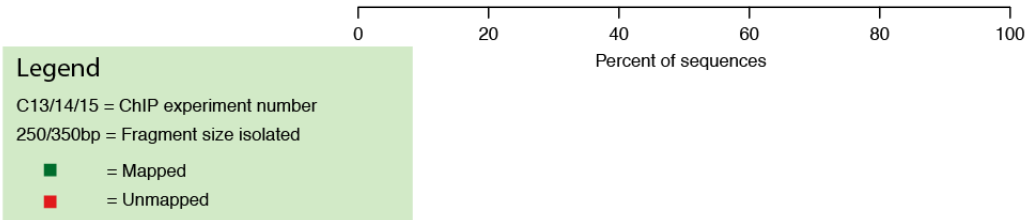
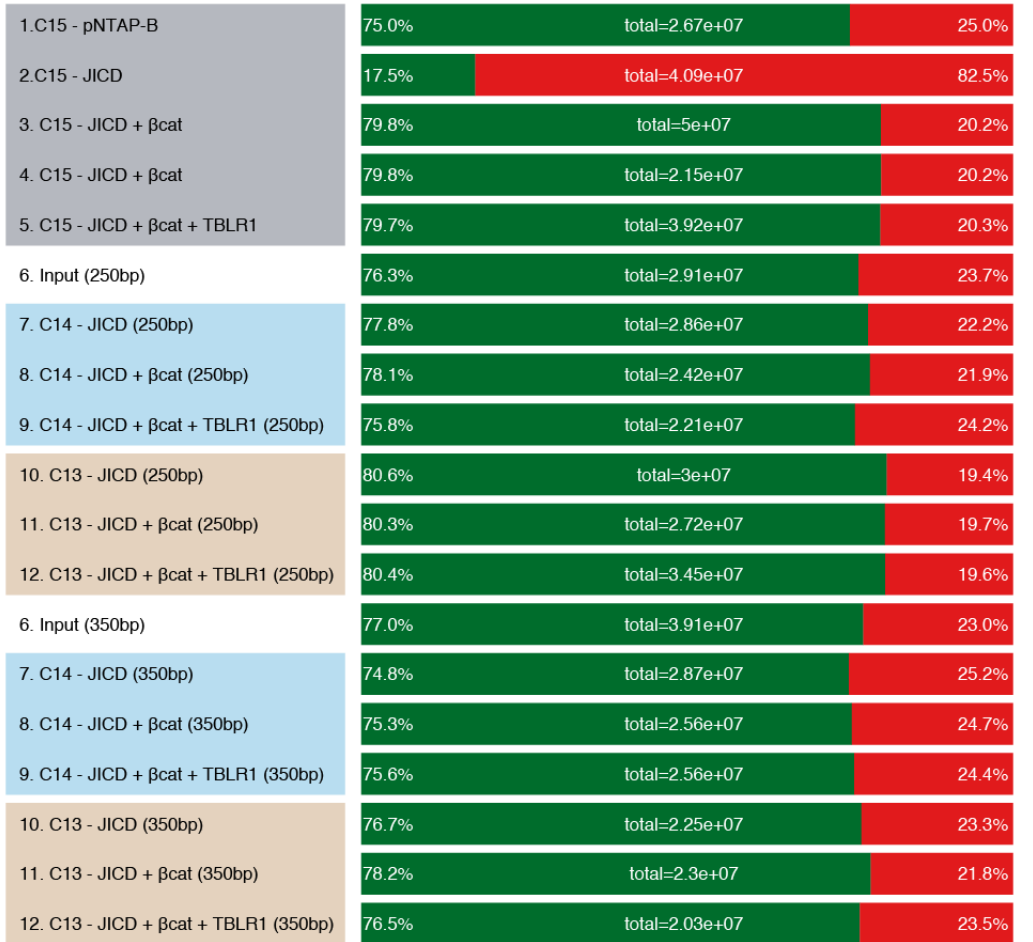


Figure 50

Number of unique reads per ChIP sample

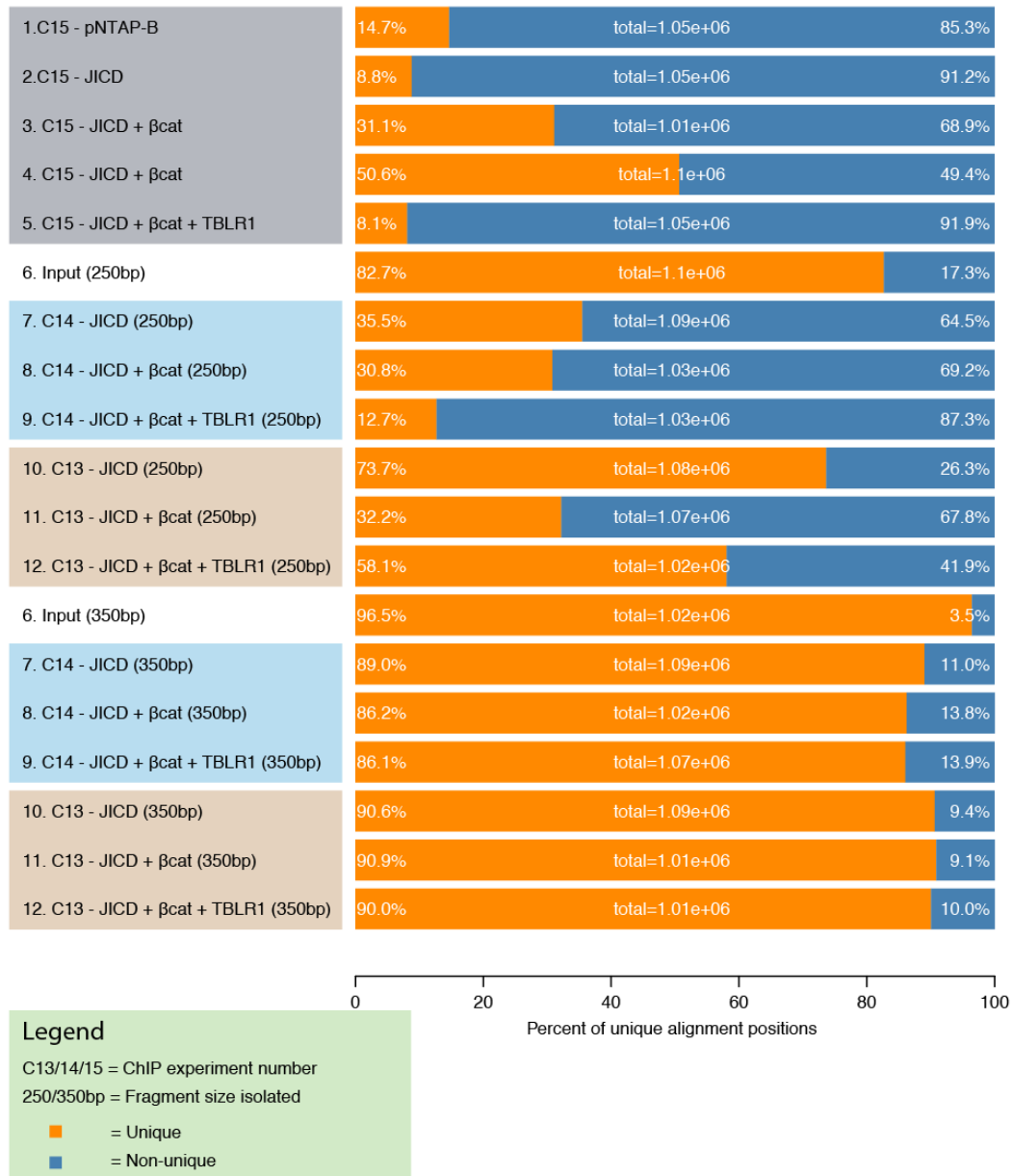
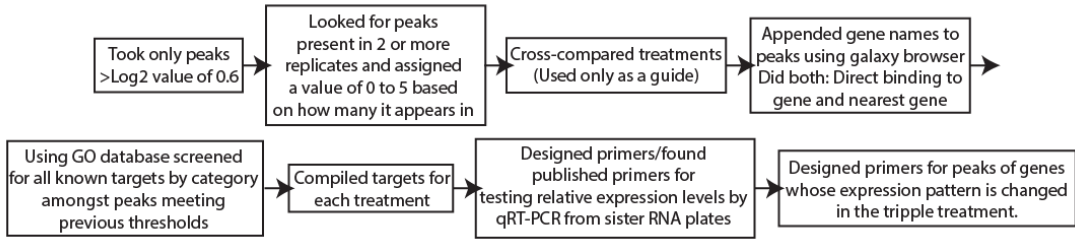


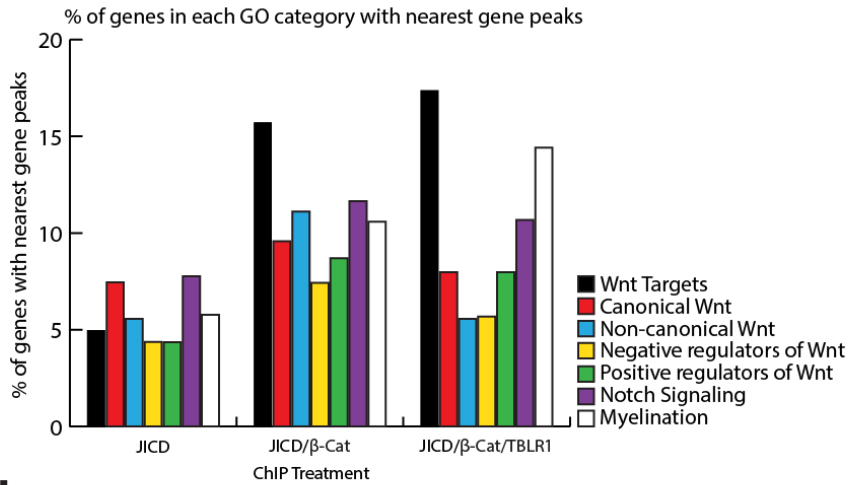
Figure 51

a

Process of target discovery and verification



b



d

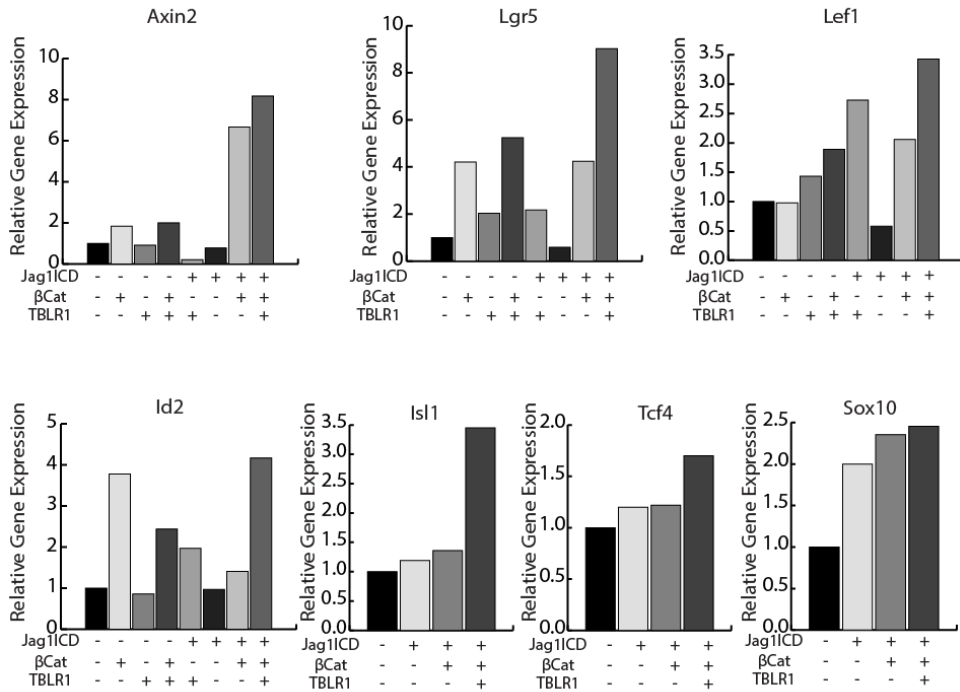


Figure 52

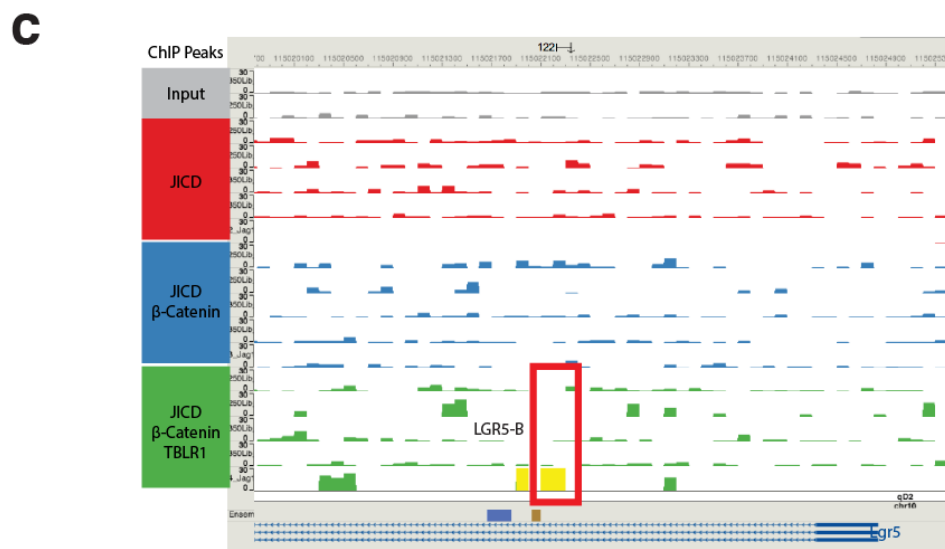
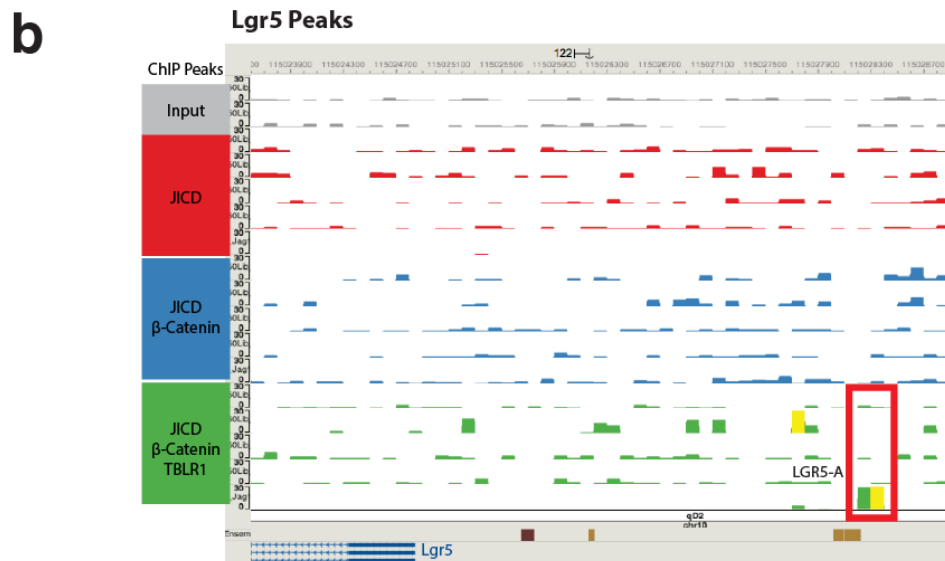
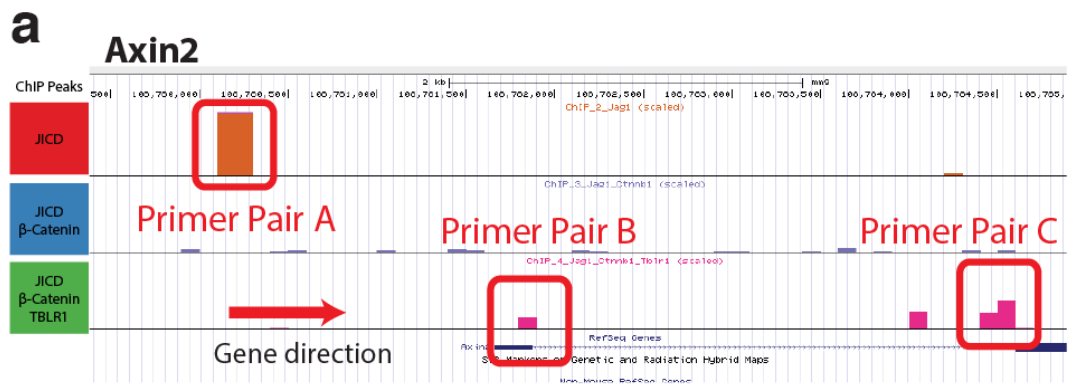


Figure 53

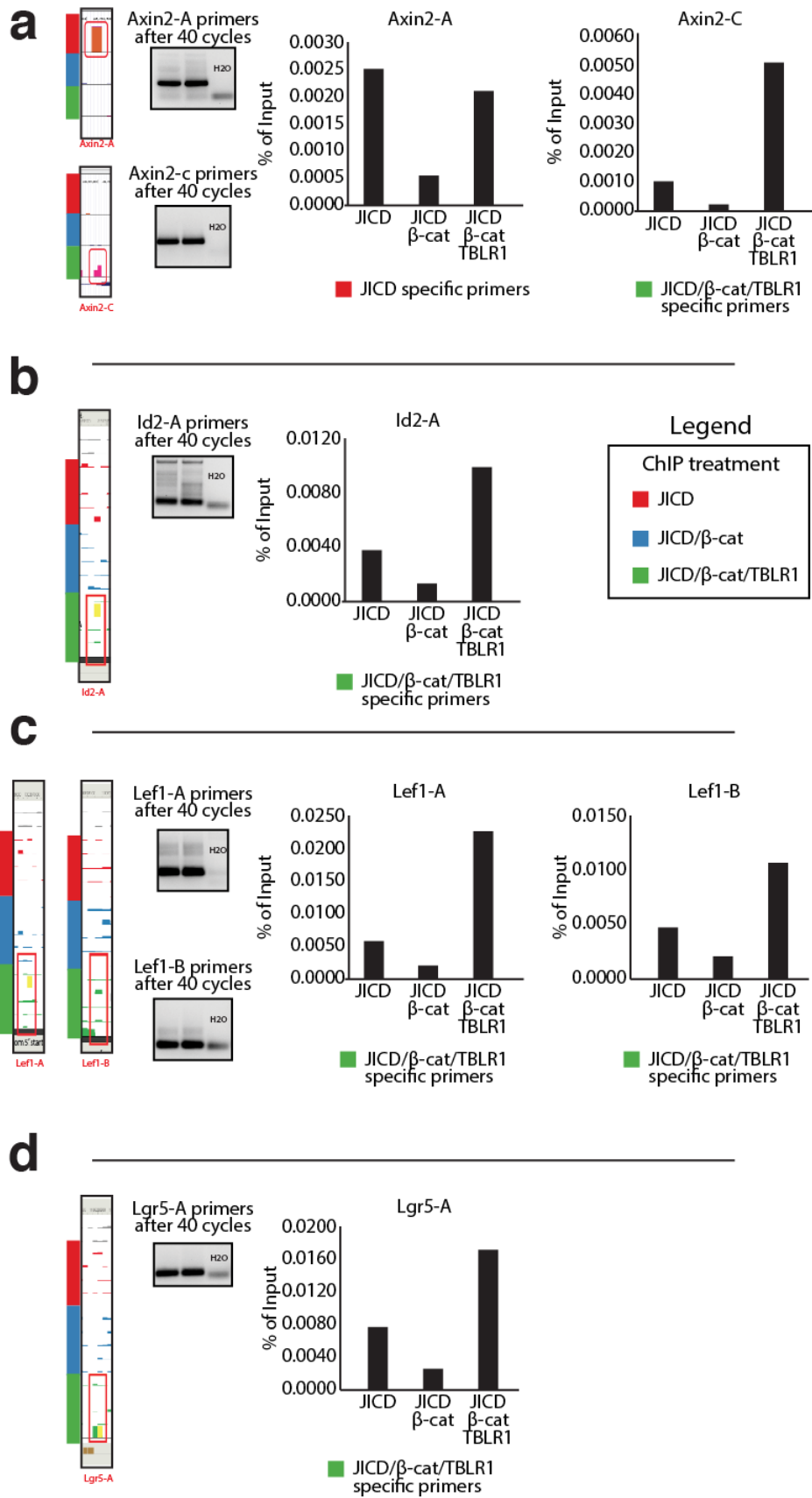


Figure 54

Supplementary table 1

| Positive control | | | | | | | RNAseq | qRT-PCR | |
|------------------|--|-------|----------|----------|-------------|-------------|--|---------|--|
| Gene Symbol | Gene Name | logFC | PValue | FDR | Fold change | Fold change | Known role | | |
| Jag1 | jagged 1 | 4.65 | 0.00E+00 | 0.00E+00 | 25.13 | 62.18 | Ligand for multiple Notch receptors and involved in the mediation of Notch signaling. (UniProtKB) | | |
| Top 15 | | | | | | | RNAseq | qRT-PCR | |
| Gene Symbol | Gene Name | logFC | PValue | FDR | Fold change | Fold change | Known role | | |
| Jag1 | jagged 1 | 4.65 | 0.00E+00 | 0.00E+00 | 25.13 | 62.18 | Ligand for multiple Notch receptors and involved in the mediation of Notch signaling. (UniProtKB) | | |
| Rnf213 | ring finger protein 213 | 2.07 | 2.91E-08 | 3.53E-06 | 4.21 | - | Probable E3 ubiquitin-protein ligase that may play a role in angiogenesis. May also have an ATPase activity (UniProtKB) | | |
| Sacs | sacsin | 2.04 | 1.59E-09 | 2.74E-07 | 4.10 | - | Co-chaperone which acts as a regulator of the Hsp70 chaperone machinery and may be involved in the processing of other ataxia-linked proteins. (UniProtKB) | | |
| Cntnap5b | contactin associated protein-like 5B | 1.99 | 6.71E-07 | 5.33E-05 | 3.97 | - | May play a role in the correct development and proper functioning of the peripheral and central nervous system and be involved in cell adhesion and intercellular communication (UniProtKB) | | |
| Syt14 | synaptotagmin XIV | 1.84 | 5.06E-06 | 2.85E-04 | 3.59 | - | May be involved in the trafficking and exocytosis of secretory vesicles in non-neuronal tissues. Is Ca(2+)-independent (UniProtKB) | | |
| Igsf9b | immunoglobulin superfamily, member 9B | 1.84 | 1.26E-28 | 4.25E-25 | 3.58 | - | Functions in dendrite outgrowth and synapse maturation. Paralog of Igsf9 (UniProtKB/GeneCards) | | |
| Tmem90a | transmembrane protein 90a | 1.83 | 8.37E-05 | 2.86E-03 | 3.55 | - | Multi-pass membrane protein (Potential). Golgi apparatus, cis-Golgi network (UniProtKB). | | |
| Pabpc5 | poly(A) binding protein, cytoplasmic 5 | 1.82 | 5.07E-07 | 4.13E-05 | 3.52 | - | Binds the poly(A) tail of mRNA. May be involved in cytoplasmic regulatory processes of mRNA metabolism. (UniProtKB) | | |
| ErbB4* | v-erb-a erythroblastic leukemia viral oncogene homolog 4 (avian) | 1.78 | 3.96E-16 | 2.97E-13 | 3.45 | - | Acts as cell-surface receptor for the neuregulins NRG1, NRG2, NRG3 and NRG4 and the EGF family members (UniProtKB) | | |
| Hipk2* | homeodomain interacting protein kinase 2 | 1.72 | 8.31E-45 | 3.73E-41 | 3.29 | 1.63 | Negative regulator through phosphorylation and subsequent proteasomal degradation of CTNNB1 and the antiapoptotic factor CTBP1. In the Wnt/beta-catenin signaling pathway acts as an intermediate kinase between MAP3K7/TAK1 and NLK to promote the proteasomal degradation of MYB. (UniProtKB). HIPK2 phosphorylate TCF/LEF factors to inhibit their interaction with DNA (Gao et al 2014, Cell & bioscience) | | |
| Tnr* | tenascin R | 1.69 | 1.91E-26 | 5.16E-23 | 3.23 | 4.31 | Neural extracellular matrix (ECM) protein involved in interactions with different cells and matrix components. (UniProtKB) | | |
| Enpp6* | ectonucleotide pyrophosphatase/phosphodiesterase 6 | 1.59 | 9.97E-05 | 3.28E-03 | 3.02 | - | Choline-specific glycerophosphodiester phosphodiesterase. (UniProtKB) | | |
| Gpr17* | G protein-coupled receptor 17 | 1.55 | 8.43E-13 | 3.44E-10 | 2.93 | - | GPRI7 expression peaks at intermediate phases of oligodendrocyte differentiation and is thereafter downregulated to allow terminal maturation. GPRI7 activation stimulates OPC migration. Pugliese et al 2013 (Glia) | | |
| Bmp4 | bone morphogenetic protein 4 | 1.55 | 8.63E-04 | 1.67E-02 | 2.92 | 9.25 | Negative regulator of oligodendrocyte maturation. | | |
| Bottom 15 | | | | | | | RNAseq | qRT-PCR | |
| Gene Symbol | Gene Name | logFC | PValue | FDR | Fold change | Fold change | Known role | | |
| Cyp27b1 | cytochrome P450, family 27, subfamily b, polypeptide 1 | -1.24 | 1.83E-02 | 1.52E-01 | 0.42 | - | Plays an important role in normal bone growth, calcium metabolism, and tissue differentiation. (UniProtKB) | | |
| Clec2d | C-type lectin domain family 2, member d | -1.25 | 2.49E-03 | 3.76E-02 | 0.42 | - | Receptor for KLRB1 that protects target cells against natural killer cell-mediated lysis. Inhibits osteoclast formation. Inhibits bone resorption. (UniProtKB) | | |
| Lepr | leptin receptor | -1.25 | 9.26E-03 | 9.79E-02 | 0.42 | - | | | |
| Cd38 | CD38 antigen | -1.32 | 1.10E-03 | 1.98E-02 | 0.40 | - | | | |
| Clcf1 | cardiotrophin-like cytokine factor 1 | -1.34 | 3.84E-03 | 5.22E-02 | 0.40 | - | | | |
| Dsc3 | desmocollin 3 | -1.34 | 7.15E-03 | 8.15E-02 | 0.40 | - | | | |
| Gp5 | glycoprotein 5 (platelet) | -1.38 | 4.49E-03 | 5.85E-02 | 0.38 | - | | | |
| Tpsg1 | trypsin gamma 1 | -1.41 | 3.33E-05 | 1.33E-03 | 0.38 | - | | | |
| Agt | angiotensinogen (serpin peptidase inhibitor, clade A, member 8) | -1.42 | 8.27E-05 | 2.83E-03 | 0.37 | 0.43 | Essential component of the renin-angiotensin system (RAS), a potent regulator of blood pressure, body fluid and electrolyte homeostasis (UniProtKB) | | |
| Wfikkn1 | WAP, FS, Ig, KU, and NTR-containing protein 1 | -1.53 | 8.66E-05 | 2.93E-03 | 0.35 | - | | | |
| Amn | amionless | -1.59 | 3.72E-04 | 9.11E-03 | 0.33 | - | | | |

Supplementary Table 1: Continued

| | | | | | | | |
|-------|--|-------|----------|----------|------|---|--|
| Lars2 | leucyl-tRNA synthetase, mitochondrial | -1.63 | 1.21E-58 | 8.13E-55 | 0.32 | - | Increased greatly in the brains of patients with bipolar disorder and schizophrenia. Both of these disorders have a high correlation of oligodendrocyte dysfunction. |
| Cd79a | CD79A antigen (immunoglobulin-associated alpha) | -1.76 | 1.37E-04 | 4.31E-03 | 0.29 | - | |
| P4ha3 | procollagen-proline, 2-oxoglutarate 4-dioxygenase (proline 4-hydroxylase), alpha polypeptide III | -2.02 | 1.71E-04 | 5.06E-03 | 0.25 | - | |
| Nfe2 | nuclear factor, erythroid derived 2 | -2.06 | 3.06E-05 | 1.23E-03 | 0.24 | - | Component of the NF-E2 complex essential for regulating erythroid and megakaryocytic maturation and differentiation. (UniProtKB) |

Astrocytic markers

| Gene Symbol | Gene Name | logFC | PValue | FDR | RNAseq Fold change | qRT-PCR Fold change | Known role |
|-------------|---|-------|----------|----------|--------------------|---------------------|---|
| Bdnf | brain derived neurotrophic factor | -0.30 | 2.31E-01 | 6.08E-01 | 0.81 | - | During development, promotes the survival and differentiation of selected neuronal populations of the peripheral and central nervous systems. (UniProtKB) |
| Gfap | glial fibrillary acidic protein | -0.90 | 1.39E-02 | 1.28E-01 | 0.53 | - | A cell-specific marker that, during the development of the central nervous system, distinguishes astrocytes from other glial cells (UniProtKB) |
| Igf1 | insulin-like growth factor 1 | -0.33 | 2.17E-01 | 5.89E-01 | 0.80 | - | Structurally and functionally related to insulin but have a much higher growth-promoting activity (UniProtKB) |
| S100b | S100 protein, beta polypeptide, neural | 0.38 | 1.40E-01 | 4.76E-01 | 1.30 | - | Weakly binds calcium but binds zinc very tightly-distinct binding sites with different affinities exist for both ions on each monomer. (UniProtKB) |
| Slc1a3 | solute carrier family 1 (glial high affinity glutamate transporter), member 3 | -0.19 | 1.06E-01 | 4.12E-01 | 0.88 | - | Transports L-glutamate and also L- and D-aspartate. (UniProtKB) |
| Vegfa | vascular endothelial growth factor A | -0.31 | 1.18E-01 | 4.37E-01 | 0.81 | - | Growth factor active in angiogenesis, vasculogenesis and endothelial cell growth (UniProtKB). |
| Vegfb | vascular endothelial growth factor B | -0.03 | 8.26E-01 | 9.60E-01 | 0.98 | - | Growth factor for endothelial cells (UniProtKB). |
| Vegfc | vascular endothelial growth factor C | -0.08 | 8.49E-01 | 9.68E-01 | 0.95 | - | Growth factor active in angiogenesis, and endothelial cell growth (UniProtKB). |

Wnt Pathway Genes

| Gene Symbol | Gene Name | logFC | PValue | FDR | RNAseq Fold change | qRT-PCR Fold change | Known role |
|-------------|--|-------|----------|----------|--------------------|---------------------|--|
| Axin2 | axin2 | 0.04 | 8.02E-01 | 9.54E-01 | 1.03 | - | Regulator of Wnt signaling |
| Ccnd1 | cyclin D1 | 0.12 | 1.98E-01 | 5.65E-01 | 1.09 | - | regulates the cell-cycle during G(1)/S transition (UniProtKB) |
| Cdh10 | cadherin 10 | -0.15 | 1.76E-01 | 5.35E-01 | 0.90 | - | Calcium-dependent cell adhesion proteins (UniProtKB) |
| Cldn1 | claudin 1 | 0.48 | 2.64E-01 | 6.44E-01 | 1.40 | - | An integral membrane protein and a component of tight junction strands (EntrezGene) |
| Disc1 | disrupted in schizophrenia 1 | 1.04 | 1.22E-06 | 8.78E-05 | 2.06 | - | Participates in the Wnt-mediated neural progenitor proliferation as a positive regulator by modulating GSK3B activity and CTNNB1 abundance (UniProtKB) |
| En1 | engrailed 1 | 0.02 | 9.53E-01 | 9.99E-01 | 1.02 | - | Control of pattern formation during development of the central nervous system (EntrezGene) |
| Fzd7 | frizzled homolog 7 | -0.11 | 4.78E-01 | 8.14E-01 | 0.92 | - | Receptor for Wnt proteins |
| Myc (C-myc) | myelocytomatosis oncogene | 0.19 | 3.80E-02 | 2.40E-01 | 1.14 | - | Participates in the regulation of gene transcription (UniProtKB) |
| Neurod1 | neurogenic differentiation 1 | 0.43 | 2.91E-01 | 6.72E-01 | 1.34 | - | Required for dendrite morphogenesis and maintenance in the cerebellar cortex (UniProtKB). |
| Neurog2 | neurogenin 2 | 0.25 | 7.63E-01 | 9.40E-01 | 1.19 | - | Transcriptional regulator. Involved in neuronal differentiation (UniProtKB). |
| Nrcam | neuron-glia-CAM-related cell adhesion molecule | -0.03 | 8.08E-01 | 9.56E-01 | 0.98 | - | Cell adhesion, ankyrin-binding protein involved in neuron-neuron adhesion. May play a role in the molecular assembly of the nodes of Ranvier (UniProtKB) |
| Vegfa | vascular endothelial growth factor A | -0.31 | 1.18E-01 | 4.37E-01 | 0.81 | - | Growth factor active in angiogenesis, vasculogenesis and endothelial cell growth (UniProtKB). |
| Vegfb | vascular endothelial growth factor B | -0.03 | 8.26E-01 | 9.60E-01 | 0.98 | - | Growth factor for endothelial cells (UniProtKB). |
| Vegfc | vascular endothelial growth factor C | -0.08 | 8.49E-01 | 9.68E-01 | 0.95 | - | Growth factor active in angiogenesis, and endothelial cell growth (UniProtKB). |
| Wisp1 | WNT1 inducible signaling pathway protein 1 | -0.55 | 1.11E-01 | 4.23E-01 | 0.68 | - | Downstream regulator in the Wnt/Frizzled-signaling pathway. (UniProtKB) |
| Wnt2 | wingless-related MMTV integration site 2 | -0.55 | 2.07E-01 | 5.77E-01 | 0.68 | - | Ligand for members of the frizzled family of seven transmembrane receptors. (UniProtKB) |
| Wnt3* | wingless-related MMTV integration site 3 | -0.78 | 2.46E-02 | 1.83E-01 | 0.58 | 0.6 | Promotes adult neurogenesis in the DG. |

Supplementary Table 1: Continued

| | | | | | | | |
|-------|---|-------|----------|----------|------|---|---|
| Wnt4 | wingless-related MMTV integration site 4 | -0.68 | 6.14E-02 | 3.14E-01 | 0.63 | - | Ligand for members of the frizzled family of seven transmembrane receptors. (UniProtKB) |
| Wnt5a | wingless-related MMTV integration site 5A | -0.15 | 2.25E-01 | 5.99E-01 | 0.90 | - | Can activate or inhibit canonical Wnt signaling, depending on receptor context. (UniProt) |
| Wnt7b | wingless-related MMTV integration site 7B | -0.23 | 8.95E-02 | 3.78E-01 | 0.85 | - | Ligand for members of the frizzled family of seven transmembrane receptors. (UniProtKB) |

Notch pathway genes

| Gene Symbol | Gene Name | logFC | PValue | FDR | RNAseq Fold change | qRT-PCR Fold change | Known role |
|-----------------|---|-------|----------|----------|--------------------|---------------------|--|
| Ascl1 | achaete-scute complex homolog 1 | 0.38 | 3.64E-04 | 8.96E-03 | 1.30 | - | Transcriptional regulator. Involved in neuronal differentiation (UniProtKB). |
| Bhlhe41 (SHARP) | basic helix-loop-helix family, member e41 | 0.30 | 3.29E-01 | 7.10E-01 | 1.23 | - | A transcriptional repressor that represses both basal and activated transcription (UniProtKB) |
| Dll1 | delta-like 1 | 0.45 | 5.33E-05 | 2.00E-03 | 1.37 | - | Acts as a ligand for Notch receptors (UniProtKB) |
| Dll3 | delta-like 3 (Drosophila) | 0.89 | 1.22E-05 | 5.87E-04 | 1.85 | - | Acts as a ligand for Notch receptors (UniProtKB) |
| Hes1 | hairy and enhancer of split 1 | -0.07 | 8.59E-01 | 9.72E-01 | 0.96 | - | Transcriptional repressor of genes that require a bHLH protein for their transcription (UniProtKB) |
| Hes5 | hairy and enhancer of split 5 | -0.19 | 2.22E-01 | 5.97E-01 | 0.88 | - | Transcriptional repressor of genes that require a bHLH protein for their transcription (UniProtKB) |
| Kat2a (GCN5) | K(lysine) acetyltransferase 2A | 0.05 | 6.05E-01 | 8.78E-01 | 1.04 | - | Functions as a histone acetyltransferase (HAT) to promote transcriptional activation (UniProtKB) |
| Maml1 | mastermind like 1 | 0.11 | 3.40E-01 | 7.20E-01 | 1.08 | - | Acts as a transcriptional coactivator for NOTCH proteins (UniProtKB). |
| Ncor2 (SMRT) | nuclear receptor co-repressor 2 | 0.50 | 4.07E-08 | 4.68E-06 | 1.41 | - | Mediates the transcriptional repression activity of some nuclear receptors by promoting chromatin condensation (UniProtKB). |
| Notch1 | Notch receptor 1 | 0.23 | 2.38E-02 | 1.79E-01 | 1.18 | - | Functions as a receptor for membrane-bound ligands Jagged1, Jagged2 and Delta 1 to regulate cell-fate determination. (UniProtKB) |
| Nrarp | Notch-regulated ankyrin repeat protein | -0.37 | 3.06E-03 | 4.38E-02 | 0.77 | - | May play a role in the formation of somites (UniProtKB). |
| Pag1 (CBP) | phosphoprotein associated with glycosphingolipid microdomains 1 | 0.78 | 9.40E-07 | 7.11E-05 | 1.71 | - | It is thought to be involved in the regulation of T cell activation (EntrezGene) |
| Rbpj | recombination signal binding protein for immunoglobulin kappa J region | 0.07 | 4.92E-01 | 8.24E-01 | 1.05 | - | Transcriptional regulator that plays a central role in Notch signaling (UniProtKB). |
| Runx1t1 (ETO) | runt-related transcription factor 1; translocated to, 1 (cydin D-related) | 1.14 | 9.92E-03 | 1.03E-01 | 2.20 | - | Transcription regulator that exerts its function by binding to histone deacetylases and transcription factors. (UniProtKB) |

Myelination

| Gene Symbol | Gene Name | logFC | PValue | FDR | RNAseq Fold change | qRT-PCR Fold change | Known role |
|-------------|--|-------|----------|----------|--------------------|---------------------|--|
| Enpp6 | ectonucleotide pyrophosphatase/phosphodiesterase 6 | 1.59 | 9.97E-05 | 3.28E-03 | 3.02 | - | Choline-specific glycerophosphodiester phosphodiesterase. (UniProtKB) |
| ErbB4 | v-erb-a erythroblastic leukemia viral oncogene homolog 4 (avian) | 1.78 | 3.96E-16 | 2.97E-13 | 3.45 | - | Cell surface receptor for neuregulins and EGF family members and regulates development of the heart, the central nervous system and the mammary gland, gene transcription, cell proliferation, differentiation, migration and apoptosis. (UniProtKB) |
| Fa2h | fatty acid 2-hydroxylase | 1.16 | 1.34E-03 | 2.32E-02 | 2.24 | - | The lipid biosynthetic enzyme responsible for the formation of 2-hydroxy fatty acid, the precursor for hFA-galactolipids (Potter et al. 2011) |
| Myrf | Myelin regulatory factor | 1.03 | 1.39E-06 | 9.61E-05 | 2.05 | 37.4 ^Δ | Essential transcription factor of oligodendrocyte maturation (Homig et al. 2013) |
| Mbp | myelin basic protein | 0.95 | 1.66E-02 | 1.42E-01 | 1.93 | - | Protein components of the myelin membrane in the CNS (UniProtKB). |
| Myt1 | myelin transcription factor 1 | 0.66 | 1.14E-10 | 2.91E-08 | 1.58 | - | Binds to the promoter regions of proteolipid proteins of the central nervous system (UniProtKB). |
| Myt1l | myelin transcription factor 1-like | 0.84 | 3.97E-02 | 2.47E-01 | 1.79 | - | Plays a role in the development of neurons and oligodendrogalia in the CNS (UniProtKB) |
| Nrg1 | neuregulin 1 | 0.63 | 5.36E-02 | 2.91E-01 | 1.55 | - | Direct ligand for ERBB3 and ERBB4 tyrosine kinase receptors (UniProtKB) |
| Omg | oligodendrocyte myelin glycoprotein | 0.13 | 1.87E-01 | 5.47E-01 | 1.10 | - | Cell adhesion molecule contributing to the interactive process required for myelination in the central nervous system (UniProtKB). |
| Plp1 | proteolipid protein (myelin) 1 | 0.66 | 3.52E-05 | 1.39E-03 | 1.58 | - | This is the major myelin protein from the central nervous system. It plays an important role in the formation or maintenance of the multilamellar structure of myelin (UniProtKB). |

Supplementary Table 1: Continued

| Tnr | tenascin R | 1.69 | 1.91E-26 | 5.16E-23 | 3.23 | 4.31 | Neural extracellular matrix (ECM) protein involved in interactions with different cells and matrix components (UniProtKB). |
|--|--|-------|----------|----------|--------------------|---------------------|--|
| Oligodendrocyte differentiation | | | | | | | |
| Gene Symbol | Gene Name | logFC | PValue | FDR | RNAseq Fold change | qRT-PCR Fold change | Known role |
| Apc | adenomatosis polyposis coli | 0.25 | 1.86E-02 | 1.53E-01 | 1.19 | - | Promotes rapid degradation of CTNNB1 and participates in Wnt signaling as a negative regulator. (UniProtKB) |
| Bmp4 | bone morphogenetic protein 4 | 1.55 | 8.63E-04 | 1.67E-02 | 2.92 | 9.25 | Negative regulator of oligodendrocyte maturation. |
| Cnp (CNPase) | 2',3'-cyclic nucleotide 3' phosphodiesterase | 0.33 | 3.30E-03 | 4.66E-02 | 1.25 | - | May participate in RNA metabolism in the myelinating cell (UniProt). |
| Cspg4 (NG2) | chondroitin sulfate proteoglycan 4 | 0.81 | 3.27E-15 | 2.00E-12 | 1.76 | 5.18 [^] | Key oligodendrocyte progenitor marker. |
| Fa2h | fatty acid 2-hydroxylase | 1.16 | 1.34E-03 | 2.32E-02 | 2.24 | - | The lipid biosynthetic enzyme responsible for the formation of 2-hydroxy fatty acid, the precursor for hFA-galactolipids (Potter et al. 2011) |
| Myrf | Myelin regulatory factor | 1.03 | 1.39E-06 | 9.61E-05 | 2.05 | - | Essential transcription factor of oligodendrocyte maturation (Hornig et al. 2013) |
| Nkx2-2 | NK2 transcription factor related, locus 2 | 0.01 | 8.14E-01 | 9.57E-01 | 1.01 | - | Controlling the expression of genes that play a role in axonal guidance. Associates with chromatin at the NEUROD1 promoter region. (UniProt) |
| Olig1 | oligodendrocyte transcription factor 1 | 0.12 | 1.84E-01 | 5.45E-01 | 1.08 | - | Promotes formation and maturation of oligodendrocytes, especially within the brain (UniProtKB) |
| Olig2 | oligodendrocyte transcription factor 2 | 0.16 | 6.48E-02 | 3.24E-01 | 1.12 | - | Required for oligodendrocyte and motor neuron specification in the spinal cord, as well as for the development of somatic motor neurons in the hindbrain. (UniProtKB) |
| Pdgfra | platelet derived growth factor receptor, alpha polypeptide | 0.84 | 1.25E-06 | 8.86E-05 | 1.79 | 8.3 [^] | Key oligodendrocyte progenitor marker. |
| Sox10 | SRY-box containing gene 10 | 0.93 | 7.64E-07 | 5.99E-05 | 1.91 | 2.8 | Key transcription factor in oligodendrocyte maturation, expressed throughout oligodendrogenesis. |
| Sox5 | SRY-box containing gene 5 | 0.87 | 6.62E-08 | 7.07E-06 | 1.83 | 1.57 | Regulates Axin2 and therefore directly disrupts Wnt signaling (Martinez-Morales et al. 2010). |
| Zfp488 | zinc finger protein 488 | 0.63 | 2.85E-05 | 1.16E-03 | 1.54 | - | An oligodendrocyte-specific zinc-finger transcription regulator cooperates with Olig2 to promote oligodendrocyte differentiation (Wang et al. 2006) |
| Other interesting genes | | | | | | | |
| Gene Symbol | Gene Name | logFC | PValue | FDR | RNAseq Fold change | qRT-PCR Fold change | Known role |
| Cbln3 | cerebellin 3 precursor protein | -1.01 | 2.07E-02 | 1.65E-01 | 0.50 | - | Involved in synaptic functions in the CNS (UniProtKB) |
| Cd68 | CD68 antigen | -1.14 | 1.52E-04 | 4.64E-03 | 0.45 | - | Glycoprotein which binds to low density lipoprotein. This is expressed by monocytes/macrophages and highly expressed in active MS lesions. Marker of reactive microglia. |
| Ednra | endothelin receptor type A | -0.29 | 1.92E-01 | 5.56E-01 | 0.82 | - | Endothelin receptor |
| Ednrb | endothelin receptor type B | -0.22 | 3.50E-02 | 2.28E-01 | 0.86 | - | Endothelin receptor |
| Epor | erythropoietin receptor | -0.96 | 9.51E-03 | 1.00E-01 | 0.51 | - | This is shown in promoting remyelination. Potentially levels of Epor are still high enough in Jag1FL cells to get induction or acting through alternative pathway. |
| Lag3 | lymphocyte-activation gene 3 | -0.93 | 1.78E-02 | 1.49E-01 | 0.53 | - | Confers susceptibility to MS |
| Nrg1 | neuregulin 1 | 0.63 | 5.36E-02 | 2.91E-01 | 1.55 | - | Provides a key axonal signal that regulates Schwann cell proliferation, migration (Newbern et al. 2010) |
| Cdnf | cerebral dopamine neurotrophic factor | 0.99 | 3.20E-02 | 2.16E-01 | 1.99 | - | overexpression of CDNF in astrocytes displayed the potential to alleviate cell damage and proinflammatory cytokine secretion (Cheng et al. Oct 2013) |
| Egr2 (Krox20) | early growth response 2 | 0.26 | 3.55E-02 | 2.30E-01 | 1.20 | - | Shown to be directly regulated by Sox10 (Hornig et al. 2013, Plos One) |
| Hdac4 | histone deacetylase 4 | 0.75 | 1.18E-06 | 8.51E-05 | 1.68 | - | Stroke increases HDAC1, HDAC2 and HDAC4 positive OPCs (Kassis, 2014) |

[^] = qRT-PCR from different set of biological replicates prepared separate from samples used in RNA-seq

* = Gene may correlate with in vivo phenotype

Supplementary Table 2:

| Treatment: JICD (J) | | | |
|---------------------|----------|--------|---------|
| All Wnt Targets | Present? | In JB? | In JBT? |
| Gja1 | 2 | TRUE | TRUE |
| Abcb1b | 1 | FALSE | FALSE |
| Jag1 | 1 | TRUE | TRUE |
| Nrcam | 1 | FALSE | FALSE |
| Dkk1 | 1 | FALSE | TRUE |
| Vegfc | 1 | TRUE | TRUE |
| Hnf1a | 1 | FALSE | TRUE |
| Met | 1 | FALSE | TRUE |
| Mitf | 1 | FALSE | FALSE |

| Canonical wnt | Present? | In JB? | In JBT? |
|---------------|----------|--------|---------|
| Pten | 3 | FALSE | TRUE |
| Disc1 | 2 | FALSE | FALSE |
| Cyld | 1 | FALSE | FALSE |
| Fgf10 | 1 | FALSE | TRUE |
| Rspo2 | 1 | TRUE | TRUE |
| Fzd1 | 1 | TRUE | TRUE |
| Cdh2 | 1 | TRUE | TRUE |
| Dab2 | 1 | TRUE | TRUE |
| Dkk1 | 1 | FALSE | TRUE |
| Dkk2 | 1 | TRUE | TRUE |
| Sox4 | 1 | TRUE | TRUE |
| Wnt2 | 1 | FALSE | TRUE |
| Dkk3 | 1 | FALSE | FALSE |
| Gata3 | 1 | FALSE | FALSE |
| Limd1 | 1 | FALSE | FALSE |
| Mitf | 1 | FALSE | FALSE |
| Smad3 | 1 | TRUE | FALSE |
| Snai2 | 1 | FALSE | FALSE |

| Non-canonical wnt | Present? | In JB? | In JBT? |
|-------------------|----------|--------|---------|
| Celsr1 | 1 | FALSE | FALSE |
| Fzd1 | 1 | TRUE | TRUE |
| Dab2 | 1 | TRUE | TRUE |

| neg reg of wnt | Present? | In JB? | In JBT? |
|----------------|----------|--------|---------|
| CYLD | 1 | FALSE | FALSE |
| NLK | 1 | TRUE | TRUE |
| WWOX | 1 | TRUE | FALSE |
| FZD1 | 1 | TRUE | TRUE |
| CDH2 | 1 | TRUE | TRUE |
| DAB2 | 1 | TRUE | TRUE |
| dkk1 | 1 | FALSE | TRUE |
| DKK2 | 1 | TRUE | TRUE |
| TLE1 | 1 | TRUE | TRUE |
| DKK3 | 1 | FALSE | FALSE |
| LIMD1 | 1 | FALSE | FALSE |
| SNAI2 | 1 | FALSE | FALSE |
| Wif1 | 1 | FALSE | FALSE |

| pos reg of wnt | Present? | In JB? | In JBT? |
|----------------|----------|--------|---------|
| DISC1 | 2 | FALSE | FALSE |
| CSNK2A1 | 1 | FALSE | TRUE |
| FGF10 | 1 | FALSE | TRUE |
| RSPO2 | 1 | TRUE | TRUE |
| ZEB2 | 1 | TRUE | TRUE |
| DAB2 | 1 | TRUE | TRUE |
| DKK2 | 1 | TRUE | TRUE |
| SOX4 | 1 | TRUE | TRUE |
| WNT2 | 1 | FALSE | TRUE |
| CDC73 | 1 | FALSE | TRUE |
| SMAD3 | 1 | TRUE | FALSE |

| Notch Signalling | Present? | In JB? | In JBT? |
|------------------|----------|--------|---------|
| Cntn6 | 2 | TRUE | TRUE |
| Fgf10 | 1 | FALSE | TRUE |
| Jag1 | 1 | TRUE | TRUE |

| Treatment: JICD/Bcat (JB) | | | |
|---------------------------|----------|-------|---------|
| All Wnt Targets | Present? | In J? | In JBT? |
| Jag1 | 3 | TRUE | TRUE |
| Vegfc | 2 | TRUE | TRUE |
| Gja1 | 2 | TRUE | TRUE |
| Cdx1 | 2 | FALSE | FALSE |
| Lgr5 | 2 | FALSE | TRUE |
| Isl1 | 1 | FALSE | TRUE |
| Atoh1 | 1 | FALSE | TRUE |
| Fgf20 | 1 | FALSE | TRUE |
| Klf5 | 1 | FALSE | TRUE |
| Prl2c3 | 1 | FALSE | TRUE |
| Axin2 | 1 | FALSE | FALSE |
| Edn1 | 1 | FALSE | FALSE |
| Fgf9 | 1 | FALSE | FALSE |
| Fzd7 | 1 | FALSE | FALSE |
| Irx3 | 1 | FALSE | FALSE |
| Six3 | 1 | FALSE | FALSE |
| Tcf15 | 1 | FALSE | FALSE |
| Tcf4 | 1 | FALSE | FALSE |
| Twist1 | 1 | FALSE | FALSE |

| Canonical wnt | Present? | In J? | In JBT? |
|---------------|----------|-------|---------|
| Cdh2 | 4 | TRUE | TRUE |
| Dab2 | 4 | TRUE | TRUE |
| Cttnb1 | 2 | FALSE | TRUE |
| Mcc | 2 | FALSE | TRUE |
| Dkk2 | 2 | TRUE | TRUE |
| Fzd1 | 2 | TRUE | TRUE |
| Ptk7 | 1 | FALSE | FALSE |
| Rspo2 | 1 | TRUE | TRUE |
| Scyl2 | 1 | FALSE | TRUE |
| Stk11 | 1 | FALSE | FALSE |
| Isl1 | 1 | FALSE | TRUE |
| Sox4 | 1 | TRUE | TRUE |
| Tbl1xr1 | 1 | FALSE | TRUE |
| Axin2 | 1 | FALSE | FALSE |
| Bambi | 1 | FALSE | FALSE |
| Bicc1 | 1 | FALSE | FALSE |
| Fgf9 | 1 | FALSE | FALSE |
| Fzd7 | 1 | FALSE | FALSE |
| G3bp1 | 1 | FALSE | FALSE |
| Hdac2 | 1 | FALSE | FALSE |
| Nkd1 | 1 | FALSE | FALSE |
| Shh | 1 | FALSE | FALSE |
| Smad3 | 1 | TRUE | FALSE |
| Tcf7 | 1 | FALSE | FALSE |

| Non-canonical wnt | Present? | In J? | In JBT? |
|-------------------|----------|-------|---------|
| Dab2 | 4 | TRUE | TRUE |
| Fzd1 | 2 | TRUE | TRUE |
| Ptk7 | 1 | FALSE | FALSE |
| Fzd7 | 1 | FALSE | FALSE |
| Nkd1 | 1 | FALSE | FALSE |

| neg reg of wnt | Present? | In J? | In JBT? |
|----------------|----------|-------|---------|
| CDH2 | 4 | TRUE | TRUE |
| DAB2 | 4 | TRUE | TRUE |
| GNB2L1 | 3 | FALSE | TRUE |
| MCC | 2 | FALSE | TRUE |
| FZD1 | 2 | TRUE | TRUE |
| TLE1 | 2 | TRUE | TRUE |
| DKK2 | 2 | TRUE | TRUE |
| GRB10 | 2 | FALSE | FALSE |
| NLK | 1 | TRUE | TRUE |
| SCYL2 | 1 | FALSE | TRUE |
| WWOX | 1 | TRUE | FALSE |
| ISL1 | 1 | FALSE | TRUE |
| AXIN2 | 1 | FALSE | FALSE |

| Treatment: JICD/Bcat/TBLR1 (JBT) | | | |
|----------------------------------|----------|-------|--------|
| All Wnt Targets | Present? | In J? | In JB? |
| Gja1 | 3 | TRUE | TRUE |
| Isl1 | 3 | FALSE | TRUE |
| Jag1 | 2 | TRUE | TRUE |
| Atoh1 | 2 | FALSE | TRUE |
| Vcan | 2 | FALSE | FALSE |
| Dkk1 | 2 | TRUE | FALSE |
| Fgf20 | 2 | FALSE | TRUE |
| Lgr5 | 1 | FALSE | TRUE |
| FGF18 | 1 | FALSE | FALSE |
| Id2 | 1 | FALSE | FALSE |
| Klf5 | 1 | FALSE | TRUE |
| Lef1 | 1 | FALSE | FALSE |
| Mycn | 1 | FALSE | FALSE |
| Rhou | 1 | FALSE | FALSE |
| Vegfc | 1 | TRUE | TRUE |
| Dspp | 1 | FALSE | FALSE |
| Egfr | 1 | FALSE | FALSE |
| Hnf1a | 1 | TRUE | FALSE |
| Il6 | 1 | FALSE | FALSE |
| Met | 1 | TRUE | FALSE |
| Nanog | 1 | FALSE | FALSE |
| Prl2c3 | 1 | FALSE | TRUE |

| Canonical wnt | Present? | In J? | In JB? |
|---------------|----------|-------|--------|
| Tbl1xr1 | 8 | FALSE | TRUE |
| Dkk2 | 3 | TRUE | TRUE |
| Rspo2 | 3 | TRUE | TRUE |
| Isl1 | 3 | FALSE | TRUE |
| Cttnb1 | 2 | FALSE | TRUE |
| Mcc | 2 | FALSE | TRUE |
| Fzd1 | 2 | TRUE | TRUE |
| Cdh2 | 2 | TRUE | TRUE |
| Dab2 | 2 | TRUE | TRUE |
| Dkk1 | 2 | TRUE | FALSE |
| Scyl2 | 1 | FALSE | TRUE |
| Stk3 | 1 | FALSE | FALSE |
| Tnks | 1 | FALSE | FALSE |
| Lats2 | 1 | FALSE | FALSE |
| Lef1 | 1 | FALSE | FALSE |
| Sox4 | 1 | TRUE | TRUE |
| Wnt2 | 1 | TRUE | FALSE |
| Bcl9l | 1 | FALSE | FALSE |
| Fgf10 | 1 | TRUE | FALSE |
| Pten | 1 | FALSE | FALSE |

| Non-canonical wnt | Present? | In J? | In JB? |
|-------------------|----------|-------|--------|
| Fzd1 | 2 | TRUE | TRUE |
| Dab2 | 2 | TRUE | TRUE |

| neg reg of wnt | Present? | In J? | In JB? |
|----------------|----------|-------|--------|
| DKK2 | 3 | TRUE | TRUE |
| ISL1 | 3 | FALSE | TRUE |
| MCC | 2 | FALSE | TRUE |
| FZD1 | 2 | TRUE | TRUE |
| GNB2L1 | 2 | FALSE | TRUE |
| CDH2 | 2 | TRUE | TRUE |
| DAB2 | 2 | TRUE | TRUE |
| dkk1 | 2 | TRUE | FALSE |
| NLK | 1 | TRUE | TRUE |
| SCYL2 | 1 | FALSE | TRUE |
| STK3 | 1 | FALSE | FALSE |
| BMP2 | 1 | FALSE | FALSE |
| LATS2 | 1 | FALSE | FALSE |
| LEF1 | 1 | FALSE | FALSE |
| TLE1 | 1 | TRUE | TRUE |
| DACT3 | 1 | FALSE | FALSE |
| mdfc | 1 | FALSE | FALSE |

Supplementary Table 2: Continued

| | | | |
|-------|---|-------|-------|
| Cdk6 | 1 | TRUE | TRUE |
| Eya1 | 1 | TRUE | TRUE |
| Ascl1 | 1 | TRUE | TRUE |
| Ascl1 | 1 | TRUE | TRUE |
| Cntn6 | 1 | TRUE | TRUE |
| Nod2 | 1 | FALSE | FALSE |
| Sel1l | 1 | TRUE | FALSE |
| Snai2 | 1 | FALSE | FALSE |

| Myelination | Present? | In JB? | In JBT? |
|-------------|----------|--------|---------|
| Pten | 3 | FALSE | TRUE |
| Qk | 2 | FALSE | FALSE |
| Ugt8a | 2 | TRUE | TRUE |
| Nab1 | 1 | FALSE | FALSE |
| Cdh2 | 1 | TRUE | TRUE |
| Egr2 | 1 | FALSE | TRUE |
| Ifng | 1 | FALSE | TRUE |
| Cntnap1 | 1 | TRUE | FALSE |

| | | | |
|-------|---|-------|-------|
| BICC1 | 1 | FALSE | FALSE |
| Fgf9 | 1 | FALSE | FALSE |
| G3BP1 | 1 | FALSE | FALSE |
| HDAC2 | 1 | FALSE | FALSE |
| Nkd1 | 1 | FALSE | FALSE |
| Notum | 1 | FALSE | FALSE |
| Shh | 1 | FALSE | FALSE |
| SIX3 | 1 | FALSE | FALSE |

| pos reg of wnt | Present? | In J? | In JBT? |
|----------------|----------|-------|---------|
| DKK2 | 2 | TRUE | TRUE |
| RSP02 | 1 | TRUE | TRUE |
| DAB2 | 4 | TRUE | TRUE |
| MBD2 | 3 | FALSE | TRUE |
| SALL1 | 1 | FALSE | TRUE |
| SOX4 | 1 | TRUE | TRUE |
| BAMBI | 1 | FALSE | FALSE |
| Fgf9 | 1 | FALSE | FALSE |
| NKD1 | 1 | FALSE | FALSE |
| SHH | 1 | FALSE | FALSE |
| SMAD3 | 1 | TRUE | FALSE |
| sox5 | 1 | FALSE | FALSE |
| ZEB2 | 1 | TRUE | TRUE |

| Notch Signalling | Present? | In J? | In JBT? |
|------------------|----------|-------|---------|
| Stat3 | 3 | FALSE | FALSE |
| Cntn6 | 4 | TRUE | TRUE |
| Cdk6 | 4 | TRUE | TRUE |
| Eya1 | 1 | TRUE | TRUE |
| Jag1 | 3 | TRUE | TRUE |
| Notch2 | 1 | FALSE | FALSE |
| Zfp423 | 1 | FALSE | TRUE |
| Ascl1 | 4 | TRUE | TRUE |
| Foxc1 | 1 | FALSE | TRUE |
| Dicer1 | 1 | FALSE | TRUE |
| Dner | 1 | FALSE | FALSE |
| Hey2 | 1 | FALSE | FALSE |
| Itgb1bp1 | 1 | FALSE | FALSE |
| Rbpj | 1 | FALSE | FALSE |
| Sel1l | 1 | TRUE | FALSE |

| Myelination | Present? | In J? | In JBT? |
|-------------|----------|-------|---------|
| Ctnnb1 | 2 | FALSE | TRUE |
| Hexa | 1 | FALSE | FALSE |
| Hexb | 1 | FALSE | FALSE |
| Mpdz | 3 | FALSE | TRUE |
| Cdh2 | 4 | TRUE | TRUE |
| Cxcr4 | 2 | FALSE | FALSE |
| Ugt8a | 1 | TRUE | TRUE |
| Dicer1 | 1 | FALSE | TRUE |
| Wasf3 | 1 | FALSE | TRUE |
| Cldn5 | 1 | FALSE | FALSE |
| Cntnap1 | 1 | TRUE | FALSE |
| Jam3 | 1 | FALSE | FALSE |
| Mtrn2 | 1 | FALSE | FALSE |
| Pou3f1 | 1 | FALSE | FALSE |

| pos reg of wnt | Present? | In J? | In JB? |
|----------------|----------|-------|--------|
| DKK2 | 3 | TRUE | TRUE |
| RSP02 | 3 | TRUE | TRUE |
| ZEB2 | 2 | TRUE | TRUE |
| DAB2 | 2 | TRUE | TRUE |
| CSNK2A1 | 1 | TRUE | FALSE |
| SOX11 | 1 | FALSE | FALSE |
| TNKS | 1 | FALSE | FALSE |
| BMP2 | 1 | FALSE | FALSE |
| MBD2 | 1 | FALSE | TRUE |
| SALL1 | 1 | FALSE | TRUE |
| SOX4 | 1 | TRUE | TRUE |
| WNT2 | 1 | TRUE | FALSE |
| CDC73 | 1 | TRUE | FALSE |
| FGF10 | 1 | TRUE | FALSE |
| RAD21 | 1 | FALSE | FALSE |

| Notch Signalling | Present? | In J? | In JB? |
|------------------|----------|-------|--------|
| Cdk6 | 3 | TRUE | TRUE |
| Eya1 | 3 | TRUE | TRUE |
| Jag1 | 2 | TRUE | TRUE |
| Foxc1 | 2 | FALSE | TRUE |
| Ascl1 | 2 | TRUE | TRUE |
| Zfp423 | 1 | FALSE | TRUE |
| Bmp2 | 1 | FALSE | FALSE |
| Cntn6 | 1 | TRUE | TRUE |
| Dicer1 | 1 | FALSE | TRUE |
| Fbxw7 | 1 | FALSE | FALSE |
| Fgf10 | 1 | TRUE | FALSE |

| Myelination | Present? | In J? | In JB? |
|-------------|----------|-------|--------|
| Ctnnb1 | 2 | FALSE | TRUE |
| Cdh2 | 2 | TRUE | TRUE |
| Egr2 | 2 | TRUE | FALSE |
| Ugt8a | 2 | TRUE | TRUE |
| Dicer1 | 1 | FALSE | TRUE |
| Mbp | 1 | FALSE | FALSE |
| Mpdz | 1 | FALSE | TRUE |
| Nf1 | 1 | FALSE | FALSE |
| Pmp22 | 1 | FALSE | FALSE |
| Wasf3 | 1 | FALSE | TRUE |
| Epb4.113 | 1 | FALSE | FALSE |
| Ifng | 1 | TRUE | FALSE |
| Kcnj10 | 1 | FALSE | FALSE |
| Plp1 | 1 | FALSE | FALSE |
| Pten | 1 | TRUE | FALSE |
| Serinc5 | 1 | FALSE | FALSE |

3.2.8 Figure Legends

Figure 20: Design and establishment of the AAV-Jag1FL viral system. **(a)** In situ RNA hybridization for Jag1 in E13.5 telencephalon demonstrating that Jag1 mRNA is broadly expressed in the embryonic mouse telencephalon including in the (VZ), subventricular zone (SVZ) and cortical plate (CP). Along the telencephalic vesicle (tel v) and the lateral ganglionic eminence (LGE), Jag1 is expressed in a “salt and pepper” like distribution. **(b)** At higher magnification Jag1 RNA is seen throughout the VZ and SVZ and also in cells within the cortical plate. **(c and d)** Jag1 is localized to the apical side of neural progenitors in the developing telencephalon (tel) of the forebrain at embryonic day 13.5 (arrowheads). This confirms the mRNA expression patterns seen within the cortical plate. **(e)** Design of the pAAV-Jag1 full-length (FL) construct, containing the entire Jag1 coding sequence between both LTR sites. **(f-h)** pAAV-Jag1FL was transfected and grown in HEK-293 cells and then quantified after purification. **(i)** IHC for Jag1 in transfected HEK-293 cells using two different Jag1 antibodies. **(j)** IHC for Jag1 in transduced HEK-293 cells **(k)** Transduced NSCs with control neurospheres expressing an endogenous GFP reporter. **(l)** IHC for Jag1 in transduced neurospheres. Scale bars = 20µm.

Figure 21: Design and establishment of the pMIG-Jag1FL retroviral system. **(a)** pMIG-Jag1FL construct was cloned containing the entire coding sequence of Jag1 and includes an IRES-GFP reporter. **(b and c)** Relative expression levels of Jag1 transcript and protein levels in transduced NIH3T3 and N2A cell lines respectively. **(d)** Experimental overview for transduction experiments. First establish *in vitro* transduction is working efficiently and then test to ensure it can transduce NSCs. Then go to *in vivo* models to study the role of Jag1FL on the stem cell niche. **(e and f)** Transduction of NIH3T3 fibroblasts with both control IRES-GFP and Jag1FL-IRES-GFP viruses and stained for Jag1. **(g and h)** Transduced NSCs with both control IRES-GFP and Jag1FL-IRES-GFP viruses and stained for Jag1. Scale bars = 20µm

Figure 22: Initial transductions of postnatal mice. **(a)** Experimental outline of the time-course used in the stereotactic viral injection experiments. Using predefined coordinates, stereotactic injections were performed in P2 mice and then chased for 3, 7, 15 or 30 days post infection (DPI). **(b)** Initial images from the cortex of a Jag1FL 30 DPI mouse, stained for Jag1 and Olig2. **(c)** Jag1FL transduced cortical cells express Sox10 by 30 DPI. Scale bars = 20 μ m

Figure 23: Time-course of Jag1FL transduced mice at **(a)** 3 DPI, **(b)** 7 DPI, **(d)** 15 DPI, and **(e)** 30 DPI. **(c)** Quantification of average migration distance of transduced cells in the cortices of 7 and 15 mice. $p=0.02$; Scale bars = 200 μ m

Figure 24: 30 DPI Jag1FL transduced cells upregulate the oligodendocyte markers Olig2 and Sox10 in all regions analyzed **(a)** Cortex **(b)** Striatum **(c)** Corpus Callosum. **(d)** Quantifications of the number of transduced cells by region which are Olig2⁺/Sox10⁺. $n = 2$; Scale bars = 20 μ m

Figure 25: *in vivo* Jag1FL expression results in the significant upregulation of Sox10. **(a)** By 30 DPI, Sox10 is upregulated in all regions brain regions containing Jag1FL-IRES-GFP⁺ cells (CC = Corpus callosum, Ctx = Cortex, Str = Striatum). **(b)** This change in Sox10 expression is already significant by 15 DPI with almost twice as many Jag1FL-IRES-GFP⁺Sox10⁺. **(c)** Jag1FL-IRES-GFP⁺Sox10⁺ cells analyzed by neural region, over the course of a 30 day time-chase. $n=3$

Figure 26: Largest shift in Jag1FL-IRES-GFP⁺Sox10⁺ populations seen in the cortex. **(a and b)** Jag1FL-IRES-GFP⁺Sox10⁺ expression plotted by region over time. Significant shifts from control treated mice are demonstrated in cortices from as early as 3 DPI, and becomes more pronounced until 15 DPI where it eventually plateaus at just below 80% Jag1FL-IRES-GFP⁺Sox10⁺. $n=3$

Figure 27: Summary of shift in Jag1FL-IRES-GFP⁺Sox10⁺ populations. **(a)** Representative images of counts used in quantifying transduced cells from

figures 5 and 6. **(b)** Shift of Jag1FL-IRES-GFP⁺Sox10⁺ are summarized in this diagram with dark blue containing low densities of Sox10⁺ transduced cells and red representing high densities. Scale bars = 200µm

Figure 28: Jag1FL-IRES-GFP⁺Sox10⁺ cells express the early oligodendrocyte marker NG2 but not PDGFR α or the neuronal marker Dcx. **(a)** Representative images of Jag1FL-IRES-GFP⁺Sox10⁺NG2⁺ cells in the cortex. **(b)** Quantifications were performed in the cortices of 7 DPI mice and **(c)** showed a significant increase in Jag1FL-IRES-GFP⁺Sox10⁺NG2⁺ cells. **(d)** However another early oligodendrocyte marker PDGFR α , **(e)** or the neuronal marker Dcx could not be detected by 30 DPI. Arrows in D and E point to Jag1FL-IRES-GFP⁻ and IRES-GFP⁻ cells but positive for PDGFR α and Dcx respectively. n=3, Scale bars = 20µm

Figure 29: Mature oligodendrocyte markers are expressed by Jag1FL-IRES-GFP⁺ cells. **(a)** Jag1FL-IRES-GFP⁺Sox10⁺CNPase⁺ cells are found frequently in the cortex of 15 DPI mice (white arrow heads) and very rarely in control treated mice. **(b)** They are prevalent still in 30 DPI cortices. By 30 DPI, many are co-positive for MBP in the striatum. Ctx – Cortex; Str – Striatum; CC – Corpus callosum. Scale bars = 20µm

Figure 30: Mature oligodendrocyte marker MBP is expressed by Jag1FL-IRES-GFP⁺ cells. **(a-c)** Representative images of transduced cells in each neural region. **(d)** Overview of Ki67 analysis done in the corpus callosum of 7 DPI cortices. **(e)** No change was seen in proliferation as measured by the expression of the cell cycle marker Ki67. Scale bars = 20µm

Figure 31: Jag1FL expression results in a loss of NSC maintenance. **(a)** Outline of proliferation assay performed in NSCs **(b)** Representative images of the variety of transduction levels seen in neurospheres. **(c)** Sphere forming capacity as measured by percentage of spheres formed from the cells plated. **(d)** Thymidine labeling experiments showed no noticeable differences in Jag1FL treated NSCs compared to control. Percentages converted to arcsin values for student t-test calculations. n=3, Scale bars = 20µm

Figure 32: Jag1FL expression results in an upregulation of oligodendrocyte lineage genes. **(a)** Outline of NSC differentiation assay. **(b)** Representative colonies after being grown for 7 days under differentiating conditions. **(c)** qRT-PCR confirmed that colonies upregulate genes associated with differentiating oligodendrocytes, including the essential transcription factors Olig2, Sox10 and Myrf. **(d)** Colonies were quantified by if they expressed a marker or not. Although both colonies express the marker O4 at the same frequency, there was a loss of colonies expressing GFAP and β -TubIII (β -TubulinIII). **(e)** Representative images of differentiated NSC colonies stained for Jag1, O4, BTubIII and Olig2. Small white circles represent location in the differentiating colony where image was photographed. n=3, Scale bars = 20 μ m

Figure 33: Sequencing of Jag1FL transduced NSC transcriptomes. **(a)** Outline of Jag1FL RNA-Seq experiment. **(b)** NSCs were sorted based on GFP from the IRES-GFP in both the control and Jag1FL viruses. Shown are representative FACS sorting gates and **(c)** a report of total cells sorted for RNA sequencing. n=2

Figure 34: FastQC reports confirm that RNA sequencing of samples went correctly. **(a)** Quality scores of reads across all base pairs in each sample. **(b)** Report of total reads (millions), unique reads (%), Passed filters (%) and % of sequences aligned per sample.

Figure 35: Cross-analysis of RNA-Seq replicates. **(a)** Comparison of % similarity of RNA-Seq replicates to one another. **(b)** Transcriptome comparison of Jag1FL treated NSCs to control NSCs. Thresholds were set at +/- Log₂ fold change of 1, with Log₂counts per million reads plotted on the x-axis.

Figure 36: Jag1FL treated NSCs express genes associated with oligodendrocyte maturation and myelination. **(a)** Summary table of the top 10 gene ontology (GO) categories upregulated in Jag1FL treated NSCs. Although not in the top 10, there were also significant odds ratios for both

oligodendrocyte development and differentiation. **(b)** Changes in genes involved in oligodendrocyte differentiation, maturation and myelination are grouped based on early, intermediate, or late expression (Introduction Fig. 16) **(c)** Wnt signaling genes were largely unchanged, however a notable decrease was seen in Wnt3.

Figure 37: Summary of target genes identified in RNA-Seq. **(a)** Lysates from NSCs prepared in parallel to the RNA-Seq samples were used to confirm targets by qRT-PCR. Although expression levels of Olig2 did not change significantly (data not shown) interestingly Sox10 levels increased nearly 3 fold. **(b)** New lysates prepared in a similar fashion to those used in the RNA-Seq, but not in parallel, confirmed additional targets such as Myrf and PDGFR α , however the relative fold changes are far more exaggerated (n=3 biological replicates). **(c)** Table summarizing the top 15 genes upregulated in Jag1FL treated NSCs. Genes with stars are of particular interest due to their reported positive roles in promoting oligodendrogenesis. Through qRT-PCR analysis, 84.21% of genes identified in the screen were true positives.

Figure 38: Summary of an on going collaboration examining the ability of grafted Jag1FL-IRES-GFP⁺ NSCs to remyelinate *in vivo*. **(a)** Overview of current experiments using both lysolecithin lesion treated mice and citron-kinase KO mice (For full summary see 0) **(b)** Representative images of NSCs used in grafting experiments, before and after FACS sorting. Scale bars = 20 μ m

Figure 39: Initial results from the first lysolecithin treated mice. **(a)** Overview images from a Jag1FL-IRES-GFP⁺ NSC grafted mouse **(b)** and an IRES-GFP control grafted mouse. **(c-e)** Jag1FL-IRES-GFP⁺ express CNPase which is not seen in control grafted cells. **(f-h)** Jag1FL-IRES-GFP⁺NG2⁺ cells are present and not seen in control grafted cells. Scale bar = 20 μ m

Figure 40: Initial results from the first Cit-K KO mice. **(a)** Overview of Jag1FL-IRES-GFP⁺ grafted cells which **(b-c)** express the mature myelinating marker CNPase. **(d-e)** Populations of cells in Jag1FL-IRES-GFP⁺ grafted

mice are quite heterogeneous and some appear more astrocytic. (f-g) Control grafted cells do not express CNPase. (h-i) Jag1FL-IRES-GFP⁺ grafted cells express NG2 (j-k) which is not seen in control grafted cells. Scale bar = 20µm

Figure 41: Jag1 signals through its ICD to regulate neurogenesis. (a) Embryonic day 10 Jag1^{-/-} mice show maintained neural progenitors (Sox2⁺) and reduced neurons (β-TubulinIII⁺) in the dorsal telencephalon compared to wild type littermates (wt). Note also the reduced β-Tub expression in the ventral telencephalon and in the hindbrain (hb) (data not shown). (Photo by Marion Rukavina) (b) Transfection of the lateral ventricular wall of E13.5 embryos using IUE. (c and d) Expression of JICD or JICD-GFP fusion in neural progenitors *in vivo* causes a precocious exit from the VZ to the SVZ/IZ (P<0.05). (e-i) JICD expressing cells down regulate progenitor marker expression (P<0.05* and <0.001**) and activate basal progenitor (Tbr2) and neuronal gene expression (β-TubIII/NF160) (P<0.001). LV - lateral ventricle; LGE - lateral ganglionic eminence. Scale bars = 20µm.

Figure 42: (a) Even though JICD induces precocious differentiation within 24 hours, and this is maintained, JICD expressing cells progress and differentiate into Tbr1⁺ neurons. Tbr1 expression of transfected cells (green) 48 hours post-electroporation. (b). Quantification shows no difference in Tbr1 expression between control and JICD expressing cells, indicating that JICD expressing cells are still able to go through a normal differentiation program. (c-f) JICD expression reduces the number of cells passing through S-phase 22-24 hours post-electroporation but does not induce cell cycle exit. (c) Scheme showing the BrdU labeling paradigm after transfection. Twenty-two hours after IUE, a single dose of BrdU was given intraperitoneal to the mother. Embryos were isolated three hours later. (d) Combined staining of cell cycle marker Ki67 (to mark cells in the cell cycle) and S-phase label BrdU in JICD (left) and GFP-only (right) transfected cells in the developing forebrain. (e) Quantification of BrdU incorporation revealed that less JICD expressing cells passed through S-Phase between 22-24 hours post-electroporation. (f) Quantification of the transfected cells expressing the cell cycle marker Ki67 indicated that JICD expressing cells remain in the cell

cycle. However, combining Ki67 and BrdU revealed that the cell cycle length on dividing JICD expressing cells is extended. VZ - ventricular, SVZ - subventricular zone and CP - cortical plate. Scale bars = 20µm. $P < 0.001$.

Figure 43: (a-c) Identification of JICD binding partners and JICD directly regulates the Wnt target Axin2. **(a)** A subset of JICD interacting proteins identified in the Yeast-2-Hybrid (Y2H) and Tandem Affinity Purification (TAP) screens. **(b)** Confirmation that full length Jag1 can interact directly with PICK1 and PKC α by co-immunoprecipitation. Both are critical in mediating regulated intramembrane proteolysis of Jag1. **(c)** Both PICK1 and PKC α were confirmed to also bind JICD. **(d)** PKC α translocates to the plasma membrane and colocalizes with Jag1 upon stimulation with phorbol ester (PMA). Full-length (FL) Jag1 GFP fusion is expressed at the cell membrane of transfected HEK293 cells. Endogenous PKC α is distributed in the cytoplasm (mock) and translocates to the plasma membrane where it co-localizes with Jag1FL only upon activation with PMA. **(e)** JICD interacts with TBLR1 **(f)** and core Histones including H3. **(g-k)** Jag1 undergoes RIP in vivo, which is controlled by PICK1 and PKC α . **(g and h)** Jag1 is a substrate for RIP to generate Jag1-CTF1 and JICD. Blockage of gamma-secretase increases CTF1 accumulation ($P < 0.05^*$) and phorbol ester (PMA) activation of PKC stimulates RIP of Jag1 ($P < 0.001^{**}$). **(i, j and k)** An 80% shRNA knockdown of PICK1 ($P < 0.001^{**}$) abolishes PMA-induced RIP and accumulation of Jag1-CTF1 compared to control shRNA (ctrl sh) expressing cells ($P < 0.001^{**}$). All data provided by Antje Grabosch. Scale bar = 5 µm.

Figure 44: (a) Endogenous Axin2 and synthetic TopFlash luciferase reporters used in studying JICDs ability to potentiate of Wnt signaling **(b)** JICD potentiates stabilized β -Catenin activity on the TopFlash Luciferase reporter and **(c)** synergizes with TBLR1 and β -Catenin to potentiate activity of the Axin2 promoter (blue bar). **(d)** Neither p300 nor CBP copurified with JICD. **(e)** Tle1, Tle2 or Tle3 did not copurify with JICD.

Figure 45: (a and b) The JICD contains a nuclear localization signal (RKRRK) downstream of the gamma-secretase cleavage site and a C-terminal PDZ-

ligand (YIV). C-terminal truncations (F1-F3) revealed that the TBLR1 interaction domain likely lies in the middle of the protein and deletion of the C-terminus does not affect TBLR binding. **(c)** Although able to bind TBLR1, JICD-F1 has lost its ability to potentiate β -Catenin activity even in the presence of TBLR1 (blue bar). **(d)** The C-terminal 25 amino acids of JICD are required for the JICD-mediated potentiation of β -Catenin-mediated transcription. HEK 293 cells were transfected with the Wnt-reporter TopFlash, pRL Renilla luciferase expression plasmid, sub maximal levels of constitutive active β -Catenin, TBLR1 expression vector, vectors expressing JICD or JICD truncation mutants (F1-F3). Truncation of JICD at the C-terminus blocked transcriptional potentiation even in the presence of TBLR1 although the truncated JICD proteins are able to bind TBLR1. Luciferase activity was determined 48 hours post-transfection. The graphs show representative mean values from three independent experiments performed in triplicate. All values are normalized to the transfection control Renilla luciferase values.

Figure 46: The PDZ-ligand domain of Jag1 and the PDZ domain of PICK1 are critical for their induction of neurogenesis. **(a)** JICD PDZ-ligand deletion mutant (JICDdelPDZ) still localizes to the nucleus of transfected cells. **(b)** JICDdelPDZ does not potentiate Wnt/ β -Catenin dependent transcription. **(c)** Blockage of PKC α activity (RO 32-0432) severely reduces the effect of JICD on Wnt/ β -Catenin signaling. **(d-g)** JICDdelPDZ does not induce loss of progenitor marker expression, exit from the ventricular zone (VZ), or induction of basal progenitor (Tbr2) or neuronal genes (Tbr1) and over expressing cells mature normally.

Figure 47: JICD is directly bound to chromatin. **(a)** Subcellular fractionation of N2A cells transfected with Jag1CD-eGFP or the eGFP control plasmid. **(b)** Provides direct evidence that JICD is bound to chromatin. Therefore to determine binding locations a **(c)** Chromatin immunoprecipitation (ChIP) followed by deep sequencing was performed. **(d)** Experimental outline of the ChIP protocol. **(e)** In parallel, sister plates of N2A cells were transfected to analyse gene transcripts by qRT-PCR. **(f)** Axin2 potentiation by JICD, stabilized β -Catenin, and TBLR1 was confirmed in transfected N2As. **(g)** JICD

expression was confirmed at the protein level. **(h)** ChIP settings were optimized, including Covaris sonication shearing times. **(i)** A summary of ChIP samples sent for sequencing. Samples from three independent ChIPs were sequenced.

Figure 48: Workflow for Illumina HiSeq2000 sequencer. (Image from (Illumina 2011))

Figure 49: Heat map comparison of promoter enrichment in all ChIP samples sequenced. Although low levels of similarity was seen amongst ChIP replicates, there were still peaks shared amongst multiple replicates.

Figure 50: A summary of all reads that mapped to the mouse genome in ChIP samples.

Figure 51: A summary of unique reads per ChIP sample.

Figure 52: The process of target discovery in JICD ChIP-Sequencing. **(a)** Outline of how ChIP-Seq analysis was performed. **(b)** Gene ontology (GO) category analysis showed an enrichment for both the promoter of Wnt target genes and genes involved in myelination. **(c)** Targets were chosen and relative expression levels screened by qRT-PCR of cDNA generated from sister transfected plates. In the treatment where JICD-NTAP/ β -Catenin/TBLR1 were co-expressed, upregulation of Axin2, Lgr5, Lef1 and Id2 was measured.

Figure 53: Analysis of peaks using UCSC and Washington genome browsers. **(a)** Peaks specific for both JICD alone and JICD-NTAP/ β -Catenin/TBLR1 co-expressed were identified for Axin2 in the immediate promoter region. **(b)** Peaks specific for JICD-NTAP/ β -Catenin/TBLR1 co-expression identified in Lgr5.

Figure 54: JICD can be enriched at the promoters of Wnt target genes in the presence of β -Catenin and TBLR1. Peak specific primers were designed and

tested on genomic DNA before performing quantitative ChIP PCR on ChIP elutes. In **(a)** Axin2 **(b)** Id2 **(c)** Lef1 and **(d)** Lgr5, peak specific enrichment could be detected in JICD-NTAP/ β -Catenin/TBLR1 ChIP samples, suggesting that JICD is bound and contributing to regulation of these genes.

Supplementary Table 1: Summary of findings in RNA-Seq, grouped by signaling pathway and function. For genes that have verified, the qRT-PCR result is listed next to the predicted relative expression.

Supplementary Table 2: Summary of ChIP-Seq peaks identified by the screen outlined in Fig. 31. Peaks are organized by treatment, with the number of times the peak occurs in the promoter of each gene. Additionally, inter-comparison of ChIP treatments shows if the peak is present in other sample (true) or not (false). J – JICD; JB - JICD-NTAP/ β -Catenin, JBT - JICD-NTAP/ β -Catenin/TBLR1.

4 Discussion

4.1 Jag1FL in the role of NSC niche maintenance

4.1.1 Jag1FL as a key regulator of stem cell fate

In this project, AAV and RV were engineered to study the gain-of-function effects of Jag1FL in the NSC niche. AAVs are well suited for gene delivery because they can transduce both dividing and non-dividing cells, making them an optimal candidate for targeting quiescent stem cell populations in the niche. Live virus production requires a high transfection efficiency of AAV-293 packaging cells (Fig. 20F) since cells must be simultaneously transfected with the pAAV-RC and the pHelper plasmids. Although high transfection efficiency was achieved, low titers of AAV-Jag1FL virus were obtained, which could be due to difficulties in packaging the long viral DNA transcript. Additionally, it has been shown that AAV viruses can stably incorporate into the genome of host cells in approximately 15% of the infection events, resulting in a high transient but relatively low stable transduction rate. RVs however can only transduce and incorporate their genome into proliferating cells and integration is a prerequisite for expression, but they can accommodate longer DNA fragments (Deregowski and Canalis 2008). Due to this, I was able to integrate an internal ribosome entry site (IRES) and reporter protein (GFP) for monitoring viral infected cells. *In vivo*, this allowed for RV transduced cells to be lineage traced based on GFP expression.

Once established, these tools allowed me to study the effects of a Jag1FL gain-of-function in the NSC niche. Surprisingly, expression of Jag1FL-IRES-GFP resulted in a fate shift of transduced cells to the oligodendrocyte lineage as measured by Sox10 expression (Fig. 25,26). Sox10 was used in this study as a marker for oligodendrocytes since there are no known Sox10⁻ oligodendrocyte lineages (Kessaris, Fogarty et al. 2006). Additionally, initial analysis demonstrated that all Sox10⁺ transduced cells were also Olig2⁺, which is another key transcription factor in oligodendrogenesis (Results Fig. 24, Introduction Fig. 14). To determine where this fate shift may be occurring, I performed a time course analysis for 30 DPI. By 15 DPI mice exhibited almost twice as many Jag1FL-IRES-GFP⁺Sox10⁺ cells in the cortex as

compared to controls. This increase was mirrored in the striatum and corpus callosum. This fate shift was reproduced *in vitro* with NSC cultures where both a decrease in sphere forming capacity (a sign of differentiation), and an increase in oligodendrocyte markers was demonstrated for Jag1FL-IRES-GFP⁺ NSCs. Taken together this would imply that Jag1FL expression results in a fate switch to differentiated oligodendrocytes.

Approximately 40% of Jag1FL-IRES-GFP⁺Sox10⁺ cells in the cerebral cortex at 7 DPI expressed the early OPC marker NG2. A difference of approximately 15% seen in the total percentage of Sox10⁺ transduced cells that were NG2⁺ when compared to the control may hint that these cells have already downregulated NG2 and progressed to a more mature state. Furthermore, no Jag1FL-IRES-GFP⁺ cells were identified with the OPC marker PDGFR α 30 DPI *in vivo*, supporting that they had progressed to a later stage of maturation or suggesting that they were derived from a PDGFR α ⁻ lineage of oligodendrocytes (Spassky, Goujet-Zalc et al. 1998, Spassky, Heydon et al. 2001). However, approximately 30% of Jag1FL-IRES-GFP⁺ cells at 15 DPI were not Sox10⁺, which leads me to ask what these remaining cells are? Analysis is ongoing but in the cerebral cortex many of these cells have astrocytic morphologies.

Oligodendrocyte maturation can be measured through temporally expressed cell markers (Fig. 16). The myelinating oligodendrocyte markers MBP and CNPase were both used to address if transduced cells progress to later stages of maturation. Both MBP⁺ and CNPase⁺ Jag1FL-IRES-GFP⁺ cells were identified throughout the cerebral cortex, corpus callosum and striatum suggesting that they were actively myelinating. Quantifications are currently ongoing, however this myelinating phenotype was not observed so frequently in control transduced cells at 15 DPI, particularly in the cortex.

Although there was a striking phenotypic increase in myelinating oligodendrocytes (based on morphology and IHC) induced by Jag1FL-IRES-GFP⁺ 30 DPI, this is not the first study that proposed Jag1 might play a role in promoting remyelination (Seifert, Bauer et al. 2007). Seifert and colleagues identified that astrocytes present Jag1 at the site of both actively demyelinating and remyelinating lesions in mice (Seifert, Bauer et al. 2007). However, they showed that remyelinating lesions contain far more Jag1⁺

astrocytes than demyelinating lesions. Additionally, Notch receptor expression was present in lesions that were remyelinating and not in non-remyelinating lesions (Seifert, Bauer et al. 2007).

Contrary to these findings there has been a long-held belief that Jag1⁺ reactive astrocytes play a negative role in remyelination. A recent publication from Hammond and colleagues demonstrates that through induction of Jag1 by the soluble Endothelin-1, Notch activity increases in OPCs at the site of lesions and results in a decrease of remyelination (Hammond, Gadea et al. 2014). Interestingly, in OPCs with the Notch1 receptor specifically KO in adult mice, no noticeable differences were seen in remyelination efficiency, suggesting that Notch or other members of the Notch family are not a rate-limiting determinant of remyelination (Stidworthy, Genoud et al. 2004). These conflicting results raise the interesting possibility that the role of Notch signaling is much more complicated in OPC development than previously thought.

On going experiments hope to address the role of Jag1 in remyelination *in vivo* (experimental outline Fig. 38a). Firstly, I am curious if Jag1FL-IRES-GFP⁺ NSCs can remyelinate an actively demyelinating lesion. Using lysolecithin, a drug known for its ability to induce demyelinating lesions, Jag1FL-IRES-GFP⁺ NSCs are being grafted into either the contra- or ipsilateral hemispheres and compared to IRES-GFP⁺ cells (experimental method from (Binder, Rukavina et al. 2011)). Contralaterally grafted cells will address whether or not Jag1FL-IRES-GFP⁺ cells can migrate to the site of lesion, and furthermore if they can begin to express markers of OPCs. These experiments will possibly determine if Jag1FL-IRES-GFP can also induce the same fate in actively demyelinating lesions.

Initial analysis of these mice show a notable increase in survival of Jag1FL-IRES-GFP grafted cells, which also appear to migrate further towards the lesion. Many of the Jag1FL-IRES-GFP⁺ cells are also Sox10⁺, but interestingly there are also many surrounding cells that express Sox10 but are negative for the reporter. Either these are native cells that have migrated to the lesion or transduced cells that silenced the virus. Virus silencing is a phenomenon we have experienced before *in vitro*, so this would not be completely unexpected. Jag1FL-IRES-GFP⁺ grafted cells also appear to

express CNPase to a certain degree, although due to the high density and overlapping processes of grafted cells, it is difficult to clearly discern. Further analysis and quantifications will be needed in order to determine what these cells may be. Additionally, it will be interesting to see if this phenotype becomes more pronounced by 30 DPI, with all Jag1FL-IRES-GFP⁺ grafted cells maturing to myelinating oligodendrocytes.

Secondly, I asked if Jag1FL-IRES-GFP⁺ NSCs can still become OPCs or furthermore, myelinate in a non-OPC-permitting environment? To address this, we are using Cit-K KO mice. Cit-K is a crucial regulator of cytokinesis in neuronal precursors and Boda and colleagues have demonstrated that these mice display a limited number of OPCs in both the cortical grey and white matter (E. Boda 2013). Grafting GFP expressing OPCs showed that they were capable of migrating and invading the entire brain, but never gave-rise to mature oligodendrocytes. They also demonstrated that Cit-K is involved in glial cell divisions and OPCs lacking Cit-K are prone to undergo apoptosis. Due to fewer myelinating oligodendrocytes in the brains of Cit-K KO mice, Jag1FL-IRES-GFP⁺ NSCs may exhibit an exaggerated OPC migration phenotype.

Surprisingly, initial analysis of Jag1FL-IRES-GFP⁺ grafted mice found multiple CNPase⁺ transduced cells which is a marker for mature myelinating oligodendrocytes. This will need to be analyzed further to determine if transduced NSCs already express CNPase at the time of grafting, or if this is upregulated post-grafting. Jag1FL-IRES-GFP⁺ grafted cells also exhibit other oligodendrocyte markers including the early OPC marker NG2. Further quantifications of both early and late oligodendrocyte markers are currently ongoing.

4.1.2 Regulation of genes involved in oligodendrocyte maturation identified by the Jag1FL-IRES-GFP⁺ NSC RNA-Seq

One of the plausible explanations for why Jag1FL induces a shift to an OPC fate *in vivo* could be that Jag1 directly regulates genes involved in oligodendrogenesis. Both Sox10 and Myrf have been reported extensively as key determinants of oligodendrocyte maturation (Introduction Fig. 17), with Sox10 being expressed throughout the oligodendrocyte lineage (Kuhlbrodt,

Herbarth et al. 1998, Stolt, Rehberg et al. 2002, Li, Lu et al. 2007, Finzsch, Stolt et al. 2008, Rivers, Young et al. 2008, Breuskin, Bodson et al. 2009, Emery, Agalliu et al. 2009, Koenning, Jackson et al. 2012). Sox10 can stimulate expression of Myrf, which together can act as a transcriptional complex regulating downstream genes involved in myelination (Hornig, Frob et al. 2013). Interestingly Sox10 and Myrf were confirmed through qRT-PCR to be upregulated in Jag1FL-IRES-GFP⁺ cells, and Jag1FL-IRES-GFP⁺Sox10⁺ cells could be detected by IHC throughout all brain regions analyzed in transduced animals. This suggests that potentially Sox10 is a downstream effector of Jag1 signaling.

Other genes known to be involved in oligodendrocyte maturation and myelination were upregulated in the Jag1FL-IRES-GFP⁺ NSC RNA-Seq including Tenascin-R (Tnr), Erbb4, Enpp6, Fatty acid 2-hydroxylase (Fa2H) and homeodomain interacting protein kinase 2 (HipK2). These genes will need to be addressed in detail through gain- and loss-of-function experiments to help elucidate the regulatory role of Jag1. The known roles of these genes and their effects on oligodendrogenesis are briefly covered below.

The first target gene that will be studied is Tnr, which is part of a family of extracellular matrix glycoproteins that are spatially and temporally controlled throughout development (Chiquet-Ehrismann, Orend et al. 2014). Of the four members of the tenascin family, Tnr is the only one shown to be exclusively expressed in the developing and adult nervous system (Rathjen, Wolff et al. 1991). In the absence of PDGFR α , Tnr was shown to both enhance adhesion and maturation of oligodendrocytes by inducing myelin gene expression (Pesheva, Gloor et al. 1997). Although recent studies have confirmed that Tnr promotes differentiation of oligodendrocytes *in vitro*, it was also shown that it could antagonize myelin membrane formation (Czopka, Von Holst et al. 2009). Tnr KO mice could be used to address the loss-of-function of Tnr in Jag1FL-IRES-GFP transduced animals (Weber, Bartsch et al. 1999).

The second target gene, is the neuregulin-1 (Nrg1) receptor Erbb4 which has been demonstrated to be an important mediator of oligodendrocyte survival and maturation (Park, Miller et al. 2001). Although KO mice display normal myelin structure, their myelin sheaths are significantly thinner (Roy, Murtie et al. 2007). Therefore, it is believed that Erbb4 may directly modulate

OPC responsiveness to Nrg1. Although this was not looked at in this study, ErbB4 was the 8th most enriched target gene in the RNA-Seq screen when NSCs expressed Jag1FL-IRES-GFP (excluding Jag1). Additionally, Nrg1 was slightly upregulated above control NSCs. Taken together, increased signaling through the ErbB4 receptor may act as a positive signal for Jag1FL-mediated OPC survival and maturation.

A third target for future analysis is Fa2H. Fa2H is an enzyme responsible for synthesizing precursor lipids which are later incorporated into the myelin sheath (Alderson, Rembiesa et al. 2004, Eckhardt, Yaghoofam et al. 2005). Fa2H KO mice display disrupted lipid membranes and severe axonal loss (Potter, Kern et al. 2011). Therefore, a positive regulatory role by Jag1 might hypothetically result in increased myelin lipid membrane formation.

However, not all upregulated genes in the RNA-Seq have been reported to promote oligodendrocyte maturation, and in fact some are known inhibitors. When over expressed, Bmp4 has been shown to drive progenitor cells *in vivo* to an astrocytic lineage at the expense of oligodendrocytes (Gomes, Mehler et al. 2003, Samanta and Kessler 2004). Bmp4 acts through activation of the Smad1/5/8 transcription factors, which translocate to the nucleus and regulate target genes (Massagué, Seoane et al. 2005). Interestingly HipK2 was also elevated in the Jag1FL-IRES-GFP RNA-Seq and is a known inhibitor of Bmp signaling, acting by limiting the level of Smad activation (Chalazonitis, Tang et al. 2011). Therefore, while Bmp4 may be expressed at high levels in Jag1FL-IRES-GFP⁺ cells (Fig. 37c), it is possible that Bmp signaling is moderated by HipK2 in Jag1FL expressing cells. In addition HipK2 has been shown to inhibit Wnt/ β -catenin signaling through phosphorylation of TCF/LEF transcription factors, preventing their binding to DNA (Gao, Xiao et al. 2014). Since Wnt signaling is both a requirement in early OPC commitment and an inhibitor in later stages of oligodendrocyte differentiation, HipK2 may be an interesting target to address oligodendrocyte regulation at different stages and by modulating different signaling pathways (Fancy, Baranzini et al. 2009). Additional genes downregulated in Jag1FL-IRES-GFP⁺ cells included Lars2, CD68, and Lag3, which are all associated with psychiatric disorders or inflammatory MS lesions (Werner, Pitt et al. 2001, Tkachev, Mimmack et al.

2003, Munakata, Iwamoto et al. 2005, Chiu, Morimoto et al. 2013). How Jag1 regulates these genes is not clear, but could be the focus of future studies.

4.1.3 Hypothesis: Wnt signal regulation by Jag1 determines OPC specification

Interestingly, the Jag1FL-IRES-GFP NSC RNA-Seq showed a general trend in Wnt signal reduction (Fig. 36c). Supporting this data, the JICD experiments in the second half of my thesis also demonstrated a regulation of Wnt target genes in a cell autonomous manner. However, the Jag1FL gain-of-function experiments do not allow us to address whether this is due to a cell autonomous or non-autonomous effect. Since Wnt signaling must be downregulated for OPCs to mature, Jag1 may play a role in mediating this transition. The Wnt transcriptional target Axin2 is known to autoregulate and repress the Wnt pathway by promoting degradation of β -catenin (Behrens, Jerchow et al. 1998, Jho, Zhang et al. 2002, Lustig, Jerchow et al. 2002, Zeng and Nusse 2010). Through inhibition of Wnt signaling, Axin2 is believed to be an essential regulator OPC progression (Fancy, Harrington et al. 2011). Sox5, a known stimulator of Axin2 expression, was upregulated at the mRNA level in Jag1FL-IRES-GFP NSCs (Martinez-Morales, Quiroga et al. 2010). However, no noticeable change was observed in Axin2 mRNA levels following expression of Jag1FL. Another known inhibitor of the Wnt pathway is APC and deletion studies have shown to result in complete dysregulation of Wnt/ β -catenin signaling (Lang, Maeda et al. 2013). Therefore it is believed that OPC maturation requires APC expression to prevent transition to a high-Wnt signaling state (Fancy, Harrington et al. 2014). Although the *in vivo* gain-of-function experiments in this study did not address this, the role of Jag1FL and its regulation of Wnt signaling in OPCs would be an interesting avenue of future inquiry.

To address these questions *in vivo* transgenic Wnt reporter mice, such as the BAT-gal or Axin2-LacZ mouse, could be used (Lustig, Jerchow et al. 2002, Maretto, Cordenonsi et al. 2003). With the BAT-gal mouse, future experiments could measure the levels of Wnt activity in Jag1FL-IRES-GFP⁺ cells *in vivo*. Similarly, the use of an Axin2 reporter mouse could characterize Jag1FL-IRES-GFP⁺ cells by Axin2 expression.

A second approach to study Wnt signaling downstream of Jag1FL could be *in vitro* OPC differentiation studies that would allow for direct manipulation of Wnt target genes in Jag1FL-IRES-GFP⁺ cells. It would be interesting to see if the ligand Wnt3, an activator of the canonical Wnt signaling pathway and downregulated in the Jag1FL-IRES-GFP RNA-Seq screen, could cause a loss-of-function when reintroduced into Jag1FL-IRES-GFP⁺ cells. Additional targets could be identified and their impact on differentiation measured using both gain- and loss- of function studies.

4.1.4 Interaction partners of JICD pertaining to the phenotype observed in Jag1FL NSC niche gain-of-function experiments

An interesting observation made when analyzing the Y2H screen for JICD interaction partners was that not only did the JICD interact with PICK1 and PKC α , but also with Galectin-3 and Pmp2, both of which have known roles in oligodendrocyte maturation and myelination (Majava, Polverini et al. 2010, Pasquini, Millet et al. 2011). This is only a tentative link and has not yet been confirmed, but co-immunoprecipitation studies should reveal if these interactions are true. The implications of these interactions are however unclear. Galectin-3 is highly expressed by activated microglia at the sites of MS lesions and was originally thought to play a negative role in remyelination by aiding myelin phagocytosis (Rotshenker, Reichert et al. 2008). However, a study by Pasquini and colleagues demonstrated that Galectin-3 actually assists myelination through promoting OPCs to differentiate and favours oligodendrocytes following differentiation of NSCs (Pasquini, Millet et al. 2011). Direct interactions would not be unexpected with Jag1 since Galectins can interact with *N*-glycans on the surface of glycoproteins, however why an extracellular protein would interact with the cytoplasmic JICD is unclear. A loss of *N*-glycans in Notch receptors has been hypothesized to increase endocytosis and potentially reduce Notch signaling (Stanley and Okajima 2010). Therefore interactions with Galectin-3 may stabilize Jag1 at the membrane, allowing for maintained activation of Notch.

4.1.5 Hypothesis: Regulation of CD4⁺ T-Cell development at the site of lesions by competition between the Notch ligands Jag1 and Dll

Due to the complicated nature of demyelinating diseases such as MS (See 2.4.6), the interplay between stem cell maintenance, autoimmune regulation and tissue homeostasis must all be addressed concurrently. Although my work has only studied the effect of Jag1FL on the NSC niche, Notch ligands Jag1 and Dll both have a known competitive role in CD4⁺ T-cell development (Stidworthy, Genoud et al. 2004, Elyaman, Bradshaw et al. 2007, Seifert, Bauer et al. 2007, Reynolds, Lukacs et al. 2011). In an animal model of MS termed experimental autoimmune encephalomyelitis (EAE), CD4⁺ Th1 T-cells induce inflammatory demyelinating lesions. Competition at the site of EAE lesions between Dll and Jag1 influences the fate of T-cells to either an inflammatory Th1 or an anti-inflammatory Th2 cell, respectively (Fig. 56) (Stidworthy, Genoud et al. 2004, Elyaman, Bradshaw et al. 2007, Seifert, Bauer et al. 2007, Reynolds, Lukacs et al. 2011). Further, proinflammatory cytokines IFN- γ , TNF- α and IL-17 all inhibit Jag1 expression at the site of actively demyelinating lesions. Thus, through forced expression of Jag1 in a focal lesion there is the potential that a stimulated Th2 response will induce a faster recovery. Understanding the molecular mechanisms and how Jag1 moderates the Th2 T-cell response will be essential for future studies of MS.

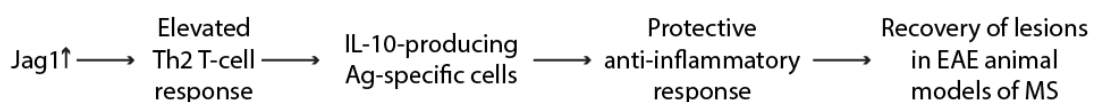


Figure 54: General theory in the literature regarding how Jag1 differentially affects T-cell development, resulting in recovery of lesions in EAE lesions. (Interpreted from (Aharoni, Teitelbaum et al. 1997, Amsen, Blander et al. 2004, Amsen, Blander et al. 2004, Rutz, Mordmüller et al. 2005, Elyaman, Bradshaw et al. 2007)). Ag: Antigen.

4.1.6 Conclusions

This study has identified a novel oligodendrocyte fate shift occurring in NSCs of the postnatal mouse mediated by Jag1FL-IRES-GFP. Populations were identified by the oligodendrocyte lineage marker Sox10 and other known

markers of OPCs, and transcriptome profiles of Jag1FL-IRES-GFP⁺ NSCs compared to controls. This revealed a global shift in mRNA transcription, expressing genes involved in differentiation of oligodendrocytes. Although many potential molecular mechanisms could be acting simultaneously in Jag1FL-IRES-GFP⁺ treated NSCs, the end result is that Sox10 is upregulated, driving cells to early OPCs. Since it has been demonstrated that Sox10 directly regulates the expression of Myrf, which was also up at the transcript level in our studies, I believe these may both be downstream effectors of the Jag1 signaling pathway (Fig. 57). Therefore studying this interplay between Sox10, Myrf and Jag1 will be fundamental to future studies of oligodendrogenesis and remyelination.

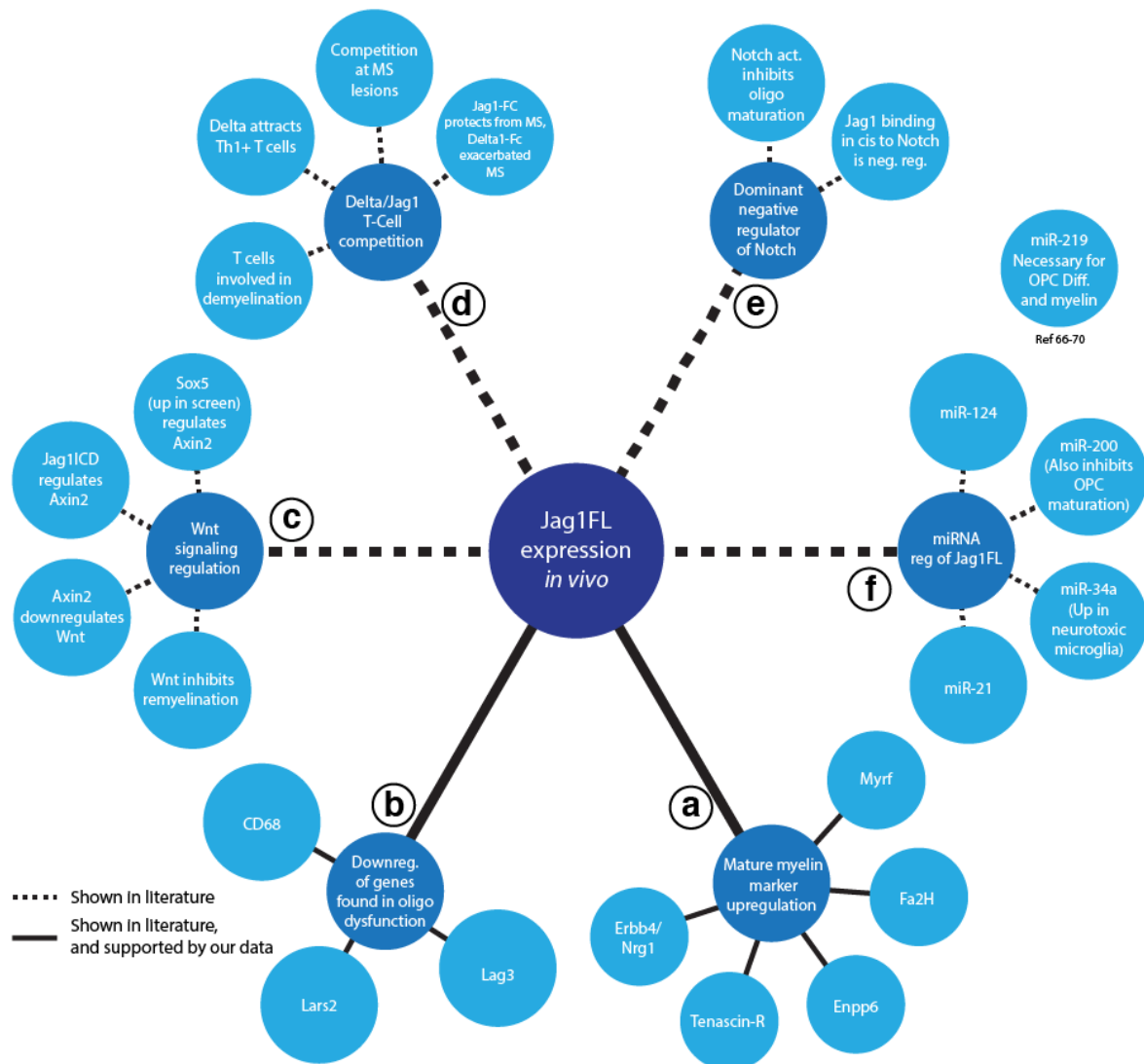


Figure 56: Summary of potential mechanisms driving the fate shift in Jag1FL-IRES-GFP⁺ NSCs. **(a)** Mature myelin genes are upregulated in the Jag1FL-IRES-GFP RNA-Seq, **(b)** Additionally, genes involved in oligodendrocyte dysfunction, including CD68, Lars2 and Lag3 were all down in the Jag1FL-IRES-GFP RNA-Seq. **(c)** Wnt signaling has a known role in inhibiting OPCs from maturing. Through regulation of Wnt antagonists, Jag1FL may play direct role in moderating Wnt signaling. **(d)** Jag1 and Dll compete with each other to regulate CD4⁺ T-cell development at the site of demyelinating MS lesions. Jag1 promotes Th2 T-cell development, resulting in an anti-inflammatory response. Dll promotes Th1 T-cell development, resulting in continued inflammation and degradation of myelin. **(e)** Notch activation has been shown in some cases to inhibit remyelination. Potentially through cis-inhibition of Notch receptor by expressing Jag1FL, this inhibits the negative effects that Notch activation has on remyelination. **(f)** miRNAs including miR-124, miR-34a and miR-200 have all been shown to regulate Jag1 expression in the literature. These miRNAs have also been shown to regulate myelin formation, and potentially there is a link between the regulation of Jag1 and myelin formation by miRNA processing. Solid lines denote data shown in my thesis that is also supported by the literature. Dashed lines have not been shown in my thesis, but are hypothetical mechanisms that have been shown in the literature.

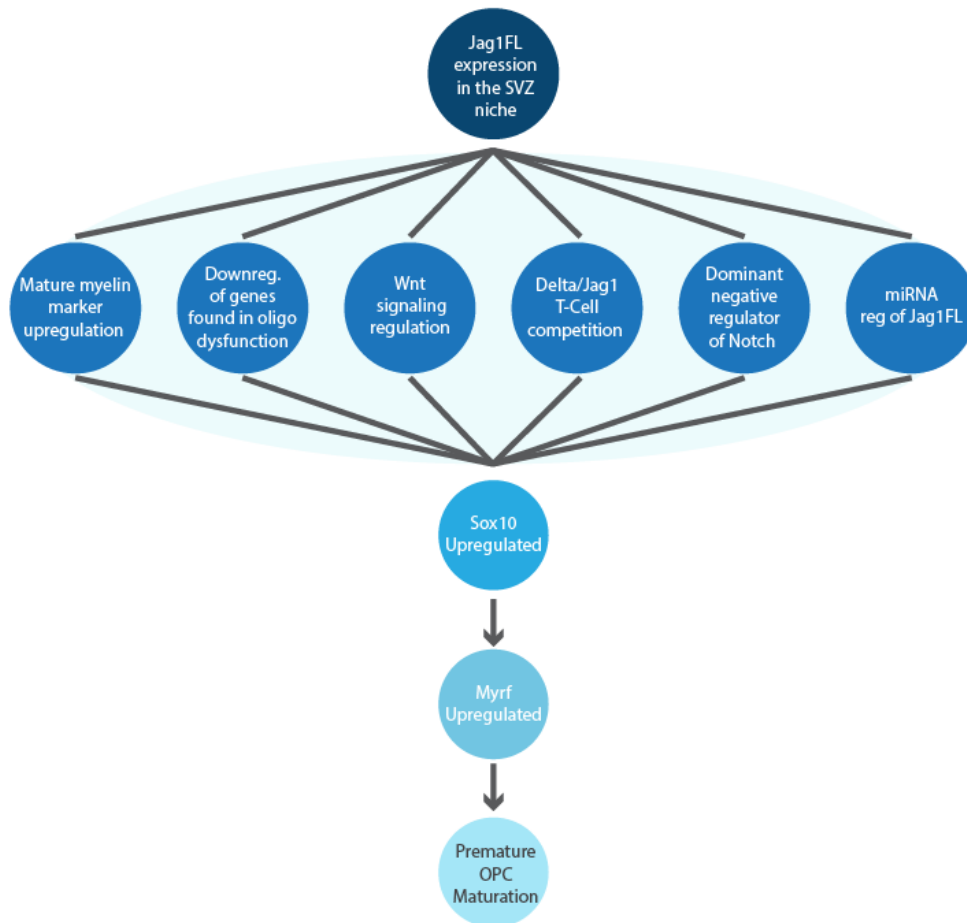


Figure 57: Summary of potential mechanisms driving Sox10 upregulation in Jag1FL-IRES-GFP⁺ NSCs. Although it is unclear what mechanism Jag1 is acting through, according to the literature, there are many potential candidates. Each has been outlined in greater detail both in the discussion and in Fig. 56. It may be that the phenotype observed *in vivo* is due to the result of multiple mechanisms outlined above, however this will need to be addressed in future studies. Based on the *in vivo* phenotype observed in this study, it suggests that Jag1 regulates Sox10 and Myrf, which are both known to promote OPC maturation *in vivo*.

5 The Cell autonomous role of JICD in NSC maintenance

5.1.1 Significant findings of this project

The significant finding of this project was the identification of the sequential proteolytic processing of Jag1, releasing the JICD that signals to the nucleus by binding to chromatin and regulating gene expression including Wnt target genes (Fig. 58). Additional data from the Taylor lab showed that upon activation, Jag1 is bound by PICK1, which then recruits PKC α . PKC α recruitment to the membrane activates ADAM17 by phosphorylation of its ICD, which proceeds to cleave the ectodomain of Jag1. The remaining Jag1-CTF1 is then rapidly processed by γ -secretase, releasing the JICD into the cytoplasm. Due to its N-terminal NLS, JICD translocates to the nucleus where it can directly bind TBLR1 in a PDZ-dependent manner. Through ChIP-Seq studies, the JICD was shown along with TBLR1 and β -catenin to bind gene promoters acting as a transcriptional regulator complex on Wnt genes including Axin2.

5.1.2 JICD can directly regulate the transcription of known Wnt targets by binding to the promoter regions

The functional role of JICD in regulating differentiation was identified through KO and IUE gain-of-function experiments. IUE allows for fast and efficient delivery of DNA constructs to NSCs lining the vesicles of the developing mouse telencephalon. This not only eliminates the need for generating expensive and time consuming transgenic reporter mice, but it also allows for quick analysis of both gain- and loss- of gene function through the additional use of silencing shRNAs. JICD gain-of-function induced a sustained exit of NSCs from the VZ and accompanied by a loss of progenitor markers and an increase in differentiation marker expression (Fig. 41). When the JICD C-terminal PDZ domain was deleted this phenotype was lost, suggesting that the interaction of JICD with PDZ proteins plays a crucial role in mediating the cell autonomous effect of Jag1 signal activation (Fig. 45 & 46). Y2H and TAP screens identified direct protein interactions of JICD with targets including PICK1, PKC α and core histones H3, H4 and H2A, all of which were confirmed through co-immunoprecipitation. Co-expression of TBLR1

and β -Catenin with JICD was shown to potentiate both synthetic Wnt luciferase reporters and endogenous Wnt target genes, implying that JICD could regulate Wnt signaling *in vivo*.

ChIP-Seq is an extremely powerful technique that can identify binding sequences of transcription factors, suggesting their possible direct regulation by the transcription factor being studied. ChIP-Seq confirmed that Jag1 was directly bound to the promoter regions of known Wnt target genes, including Axin2, Lgr5, Id2 and Lef1. Transcript levels from mRNA sister transfected plates demonstrated that when JICD was bound to the promoters of these genes in the presence of TBLR1 and β -Catenin, their expression was potentiated. Taken together, JICD binding to these promoter sequences in combination with β -Catenin regulated the genes expression. However, to properly confirm this claim additional experiments could identify putative consensus binding sequences and then mutate them.

Although there was significant background signal noise in many of the ChIP samples, enriched peaks could still be identified in the ChIP samples in which JICD-NTAP/ β -Catenin/TBLR1 were co-expressed. Analysis of target genes Axin2, Lgr5, Id2, and Lef1 reveals varying roles in Wnt signaling and development. As discussed earlier, Axin2 is a known repressor of Wnt signaling. Contradictory to this, Lgr5 plays a role in activating canonical Wnt signaling. Therefore, JICD may play a role in fine-tuning downstream effectors of the Wnt pathway, exhibiting both a positive and negative regulation in a cell autonomous fashion.

5.1.3 Future outlooks

To address the cell autonomous effects JICD may have on global transcriptome regulation, RNA-Seq experiments of NSCs expressing JICD are currently ongoing (experimental outline Fig. 59). Through cross analysis of transcriptomes from both Jag1FL-IRES-GFP⁺ NSCs, where Jag1 could exhibit both a cell autonomous and non-autonomous effect on NSCs, and JICD NSCs where Jag1 acts autonomously, similarities and differences in transcript profiles can hopefully be identified. Potentially, signaling regulation similarities might explain the effects on Wnt regulation and cellular

differentiation exhibited by both Jag1FL-IRES-GFP and JICD gain-of-function experiments (Outlined in Fig. 60).

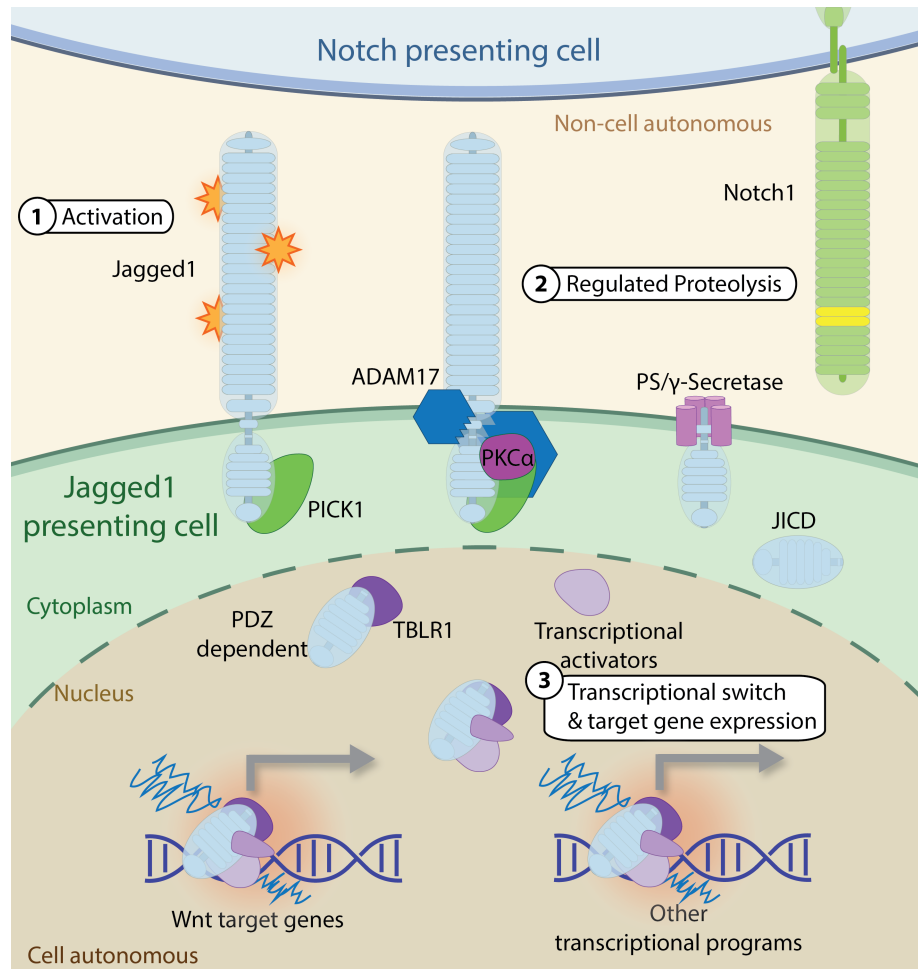


Figure 58: Working model of Jagged1 cell autonomous signaling. Activation of Jag1 results in recruitment of PICK1 and activated PKC α . PKC α phosphorylates the ICD of ADAM17, which leads to the sequential proteolytic cleavage of Jag1 first by ADAM17, releasing the extracellular domain. Jag1-CTF1 is then recognized and processed by γ -secretase, releasing the JICD into the cytoplasm. JICD translocates to the nucleus where it can directly bind TBLR1 in a PDZ-dependent manner. Along with TBLR1 and β -catenin, the JICD can bind promoters of genes including Wnt genes, resulting in a transcriptional switch and target gene expression.

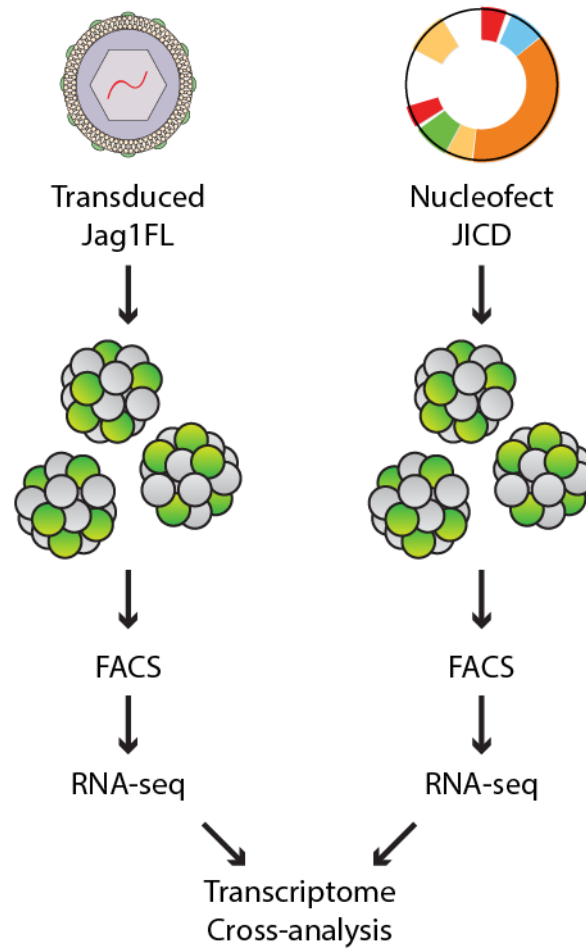


Figure 59: Outline of future RNA-Seq experiments to analyze the cell autonomous role of JICD. Similar to the Jag1FL studies performed in the first half of my thesis, JICD will be transfected into NSCs and then maintained in culture as neurospheres. On the 5th day, neurospheres will be dissociated and NSCs sorted for GFP expression by FACS. RNA will then be immediately isolated and sent for RNA-Seq. The transcriptome profiles of NSCs transfected with only the JICD will then be cross-analyzed with Jag1FL-IRES-GFP⁺ NSCs transcriptome profiles to determine which effects are due to Jag1 non-autonomous and autonomous signaling effects.

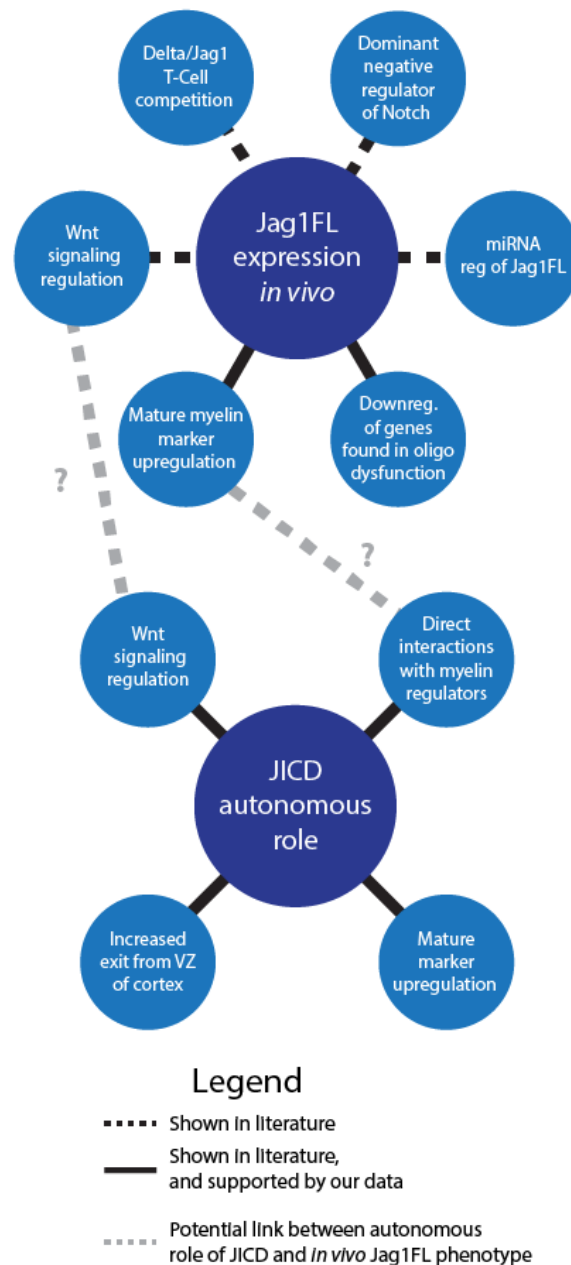


Figure 60: Illustration of the potential links seen in the autonomous role of JICD that may explain phenotypes expressed in Jag1FL-IRES-GFP⁺ NSCs. Based on both the Wnt luciferase reporter data and the JICD ChIP-Seq data, Wnt genes can be regulated by the JICD. Similarly, in the Jag1FL gain-of-function experiments a regulation of Wnt targets was observed. Additionally the JICD directly interacted with both Galectin-3 and Pmp2 both of which have known roles in oligodendrocyte maturation and myelination. Potentially there is a link between the autonomous role of JICD and the *in vivo* Jag1FL phenotype. Discerning if this is due to a cell autonomous or non-autonomous effect will be addressed with on going RNA-Seq experiments, which are outlined in Fig. 59. Solid lines denote data shown in my thesis that is also supported by the literature. Black dashed lines have not been shown in my thesis, but are hypothetical mechanisms that have been shown in the literature. Grey dashed lines are potential links between the autonomous role of JICD and the *in vivo* phenotype based on data and observations presented in this thesis.

6 Materials and Methods

6.1 Methods

6.1.1 Animals and husbandry

Mice were maintained and housed in animal facilities with a 12-hour day/night cycle with adequate food and water under conditions according to DBM University of Basel institutional regulations and under license numbers and 2462 2537, 2538 (Kantonales Veterinäramt, Basel).

6.1.2 Preparation of tissue

Using a ketamine/xylazine/flunitrazepam solution (150 mg, 7.5 and 0.6 mg/kg body weight, respectively), mice were deeply anesthetized by injection and verified to be unresponsive through pinching the paw. Perfusion was performed with ice-cold 0.1M phosphate buffer (PB) followed immediately by 4% PFA prepared in 0.1M PB. Additional fixation over night with 4% PFA was done to ensure full tissue fixation. Next morning, brains were washed 4 times for approximately 10 minutes each, with 0.1M PB and cryopreserved with 30% sucrose solution in 0.1M PB for 48 hours. Brains were embedded in O.C.T. (Sysmex Digitana SA) and coronal sections of 20µm were collected in 24 multiwell dishes (Corning) and stored at -20°C in antifreeze solution until use.

6.1.3 Immunohistochemistry

Tissue sections were incubated for 30 minutes in a blocking buffer solution of 2% normal donkey serum (Jackson ImmunoResearch) 1% Triton X-100 in phosphate-buffered saline (PBS) in a 24 multiwell dish (Corning). Primary antibody was diluted (see table) in blocking buffer solution and incubated with the tissue overnight on a rocking table at 4°C. Next morning sections were washed 4 times with PBS, and incubated for 1 hour with the corresponding secondary antibody diluted in blocking buffer solution. For primary antibodies requiring antigen retrieval, tissue was first incubated in sodium citrate buffer (10mM Sodium Citrate, 0.05% Tween 20, pH 6.0) at 80°C for 10 minutes, and then allowed to cool to room temperature before washing with PBS and proceeding with the standard protocol. For biotinylated secondary antibodies,

sections were washed with PBS after secondary antibody incubation and then incubated for 1 hour with the corresponding peroxidase-conjugated streptavidin antibody (Jackson ImmunoResearch; 1:1000). Sections were incubated with 0.015% 3,3'-diaminobenzidine, 0.0024% H₂O₂ in 0.05 M Tris-HCl, pH 7.6. Sections were mounted on glass slides (VWR), dehydrated and embedded in mounting medium containing 1,4-diazabicyclooctane (DABCO; Sigma) to prevent fading. Sections were then visualized using either a Zeiss LSM510 confocal microscope or a Zeiss Observer microscope with apotome.

Table 1: Antibodies

a) Primary antibodies

| Antigen | Species | Working concentration | Company | Product # |
|-----------------|---------|-----------------------|----------------------|-----------------|
| Beta-TubulinIII | | 1:500 | Sigma | T8660-.2ML |
| Btub3 | Mouse | 1:200 | Sigma | T8660 |
| CNPase | | 1:600 | | |
| Dcx | Goat | 1:400 | Santa Cruz | sc-8066 |
| GAPDH | Mouse | 1:5000 | Biocam | |
| GFAP | Mouse | 1:500 | Sigma | 11814460001 |
| GFP | Rabbit | 1:250 | Invitrogen | A11122 |
| GFP | Sheep | 1:300 | AbD Serotec/Biorad | 4745-1051 |
| GFP | Chicken | 1:250 | Aves labs | GFP-1020 |
| H2A | Rabbit | 1:1000 | | |
| H3 | Mouse | 1:10000 | abcam | |
| Jag1 | Rabbit | 1:500 | Nyfeler et al., 2005 | - |
| Jag1 | Goat | 1:200 | Santa Cruz | sc-6011 |
| Ki67 | mouse | 1:25 | Novocastra | |
| MBP | Rat | 1:500 | Millipore | MAB 386 |
| NG2 | Rat | 1:5 (supernatent) | | AN2 clone 1E6-4 |
| O4 | Mouse | 1:25 | Dr. M. Schwab | |
| Olig2 | Rabbit | 1:600 | Chemicon | AB9610 |
| Pax6* | Rabbit | 1:400 | Covance | PRB-278P |
| PDGFRa | Goat | 1:25 | R&D | AF1062 |
| PICK1 | Goat | 1:1000 | Santa Cruz | sc-9539 |
| Myc-tag | Mouse | 1:1000 | Santa Cruz | |
| Sox2 | Goat | 1:250 | Santa Cruz | sc-17320 |
| Sox10 | Goat | 1:100 | Santa Cruz | sc-17342 |
| Tbr1* | Rabbit | 1:500 | Abcam | AB31940-100 |
| Tbr2* | Rabbit | 1:500 | Abcam | AB23345 |

* Requires antigen retrieval

b) Secondary antibodies

| Species | Fluorophore | Raised in | Company | Product # | Working concentration |
|--------------|-------------|-----------|------------------------|-----------|-----------------------|
| Mouse | Cy3 | donkey | Jackson ImmunoResearch | 715165151 | 1:500 |
| Mouse | Alexa488 | donkey | Jackson ImmunoResearch | 715165151 | 1:500 |
| Rat | Cy5 | donkey | Jackson ImmunoResearch | 712175153 | 1:500 |
| Rabbit | Cy3 | donkey | Jackson ImmunoResearch | 711165152 | 1:500 |
| Rabbit | Alexa488 | donkey | Jackson ImmunoResearch | 715486151 | 1:500 |
| Rabbit | DyLight649 | donkey | Jackson ImmunoResearch | 711496152 | 1:500 |
| Chicken | HRP | donkey | Jackson ImmunoResearch | 703036155 | 1:500 |
| Streptavidin | Alexa488 | donkey | Jackson ImmunoResearch | 16540084 | 1:500 |
| Goat | Cy3 | donkey | Jackson ImmunoResearch | 705165147 | 1:500 |
| Goat | DyLight649 | donkey | Jackson ImmunoResearch | 705495147 | 1:500 |
| Sheep | Cy3 | donkey | Jackson ImmunoResearch | 713165147 | 1:500 |
| Sheep | Alexa488 | donkey | Jackson ImmunoResearch | 711545152 | 1:500 |

6.1.4 Stereotactic injection of RV into postnatal mice

Flaming/Brown micropipette puller (Sutter Instruments) was used to prepare borosilicate glass micro capillaries for viral delivery (Kwick-Fil™). Concentrated RV was prepared by mixing in a 10:1 ratio of virus:Fast Green (10%) (Sigma). Micro capillaries were backfilled with viral suspension, loaded into a microinjector (Pneumatic Pico Pump, WPI Rnage) and secured onto the stereotaxic apparatus (David Kopf Instruments). Postnatal (P2) wild type C57BL/6 mice were anesthetized by incubating on ice for approximately 5-10 minutes before positioning into the stereotaxic apparatus. A small incision using the tip of a needle was made halfway between the bregma line and the eye in the right hemisphere. The capillary was positioned over the incision and the tip aided past the skull with the needle. The capillary was lowered 1 mm down to the lateral ventricle, and approximately 1 µl of virus injected. The capillary was then removed and mouse returned under a heat lamp to recover. Paws were tattooed to denote treatment and pups then returned to the cage with their mother. Time-chases were done for 3, 7, 15 and 30 days post infection. At the end of the experiment, mice were heavily anesthetized with ketamine/xylazine/ flunitrazepam solution (150 mg, 7.5 and 0.6 mg/kg body weight, respectively) and perfused as outlined in “Preparation of tissue.”

6.1.5 Quantification of transduced mice

Immunostained brain sections of transduced mice were analyzed on a Zeiss Observer with apotome microscope. 3 images at 20x magnification were taken at random in the cortex, the striatum and the corpus callosum of each brain section, and 3 brain sections photographed from each animal. Images were then imported into Fiji imaging software and cells counted manually based on marker expression. Quantification of migration in the cortex was done using 20x magnification tiled images in Fiji imaging software. The boundary of the corpus callosum was traced out and then individual measurements from the edge of the corpus callosum to approximately 75-100 cells per mouse were taken. Statistical comparisons was done by two-tailed unpaired Student's t-test. In the case where t-test was used on two sets of percentages, values were first converted to arcsin values. Significance was

established at $p < 0.05$. In all graphs error bars represent standard error of the mean (s.e.m.).

6.1.6 Maintenance of cell culture lines (N2A, NIH3T3, HEK293 and Platinum-E HEK293 cells)

Throughout this study, multiple cell lines were used that were all grown, maintained and passaged under similar conditions. These include the mouse neuroblastoma (N2A), NIH3T3 fibroblasts, Human embryonic kidney (HEK293), and Platinum-E HEK293 cell lines. Frozen aliquots of all cell lines were thawed quickly in a 37°C water bath and immediately transferred to a 15 mL canonical tube containing 10 mL of DMEM culture medium (Gibco) and centrifuged at 80g for 5 minutes. Pellets were resuspended in DMEM culture medium containing 10% fetal bovine serum (FBS) (PAA), and 1% Penicillin streptomycin (Life technologies) and plated in T75 culture flasks (Greiner). Cells were grown and maintained at 37°C in 5% CO₂. When cells became 80-90% confluent (approximately two to three days after plating) cells were incubated with Trypsin diluted in Versene (Gibco) and incubated at 37°C for 2 minutes. Cells were then removed and resuspended in 10mL of cell culture PBS (Gibco) before centrifuging for 5 minutes at 80g. Cells were resuspended in DMEM culture medium, counted using a Neubauer chamber and replated in a T25 flask containing DMEM culture medium containing 10% FBS. To store cells for length periods of time, cells were frozen down. One T75 flask of cells was dissociated as described above and resuspended in 1 mL of freezing solution (50% DMEM+Glutamax, 40% FBS, 10% DMSO, filter sterilized). Cells were aliquoted into 500 µl/cryotube (Starlab) and placed in a Mr. Frosty cooling box at -80°C to ensure gradual cooling of cells at about -1°C per minute. For long-term storage, cells were then transferred to liquid nitrogen.

Uniquely, Platinum-E HEK293 cells contain a blasticidin/puromycin selection cassette allowing for selection and maintenance of retroviral packaging genes. Cells were grown in selection medium (DMEM, 10% FBS, 1 µg/mL puromycin, 10 µg/mL blasticidin, penicillin and streptomycin) for at least 24 hours and then allowed to recover in standard DMEM culture medium for approximately 24 hours prior to transfection with retroviral plasmids.

6.1.7 Transfection of cell culture lines by Calcium Phosphate

Calcium phosphate transfection was performed according to manufacturer's instructions (ClonTech). A 10 cm plate of cells was grown to approximately 70% confluency. Solution A was prepared by mixing 15-20 μg of plasmid DNA with 85 μl of 2M calcium solution and 680 μl of sterile H₂O in a 15 mL conical tube. 700 μl of 2xHepes buffered saline (HBS) solution was added drop wise (approximately 1 drop every 2 seconds) to solution A while vortexing at 1400rpm. The solution was then incubated for 10 minutes at room temperature before briefly vortexing and adding drop wise to the pre-seeded cells. Plates were then rocked to ensure even distribution of transfection mix and incubated overnight at 37°C in 5% CO₂. Medium was replaced 12 hours later with fresh DMEM 10% FBS.

6.1.8 Transfection of Cell culture lines by TransFectin (BioRad)

TransFectin lipid reagent (BioRad) was used to transiently transfect foreign plasmids into cell culture lines (approx. 70% confluent). Transfection solution for a 24 well plate was prepared by mixing 50 μl of serum-free medium with 1 μg of plasmid DNA. 4 μl of TransFectin reagent was added to a second 50 μl volume of serum-free medium. Both solutions were then mixed together and incubated at room temperature for 20 minutes. The transfection solution was then directly applied to one well of cells in a 24 well plate and cells were incubated as outline in maintenance of cell culture lines.

6.1.9 Subcellular fractionation of N2A cells

Cells were grown in a T25 flask and transfected with approximately 4 μg of plasmid DNA when cells were approximately 70% confluent using TransFectin (BioRad). Cells were then incubated for 48 hours at 37°C in 5% CO₂. Before harvesting, cells were washed twice with 5 mL of cold PBS (Gibco). 300 μL of Buffer A (10 mM Hepes pH 7.9, 10 mM KCl, 1.5 mM MgCl₂, 0.34 M Sucrose, 0.1% Triton, 1x complete protease inhibitor (Roche), 10% glycerol, 0.1 M PMSF, 1 mM DTT) was added directly to the cells, and then cells scraped from the flask with a cell scraper before being pipetted up and down to disrupt the cell membrane. Lysates were then transferred to a fresh tube and centrifuged for 5 minutes, 1000 g at 4°C. Supernatant was isolated (cytosolic

proteins, S1) and stored at -80°C until further analysis. The pellet was washed in 400 μL of Buffer A and rotated on a rotating platform (Stuart) at 4°C for 5 minutes. Lysate was centrifuged for 5 minutes, 1000 g at 4°C , and supernatant discarded. The pellet was resuspended in 75 μL of Buffer B (10 mM Hepes pH 7.9, 3 mM EDTA pH 8, 0.02 mM EGTA pH 8, 1x complete protease inhibitor, 0.1 mM PMSF, 1 mM DTT) and left to lyse on ice for 30 minutes with no pipetting. Nuclear lysate was centrifuged for 5 minutes, 1500 g at 4°C , and the supernatant collected and stored at -80°C until further analysis (soluble nuclear lysis, S2). Chromatin pellet was then washed with 400 μL of Buffer B, and rotated at 4°C for 5 minutes. Chromatin was centrifuged for 5 minutes, 1500 g at 4°C , and then resuspended in 150 μL of Buffer A without glycerol. Chromatin bound proteins were released by adding 1 μL /sample of Benzonase and incubating for 1 hour at room temperature with low (ie. 300 rpm) shaking. Once complete, samples were stored until further analysis at -80°C . Samples were analyzed by SDS-Page western blot using approximately 10 μg of protein per lane and a loading control antibody specific for H2A was used to ensure that fractionation occurred cleanly.

6.1.10 Cloning of retroviral and AAV and retroviral constructs

Full-length cDNA of Jag1 was subcloned into a modified pAAV vector containing the SV40 polyA sequence from pAAV-LacZ plasmid (pAAV-Jag1FL). The identical full-length Jag1 cDNA was subcloned into the pMIG vector, in frame with the IRES-GFP (pMIG-Jag1FL). Both plasmids were confirmed to by sequencing.

6.1.11 Purification of AAV via iodixanol centrifugation

A 50-60% confluent 10cm plate (Corning) of HEK293 cells was transfected with 10 μg of plasmid DNA (pHelper, pAAV-RC, and pAAV-GFP or pAAV-Jag1FL) using the calcium phosphate transfection method. 72 hours later, cells were scraped from the plate in 37°C 3.5 ml PBS and transferred to a 50 ml conical tube and centrifuged at 1000 rpm for 5 minutes at 4°C . Pellets were resuspended in 8.5 mL of prechilled Tris/NaCl (50mM, 150mM, pH: 8) and 500 μL of NaDOC (10%) /5 μL Benzonase (Sigma) (ca. 1400U) added. Cell pellet was incubated for 20 minutes at 37°C and then 584mg of NaCl was

dissolved in the buffer and incubated an additional 5 minutes at room temperature. Virus was snap frozen in liquid nitrogen (N₂) and thawed at 37°C before centrifuging at 5000rpm for 20 minutes. An iodixanol gradient was prepared by loading 6 mL of iodixanol in a Beckman centrifuge tube followed by first an underlying layer of 4 ml 25% Iodixanol, then 3 mL 40% iodixanol and finally 3 ml 54% iodixanol, which remains separated as four visible phases. Virus was loaded on the iodixanol gradient, keeping 100 µl of lysate for future analysis. Ultra centrifuge was then performed at 60 000rpm for 1.5 hours at 18°C. 40% iodixanol (3 mL) top phase was removed with a syringe and diluted 1:1 with PBS-MK (PBS, 1 mM MgCl₂, 2.5 mM KCl), taking care not to disturb the cellular debris layer (white film) at the iodixanol boundary. Virus was further concentrated in an Amicon Concentrator (Millipore) (100kDa) three times at 2000g by refilling with PBS-MK. The final pellet was resuspended in 250 µl PBS-MK and filtered through 0.2µm Acrodisc (Sigma), and immediately aliquoted in 25 µl units and snap frozen in liquid nitrogen. Analysis was confirmed by infecting HEK293 and titer determined through GelCode-Blue-Stain solution (Pierce) on a 10% SDS-polyacrylamide gel.

6.1.12 Purification of RV with Retro-X concentrator (ClonTech)

A 10cm plate of 70% confluent Platinum-E HEK293 cells were transfected with 20 µg of pMIG viral plasmid DNA by the calcium phosphate method (ClonTech). Supernatant was collected at 48 hours and 72 hours post transfection, and stored at 4°C. Supernatant was pooled and filtered through a polyethersulfone (PES) low protein binding filter (Millipore) and clarified supernatant purified according to the standard Retro-X concentrator protocol (ClonTech). Viral pellet was gently suspended in 200 µl of PBS containing 10% DMSO, and immediately snap frozen on dry ice and stored at -80°C. Viral titer was calculated by serial diluting the virus and transducing a NIH3T3 fibroblast cell line and then 48 hours later quantifying the percentage of cells transduced.

6.1.13 Isolation of NSCs and maintenance of Neurospheres

Neurospheres were isolated and maintained *in vitro* as previously described (Giachino, Basak et al. 2009). Brains were isolated from postnatal wild type C57BL/6 mice (P2-P5) and transferred to L15 medium (GIBCO). The SVZ and cortices were micro-dissected using a binocular (Leica), and tissue digested with freshly prepared Papain based solution (L15 medium (Gibco), Papain (Sigma) 30 U/mL, Cysteine (Sigma) 0.24 mg/mL, DNaseI Type IV (Roche) 40 µg/mL, sterile filter) for 10 minutes at 37°C. The reaction was terminated by adding an equal volume of Ovomuroid mix (stored at 4°C for a maximum of one week, Ovomuroid trypsin inhibitor (Sigma) 45 mg, BSA (Sigma) 21 mg, DNaseI Type IV (Roche) 40 µg/mL, L15 medium (Gibco) 39 mL, sterile filter) and incubated for 5 minutes to ensure digestion has completed. Spheres were then triturated with a fire polished Pasteur pipette by pipetting up and down at least 10-15x or until completely homogenous. Cells were resuspended in 9 mL of prewarmed DMEM/F12 culture medium (Gibco) and centrifuged for 5 minutes at 80g. Pellets were resuspended in 4.5 mL of NS culture medium (DMEM/F12, Penicillin 10 U/mL, Streptomycin 10 µg/mL, B27 supplement (1:50) (Gibco), FGF-2 20ng/mL (R&D), EGF 10ng/mL (R&D)) and transferred to a T25 culture flask (Greiner). Cells were incubated at 37°C, with 5% CO₂. 2 mL of fresh NS culture medium was provided after 2 days in culture and neurospheres were passaged on day 5.

At day 5 neurospheres were transferred to a 15 mL conical tube and centrifuged at 80g for 5 minutes. The pellet was resuspended in 500 µl of 0.05% Trypsin diluted in Versene (Gibco) and incubated at 37°C for 10 minutes with agitation. The trypsin reaction was stopped by adding 0.5 mL of Ovomuroid mix and incubating at room temperature for 5 minutes. Neurospheres were then triturated with a fire-polished Pasteur pipette and resuspended in 9 mL of DMEM/F12 medium in a 15 mL tube to wash them and centrifuged at 80g for 5 minutes. Cells were resuspended in 1 mL of NS medium and gently triturated with a fire polished pipette before counting cell numbers using a Neubauer chamber and replating in a T25 flask containing NS medium.

6.1.14 Transduction of NSC cultures

Low-passage neurospheres (passage 1-3) were dissociated with 0.05% Trypsin diluted in Versene (Gibco) and triturated with a fire polished pipette before counting cell numbers using a Neubauer chamber. Dissociated cells (approximately $7-10 \times 10^7$) were transferred to a 1.5 mL tube and resuspended in a minimal volume of approximately 200 μ l of NS medium (see NS maintenance) and 10 μ l of a previously prepared retroviral stock (see retroviral purification) was added directly to the cell suspension for an approximate MOI of 1. Cells were then incubated at 37°C with 5% CO₂, for 3 hours with the virus and then replated in a T25 flask with NS medium containing growth factors. Cells were examined for reporter expression after 48 hours using a fluorescent binocular (Leica). Neurospheres were maintained as outlined in the NS maintenance protocol.

6.1.15 FACS sorting of transduced NSCs

NSCs were dissociated as single cells as outlined in the NS maintenance protocol. Cells were resuspended in 500 μ l of cell culture PBS (Gibco) and filtered through a 30 μ m cell sieve (Miltenyi Biotec) and sorted by forward and side-scatter for live cells and gated for GFP⁺. Cells were then either directly used for RNA isolation or cultured in NS culture media (NS maintenance protocol).

6.1.16 Differentiation of transduced NSCs

FACS sorted transduced neurospheres were plated on 30 mm coverslips (Biosystems) coated with poly-L-lysine (Sigma) and laminin (Sigma). Cells were grown in differentiating medium containing reduced growth factors (DMEM/F12 (Gibco), B27 supplement (1:50) (Gibco), FGF-2 10ng/mL (R&D), EGF 5ng/mL (R&D)), with fresh medium provided every two days. After 7 days of differentiation, colonies were fixed by adding 12% PFA directly to the medium, for a final concentration of 4% PFA and incubated with rocking at room temperature. Colonies were then washed 4 times with PBS and analyzed by immunohistochemistry.

6.1.17 Thymidine pulse chase assay of transduced NSCs

Thymidine pulse experiments of NSCs were performed using the Click-iT EdU kit (Invitrogen) as outlined by the manufacturers protocol. NSCs were dissociated and plated on coverslips as outlined in the differentiation of transduced NSCs method, but instead grown in NS medium (DMEM/F12 + Glutamax (Gibco), B27 supplement (1:50) (Gibco), FGF-2 20ng/mL (R&D), EGF 10ng/mL (R&D)). 24 hours after plating, cells were incubated with EdU for a 3 hour pulse, and then immediately fixed with 4% PFA and permeabilized followed by immediate EdU detection. Immunohistochemistry for Ph3 was performed in parallel.

6.1.18 RNA Isolation

RNA isolation from cells was performed using TRIzol Reagent as outlined by the manufacturers protocol. Adherent cells (ie. CHIP and NSC differentiation assays) and dissociated cells (ie. FACS sorted NSCs) were homogenized by adding 1 mL of TRIzol reagent directly to cells. Cells were pipetted up and down several times and transferred to a clean 1.5 mL tube and left to sit for 5 minutes at room temperature. 0.2 mL of chloroform was added and sample shaken for 15 seconds by hand, and then incubated for an additional 3 minutes at room temperature. Samples were then centrifuged at 12 000g for 15 minutes at 4°C, separating out the aqueous phase, interphase, and organic phase. The aqueous phases containing the RNA were carefully isolated, transferred to a new tube and Glycogen blue added to improve efficiency of RNA precipitation (Life Technologies). 0.5 mL of isopropanol was added to the aqueous phase, incubated at room temperature for 10 minutes, and then centrifuged at 12 000g for 10 minutes at 4°C. The RNA was then washed with 75% ethanol and centrifuged at 7 500g for 5 minutes at 4°C. Pellets were air dried and redissolved in 30 µl of RNase-free water and incubated in a heating block at 55°C for 10 minutes.

6.1.19 RNA-Sequencing of NSCs

NSCs were derived from postnatal wild type C57BL/6 mice as outlined in Isolation of NSCs and maintenance of Neurospheres and were transduced as described in Transduction of NSC cultures. At 5 days post-transduction,

neurospheres were dissociated and FACS sorted as explained in, FACS sorting of transduced NSCs, and RNA immediately isolated as described in, RNA Isolation. Sample libraries were then assembled by the D-BSSE Quantitative genomics facility (Basel Switzerland) and analyzed using an Agilent Bioanalyzer 2100. Multiplex sequencing was performed with Illumina Next Generation sequencing (HiSeq2000). Peak alignment and mapping to the genome of *Mus musculus* build NCBI37/mm9 was performed by Robert Ivanek of the DBM (University of Basel, Basel, Switzerland). Intra-comparison of RNA-Seq replicates was performed to find reproducible gene profiles changes. Jag1FL-IRES-GFP⁺ NSCs samples were then compared to control NSCs to determine fold change of transcripts. Analysis of sequencing datasets was done with GO and KEGG database software to identify gene targets that were later quantified through gene specific qRT-PCR as described in qRT-PCR analysis below.

6.1.20 cDNA synthesis and quantitative reverse transcriptase PCR (qRT-PCR) analysis

Using 1-2 µg of starting RNA, first-strand cDNA synthesis was performed using SuperScriptIII (Invitrogen) exactly as outlined by the manufacturers protocol. Gene specific qRT-PCR primers were both obtained and verified from previous publications, obtained from the verified primers in the Harvard PrimerBank (<http://pga.mgh.harvard.edu/primerbank/>) or designed using Primer3 software. Criteria for primers included: a single PCR product as determined by analysis on agarose gel; a single peak in the melting curve of primer pairs; a PCR product of approximately 100-150 bp; and binding of both primers on different exons. Primers that met these criteria were used to determine relative levels of transcripts, using the house-keeping gene β -actin as an internal sample standardization control. 10 µl qRT-PCR reactions were performed in 0.1 mL strip tubes (Labgene Scientific Biolab) with SensiMix SYBR Kit (Labgene Scientific Biolab) and samples run on a RotorGene qPCR machine (Corbett). cT values and melting curves were generated by RotorGene software, and statistics and follow-up analysis performed in Excel.

6.1.21 Production of endotoxin free plasmid DNA

Endotoxin free plasmid DNA was used for IUEs and purified according to manufacturers protocol (Qiagen).

6.1.22 *In Utero* Electroporation

IUE was performed as previously described (De Pietri Tonelli, Calegari et al. 2006). Flaming/Brown micropipette puller (Sutter Instruments) was used to prepare borosilicate glass micro capillaries for plasmid DNA delivery (settings: heat = 540°C; pull = 50; velocity = 50; time = 200 sec) (Kwick-Fil™). The tip of the capillary was sharpened using a capillary sharpener (Bachofer). Endotoxin free plasmid DNA was prepared with fast green (10%) (Sigma) in a 10:1 ratio, for a final DNA concentration of 2 µg/µl. Since all plasmids used in IUEs contained fluorescent tags, there was no need for co-electroporation of a second reporter plasmid. Capillaries were backfilled with viral suspension and loaded into a microinjector (Pneumatic Pico Pump, WPI Rnage). Pregnant mothers at day E13.5 of gestation were anesthetized with Isofluran (Baxter), diluted in O₂ and carefully secured to the heated operating table. The eyes were coated with Bepanthen cream to prevent drying and temgesic was delivered subcutaneously to relieve pain (0.1mg/kg). Fur was removed from the stomach using depilation cream and then disinfected with 70% ethanol. A small, 1 cm incision along the midline, was made beginning at the bottom of the abdomen and moving upwards. This was done first by cutting through the skin, and then the muscle layer. The uterine horns containing the embryos were gently removed from the abdominal cavity using pincets and rested on the skin. Embryos were kept moist throughout the remainder of the experiment with HBSS/PenStrept (1:1000). Beginning at one end of the uterine horn, embryos were injected into the left lateral ventricle with 1-2 µl of DNA solution. To aid in visualization of the ventricle, a cold light source was used to backlight the embryo. Electroporation paddles were held directly adjacent to the site of injection with the positive pole oriented towards the injection site. Two consecutive rounds of pulses were delivered to each embryo (Electro Square Pavator™, BTX® Harvard Apparatus, 40V, pulse length: 50 ms, 5 pulses, interval: 950ms). After all embryos had been electroporated, they were returned into the abdomen and the chest cavity

filled with HBSS/PenStrept to aid the recovery. The muscle layer and then the skin were sutured with 3 stitches each and the animals placed under a heat lamp to recover. Recovery was carefully monitored throughout the day.

6.1.23 IUE tissue preparation and quantification

24 or 48 hours post-IUE, mothers were sacrificed and their embryos dissected in HBSS. Brains were micro-dissected and electroporation efficiency measured using a fluorescent binocular (Leica). Positive brains were fixed overnight in 4% PFA, and washed 4 times with PBS. Brains were processed through sequential rounds of cryopreservation, first with 15% and then 30% PB-sucrose solution. Brains were embedded in embryo molds with O.C.T. (Sysmex Digitana SA) and frozen on dry ice. Brains were sectioned horizontally and mounted directly onto glass slides and stored in PBS at 4°C until analyzed by immunohistochemistry.

6.1.24 SDS-Page Western Blot

Media was removed and cells scraped into 300 μ l lysis buffer (20 mM Tris-HCl pH7.6, 150 mM NaCl, 2 mM MgCl₂, 2 mM EDTA, 0.5% Triton-X-100, 0.5% Nonidet P40, 10% Glycerol and Complete protease inhibitor 1x (Roche)). Cells were lysed by pipetting up and down and vortexing for about 2-3 minutes. Lysates were centrifuged at maximum speed (17 000g) for 5 minutes and then transferred to a new tube to measure protein concentration with the BCA protein assay (Pierce) kit (followed manufacturers protocol exactly). The volume of lysate required for 30 μ g of protein per sample was prepared and β -mercaptoethanol added. 5x loading buffer was added to bring the total loading volume to 30 μ l. Proteins were denatured for 10 minutes at 95°C followed by immediately placing samples on ice. Samples were then loaded on a 10% SDS-Page gel and run at 60V until samples reach the separating gel. Once in the separation gel, voltage was then increased to 120V and run as long as needed for correct protein band separation. Proteins were then transferred to an activated PVDF membrane run at 150 mA for 50 minutes and then ponceau stained to confirm that transfer worked successfully. Ponceau was destained from the membrane with 3, 5 minute washes with PBS. Membranes were then blocked with 5% milk powder in

0.05% Tween TBS (TTBS) for 30 minutes at room temperature. Primary antibody in blocking buffer was then incubated over night at 4°C on rollers with the membrane. Membranes were washed with 3 times for 15 minutes with TTBS. Membranes were then incubated with secondary antibody in blocking buffer for 1 hour and again washed for 15 minutes 3 times with TTBS. ECL detection (GE Healthcare, ECL Plus western blot detection reagents) was performed according to manufactures protocol and imaged using a ChemiDoc MP imager (BioRad).

6.1.25 Yeast-2-Hybrid and TAP-tag proteomics screen screening.

cDNA encoding JICD in the pGBT9 expression vector was used as a bait in the yeast two-hybrid screen. A Gal4-based system (Out-sourced: RZPD, Heidelberg, Germany) was used to screen in parallel a human fetal brain expression library and a human full-length clone library with three times genome coverage. A positive two-hybrid interaction was determined based on fluorescent signal and screened for specificity and background interaction (RZPD).

Tandam affinity purification (TAP), was performed on N-terminal TAP-JICD and control plasmid transfected N2A cells (>10⁸ cells). The InterPlay N-terminal Mammalian TAP system was used (according to manufactures protocols) to TAP protein complexes associated with JICD (Stratagene). 3 freeze-thaw cycles were performed in lysis buffer to lyse N2As and lysates incubated with streptavidin resin. TAP-tagged protein complexes bound to streptavidin resin were eluted from the beads after several washes with biotin solution. Elute was incubated with calmodulin resin in the presence of Ca²⁺. Bound protein complexes were eluted by boiling the resin in SDS sample buffer. Samples were separated by gradient denaturing SDS-PAGE and visualized with silver staining. Protein bands were excised and enzymatically digested with trypsin. Before LC-mass spectroscopic analysis, tryptic peptide mixtures were desalted using STAGE tips. Nanoscale LC (MDLC; GE Healthcare) was coupled to a 7-tesla linear ion-trap Fourier-transform ion cyclotron resonance mass spectrometer (LTQ-FT; Thermo Electron) equipped with a nanoelectrospray source (Proxeon). Peptides were eluted from an analytical column by a linear gradient running from 2 to 60% (vol/vol)

acetonitrile (in 0.5% acetic acid) with a flow rate of 250 nl/min in 35 min and sprayed directly into the aperture of the mass spectrometer. Information-dependent acquisition of MS, MS/MS, and MS³ spectra was performed as described previously (Olsen, Blagoev et al. 2006). Acquired spectra were then searched with Mascot (Matrix Science) against the human and mouse International Protein Index protein database (version 3.14, available at <http://www.ebi.ac.uk/IPI/>), to which we added frequently observed contaminants. Tryptic enzyme specificity with up to two missed cleavages was applied to all searches. Protein identifications were further analyzed and manually verified by the use of MSQuant (available at <http://msquant.sourceforge.net>).

6.1.26 Luciferase reporter assays.

Luciferase reporter constructs TopFlash, Axin2-Luc (Aulehla, Wehrle et al. 2003) were cotransfected with expression constructs (see supplementary table) for JICD, TBLR1, constitutive active β -catenin (S33A), and pCS2 into HEK 293 cells by calcium phosphate precipitation. Luciferase and Renilla luciferase (pRL; Promega) activity was assayed 48 hours after transfection. 10 μ l of cell lysate was mixed with 100 μ l of Luciferase Assay Reagent (Promega) and the light produced was measured using a Berthold Tech Centro LB960. To control for differences in transfection efficiency, the luciferase values were normalized to Renilla luciferase expression of the same sample.

6.1.27 Chromatin immunoprecipitation (ChIP) and ChIP-Sequencing

8, 10cm plates of 70% confluent N2As (approximately 7x10⁶ cells/plate) were each transfected using Transfectin (BioRad) with 15 μ g of plasmid DNA. The four transfection conditions included, i) pNTAP-B only (empty control vector), ii) TAP-JICD with pNTAP-B, iii) TAP-JICD with active β -catenin (S33A) and pNTAP-B and, iv) TAP-JICD with β -catenin and TBLR1. Cells were incubated for 48 hours and then 4 of the plates were cross-linked using 200 μ l of 37% formaldehyde per plate, and rocked gently for 10 minutes. The other 4 plates were used for RNA extraction (see RNA isolation protocol). Glycine was added to a final concentration of 125mM (for 10 mL of media, 500 μ L of 2.5M

solution) to the media to stop the cross-linking. Cells were then rinsed twice with 10 mL of cold PBS and scraped into 5 mL cold PBS and transferred to a 15 mL tube (Falcon) (approximately 1×10^7 cells). Lysates were centrifuged for 5 minutes, 1000g at 4°C, and pellets resuspended in 1 mL of FA lysis buffer. A covaris sonicator was used with the following settings, keeping samples on ice at all times when not being sonicated: Duty cycle: 5%, Intensity: 4, Peak incident power: 140 watts, Cycles per burst: 200, Processing time: 20 min, Temperature: 4°C, Power mode: Frequency sweeping, Degassing mode: continuous, Volume: 1 mL in a TC12x12 AFA Tube. 50 μ L of washed streptavidin resin was added to the sonicated lysate and incubated while rotating for 16 hours at 4°C (InterPlay Mammalian TAP system). Resin was collected by centrifugation at 1500g for 5 minutes and supernatant stored for future analysis. Resin was resuspended and washed with Streptavidin binding buffer (SBB) by rotating the tube at 4°C, and then recollected by centrifugation at 1500g for 5 minutes. 120 μ L of Streptavidin Elution Buffer (SEB) was added to resin and rotated at room temperature for 30 minutes to elute the protein complexes. Resin was collected by centrifugation at 1500g for 5 minutes and supernatant transferred to a new tube. Reverse cross-linking of each sample was done by incubating at 65°C for 16 hours with RNaseA (24mg/ml, Sigma). Purification of DNA done according to Qiagen QIAquick kit standard protocol, with 600 μ L of buffer PB is added to the 120 μ L of CHIP DNA. DNA was eluted with 30 μ L of prewarmed Buffer EB, allowing it to incubate on the filter for 2-3 minutes. After elution, a second volume of 30 μ L of prewarmed Buffer EB was added to the filter to ensure all DNA was eluted. Libraries were prepared for sequencing by excising a 250 bp band (D-BSSE Quantitative genomics facility, Basel, Switzerland) and DNA concentration was then verified by ND3300 using PicoGreen and multiplex sequencing performed with Illumina Next Generation sequencing (HiSeq2000). Peak alignment and mapping to the genome of *Mus musculus* build NCBI37/mm9 was performed by Robert Ivanek of the DBM (University of Basel, Basel, Switzerland). Targets were then identified by a Union of peaks shared in multiple replicates and verified with peak specific qRT-PCR primers on CHIP elutes.

6.2 Materials

Table 2: Plasmids used in experiments.

| Construct name | Insert | Vector backbone | Used for |
|--------------------|-----------------------------------|-----------------|---|
| pcDNA3.1-Jag1FL | Jag1FL | pcDNA3.1+neo | Transfection, Luciferase assay |
| pCS2+MT | - | pCS2+MT | Transfection |
| peGFP-N1 | eGFP | peGFPN1 | IUE, Transfection, Co-IP |
| pCAGs-mCherry | mCherry | pCAG | IUE |
| Jag1FL-eGFP | Jag1FL eGFP fusion | peGFPN3 | IUE, Transfection |
| Jag1ICD-eGFP | Jag1ICD eGFP fusion | peGFPN1 | Transfection, Co-IP |
| Jag1ICD-IRES-hrGFP | Jag1ICD | pAAV | Transfection |
| hrGFP-IRES | IRES-hrGFP | pAAV | Transfection |
| pGBT9-Jagged1ICD | Jag1ICD | pGBT | Yeast-2-Hybrid bait |
| pNTAP-B | - | pNTAP-B | Transfection, ChIP |
| pNTAP-Jagged1ICD | Jag1ICD | pNTAP-B | Transfection, Affinity purification, ChIP |
| Jagged1FL-MT | Jag1FL (myc tagged) | pCS2+MT | Transfection, Co-IP |
| HA-TBLR1 | TBLR1 (HA tagged) | pSG-5 | Transfection, Co-IP, Luciferase assay, ChIP |
| TBL1-cmyc | TBL1 (myc tagged) | pSG-5 | Transfection, Co-IP |
| Jag1ICDdelIPDZ-GFP | Jag1ICDdelIPDZ | peGFPN3 | Transfection, IUE |
| beta-Catenin | beta-Catenin (S33A) | pCS2 | Transfection, Co-IP, Luciferase assay, ChIP |
| Axin2-Luciferase | Axin2 promoter driving Luciferase | pBS | Transfection, Luciferase assay |
| Topflash | | pBS | Transfection, Luciferase assay |
| pRL | Renilla luciferase | pRL | Transfection control, Luciferase assay |
| pMIG | IRES-GFP | pMIG | Retrovirus production |
| pMIG-Jag1FL | Jag1FL-IRES-GFP | pMIG | Retrovirus production |
| pVPack VSV-G | VSV-G | pVPACK | Retrovirus production with VSV-G |
| pGEMT SV40 | SV40 | pGEMT | Cloning |
| pHelper | E2A, E4, and VA RNA genes | pHelper | AAV production |
| AAV-RC | Rep and Cap genes | AAV | AAV production |
| AAV-IRES-GFP | IRES-GFP | AAV | AAV production |
| AAV-Jag1FL | Jag1FL | AAV | AAV production |
| JICD-IRES-GFP | JICD-IRES-GFP | AAV | AAV production |

Table 3: Primers used in experiments.

| Primer name | Primer sequence (5'-3') | Primer Use |
|------------------|-------------------------------|--|
| 1233-SV40f-BamHI | TggatccACCATGGCCCAACTTGTATTAT | Clone out SV40 and add BamHI site |
| 1234-SV40r-BamHI | TggatccGCGGCCGCTCGGTCCGCACG | Clone out SV40 and add BamHI site |
| 1247-AAVquantify | GACGTCAATAATGACGTATG | Quantifying # of AAV genome copies, (Mochizuki H., 2011) |
| 1248-AAVquantify | GGTAATAGCGATGACTAATACG | Quantifying # of AAV genome copies, (Mochizuki H., 2011) |
| 443-Jag1 seq1 | TAGCGCTGGTGTCTCCCGCCGAG | Confirm Jag1 sequence |
| 444-Jag1 seq2 | ATGACACTATTCAACCTGATAGC | Confirm Jag1 sequence |
| 445-Jag1 seq3 | TACCAGTGCTCCTGCCAGAG | Confirm Jag1 sequence |
| 446-Jag1 seq4 | ATCACTGTGAGAGAGACATCGATG | Confirm Jag1 sequence |
| 447-Jag1 seq5 | TACTGTGACTGCAAAAATGGCTG | Confirm Jag1 sequence |
| 448-Jag1 seq6 | TAGTGGTGCCAAGTGCCATGAAG | Confirm Jag1 sequence |
| 449-Jag1 seq7 | ATCCGGGATGATGGGAACCCTGTC | Confirm Jag1 sequence |
| 450-Jag1 seq8 | ATACGCTGGTAGACAGAGAGGAG | Confirm Jag1 sequence |
| 455-Jag1-r | AGGGCGAGCAGAAGACTCAG | Reads out of the 5' end of Jagged |
| 1231-pEGFP-N-ter | CTGGTCGAGCTGGACGGCGACG | Used to sequence out of EGFP |
| 1232-pEGFP-C-ter | CATGGTCCTGCTGGAGTTCGTG | Used to sequence out of EGFP |
| 1235-b-globin-f | ATTCTGAGTCCAAGCTAGGC | Used to confirm AAV constructs |
| 1236-left ITR-f | CCTCTGACTTGAGCGTCGAT | Used to confirm AAV constructs |
| 1237-Right ITR-r | TACTATGGTTGCTTTGACGT | Used to confirm AAV constructs |
| 1240-pUC-r | TTTTTGTGATGCTCGTCAGG | Sequencing pCMV-MCS after hGH removed(AAV) |
| 1241-CMV-r | TTATGTAACGCGGAACTCCA | Sequencing of AAV vectors. Reads out of insert into the ITR. |
| 1242-hGH-polyA-f | GTAGAGACGGGGTTTCACCA | Sequencing of AAV vectors. Reads out of hGH into the ITR. |
| 1243-hGH-polyA-r | TAGAAGGACACCTAGTCAGA | Sequencing of AAV vectors. Reads into the insert. |

| Gene abbreviation | Primer name | Primer sequence (5'-3') | Primer Source |
|-------------------|-----------------|-------------------------|---|
| Axin2 | Axin2_ChIPA_Fwd | AACACGCTTCCTCTGGTCTT | Designed for JICD specific peak in ChIPseq. Designed with the help of Primer3. |
| | Axin2_ChIPA_Rev | CTCACACACCTTAGGCCTCA | |
| Axin2 | Axin2_ChIPC_Fwd | CCCCTCCTTTCTTTCCAGAG | Designed for JICD/Bcat/TBLR1 specific peak in ChIPseq. Designed with the help of Primer3. |
| | Axin2_ChIPC_Rev | ACTAACACGGCGCTACTCAT | |
| Lgr5 | 1583_Lgr5_A_F | GCCACTTATCGACTGTAGAGC | Designed for JICD/Bcat/TBLR1 specific peak in ChIPseq. Designed with the help of Primer3. |
| | 1584_Lgr5_A_R | TCTTGCTTTACAGTTGTGGGA | |
| Id2 | 1599_Id2_A_F | AAGAGGCTCGAACTGTTGGG | Designed for JICD/Bcat/TBLR1 specific peak in ChIPseq. Designed with the help of Primer3. |
| | 1600_Id2_A_R | GCCTCTGTTATTAAGCCTGGA | |
| Lef1 | 1603_Lef1_A_F | CTGGACTGGTACCCACTTTTAA | Designed for JICD/Bcat/TBLR1 specific peak in ChIPseq. Designed with the help of Primer3. |
| | 1604_Lef1_A_R | CATGTGGGTTGACAGGCAC | |

Table 4: qRT-PCR Primers used in experiments

| Gene abbreviation | Primer name | Primer sequence (5'-3') | Primer Source |
|-------------------|----------------|----------------------------|---|
| Agt | 1423-Agt-F | TCTCCTTTACCACAACAAGAGCA | http://pga2.mgh.harvard.edu:8080/rtpcr/displayResult.do?primerPairId=19705566a1 |
| | 1424-Agt-R | CTTCTCATTACAGGGGAGGT | |
| Axin2 | 140-Axin2 | GGAAGGTGCTGACTGATGTGTA | Designed with the help of Primer3 |
| | 141-Axin2 | GATGAAGATGGGCGGTTG | |
| Bmp4 | 1383-Bmp4-F | TTCCTGGTAACCGAATGCTGA | http://pga2.mgh.harvard.edu:8080/rtpcr/displayResult.do?primerPairId=6680796a1 |
| | 1384-Bmp4-R | CCTGAATCTCGGCGACTTTTT | |
| Cnp | 1646_CNPase_F | GTTCTGAGACCTCCGAAAA | Koenning et al, The Journal of Neuroscience, September 5, 2012 • 32(36):12528 –12542 |
| | 1647_CNPase_R | CCTTGGGTTTCATCTCCAGAA | |
| Dcx | 1525_Dcx_fwd | CTCAGGGAGTGCCTACATT | Designed with the help of Primer3 |
| | 1526_Dcx_rev | ACAGACCAGTTGGGTTGAC | |
| Dkk3 | 1419-Dkk3-F | CTCGGGGGTATTTTGCTGTGT | http://pga2.mgh.harvard.edu:8080/rtpcr/displayResult.do?primerPairId=7657027a1 |
| | 1420-Dkk3-R | TCCTCCTGAGGGTAGTTGAGA | |
| Dscam | 1387-Dscam-F | CCCTCCTGTGACTCTCAGATG | http://pga2.mgh.harvard.edu:8080/rtpcr/displayResult.do?primerPairId=13626028a1 |
| | 1388-Dscam-R | CCCGTAAACAGCCTTGATGTG | |
| FGF20 | 1575_FGF20_Fwd | ATCAGAGGTGTGGACAGTGG | Designed with the help of Primer3 |
| | 1576_FGF20_Rev | CAAATACCTGCGACCCGTG | |
| Hipk2 | 1417-Hipk2-F | TTTCTCCCCTCACACCCTCA | http://pga2.mgh.harvard.edu:8080/rtpcr/displayResult.do?primerPairId=5815139a1 |
| | 1418-Hipk2-R | CCAGTTGGAAGTTGGCTCTACT | |
| Htt | 1393-Htt-F | CTCCATGCTGTTACGACTCATC | http://pga2.mgh.harvard.edu:8080/rtpcr/displayResult.do?primerPairId=438805a1 |
| | 1394-Htt-R | AGGGAGGAAGGAGCCAAAATC | |
| Id2 | 1567_Id2_fwd | CATCTTGGACCTGCAGATCG | Designed with the help of Primer3 |
| | 1568_Id2_rev | TCGACATAAGCTCAGAAGGGA | |
| Isl1 | 1453-Isl1-F | ATGATGGTGGTTTACAGGCTAAC | http://pga2.mgh.harvard.edu:8080/rtpcr/displayResult.do?primerPairId=31543007a1 |
| | 1454-Isl1-R | TCGATGCTACTTCACTGCCAG | |
| Jag1 | 1581_Jag1_Fwd | CTTCAATCTCAAGGCCAGCC | Designed with the help of Primer3 |
| | 1582_Jag1_Rev | ATGCCCTGAGTGAGAAGCCTT | |
| Lef1 | 1559_Lef1_fwd | TGAGTGCACGCTAAAGGAGA | Published: Cell Rep. 2013 Jun 27;3(6):2113-26. doi: 10.1016/j.celrep.2013.05.015. Epub 2013 Jun 20. |
| | 1560_Lef1_rev | ATAATTGTCTCGCGCTGACC | |
| Lgr5 | 1542_Lgr5_fwd | CCAATGGAATAAAGACGACGGCAACA | Published: Development. 2011 Nov;138(22):4843-52. doi: 10.1242/dev.070284 |
| | 1543_Lgr5_rev | GGGCCTTCAGGTCTTCTCAAAGTCA | |
| Lrp6 | 1391-Lrp6-F | TTGTTGCTTTATGCAACAGACG | http://pga2.mgh.harvard.edu:8080/rtpcr/displayResult.do?primerPairId=6678718a1 |
| | 1392-Lrp6-R | GTTTCGTTAATGGCTTCTTCGC | |
| Math1 | 1571_Atoh1_Fwd | GAGTGGGCTGAGGTAAGAGT | http://pga2.mgh.harvard.edu:8080/rtpcr/displayResult.do?primerPairId=6680742a1 |
| | 1572_Atoh1_Rev | GGTCGGTGCTATCCAGGAG | |
| MBP | 1654_MBP_F | CCCGTGGAGCCGTGATC | Koenning et al, The Journal of Neuroscience, September 5, 2012 • 32(36):12528 –12542 |
| | 1655_MBP_R | TCTTCAAACGAAAAGGGA | |
| Mib1 | 1413-Mib1-F | AGTAACTCCCGCAACAACCG | http://pga2.mgh.harvard.edu:8080/rtpcr/displayResult.do?primerPairId=32189428a1 |
| | 1414-Mib1-R | CAGTGCCTACATGGCCCTC | |
| Myrf | 1642_Myrf_F | GCATGGGCACCCCTAAG | Koenning et al, The Journal of Neuroscience, September 5, 2012 • 32(36):12528 –12542 |
| | 1643_Myrf_R | GGGGCGAGTCTGGCAGTGTG | |
| Ngn1 | 1579_Ngn1_Fwd | CCAGCGACACTGAGTCTCG | http://pga2.mgh.harvard.edu:8080/rtpcr/displayResult.do?primerPairId=6754826a1 |
| | 1580_Ngn1_Rev | CGGGCCATAGGTGAAGTCTT | |
| Pak3 | 1441-Pak3-F | TTGATAACGAAGAAAAACCCCC | http://pga2.mgh.harvard.edu:8080/rtpcr/displayResult.do?primerPairId=6679205a1 |
| | 1442-Pak3-R | GAGTCTCGTTGTTACTGTTTCAT | |
| PDGFRa | 1648_PDGFRa_F | GGAAGGACTGGAAGCTTGGGGC | Koenning et al, The Journal of Neuroscience, September 5, 2012 • 32(36):12528 –12542 |
| | 1649_PDGFRa_R | GAGATGAGGCCCGCCCTGTGA | |
| Plp1 | 1644_Plp1_F | GCCCTACCAGACATCTAGC | Koenning et al, The Journal of Neuroscience, September 5, 2012 • 32(36):12528 –12542 |
| | 1645_Plp1_R | AGTCAGCCGCAAAACAGACT | |
| Prox1 | 1527_Prox1_fwd | GAAGGGCTATCACCAATCA | Designed with the help of Primer3 |
| | 1528_Prox1_rev | AGTGGTTCAGCAATTTCCGT | |
| Ptch1 | 1395-Ptch1-F | AAAGAACTGCGGCAAGTTTTTG | http://pga2.mgh.harvard.edu:8080/rtpcr/displayResult.do?primerPairId=6679519a1 |
| | 1396-Ptch1-R | CTTCTCCTATCTTCTGACGGGT | |
| Sox10 | 1411-Sox10-F | ACACCTTGGGACACGGTTTTTC | http://pga2.mgh.harvard.edu:8080/rtpcr/displayResult.do?primerPairId=2826523a1 |
| | 1412-Sox10-R | TAGGTCTTGTCTCGGCCAT | |
| Sox5 | 1409-Sox5-F | AGCCGCAATGCAGGTTTCT | http://pga2.mgh.harvard.edu:8080/rtpcr/displayResult.do?primerPairId=26349395a1 |
| | 1410-Sox5-R | TTGTGCTCTTGTCTGTGTGAAT | |
| Tcf4 | 1557_Tcf4_fwd | CGAAAAGTTCTCCGGGTTTG | http://pga2.mgh.harvard.edu:8080/rtpcr/displayResult.do?primerPairId=7305551a1 |
| | 1558_Tcf4_rev | CGTAGCCGGGCTGATTCAT | |
| Tnr | 1407-Tnr-F | GGCTGGAGGTGACTACAGAAA | http://pga2.mgh.harvard.edu:8080/rtpcr/displayResult.do?primerPairId=29789028a1 |
| | 1408-Tnr-R | GAAGACCATAGGCTGTTCTTG | |
| Wnt3 | 1415-Wnt3-F | TAAAGTGTAATGCCACGGGTT | http://pga.mgh.harvard.edu/cgi-bin/primerbank/new_search2.cgi |
| | 1416-Wnt3-R | CGGAGGCACTGTCGACTTGG | |

Table 5: Chemicals and consumables used in experiments

| Product | Vendor | Product # |
|---|----------------------------|-----------------|
| 0.1 ml StripTubes & caps for RotorGene | Labgene Scientific Biolabo | 3001 - 002 |
| 1 kb Plus DNA Ladder | Life Technologies | 10787018 |
| 1:5000 Versene, 100ML | Life Technologies | 15040033 |
| 15ml tubes | Faust | TPP91015 |
| 1N HCl (1M/L), 1L | Roth | K025.1 |
| 1N NaOH (Natronlaug), 1L | Roth | K021.1 |
| 2- Propanol, Isopropanol, 2,5l | VWR | 8.18766.2500 |
| 2.5% Trypsin (10x), no Phenol Red, 100ml | Life Technologies | 15090-046 |
| 24 well Zellkulturplatte | Huber & Co AG | 7.662.160 |
| 2x SensiMix SYBR Kit | Labgene Scientific Biolabo | QT605-05 |
| 2x SensiMix SYBR- Kit, 2000rxns (50µl ^o 40x | Labgene Scientific Biolabo | QT605-20 |
| 5x FIREPol Master Mix (12.5 mM MgCl ₂), 1ml | Lucerna Chem AG | 04 - 11 - 00125 |
| 8-strip 0.2ml tubes and flat caps, 125 stripes | Starlab | 4ti-0784 |
| Acetic acid | VWR | 20102.292. |
| Albumin, from bovine serum | Sigma | A3294-10G |
| Ampicilin, 10g | Roth | K029.1 |
| Ascorbic Acid, 100g | Sigma | A4034 |
| B27 Supplement, 10ML | Life Technologies | 17504044 |
| BioScript for First Strand cDNA Synthesis,10000 units | Labgene | BIO-27036-4 |
| Bioscript Reverse Transcriptase | Labgene Scientific Biolabo | BIO-27036 |
| Biotin-Sp-AffiniPure Dnk Anti-Goat IgG (H+L) | Milan | 705-066-147 |
| BIS- Tris (CAS 6976-37-0), Ultrapure,100G | Lucerna Chem AG | BB0079-100G |
| Blasticidin S HCl, 150mg | Life Technologies | R21001 |
| BSA | Sigma | A3294-10G |
| BSA: Albumine from bovine serum | Sigma | A3294-50G |
| CaCl ₂ -2H ₂ O | Sigma | C7902-500G |
| CalPhos Mammalian Transfection Kit, 700 Rxns | Takara Bio Europe | 631312 |
| Cell Culture 12 well plates | Thermo Fisher Scientific | W2128R |
| Click EDU Alexa 594 Imaging Kit | Life Technologies | C10339 |
| Complete, Proteinase inhibitor Cockail tablets,20St | Roche | 11 697 498 001 |
| Corn oil | Sigma | C8267-500ML |
| Costar 12 well plate, 100St | Vitaris | 3512-Cor |
| Costar 6 well plate, 50St | Vitaris | 3516-Cor |
| Cryogenic Vials, InternalThreated Tubes, silicon Seal in Cap, 500St | Starlab | E3110-6122 |
| Coverslip 24x50mm | VWR | 632-1575 |
| Round Coverslip, 13mm, 1000St | Biosystems | 85-0271-00 |
| Round Coverslip,18mm, 1000St | Biosystems | 85-0296-00 |
| Deoxyribonuclease I from bovine pancreas | Sigma | D5025-150KU |
| DL- Dithiothreitol- Solution, DTT, 1M in H ₂ O, BioUltra | Sigma | 43816-10ML |
| DMEM + Glutamax | LuBioScience GmbH | 31966047 |
| DMEM-F12, 11330-032,10x500ml | Life Technologies | 31330095 |
| DMEM, High Glucose, Glutamax, Pyrovate, 10x 500ml | Life Technologies | 31966-047 |
| DMSO, 100nl | | D8418-100ML |
| DTT, DL-Dithiothreitol, 5G | Sigma | P9155-5MG |
| Dual Luciferase Reporter Assay System | Promega | E1980 |
| Dynabeads M-280 Streptavidin 2ML | Life Technologies | 11205D |
| EDTA | Sigma | ED-500G |
| Einmalsalpellet, 10 Stueck | Huber & Co AG | 3.7657.21 |
| Electroporations Cuvettes, 2mm, ind. wrapp, 50x | Axon Lab AG | EP-102 |
| Ethanol 96% | VWR | 20905.320. |
| Ethanol 99% | VWR | 20905.265. |
| Ethanol absolut, 2.5L | VWR | 1.20603.2511 |
| Ethylene glycol-bis(2-aminoethylether)-N,N,N',N',-tetraacetic acid | Sigma | 34596-25G |
| Fast green | Sigma | F7258 |
| FBS Good, Filtrated bovine serum, EU approved, 500ml | Brunschwig | P40-37500 |
| FIRERPol 5x MasterMix 12.5mM | Lucerna | 04/11/0124 |
| Foetal Bovine Serum, EU approved | Brunschwig | A10112-2170 |
| Forceps | F.S.T. | |
| Forceps, type 5, light shanks, very thin tips | Dumont SA | 0203-55-PO |
| Formaldehyde | Sigma | F1635-500ML |
| GBSS | Sigma | G9779-500MI |
| Gluteraldehyde 1L | VWR | 8.20603.1000 |
| Glycerol 99%, 1L | Axon Lab AG | A4443.1000 |
| Glyco Blue Coprecipitant, 300µl | Life Technologies | AM9515 |
| Green Fluor Protein (GFP) | Millipore | MAB3580 |
| HBSS 10x | Life Technologies | 14180-048 |
| HBSS, no Ca, no Mg, No Phenol Red, 10x 500 ml | Life Technologies | 14175-129 |
| HEPES | Sigma | H3375-100G |

Table 5: Chemicals and consumables used in experiments (*continued*)

| Product | Vendor | Product # |
|--|---------------------------|---------------|
| Hexadimethrine bromide | Sigma | 107689-10G |
| Hydrochloric acid | VWR | 20255.290. |
| Hydrogen peroxide, 30%, 1L | VWR | 23622.298. |
| InterPlay TAP Purification Kit | Agilent | 240107 |
| Isopropamol, 2,5L | VWR | 20904.320. |
| Kappa2G Robust KK5005 Genotyping Kit | Axon Lab AG | KK5005 |
| L- Glutamine 200MM | Life Technologies | 25030024 |
| L-Cysteine from non- animal source, BioReagent | Sigma | C7352-25G |
| L15 Medium (1x) + GlutaMAX, 1VE = 10x500ml | Life Technologies | 31415086 |
| Laminin from Engelbreth-Holm-Swarm... | Sigma | L2020-1MG |
| Laminin, 1mg | Sigma | L2020 |
| Lipofectamine 2000 Reagent 1.5 ML | Life Technologies | 11668019 |
| Magnesium Chloride Hexahydrate | Sigma | M2670-500G |
| Methanol | VWR | 1.06009.1000 |
| Methanol, 2.5l | VWR | 1.06009.1000 |
| MgSo4 | Sigma | M2643-500G |
| MOPS | Sigma | M3183-100G |
| Mouse Anaesthesia Mask | Bilaney | DKI 907 |
| Normal Donkey Serum 500ml | Lucerna Cem AG | GTX73245 |
| O.C.T.Compound, Sparpaket a 12 x 125 ml | Sysmex Digitana SA | 4583 |
| Microscope glass slides Superfrost/Plus | Biosystems Switzerland AG | 85-0911-00 |
| Microscope glass slides untreated | VWR | ECN631-1551 |
| Papain | Sigma | P3125-100MG |
| Parafilm, 75M, 10cm | Fisher | 11772644 |
| Paraformaldehyde, 1kg | Sigma | P6148-1KG |
| PBS PH7.4 W/O CaMg, 10x 500ml | Life Technologies | 10010056 |
| PBS PH7.4 W/O CaMg, 10x500ml | Life Technologies | 10010056 |
| PBS, Dubelcos PBS without Ca & Mg 500ml | Brunschwig | H15-002 |
| PDGF-AA, Recombinant Human PDGF-AA, 10µg | R&DSYSTEMS | 221-AA-010 |
| Penicilin Streptomycin Sol | Life Technologies | 15070063 |
| PFU DNA Polymerase | Fisher | 10202830 |
| Phenol red solution | Sigma | P0290-100ML |
| Pierce BCA Protein Assay Kit, Number 23250 | Fisher | 10750985 |
| Pierce BCA Protein Assay Reagent A, 500ml | Fisher | 11801355 |
| Pierce BCA Protein Assay Reagent B, 25ml | Fisher | 11891345 |
| Pierce ECL Plus Western Blotting Substrate 100ml (f. 1000m2) | Fisher | 32132 |
| Platinum- E Retroviral Packaging Cell Line | LuBioScience GmbH | RV- 101 |
| poly-L-Lysine, 5mg | Sigma | P9155-5MG |
| Protein G-Sepharose 4 fast Flow, 5ml | VWR | 17-0618-01 |
| Proteinase K | VWR | A7932.0025 |
| Proteinase K, 500mg | Roth | 7528.2 |
| Random Hexamers | Life Technologies | N8080127 |
| Recombinant Human FGF basic | R&DSYSTEMS | 233-FB |
| Recombinant Human FGF basic, 1mg | R&DSYSTEMS | 233-FB-01M |
| Retro-X Concentrator, 100 ml | Takara Bio Europe | 631455 |
| rhEGF, Epidermal Grow Factor, recombinant human | R&DSYSTEMS | 236-EG |
| Ribonuclease A from bovine pancreas | Sigma | R4642-10MG |
| RNase Zap | Life Technologies | AM9780 |
| RNaseOUT Recombinant Ribonuclease Inhibitor 5000U | Life Technologies | 10777-019 |
| Sodium bicarbonate | Sigma | S5761-500G |
| Sodium cacodylate trihydrate, 100g | Sigma | 20840-100G |
| Sodium Carbonate | Sigma | 223484-500G |
| Sodium deoxycholate | Sigma | 30970-100G |
| Sodium pyrovate | Life Technologies | 11360-039 |
| Succrose, 1KG | Sigma | 84100-1KG |
| T125 cell culture flask | Huber & Co AG | 7.661 175 |
| T25 cell culture flask | Huber & Co AG | 7.690175 |
| T75 cell culture flask | Huber & Co AG | 7.658 175 |
| Tamoxifen | Sigma | T5648-1G |
| TAQ DNA Polymerase, Cloned 150 UN(3x500) | Life Technologies | 10342046 |
| TransFectin Lipid Reagent | BioRad | 170-3351 |
| Tris-HCl | VWR | M108- 1KG |
| Trizma, 1kg | Sigma | 1503-1KG |
| TRIzol Reagent 100ml | Life Technologies | 15596026 |
| Trypsin Inhibitor 5x100MG | Sigma | T6522-5x100MG |
| Trypsin Inhibitor, 5x 100mg | Sigma | T6522-5x100MG |
| Trypan blue solution | Sigma | T8154-20ML |

7 References

- Abe, M. and N. M. Bonini (2013). "MicroRNAs and neurodegeneration: role and impact." *Trends Cell Biol* **23**(1): 30-36.
- Ables, J. L., N. A. Decarolis, M. A. Johnson, P. D. Rivera, Z. Gao, D. C. Cooper, F. Radtke, J. Hsieh and A. J. Eisch (2010). "Notch1 is required for maintenance of the reservoir of adult hippocampal stem cells." *J Neurosci* **30**(31): 10484-10492.
- Aguirre, A., M. E. Rubio and V. Gallo (2010). "Notch and EGFR pathway interaction regulates neural stem cell number and self-renewal." *Nature* **467**(7313): 323-327.
- Aharoni, R., D. Teitelbaum, M. Sela and R. Arnon (1997). "Copolymer 1 induces T cells of the T helper type 2 that crossreact with myelin basic protein and suppress experimental autoimmune encephalomyelitis." *Proceedings of the National Academy of Sciences* **94**(20): 10821-10826.
- Alderson, N. L., B. M. Rembiesa, M. D. Walla, A. Bielawska, J. Bielawski and H. Hama (2004). "The human FA2H gene encodes a fatty acid 2-hydroxylase." *Journal of Biological Chemistry* **279**(47): 48562-48568.
- Amsen, D., J. M. Blander, G. R. Lee, K. Tanigaki, T. Honjo and R. A. Flavell (2004). "Instruction of distinct CD4 T helper cell fates by different notch ligands on antigen-presenting cells." *Cell* **117**(4): 515-526.
- Andreu-Agulló, C., J. M. Morante-Redolat, A. C. Delgado and I. Fariñas (2009). "Vascular niche factor PEDF modulates Notch-dependent stemness in the adult subependymal zone." *Nature neuroscience* **12**(12): 1514-1523.
- Androutsellis-Theotokis, A., R. R. Leker, F. Soldner, D. J. Hoepfner, R. Ravin, S. W. Poser, M. A. Rueger, S. K. Bae, R. Kittappa and R. D. McKay (2006). "Notch signalling regulates stem cell numbers in vitro and in vivo." *Nature* **442**(7104): 823-826.
- Aparicio, E., P. Mathieu, M. Pereira Luppi, M. F. Almeida Gubiani and A. M. Adamo (2013). "The Notch signaling pathway: its role in focal CNS demyelination and apotransferrin-induced remyelination." *J Neurochem* **127**(6): 819-836.
- Arnett, H. A., J. Mason, M. Marino, K. Suzuki, G. K. Matsushima and J. P.-Y. Ting (2001). "TNF α promotes proliferation of oligodendrocyte progenitors and remyelination." *Nature neuroscience* **4**(11): 1116-1122.
- Ascano, J. M., L. J. Beverly and A. J. Capobianco (2003). "The C-terminal PDZ-ligand of JAGGED1 is essential for cellular transformation." *J Biol Chem*. **278**(10): 8771-8779. Epub 2002 Dec 8720.
- Ascano, J. M., L. J. Beverly and A. J. Capobianco (2003). "The C-terminal PDZ-ligand of JAGGED1 is essential for cellular transformation." *Journal of Biological Chemistry* **278**(10): 8771-8779.
- Aulehla, A., C. Wehrle, B. Brand-Saberi, R. Kemler, A. Gossler, B. Kanzler and B. G. Herrmann (2003). "Wnt3a plays a major role in the segmentation clock controlling somitogenesis." *Dev Cell*. **4**(3): 395-406.
- Azim, K., A. Rivera, O. Raineteau and A. M. Butt (2014). "GSK3beta regulates oligodendrogenesis in the dorsal microdomain of the subventricular zone via Wnt-beta-catenin signaling." *Glia* **62**(5): 778-779.
- Back, S. A., A. Riddle and M. M. McClure (2007). "Maturation-dependent vulnerability of perinatal white matter in premature birth." *Stroke* **38**(2 Suppl): 724-730.
- Bafico, A., G. Liu, A. Yaniv, A. Gazit and S. A. Aaronson (2001). "Novel mechanism of Wnt signalling inhibition mediated by Dickkopf-1 interaction with LRP6/Arrow." *Nature cell biology* **3**(7): 683-686.
- Bak, M., A. Silahtaroglu, M. Møller, M. Christensen, M. F. Rath, B. Skryabin, N. Tommerup and S. Kauppinen (2008). "MicroRNA expression in the adult mouse central nervous system." *Rna* **14**(3): 432-444.
- Balashov, K. E., D. R. Smith, S. J. Khoury, D. A. Hafler and H. L. Weiner (1997). "Increased interleukin 12 production in progressive multiple sclerosis: induction by activated CD4+ T cells via CD40 ligand." *Proceedings of the National Academy of Sciences* **94**(2): 599-603.
- Bar, E. E., A. Lin, V. Mahairaki, W. Matsui and C. G. Eberhart (2010). "Hypoxia increases the expression of stem-cell markers and promotes clonogenicity in glioblastoma neurospheres." *The American journal of pathology* **177**(3): 1491-1502.
- Barres, B., I. Hart, H. Coles, J. Burne, J. Voyvodic, W. Richardson and M. Raff (1992). "Cell death and control of cell survival in the oligodendrocyte lineage." *Cell* **70**(1): 31-46.

- Barres, B., I. Hart, H. Coles, J. Burne, J. Voyvodic, W. Richardson and M. Raff (1992). "Cell death in the oligodendrocyte lineage." Journal of neurobiology **23**(9): 1221-1230.
- Barros, C. S., T. Nguyen, K. S. R. Spencer, A. Nishiyama, H. Colognato and U. Müller (2009). "β1 integrins are required for normal CNS myelination and promote AKT-dependent myelin outgrowth." Development **136**(16): 2717-2724.
- Basak, O., C. Giachino, E. Fiorini, H. R. Macdonald and V. Taylor (2012). "Neurogenic subventricular zone stem/progenitor cells are Notch1-dependent in their active but not quiescent state." J Neurosci **32**(16): 5654-5666.
- Basak, O. and V. Taylor (2007). "Identification of self-replicating multipotent progenitors in the embryonic nervous system by high Notch activity and Hes5 expression." Eur J Neurosci **25**(4): 1006-1022.
- Basak, O. and V. Taylor (2009). "Stem cells of the adult mammalian brain and their niche." Cell Mol Life Sci **66**(6): 1057-1072.
- Beckervordersandforth, R., P. Tripathi, J. Ninkovic, E. Bayam, A. Lepier, B. Stempfhuber, F. Kirchhoff, J. Hirrlinger, A. Haslinger, D. C. Lie, J. Beckers, B. Yoder, M. Irmeler and M. Gotz (2010). "In vivo fate mapping and expression analysis reveals molecular hallmarks of prospectively isolated adult neural stem cells." Cell Stem Cell **7**(6): 744-758.
- Behrens, J., B. A. Jerchow, M. Wurtele, J. Grimm, C. Asbrand, R. Wirtz, M. Kuhl, D. Wedlich and W. Birchmeier (1998). "Functional interaction of an axin homolog, conductin, with beta-catenin, APC, and GSK3beta." Science **280**(5363): 596-599.
- Behrens, J., J. P. von Kries, M. Kühl, L. Bruhn, D. Wedlich, R. Grosschedl and W. Birchmeier (1996). "Functional interaction of β-catenin with the transcription factor LEF-1." Nature **382**(6592): 638-642.
- Bergamaschi, R., S. Villani, M. Crabbio, M. Ponzio, A. Romani, A. Verri, V. Bargiggia and V. Cosi (2009). "Inverse relationship between multiple sclerosis and allergic respiratory diseases." Neurological sciences **30**(2): 115-118.
- Bhalala, O. G., M. Srikanth and J. A. Kessler (2013). "The emerging roles of microRNAs in CNS injuries." Nat Rev Neurol **9**(6): 328-339.
- Binder, E., M. Rukavina, H. Hassani, M. Weber, H. Nakatani, T. Reiff, C. Parras, V. Taylor and H. Rohrer (2011). "Peripheral nervous system progenitors can be reprogrammed to produce myelinating oligodendrocytes and repair brain lesions." J Neurosci **31**(17): 6379-6391.
- Boulanger, J. J. and C. Messier (2014). "From precursors to myelinating oligodendrocytes: Contribution of intrinsic and extrinsic factors to white matter plasticity in the adult brain." Neuroscience **269C**: 343-366.
- Brabletz, S., K. Bajdak, S. Meidhof, U. Burk, G. Niedermann, E. Firat, U. Wellner, A. Dimmler, G. Faller, J. Schubert and T. Brabletz (2011). "The ZEB1/miR-200 feedback loop controls Notch signalling in cancer cells." EMBO J **30**(4): 770-782.
- Brady, S. T., A. S. Witt, L. L. Kirkpatrick, S. M. de Waegh, C. Readhead, P.-H. Tu and V. M.-Y. Lee (1999). "Formation of Compact Myelin Is Required for Maturation of the Axonal Cytoskeleton." The Journal of Neuroscience **19**(17): 7278-7288.
- Braun, P. E., F. Sandillon, A. Edwards, J.-M. Matthieu and A. Privat (1988). "Immunocytochemical localization by electron microscopy of 2'3'-cyclic nucleotide 3'-phosphodiesterase in developing oligodendrocytes of normal and mutant brain." The Journal of neuroscience **8**(8): 3057-3066.
- Braun, S. M. and S. Jessberger (2014). "Adult neurogenesis: mechanisms and functional significance." Development **141**(10): 1983-1986.
- Breunig, J. J., J. Silbereis, F. M. Vaccarino, N. Sestan and P. Rakic (2007). "Notch regulates cell fate and dendrite morphology of newborn neurons in the postnatal dentate gyrus." Proc Natl Acad Sci U S A **104**(51): 20558-20563.
- Breuskin, I., M. Bodson, N. Thelen, M. Thiry, L. Borgs, L. Nguyen, P. P. Lefebvre and B. Malgrange (2009). "Sox10 promotes the survival of cochlear progenitors during the establishment of the organ of Corti." Dev Biol **335**(2): 327-339.
- Brou, C., F. Logeat, N. Gupta, C. Bessia, O. LeBail, J. R. Doedens, A. Cumano, P. Roux, R. A. Black and A. Israel (2000). "A novel proteolytic cleavage involved in Notch signaling: the role of the disintegrin-metalloprotease TACE." Mol Cell **5**(2): 207-216.
- Bujalka, H., M. Koenning, S. Jackson, V. M. Perreau, B. Pope, C. M. Hay, S. Mitew, A. F. Hill, Q. R. Lu, M. Wegner, R. Srinivasan, J. Svaren, M. Willingham, B. A. Barres and B. Emery (2013). "MYRF is a membrane-associated transcription factor that autoproteolytically cleaves to directly activate myelin genes." PLoS Biol **11**(8): e1001625.

- Bultje, R. S., D. R. Castaneda-Castellanos, L. Y. Jan, Y.-N. Jan, A. R. Kriegstein and S.-H. Shi (2009). "Mammalian Par3 regulates progenitor cell asymmetric division via notch signaling in the developing neocortex." *Neuron* **63**(2): 189-202.
- Carlén, M., K. Meletis, C. Göritz, V. Darsalia, E. Evergren, K. Tanigaki, M. Amendola, F. Barnabé-Heider, M. S. Yeung and L. Naldini (2009). "Forebrain ependymal cells are Notch-dependent and generate neuroblasts and astrocytes after stroke." *Nature neuroscience* **12**(3): 259-267.
- Celis de, J. F. and S. Bray (1997). "Feed-back mechanisms affecting Notch activation at the dorsoventral boundary in the *Drosophila* wing." *Development* **124**(17): 3241-3251.
- Chalazonitis, A., A. A. Tang, Y. Shang, T. D. Pham, I. Hsieh, W. Setlik, M. D. Gershon and E. J. Huang (2011). "Homeodomain interacting protein kinase 2 regulates postnatal development of enteric dopaminergic neurons and glia via BMP signaling." *J Neurosci* **31**(39): 13746-13757.
- Chapouton, P., P. Skupien, B. Hesl, M. Coolen, J. C. Moore, R. Madelaine, E. Kremmer, T. Faus-Kessler, P. Blader, N. D. Lawson and L. Bally-Cuif (2010). "Notch activity levels control the balance between quiescence and recruitment of adult neural stem cells." *J Neurosci* **30**(23): 7961-7974.
- Chen, B., L. R. Schaevitz and S. K. McConnell (2005). "Fezl regulates the differentiation and axon targeting of layer 5 subcortical projection neurons in cerebral cortex." *Proc Natl Acad Sci U S A* **102**(47): 17184-17189.
- Chen, X., A. Stoeck, S. J. Lee, I.-M. Shih, M. M. Wang and T.-L. Wang (2010). Jagged1 expression regulated by Notch3 and Wnt/ β -catenin signaling pathways in ovarian cancer.
- Chenn, A. and C. A. Walsh (2002). "Regulation of cerebral cortical size by control of cell cycle exit in neural precursors." *Science* **297**(5580): 365-369.
- Chien, C. T., C. D. Hsiao, L. Y. Jan and Y. N. Jan (1996). "Neuronal type information encoded in the basic-helix-loop-helix domain of proneural genes." *Proc Natl Acad Sci U S A* **93**(23): 13239-13244.
- Chiquet-Ehrismann, R., G. Orend, M. Chiquet, R. P. Tucker and K. S. Midwood (2014). "Tenascins in stem cell niches." *Matrix Biol.*
- Chiu, I. M., E. T. Morimoto, H. Goodarzi, J. T. Liao, S. O'Keeffe, H. P. Phatnani, M. Muratet, M. C. Carroll, S. Levy, S. Tavazoie, R. M. Myers and T. Maniatis (2013). "A neurodegeneration-specific gene-expression signature of acutely isolated microglia from an amyotrophic lateral sclerosis mouse model." *Cell Rep* **4**(2): 385-401.
- Ciani, L. and P. C. Salinas (2005). "WNTS in the vertebrate nervous system: from patterning to neuronal connectivity." *Nat Rev Neurosci* **6**(5): 351-362.
- Clevers, H. and R. Nusse (2012). "Wnt/beta-catenin signaling and disease." *Cell* **149**(6): 1192-1205.
- Codega, P., V. Silva-Vargas, A. Paul, A. R. Maldonado-Soto, A. M. DeLeo, E. Pastrana and F. Doetsch (2014). "Prospective Identification and Purification of Quiescent Adult Neural Stem Cells from Their In Vivo Niche." *Neuron* **82**(3): 545-559.
- Cohen, M., J. Briscoe and R. Blassberg (2013). "Morphogen interpretation: the transcriptional logic of neural tube patterning." *Curr Opin Genet Dev* **23**(4): 423-428.
- Copp, A. J. (2005). "Neurulation in the cranial region--normal and abnormal." *J Anat* **207**(5): 623-635.
- Copp, A. J., N. D. Greene and J. N. Murdoch (2003). "The genetic basis of mammalian neurulation." *Nat Rev Genet* **4**(10): 784-793.
- Cordle, J., S. Johnson, J. Z. Tay, P. Roversi, M. B. Wilkin, B. H. de Madrid, H. Shimizu, S. Jensen, P. Whiteman, B. Jin, C. Redfield, M. Baron, S. M. Lea and P. A. Handford (2008). "A conserved face of the Jagged/Serrate DSL domain is involved in Notch trans-activation and cis-inhibition." *Nat Struct Mol Biol* **15**(8): 849-857.
- Crawford, M. P., S. X. Yan, S. B. Ortega, R. S. Mehta, R. E. Hewitt, D. A. Price, P. Stastny, D. C. Douek, R. A. Koup and M. K. Racke (2004). "High prevalence of autoreactive, neuroantigen-specific CD8+ T cells in multiple sclerosis revealed by novel flow cytometric assay." *Blood* **103**(11): 4222-4231.
- Cubelos, B., A. Sebastian-Serrano, S. Kim, C. Moreno-Ortiz, J. M. Redondo, C. A. Walsh and M. Nieto (2008). "Cux-2 controls the proliferation of neuronal intermediate precursors of the cortical subventricular zone." *Cereb Cortex* **18**(8): 1758-1770.

Czopka, T., A. Von Holst, G. Schmidt, C. Ffrench-Constant and A. Faissner (2009). "Tenascin C and tenascin R similarly prevent the formation of myelin membranes in a RhoA-dependent manner, but antagonistically regulate the expression of myelin basic protein via a separate pathway." *Glia* **57**(16): 1790-1801.

D'Souza, B., A. Miyamoto and G. Weinmaster (2008). "The many facets of Notch ligands." *Oncogene* **27**(38): 5148-5167.

De Pietri Tonelli, D., F. Calegari, J. F. Fei, T. Nomura, N. Osumi, C. P. Heisenberg and W. B. Huttner (2006). "Single-cell detection of microRNAs in developing vertebrate embryos after acute administration of a dual-fluorescence reporter/sensor plasmid." *Biotechniques* **41**(6): 727-732.

Dequéant, M.-L., E. Glynn, K. Gaudenz, M. Wahl, J. Chen, A. Mushegian and O. Pourquié (2006). "A Complex Oscillating Network of Signaling Genes Underlies the Mouse Segmentation Clock." *Science* **314**(5805): 1595-1598.

Deregowski, V. and E. Canalis (2008). "Gene delivery by retroviruses." *Methods Mol Biol* **455**: 157-162.

Desai, A. R. and S. K. McConnell (2000). "Progressive restriction in fate potential by neural progenitors during cerebral cortical development." *Development* **127**(13): 2863-2872.

Doetsch, F. (2003). "A niche for adult neural stem cells." *Current opinion in genetics & development* **13**(5): 543-550.

Doetsch, F., J. M. Garcia-Verdugo and A. Alvarez-Buylla (1997). "Cellular composition and three-dimensional organization of the subventricular germinal zone in the adult mammalian brain." *J Neurosci* **17**(13): 5046-5061.

Dong, Z., N. Yang, S.-Y. Yeo, A. Chitnis and S. Guo (2012). "Intralineage directional notch signaling regulates self-renewal and differentiation of asymmetrically dividing radial glia." *Neuron* **74**(1): 65-78.

Dou, S., X. Zeng, P. Cortes, H. Erdjument-Bromage, P. Tempst, T. Honjo and L. D. Vales (1994). "The recombination signal sequence-binding protein RBP-2N functions as a transcriptional repressor." *Mol Cell Biol* **14**(5): 3310-3319.

Duryagina, R., S. Thieme, K. Anastassiadis, C. Werner, S. Schneider, M. Wobus, S. Brenner and M. Bornhauser (2013). "Overexpression of Jagged-1 and its intracellular domain in human mesenchymal stromal cells differentially affect the interaction with hematopoietic stem and progenitor cells." *Stem Cells Dev* **22**(20): 2736-2750.

E. Boda, S. P., F. Bianchi, D. Cunto, Analissa Buffo (2013). Intrinsic mechanisms regulating oligodendrocyte progenitor cell division: the role of citron-kinase. *Glia*.

Eckhardt, M., A. Yaghootfam, S. FEWOU, I. Zoller and V. Gieselmann (2005). "A mammalian fatty acid hydroxylase responsible for the formation of alpha-hydroxylated galactosylceramide in myelin." *Biochem. J* **388**: 245-254.

Ehm, O., C. Goritz, M. Covic, I. Schaffner, T. J. Schwarz, E. Karaca, B. Kempkes, E. Kremmer, F. W. Pfrieger, L. Espinosa, A. Bigas, C. Giachino, V. Taylor, J. Frisen and D. C. Lie (2010). "RBPJkappa-dependent signaling is essential for long-term maintenance of neural stem cells in the adult hippocampus." *J Neurosci* **30**(41): 13794-13807.

Einheber, S., G. Zanazzi, W. Ching, S. Scherer, T. A. Milner, E. Peles and J. L. Salzer (1997). "The Axonal Membrane Protein Caspr, a Homologue of Neurexin IV, Is a Component of the Septate-like Paranodal Junctions That Assemble during Myelination." *The Journal of Cell Biology* **139**(6): 1495-1506.

Eldadah, Z. A., A. Hamosh, N. J. Biery, R. A. Montgomery, M. Duke, R. Elkins and H. C. Dietz (2001). "Familial Tetralogy of Fallot caused by mutation in the jagged1 gene." *Hum Mol Genet* **10**(2): 163-169.

Elyaman, W., E. M. Bradshaw, Y. Wang, M. Oukka, P. Kivisakk, S. Chiba, H. Yagita and S. J. Khoury (2007). "JAGGED1 and delta1 differentially regulate the outcome of experimental autoimmune encephalomyelitis." *J Immunol* **179**(9): 5990-5998.

Elyaman, W., E. M. Bradshaw, Y. Wang, M. Oukka, P. Kivisakk, S. Chiba, H. Yagita and S. J. Khoury (2007). "Jagged1 and Delta1 Differentially Regulate the Outcome of Experimental Autoimmune Encephalomyelitis." *The Journal of Immunology* **179**(9): 5990-5998.

Emery, B. (2013). "Playing the field: Sox10 recruits different partners to drive central and peripheral myelination." *PLoS Genet* **9**(10): e1003918.

Emery, B., D. Agalliu, J. D. Cahoy, T. A. Watkins, J. C. Dugas, S. B. Mulinyawe, A. Ibrahim, K. L. Ligon, D. H. Rowitch and B. A. Barres (2009). "Myelin gene regulatory factor is a critical transcriptional regulator required for CNS myelination." *Cell* **138**(1): 172-185.

Englund, C., A. Fink, C. Lau, D. Pham, R. A. Daza, A. Bulfone, T. Kowalczyk and R. F. Hevner (2005). "Pax6, Tbr2, and Tbr1 are expressed sequentially by radial glia, intermediate progenitor cells, and postmitotic neurons in developing neocortex." *J Neurosci* **25**(1): 247-251.

- Esper, R. M., M. S. Pankonin and J. A. Loeb (2006). "Neuregulins: versatile growth and differentiation factors in nervous system development and human disease." *Brain Res Rev* **51**(2): 161-175.
- Estrach, S., J. Legg and F. M. Watt (2007). "Syntenin mediates Delta1-induced cohesiveness of epidermal stem cells in culture." *Journal of cell science* **120**(16): 2944-2952.
- Faigle, R. and H. Song (2013). "Signaling mechanisms regulating adult neural stem cells and neurogenesis." *Biochim Biophys Acta* **1830**(2): 2435-2448.
- Fancy, S. P., S. E. Baranzini, C. Zhao, D. I. Yuk, K. A. Irvine, S. Kaing, N. Sanai, R. J. Franklin and D. H. Rowitch (2009). "Dysregulation of the Wnt pathway inhibits timely myelination and remyelination in the mammalian CNS." *Genes Dev* **23**(13): 1571-1585.
- Fancy, S. P., J. R. Chan, S. E. Baranzini, R. J. Franklin and D. H. Rowitch (2011). "Myelin regeneration: a recapitulation of development?" *Annu Rev Neurosci* **34**: 21-43.
- Fancy, S. P., E. P. Harrington, S. E. Baranzini, J. C. Silbereis, L. R. Shiow, T. J. Yuen, E. J. Huang, S. Lomvardas and D. H. Rowitch (2014). "Parallel states of pathological Wnt signaling in neonatal brain injury and colon cancer." *Nat Neurosci* **17**(4): 506-512.
- Fancy, S. P., E. P. Harrington, T. J. Yuen, J. C. Silbereis, C. Zhao, S. E. Baranzini, C. C. Bruce, J. J. Otero, E. J. Huang, R. Nusse, R. J. Franklin and D. H. Rowitch (2011). "Axin2 as regulatory and therapeutic target in newborn brain injury and remyelination." *Nat Neurosci* **14**(8): 1009-1016.
- Fang, W. Q., W. W. Chen, A. K. Fu and N. Y. Ip (2013). "Axin directs the amplification and differentiation of intermediate progenitors in the developing cerebral cortex." *Neuron* **79**(4): 665-679.
- Ferron, S. R., M. Charalambous, E. Radford, K. McEwen, H. Wildner, E. Hind, J. M. Morante-Redolat, J. Laborda, F. Guillemot, S. R. Bauer, I. Farinas and A. C. Ferguson-Smith (2011). "Postnatal loss of Dlk1 imprinting in stem cells and niche astrocytes regulates neurogenesis." *Nature* **475**(7356): 381-385.
- Ferron, S. R., N. Pozo, A. Laguna, S. Aranda, E. Porlan, M. Moreno, C. Fillat, S. de la Luna, P. Sánchez, M. L. Arbonés and I. Fariñas (2010). "Regulated Segregation of Kinase Dyrk1A during Asymmetric Neural Stem Cell Division Is Critical for EGFR-Mediated Biased Signaling." *Cell Stem Cell* **7**(3): 367-379.
- Filipe Palavraa, L. A. (2014). "Remyelination in Multiple Sclerosis – How Close are We?" *Journal of Neurology & Neurophysiology* **05**(02).
- Finzsch, M., C. C. Stolt, P. Lommes and M. Wegner (2008). "Sox9 and Sox10 influence survival and migration of oligodendrocyte precursors in the spinal cord by regulating PDGF receptor alpha expression." *Development* **135**(4): 637-646.
- Fish, J. L., C. Dehay, H. Kennedy and W. B. Huttner (2008). "Making bigger brains-the evolution of neural-progenitor-cell division." *J Cell Sci* **121**(Pt 17): 2783-2793.
- Fishell, G. and A. R. Kriegstein (2003). "Neurons from radial glia: the consequences of asymmetric inheritance." *Current Opinion in Neurobiology* **13**(1): 34-41.
- Fiuza, U. M. and A. M. Arias (2007). "Cell and molecular biology of Notch." *J Endocrinol* **194**(3): 459-474.
- Fleming, R. J., K. Hori, A. Sen, G. V. Filloramo, J. M. Langer, R. A. Obar, S. Artavanis-Tsakonas and A. C. Maharaj-Best (2013). "An extracellular region of Serrate is essential for ligand-induced cis-inhibition of Notch signaling." *Development* **140**(9): 2039-2049.
- Foster, R. E., B. W. Connors and S. G. Waxman (1982). "Rat optic nerve: Electrophysiological, pharmacological and anatomical studies during development." *Developmental Brain Research* **3**(3): 371-386.
- Franco, S. J., C. Gil-Sanz, I. Martinez-Garay, A. Espinosa, S. R. Harkins-Perry, C. Ramos and U. Muller (2012). "Fate-restricted neural progenitors in the mammalian cerebral cortex." *Science* **337**(6095): 746-749.
- Franco, S. J. and U. Muller (2013). "Shaping our minds: stem and progenitor cell diversity in the mammalian neocortex." *Neuron* **77**(1): 19-34.
- Franklin, R. J. (2002). "Why does remyelination fail in multiple sclerosis?" *Nature Reviews Neuroscience* **3**(9): 705-714.
- Franklin, R. J. and C. ffrench-Constant (2008). "Remyelination in the CNS: from biology to therapy." *Nat Rev Neurosci* **9**(11): 839-855.

Franklin, R. J., C. French-Constant, J. M. Edgar and K. J. Smith (2012). "Neuroprotection and repair in multiple sclerosis." Nat Rev Neurol **8**(11): 624-634.

Gaiano, N., J. S. Nye and G. Fishell (2000). "Radial Glial Identity Is Promoted by Notch1 Signaling in the Murine Forebrain." Neuron **26**(2): 395-404.

Gal, J. S., Y. M. Morozov, A. E. Ayoub, M. Chatterjee, P. Rakic and T. F. Haydar (2006). "Molecular and morphological heterogeneity of neural precursors in the mouse neocortical proliferative zones." J Neurosci **26**(3): 1045-1056.

Gao, C., G. Xiao and J. Hu (2014). "Regulation of Wnt/ β -catenin signaling by posttranslational modifications." Cell & bioscience **4**(1): 13.

Gauthier, M.-K., K. Kosciuczyk, L. Tapley and S. Karimi-Abdolrezaee (2013). "Dysregulation of the neuregulin-1–ErbB network modulates endogenous oligodendrocyte differentiation and preservation after spinal cord injury." European Journal of Neuroscience **38**(5): 2693-2715.

Geschwind, D. H. and P. Rakic (2013). "Cortical evolution: judge the brain by its cover." Neuron **80**(3): 633-647.

Ghislain, J. and P. Charnay (2006). "Control of myelination in Schwann cells: a Krox20 cis - regulatory element integrates Oct6, Brn2 and Sox10 activities." EMBO reports **7**(1): 52-58.

Giachino, C., O. Basak, S. Lugert, P. Knuckles, K. Obernier, R. Fiorelli, S. Frank, O. Raineteau, A. Alvarez-Buylla and V. Taylor (2014). "Molecular diversity subdivides the adult forebrain neural stem cell population." Stem Cells **32**(1): 70-84.

Giachino, C., O. Basak and V. Taylor (2009). "Isolation and manipulation of mammalian neural stem cells in vitro." Methods Mol Biol **482**: 143-158.

Giachino, C. and V. Taylor (2014). "Notching up neural stem cell homogeneity in homeostasis and disease." Front Neurosci **8**: 32.

Glezer, I., A. Lapointe and S. Rivest (2006). "Innate immunity triggers oligodendrocyte progenitor reactivity and confines damages to brain injuries." The FASEB journal **20**(6): 750-752.

Gomes, W. A., M. F. Mehler and J. A. Kessler (2003). "Transgenic overexpression of BMP4 increases astroglial and decreases oligodendroglial lineage commitment." Developmental Biology **255**(1): 164-177.

Gotz, M. and W. B. Huttner (2005). "The cell biology of neurogenesis." Nat Rev Mol Cell Biol **6**(10): 777-788.

Grbavec, D. and S. Stifani (1996). "Molecular interaction between TLE1 and the carboxyl-terminal domain of HES-1 containing the WRPW motif." Biochemical and biophysical research communications **223**(3): 701-705.

Greig, L. C., M. B. Woodworth, M. J. Galazo, H. Padmanabhan and J. D. Macklis (2013). "Molecular logic of neocortical projection neuron specification, development and diversity." Nat Rev Neurosci **14**(11): 755-769.

Greiner-Tollersrud, L., T. Berg, H. M. Stensland, G. Evjen and O. K. Greiner-Tollersrud (2013). "Bovine brain myelin glycerophosphocholine choline phosphodiesterase is an alkaline lysosphingomyelinase of the eNPP-family, regulated by lysosomal sorting." Neurochem Res **38**(2): 300-310.

Griffiths, I., M. Klugmann, T. Anderson, D. Yool, C. Thomson, M. H. Schwab, A. Schneider, F. Zimmermann, M. McCulloch, N. Nadon and K. A. Nave (1998). "Axonal swellings and degeneration in mice lacking the major proteolipid of myelin." Science **280**(5369): 1610-1613.

Guegan, K., K. Stals, M. Day, P. Turnpenny and S. Ellard (2012). "JAG1 mutations are found in approximately one third of patients presenting with only one or two clinical features of Alagille syndrome." Clin Genet **82**(1): 33-40.

Guerau-de-Arellano, M., K. M. Smith, J. Godlewski, Y. Liu, R. Winger, S. E. Lawler, C. C. Whitacre, M. K. Racke and A. E. Lovett-Racke (2011). "Micro-RNA dysregulation in multiple sclerosis favours pro-inflammatory T-cell-mediated autoimmunity." Brain **134**(Pt 12): 3578-3589.

Guillemot, F. (2005). "Cellular and molecular control of neurogenesis in the mammalian telencephalon." Curr Opin Cell Biol **17**(6): 639-647.

Guo, C., M. J. Eckler, W. L. McKenna, G. L. McKinsey, J. L. Rubenstein and B. Chen (2013). "Fezf2 expression identifies a multipotent progenitor for neocortical projection neurons, astrocytes, and oligodendrocytes." Neuron **80**(5): 1167-1174.

- Gustafsson, M. V., X. Zheng, T. Pereira, K. Gradin, S. Jin, J. Lundkvist, J. L. Ruas, L. Poellinger, U. Lendahl and M. Bondesson (2005). "Hypoxia requires notch signaling to maintain the undifferentiated cell state." *Developmental cell* **9**(5): 617-628.
- Hamada, Y., Y. Kadokawa, M. Okabe, M. Ikawa, J. R. Coleman and Y. Tsujimoto (1999). "Mutation in ankyrin repeats of the mouse Notch2 gene induces early embryonic lethality." *Development* **126**(15): 3415-3424.
- Hammond, T. R., A. Gadea, J. Dupree, C. Kerninon, B. Nait-Oumesmar, A. Aguirre and V. Gallo (2014). "Astrocyte-Derived Endothelin-1 Inhibits Remyelination through Notch Activation." *Neuron* **81**(3): 588-602.
- Han, W. and N. Sestan (2013). "Cortical projection neurons: sprung from the same root." *Neuron* **80**(5): 1103-1105.
- Hanley, J. G. (2008). "PICK1: a multi-talented modulator of AMPA receptor trafficking." *Pharmacol Ther.* **118**(1): 152-160. Epub 2008 Feb 2020.
- Hashimi, S. T., J. A. Fulcher, M. H. Chang, L. Gov, S. Wang and B. Lee (2009). "MicroRNA profiling identifies miR-34a and miR-21 and their target genes JAG1 and WNT1 in the coordinate regulation of dendritic cell differentiation." *Blood* **114**(2): 404-414.
- Hatakeyama, J., Y. Bessho, K. Katoh, S. Ookawara, M. Fujioka, F. Guillemot and R. Kageyama (2004). "Hes genes regulate size, shape and histogenesis of the nervous system by control of the timing of neural stem cell differentiation." *Development* **131**(22): 5539-5550.
- Hatakeyama, J. and R. Kageyama (2006). "Notch1 expression is spatiotemporally correlated with neurogenesis and negatively regulated by Notch1-independent Hes genes in the developing nervous system." *Cereb Cortex* **16 Suppl 1**: i132-137.
- Haubensak, W., A. Attardo, W. Denk and W. B. Huttner (2004). "Neurons arise in the basal neuroepithelium of the early mammalian telencephalon: a major site of neurogenesis." *Proc Natl Acad Sci U S A* **101**(9): 3196-3201.
- He, M., Y. Liu, X. Wang, M. Q. Zhang, G. J. Hannon and Z. J. Huang (2012). "Cell-type-based analysis of microRNA profiles in the mouse brain." *Neuron* **73**(1): 35-48.
- He, Y., J. Dupree, J. Wang, J. Sandoval, J. Li, H. Liu, Y. Shi, K. A. Nave and P. Casaccia-Bonnel (2007). "The transcription factor Yin Yang 1 is essential for oligodendrocyte progenitor differentiation." *Neuron* **55**(2): 217-230.
- Hebert, J. M. and G. Fishell (2008). "The genetics of early telencephalon patterning: some assembly required." *Nat Rev Neurosci* **9**(9): 678-685.
- Heng, J. I., L. Nguyen, D. S. Castro, C. Zimmer, H. Wildner, O. Armant, D. Skowronska-Krawczyk, F. Bedogni, J. M. Matter, R. Hevner and F. Guillemot (2008). "Neurogenin 2 controls cortical neuron migration through regulation of Rnd2." *Nature* **455**(7209): 114-118.
- Hicks, C., S. H. Johnston, G. diSibio, A. Collazo, T. F. Vogt and G. Weinmaster (2000). "Fringe differentially modulates Jagged1 and Delta1 signalling through Notch1 and Notch2." *Nat Cell Biol* **2**(8): 515-520.
- Hirabayashi, Y., Y. Itoh, H. Tabata, K. Nakajima, T. Akiyama, N. Masuyama and Y. Gotoh (2004). "The Wnt/beta-catenin pathway directs neuronal differentiation of cortical neural precursor cells." *Development* **131**(12): 2791-2801.
- Hitoshi, S., T. Alexson, V. Tropepe, D. Donoviel, A. J. Elia, J. S. Nye, R. A. Conlon, T. W. Mak, A. Bernstein and D. van der Kooy (2002). "Notch pathway molecules are essential for the maintenance, but not the generation, of mammalian neural stem cells." *Genes Dev* **16**(7): 846-858.
- Hock, B., B. Bohme, T. Karn, T. Yamamoto, K. Kaibuchi, U. Holtrich, S. Holland, T. Pawson, H. Rubsamens-Waigmann and K. Strebhardt (1998). "PDZ-domain-mediated interaction of the Eph-related receptor tyrosine kinase EphB3 and the ras-binding protein AF6 depends on the kinase activity of the receptor." *Proc Natl Acad Sci U S A*. **95**(17): 9779-9784.
- Hornig, J., F. Frob, M. R. Vogl, I. Hermans-Borgmeyer, E. R. Tamm and M. Wegner (2013). "The transcription factors Sox10 and Myrf define an essential regulatory network module in differentiating oligodendrocytes." *PLoS Genet* **9**(10): e1003907.
- Houart, C., L. Caneparo, C.-P. Heisenberg, K. A. Barth, M. Take-Uchi and S. W. Wilson (2002). "Establishment of the Telencephalon during Gastrulation by Local Antagonism of Wnt Signaling." *Neuron* **35**(2): 255-265.
- Hsieh, J. J. and S. D. Hayward (1995). "Masking of the CBF1/RBPJ kappa transcriptional repression domain by Epstein-Barr virus EBNA2." *Science* **268**(5210): 560-563.

- Huttner, W. B. and M. Brand (1997). "Asymmetric division and polarity of neuroepithelial cells." Curr Opin Neurobiol **7**(1): 29-39.
- Ihrie, R. A. and A. Alvarez-Buylla (2011). "Lake-front property: a unique germinal niche by the lateral ventricles of the adult brain." Neuron **70**(4): 674-686.
- Illumina (2011). Specification Sheet: Illumina HiSeq2000 specification sheet.
- Imayoshi, I. (2012). "[Neurogenesis in the postnatal and adult brain]." Nihon Shinkei Seishin Yakurigaku Zasshi **32**(5-6): 293-297.
- Imayoshi, I. and R. Kageyama (2014). "bHLH Factors in Self-Renewal, Multipotency, and Fate Choice of Neural Progenitor Cells." Neuron **82**(1): 9-23.
- Imayoshi, I., M. Sakamoto, M. Yamaguchi, K. Mori and R. Kageyama (2010). "Essential roles of Notch signaling in maintenance of neural stem cells in developing and adult brains." J Neurosci **30**(9): 3489-3498.
- Irvin, D. K., I. Nakano, A. Paucar and H. I. Kornblum (2004). "Patterns of Jagged1, Jagged2, Delta-like 1 and Delta-like 3 expression during late embryonic and postnatal brain development suggest multiple functional roles in progenitors and differentiated cells." J Neurosci Res **75**(3): 330-343.
- Irvin, D. K., S. D. Zurcher, T. Nguyen, G. Weinmaster and H. I. Kornblum (2001). "Expression patterns of Notch1, Notch2, and Notch3 suggest multiple functional roles for the Notch-DSL signaling system during brain development." J Comp Neurol **436**(2): 167-181.
- Jacques, B. E., C. Puligilla, R. M. Weichert, A. Ferrer-Vaquer, A. K. Hadjantonakis, M. W. Kelley and A. Dabdoub (2012). "A dual function for canonical Wnt/beta-catenin signaling in the developing mammalian cochlea." Development **139**(23): 4395-4404.
- Jang, M. H., M. A. Bonaguidi, Y. Kitabatake, J. Sun, J. Song, E. Kang, H. Jun, C. Zhong, Y. Su, J. U. Guo, M. X. Wang, K. A. Sailor, J. Y. Kim, Y. Gao, K. M. Christian, G. L. Ming and H. Song (2013). "Secreted frizzled-related protein 3 regulates activity-dependent adult hippocampal neurogenesis." Cell Stem Cell **12**(2): 215-223.
- Jessell, T. M. and J. R. Sanes (2000). Principles of neural science: The Induction and Patterning of the Nervous System. New York, McGraw-Hill, Health Professions Division.
- Jho, E. H., T. Zhang, C. Domon, C. K. Joo, J. N. Freund and F. Costantini (2002). "Wnt/beta-catenin/Tcf signaling induces the transcription of Axin2, a negative regulator of the signaling pathway." Mol Cell Biol **22**(4): 1172-1183.
- John, G. R., S. L. Shankar, B. Shafit-Zagardo, A. Massimi, S. C. Lee, C. S. Raine and C. F. Brosnan (2002). "Multiple sclerosis: re-expression of a developmental pathway that restricts oligodendrocyte maturation." Nature medicine **8**(10): 1115-1121.
- Johnston, D. A., B. Dong and C. C. Hughes (2009). "TNF induction of jagged-1 in endothelial cells is NFkappaB-dependent." Gene **435**(1-2): 36-44.
- Jurynczyk, M., A. Jurewicz, B. Bielecki, C. S. Raine and K. Selmaj (2008). "Overcoming failure to repair demyelination in EAE: γ -secretase inhibition of Notch signaling." Journal of the Neurological Sciences **265**(1-2): 5-11.
- Kadowaki, M., S. Nakamura, O. Machon, S. Krauss, G. L. Radice and M. Takeichi (2007). "N-cadherin mediates cortical organization in the mouse brain." Developmental biology **304**(1): 22-33.
- Kageyama, R., T. Ohtsuka and T. Kobayashi (2007). "The Hes gene family: repressors and oscillators that orchestrate embryogenesis." Development **134**(7): 1243-1251.
- Kageyama, R., T. Ohtsuka, H. Shimojo and I. Imayoshi (2008). "Dynamic Notch signaling in neural progenitor cells and a revised view of lateral inhibition." Nature neuroscience **11**(11): 1247-1251.
- Kamakura, S., K. Oishi, T. Yoshimatsu, M. Nakafuku, N. Masuyama and Y. Gotoh (2004). "Hes binding to STAT3 mediates crosstalk between Notch and JAK-STAT signalling." Nature cell biology **6**(6): 547-554.
- Kato, H., Y. Taniguchi, H. Kurooka, S. Minoguchi, T. Sakai, S. Nomura-Okazaki, K. Tamura and T. Honjo (1997). "Involvement of RBP-J in biological functions of mouse Notch1 and its derivatives." Development **124**(20): 4133-4141.
- Kawaguchi, D., S. Furutachi, H. Kawai, K. Hozumi and Y. Gotoh (2013). "Dil1 maintains quiescence of adult neural stem cells and segregates asymmetrically during mitosis." Nat Commun **4**: 1880.

- Kebir, H., K. Kreymborg, I. Ifergan, A. Dodelet-Devillers, R. Cayrol, M. Bernard, F. Giuliani, N. Arbour, B. Becher and A. Prat (2007). "Human TH17 lymphocytes promote blood-brain barrier disruption and central nervous system inflammation." *Nature medicine* **13**(10): 1173-1175.
- Kessaris, N., M. Fogarty, P. Iannarelli, M. Grist, M. Wegner and W. D. Richardson (2006). "Competing waves of oligodendrocytes in the forebrain and postnatal elimination of an embryonic lineage." *Nat Neurosci* **9**(2): 173-179.
- Kiecker, C. and A. Lumsden (2005). "Compartments and their boundaries in vertebrate brain development." *Nat Rev Neurosci* **6**(7): 553-564.
- Kiernan, A. E., J. Xu and T. Gridley (2006). "The Notch ligand JAG1 is required for sensory progenitor development in the mammalian inner ear." *PLoS Genet.* **2**(1): e4. Epub 2006 Jan 2006.
- Klein, T., K. Brennan and A. M. Arias (1997). "An Intrinsic Dominant Negative Activity of Serrate That Is Modulated during Wing Development in *Drosophila*." *Developmental Biology* **189**(1): 123-134.
- Knoblich, J. A. (2008). "Mechanisms of asymmetric stem cell division." *Cell* **132**(4): 583-597.
- Knuckles, P., M. A. Vogt, S. Lugert, M. Milo, M. M. Chong, G. M. Hautbergue, S. A. Wilson, D. R. Littman and V. Taylor (2012). "Drosha regulates neurogenesis by controlling neurogenin 2 expression independent of microRNAs." *Nat Neurosci* **15**(7): 962-969.
- Koenning, M., S. Jackson, C. M. Hay, C. Faux, T. J. Kilpatrick, M. Willingham and B. Emery (2012). "Myelin gene regulatory factor is required for maintenance of myelin and mature oligodendrocyte identity in the adult CNS." *J Neurosci* **32**(36): 12528-12542.
- Kopan, R. and M. X. Ilagan (2009). "The canonical Notch signaling pathway: unfolding the activation mechanism." *Cell* **137**(2): 216-233.
- Kosik, K. S. (2006). "The neuronal microRNA system." *Nature Reviews Neuroscience* **7**(12): 911-920.
- Kriegstein, A. and A. Alvarez-Buylla (2009). "The glial nature of embryonic and adult neural stem cells." *Annu Rev Neurosci.* **32**: 149-184.
- Kriegstein, A. R. and M. Gotz (2003). "Radial glia diversity: a matter of cell fate." *Glia* **43**(1): 37-43.
- Kuhlbrodt, K., B. Herbarth, E. Sock, I. Hermans-Borgmeyer and M. Wegner (1998). "Sox10, a Novel Transcriptional Modulator in Glial Cells." *The Journal of Neuroscience* **18**(1): 237-250.
- Kuhn, H. G., H. Dickinson-Anson and F. H. Gage (1996). "Neurogenesis in the dentate gyrus of the adult rat: age-related decrease of neuronal progenitor proliferation." *The Journal of neuroscience* **16**(6): 2027-2033.
- Kuo, C. T., Z. Mirzadeh, M. Soriano-Navarro, M. Rasin, D. Wang, J. Shen, N. Sestan, J. Garcia-Verdugo, A. Alvarez-Buylla, L. Y. Jan and Y. N. Jan (2006). "Postnatal deletion of Numb/Numbl like reveals repair and remodeling capacity in the subventricular neurogenic niche." *Cell* **127**(6): 1253-1264.
- Kurooka, H., K. Kuroda and T. Honjo (1998). "Roles of the ankyrin repeats and C-terminal region of the mouse notch1 intracellular region." *Nucleic Acids Res* **26**(23): 5448-5455.
- Kusek, G., M. Campbell, F. Doyle, S. A. Tenenbaum, M. Kiebler and S. Temple (2012). "Asymmetric segregation of the double-stranded RNA binding protein Staufen2 during mammalian neural stem cell divisions promotes lineage progression." *Cell Stem Cell* **11**(4): 505-516.
- Küspert, M., A. Hammer, M. R. Bösl and M. Wegner (2011). "Olig2 regulates Sox10 expression in oligodendrocyte precursors through an evolutionary conserved distal enhancer." *Nucleic acids research* **39**(4): 1280-1293.
- Kuwabara, T., J. Hsieh, A. Muotri, G. Yeo, M. Warashina, D. C. Lie, L. Moore, K. Nakashima, M. Asashima and F. H. Gage (2009). "Wnt-mediated activation of NeuroD1 and retro-elements during adult neurogenesis." *Nature neuroscience* **12**(9): 1097-1105.
- Kuwahara, A., Y. Hirabayashi, P. S. Knoepfler, M. M. Taketo, J. Sakai, T. Kodama and Y. Gotoh (2010). "Wnt signaling and its downstream target N-myc regulate basal progenitors in the developing neocortex." *Development* **137**(7): 1035-1044.
- Kwan, K. Y., N. Sestan and E. S. Anton (2012). "Transcriptional co-regulation of neuronal migration and laminar identity in the neocortex." *Development* **139**(9): 1535-1546.
- Lagos-Quintana, M., R. Rauhut, A. Yalcin, J. Meyer, W. Lendeckel and T. Tuschl (2002). "Identification of tissue-specific microRNAs from mouse." *Current Biology* **12**(9): 735-739.

Landgraf, P., M. Rusu, R. Sheridan, A. Sewer, N. Iovino, A. Aravin, S. Pfeffer, A. Rice, A. O. Kamphorst and M. Landthaler (2007). "A mammalian microRNA expression atlas based on small RNA library sequencing." *Cell* **129**(7): 1401-1414.

Lang, J., Y. Maeda, P. Bannerman, J. Xu, M. Horiuchi, D. Pleasure and F. Guo (2013). "Adenomatous polyposis coli regulates oligodendroglial development." *J Neurosci* **33**(7): 3113-3130.

Larsen, P. H., J. E. Wells, W. B. Stallcup, G. Opdenakker and V. W. Yong (2003). "Matrix metalloproteinase-9 facilitates remyelination in part by processing the inhibitory NG2 proteoglycan." *The Journal of neuroscience* **23**(35): 11127-11135.

Lasiene, J., L. Shupe, S. Perlmutter and P. Horner (2008). "No evidence for chronic demyelination in spared axons after spinal cord injury in a mouse." *The Journal of Neuroscience* **28**(15): 3887-3896.

Lavado, A. and G. Oliver (2014). "Jagged1 is necessary for postnatal and adult neurogenesis in the dentate gyrus." *Dev Biol* **388**(1): 11-21.

LaVoie, M. J. and D. J. Selkoe (2003). "The Notch ligands, Jagged and Delta, are sequentially processed by alpha-secretase and presenilin/gamma-secretase and release signaling fragments." *J Biol Chem* **278**(36): 34427-34437.

LeBlanc, S. E., S.-W. Jang, R. M. Ward, L. Wrabetz and J. Svaren (2006). "Direct regulation of myelin protein zero expression by the Egr2 transactivator." *Journal of Biological Chemistry* **281**(9): 5453-5460.

Lee, K. K., Y. De Repentigny, R. Saulnier, P. Rippstein, W. B. Macklin and R. Kothary (2006). "Dominant - negative β 1 integrin mice have region - specific myelin defects accompanied by alterations in MAPK activity." *Glia* **53**(8): 836-844.

Lee, S., M. K. Leach, S. A. Redmond, S. Y. C. Chong, S. H. Mellon, S. J. Tuck, Z.-Q. Feng, J. M. Corey and J. R. Chan (2012). "A culture system to study oligodendrocyte myelination processes using engineered nanofibers." *Nat Meth* **9**(9): 917-922.

Leone, D. P., K. Srinivasan, B. Chen, E. Alcamo and S. K. McConnell (2008). "The determination of projection neuron identity in the developing cerebral cortex." *Curr Opin Neurobiol* **18**(1): 28-35.

Leung, J. Y., F. T. Kolligs, R. Wu, Y. Zhai, R. Kuick, S. Hanash, K. R. Cho and E. R. Fearon (2002). "Activation of AXIN2 expression by beta-catenin-T cell factor. A feedback repressor pathway regulating Wnt signaling." *J Biol Chem* **277**(24): 21657-21665.

Li, H., Y. He, W. D. Richardson and P. Casaccia (2009). "Two-tier transcriptional control of oligodendrocyte differentiation." *Curr Opin Neurobiol* **19**(5): 479-485.

Li, H., Y. Lu, H. K. Smith and W. D. Richardson (2007). "Olig1 and Sox10 interact synergistically to drive myelin basic protein transcription in oligodendrocytes." *J Neurosci* **27**(52): 14375-14382.

Li, J. and C. Y. Wang (2008). "TBL1-TBLR1 and beta-catenin recruit each other to Wnt target-gene promoter for transcription activation and oncogenesis." *Nat Cell Biol.* **10**(2): 160-169. Epub 2008 Jan 2013.

Li, L., I. D. Krantz, Y. Deng, A. Genin, A. B. Banta, C. C. Collins, M. Qi, B. J. Trask, W. L. Kuo, J. Cochran, T. Costa, M. E. Pierpont, E. B. Rand, D. A. Piccoli, L. Hood and N. B. Spinner (1997). "Alagille syndrome is caused by mutations in human Jagged1, which encodes a ligand for Notch1." *Nat Genet* **16**(3): 243-251.

Li, V. S., S. S. Ng, P. J. Boersema, T. Y. Low, W. R. Karthaus, J. P. Gerlach, S. Mohammed, A. J. Heck, M. M. Maurice, T. Mahmoudi and H. Clevers (2012). "Wnt signaling through inhibition of beta-catenin degradation in an intact Axin1 complex." *Cell* **149**(6): 1245-1256.

Li, Y. and N. E. Baker (2004). "The roles of cis-inactivation by Notch ligands and of neuralized during eye and bristle patterning in Drosophila." *BMC Dev Biol* **4**: 5.

Lindsell, C. E., J. Boulter, G. diSibio, A. Gossler and G. Weinmaster (1996). "Expression patterns of Jagged, Delta1, Notch1, Notch2, and Notch3 genes identify ligand-receptor pairs that may function in neural development." *Mol Cell Neurosci* **8**(1): 14-27.

Lindsell, C. E., J. Boulter, G. diSibio, A. Gossler and G. Weinmaster (1996). "Expression Patterns of Jagged, Delta1, Notch1, Notch2, and Notch3 Genes Identify Ligand-Receptor Pairs That May Function in Neural Development." *Molecular and Cellular Neuroscience* **8**(1): 14-27.

Liu, A. and L. A. Niswander (2005). "Bone morphogenetic protein signalling and vertebrate nervous system development." *Nat Rev Neurosci* **6**(12): 945-954.

- Liu, C., Z. Q. Teng, N. J. Santistevan, K. E. Szulwach, W. Guo, P. Jin and X. Zhao (2010). "Epigenetic regulation of miR-184 by MBD1 governs neural stem cell proliferation and differentiation." *Cell Stem Cell* **6**(5): 433-444.
- Liu, X. S., M. Chopp, R. L. Zhang, T. Tao, X. L. Wang, H. Kassis, A. Hozeska-Solgot, L. Zhang, C. Chen and Z. G. Zhang (2011). "MicroRNA profiling in subventricular zone after stroke: MiR-124a regulates proliferation of neural progenitor cells through Notch signaling pathway." *PLoS One* **6**(8): e23461.
- Louvi, A. and S. Artavanis-Tsakonas (2006). "Notch signalling in vertebrate neural development." *Nat Rev Neurosci* **7**(2): 93-102.
- Lugert, S., O. Basak, P. Knuckles, U. Haussler, K. Fabel, M. Gotz, C. A. Haas, G. Kempermann, V. Taylor and C. Giachino (2010). "Quiescent and active hippocampal neural stem cells with distinct morphologies respond selectively to physiological and pathological stimuli and aging." *Cell Stem Cell* **6**(5): 445-456.
- Lui, J. H., D. V. Hansen and A. R. Kriegstein (2011). "Development and evolution of the human neocortex." *Cell* **146**(1): 18-36.
- Lupo, G., W. A. Harris and K. E. Lewis (2006). "Mechanisms of ventral patterning in the vertebrate nervous system." *Nat Rev Neurosci* **7**(2): 103-114.
- Lustig, B., B. Jerchow, M. Sachs, S. Weiler, T. Pietsch, U. Karsten, M. van de Wetering, H. Clevers, P. M. Schlag, W. Birchmeier and J. Behrens (2002). "Negative feedback loop of Wnt signaling through upregulation of conductin/axin2 in colorectal and liver tumors." *Mol Cell Biol* **22**(4): 1184-1193.
- Lütolf, S., F. Radtke, M. Aguet, U. Suter and V. Taylor (2002). "Notch1 is required for neuronal and glial differentiation in the cerebellum." *Development* **129**(2): 373-385.
- Maden, M. (2007). "Retinoic acid in the development, regeneration and maintenance of the nervous system." *Nat Rev Neurosci* **8**(10): 755-765.
- Majava, V., E. Polverini, A. Mazzini, R. Nanekar, W. Knoll, J. Peters, F. Natali, P. Baumgärtel, I. Kursula and P. Kursula (2010). "Structural and functional characterization of human peripheral nervous system myelin protein P2." *PLoS One* **5**(4): e10300.
- Malatesta, P., E. Hartfuss and M. Gotz (2000). "Isolation of radial glial cells by fluorescent-activated cell sorting reveals a neuronal lineage." *Development* **127**(24): 5253-5263.
- Maretto, S., M. Cordenonsi, S. Dupont, P. Braghetta, V. Broccoli, A. B. Hassan, D. Volpin, G. M. Bressan and S. Piccolo (2003). "Mapping Wnt/ β -catenin signaling during mouse development and in colorectal tumors." *Proceedings of the National Academy of Sciences* **100**(6): 3299-3304.
- Martinez-Morales, P. L., A. C. Quiroga, J. A. Barbas and A. V. Morales (2010). "SOX5 controls cell cycle progression in neural progenitors by interfering with the WNT-beta-catenin pathway." *EMBO Rep* **11**(6): 466-472.
- Martini, R. and M. Schachner (1986). "Immunoelectron microscopic localization of neural cell adhesion molecules (L1, N-CAM, and MAG) and their shared carbohydrate epitope and myelin basic protein in developing sciatic nerve." *The Journal of cell biology* **103**(6): 2439-2448.
- Mason, J. L., K. Suzuki, D. D. Chaplin and G. K. Matsushima (2001). "Interleukin-1 β promotes repair of the CNS." *The Journal of Neuroscience* **21**(18): 7046-7052.
- Massagué, J., J. Seoane and D. Wotton (2005). "Smad transcription factors." *Genes & development* **19**(23): 2783-2810.
- McConnell, S. K. (1988). "Fates of visual cortical neurons in the ferret after isochronic and heterochronic transplantation." *J Neurosci* **8**(3): 945-974.
- McCright, B., X. Gao, L. Shen, J. Lozier, Y. Lan, M. Maguire, D. Herzlinger, G. Weinmaster, R. Jiang and T. Gridley (2001). "Defects in development of the kidney, heart and eye vasculature in mice homozygous for a hypomorphic Notch2 mutation." *Development* **128**(4): 491-502.
- Meijer, D. H., M. F. Kane, S. Mehta, H. Liu, E. Harrington, C. M. Taylor, C. D. Stiles and D. H. Rowitch (2012). "Separated at birth? The functional and molecular divergence of OLIG1 and OLIG2." *Nat Rev Neurosci* **13**(12): 819-831.
- Menn, B., J. M. Garcia-Verdugo, C. Yaschine, O. Gonzalez-Perez, D. Rowitch and A. Alvarez-Buylla (2006). "Origin of oligodendrocytes in the subventricular zone of the adult brain." *J Neurosci* **26**(30): 7907-7918.

- Merlos-Suarez, A., S. Ruiz-Paz, J. Baselga and J. Arribas (2001). "Metalloprotease-dependent protransforming growth factor-alpha ectodomain shedding in the absence of tumor necrosis factor-alpha-converting enzyme." J Biol Chem **276**(51): 48510-48517. Epub 2001 Oct 48512.
- Micchelli, C. A., E. J. Rulifson and S. S. Blair (1997). "The function and regulation of cut expression on the wing margin of *Drosophila*: Notch, Wingless and a dominant negative role for Delta and Serrate." Development **124**(8): 1485-1495.
- Mira, H., Z. Andreu, H. Suh, D. C. Lie, S. Jessberger, A. Consiglio, J. San Emeterio, R. Hortigüela, M. Á. Marqués-Torrejón, K. Nakashima, D. Colak, M. Götz, I. Fariñas and F. H. Gage (2010). "Signaling through BMPR-IA Regulates Quiescence and Long-Term Activity of Neural Stem Cells in the Adult Hippocampus." Cell Stem Cell **7**(1): 78-89.
- Mirzadeh, Z., F. T. Merkle, M. Soriano-Navarro, J. M. Garcia-Verdugo and A. Alvarez-Buylla (2008). "Neural stem cells confer unique pinwheel architecture to the ventricular surface in neurogenic regions of the adult brain." Cell Stem Cell **3**(3): 265-278.
- Mitew, S., C. M. Hay, H. Peckham, J. Xiao, M. Koenning and B. Emery (2014). "Mechanisms regulating the development of oligodendrocytes and central nervous system myelin." Neuroscience **276**: 29-47.
- Miyata, T., A. Kawaguchi, H. Okano and M. Ogawa (2001). "Asymmetric inheritance of radial glial fibers by cortical neurons." Neuron **31**(5): 727-741.
- Mizuhara, E., T. Nakatani, Y. Minaki, Y. Sakamoto, Y. Ono and Y. Takai (2005). "MAGI1 recruits Dll1 to cadherin-based adherens junctions and stabilizes it on the cell surface." Journal of Biological Chemistry **280**(28): 26499-26507.
- Mizutani, K., K. Yoon, L. Dang, A. Tokunaga and N. Gaiano (2007). "Differential Notch signalling distinguishes neural stem cells from intermediate progenitors." Nature **449**(7160): 351-355.
- Molyneaux, B. J., P. Arlotta, J. R. Menezes and J. D. Macklis (2007). "Neuronal subtype specification in the cerebral cortex." Nat Rev Neurosci **8**(6): 427-437.
- Morrens, J., W. Van Den Broeck and G. Kempermann (2012). "Glial cells in adult neurogenesis." Glia **60**(2): 159-174.
- Mumm, J. S., E. H. Schroeter, M. T. Saxena, A. Griesemer, X. Tian, D. J. Pan, W. J. Ray and R. Kopan (2000). "A ligand-induced extracellular cleavage regulates gamma-secretase-like proteolytic activation of Notch1." Mol Cell **5**(2): 197-206.
- Munakata, K., K. Iwamoto, M. Bundo and T. Kato (2005). "Mitochondrial DNA 3243A>G mutation and increased expression of LARS2 gene in the brains of patients with bipolar disorder and schizophrenia." Biol Psychiatry **57**(5): 525-532.
- Mutch, C. A., J. D. Schulte, E. Olson and A. Chenn (2010). "Beta-catenin signaling negatively regulates intermediate progenitor population numbers in the developing cortex." PLoS One **5**(8): e12376.
- Nakahara, J., K. Kanekura, M. Nawa, S. Aiso and N. Suzuki (2009). "Abnormal expression of TIP30 and arrested nucleocytoplasmic transport within oligodendrocyte precursor cells in multiple sclerosis." The Journal of clinical investigation **119**(1): 169.
- Nave, K. A. and B. D. Trapp (2008). "Axon-glial signaling and the glial support of axon function." Annu Rev Neurosci **31**: 535-561.
- Neves, J., C. Parada, M. Chamizo and F. Giraldez (2011). "Jagged 1 regulates the restriction of Sox2 expression in the developing chicken inner ear: a mechanism for sensory organ specification." Development **138**(4): 735-744.
- Nielsen, J. A., L. D. Hudson and R. C. Armstrong (2002). "Nuclear organization in differentiating oligodendrocytes." Journal of cell science **115**(21): 4071-4079.
- Nieto, M., E. S. Monuki, H. Tang, J. Imitola, N. Haubst, S. J. Khoury, J. Cunningham, M. Gotz and C. A. Walsh (2004). "Expression of Cux-1 and Cux-2 in the subventricular zone and upper layers II-IV of the cerebral cortex." J Comp Neurol **479**(2): 168-180.
- Nishiyama, A., A. Chang and B. D. Trapp (1999). "NG2+ glial cells: a novel glial cell population in the adult brain." Journal of Neuropathology & Experimental Neurology **58**(11): 1113-1124.
- Noctor, S. C., A. C. Flint, T. A. Weissman, R. S. Dammerman and A. R. Kriegstein (2001). "Neurons derived from radial glial cells establish radial units in neocortex." Nature **409**(6821): 714-720.

- Noctor, S. C., V. Martinez-Cerdeno, L. Ivic and A. R. Kriegstein (2004). "Cortical neurons arise in symmetric and asymmetric division zones and migrate through specific phases." *Nat Neurosci* **7**(2): 136-144.
- Nyfeler, Y., R. D. Kirch, N. Mantei, D. P. Leone, F. Radtke, U. Suter and V. Taylor (2005). "Jagged1 signals in the postnatal subventricular zone are required for neural stem cell self-renewal." *The EMBO Journal* **24**(19): 3504.
- Oda, T., A. G. Elkahloun, B. L. Pike, K. Okajima, I. D. Krantz, A. Genin, D. A. Piccoli, P. S. Meltzer, N. B. Spinner, F. S. Collins and S. C. Chandrasekharappa (1997). "Mutations in the human Jagged1 gene are responsible for Alagille syndrome." *Nat Genet* **16**(3): 235-242.
- Ohtsuka, T., M. Ishibashi, G. Gradwohl, S. Nakanishi, F. Guillemot and R. Kageyama (1999). "Hes1 and Hes5 as Notch effectors in mammalian neuronal differentiation." *The EMBO Journal* **18**(8): 2196-2207.
- Ohtsuka, T. and R. Kageyama (2010). *The Basic Helix-Loop-Helix Transcription Factors in Neural Differentiation. Cell Cycle Regulation and Differentiation in Cardiovascular and Neural Systems*. A. Giordano and U. Galderisi, Springer New York: 15-34.
- Olsen, J. V., B. Blagoev, F. Gnad, B. Macek, C. Kumar, P. Mortensen and M. Mann (2006). "Global, In Vivo, and Site-Specific Phosphorylation Dynamics in Signaling Networks." *Cell* **127**(3): 635-648.
- Ortega, M. C., A. Bribián, S. Peregrín, M. T. Gil, O. Marín and F. de Castro (2012). "Neuregulin-1/ErbB4 signaling controls the migration of oligodendrocyte precursor cells during development." *Experimental Neurology* **235**(2): 610-620.
- Oswald, F., M. Winkler, Y. Cao, K. Astrahantseff, S. Bourteele, W. Knöchel and T. Borggreffe (2005). "RBP-Jk/SHARP recruits CtIP/CtBP corepressors to silence Notch target genes." *Molecular and cellular biology* **25**(23): 10379-10390.
- Paridaen, J. T. and W. B. Huttner (2014). "Neurogenesis during development of the vertebrate central nervous system." *EMBO Rep* **15**(4): 351-364.
- Park, H., Z. Li, X. O. Yang, S. H. Chang, R. Nurieva, Y.-H. Wang, Y. Wang, L. Hood, Z. Zhu and Q. Tian (2005). "A distinct lineage of CD4 T cells regulates tissue inflammation by producing interleukin 17." *Nature immunology* **6**(11): 1133-1141.
- Park, S. K., R. Miller, I. Krane and T. Vartanian (2001). "The erbB2 gene is required for the development of terminally differentiated spinal cord oligodendrocytes." *J Cell Biol* **154**(6): 1245-1258.
- Parr-Sturgess, C. A., D. J. Rushton and E. T. Parkin (2010). "Ectodomain shedding of the Notch ligand Jagged1 is mediated by ADAM17, but is not a lipid-raft-associated event." *Biochem J* **432**(2): 283-294.
- Pasquinelli, A. E. (2012). "MicroRNAs and their targets: recognition, regulation and an emerging reciprocal relationship." *Nat Rev Genet* **13**(4): 271-282.
- Pasquini, L. A., V. Millet, H. C. Hoyos, J. P. Giannoni, D. O. Croci, M. Marder, F. T. Liu, G. A. Rabinovich and J. M. Pasquini (2011). "Galectin-3 drives oligodendrocyte differentiation to control myelin integrity and function." *Cell Death Differ* **18**(11): 1746-1756.
- Pastrana, E., L. C. Cheng and F. Doetsch (2009). "Simultaneous prospective purification of adult subventricular zone neural stem cells and their progeny." *Proc Natl Acad Sci U S A* **106**(15): 6387-6392.
- Pedotti, R., M. Farinotti, C. Falcone, L. Borgonovo, P. Confalonieri, A. Campanella, R. Mantegazza, E. Pastorello and G. Filippini (2009). "Allergy and multiple sclerosis: a population-based case-control study." *Multiple sclerosis* **15**(8): 899-906.
- Perissi, V., A. Aggarwal, C. K. Glass, D. W. Rose and M. G. Rosenfeld (2004). "A corepressor/coactivator exchange complex required for transcriptional activation by nuclear receptors and other regulated transcription factors." *Cell* **116**(4): 511-526.
- Perissi, V., C. Scafoglio, J. Zhang, K. A. Ohgi, D. W. Rose, C. K. Glass and M. G. Rosenfeld (2008). "TBL1 and TBLR1 phosphorylation on regulated gene promoters overcomes dual CtBP and NCoR/SMRT transcriptional repression checkpoints." *Mol Cell* **29**(6): 755-766.
- Pesheva, P., S. Gloor, M. Schachner and R. Probstmeier (1997). "Tenascin-R Is an Intrinsic Autocrine Factor for Oligodendrocyte Differentiation and Promotes Cell Adhesion by a Sulfatide-Mediated Mechanism." *The Journal of Neuroscience* **17**(12): 4642-4651.

- Petrovic, J., P. Formosa-Jordan, J. C. Luna-Escalante, G. Abello, M. Ibanes, J. Neves and F. Giraldez (2014). "Ligand-dependent Notch signaling strength orchestrates lateral induction and lateral inhibition in the developing inner ear." Development.
- Pfeiffer, S. E., A. E. Warrington and R. Bansal (1993). "The oligodendrocyte and its many cellular processes." Trends in cell biology **3**(6): 191-197.
- Piccoli, D. A. and N. B. Spinner (2001). "Alagille syndrome and the Jagged1 gene." Semin Liver Dis **21**(4): 525-534.
- Piccolo, S., E. Agius, L. Leyns, S. Bhattacharyya, H. Grunz, T. Bouwmeester and E. M. De Robertis (1999). "The head inducer Cerberus is a multifunctional antagonist of Nodal, BMP and Wnt signals." Nature **397**(6721): 707-710.
- Pintar, A., A. De Biasio, M. Popovic, N. Ivanova and S. Pongor (2007). "The intracellular region of Notch ligands: does the tail make the difference." Biol Direct **2**: 19.
- Pompa de la, J. L., A. Wakeham, K. M. Correia, E. Samper, S. Brown, R. J. Aguilera, T. Nakano, T. Honjo, T. W. Mak, J. Rossant and R. A. Conlon (1997). "Conservation of the Notch signalling pathway in mammalian neurogenesis." Development **124**(6): 1139-1148.
- Potter, K. A., M. J. Kern, G. Fullbright, J. Bielawski, S. S. Scherer, S. W. Yum, J. J. Li, H. Cheng, X. Han, J. K. Venkata, P. A. Khan, B. Rohrer and H. Hama (2011). "Central nervous system dysfunction in a mouse model of FA2H deficiency." Glia **59**(7): 1009-1021.
- Radtke, F. and H. Clevers (2005). "Self-renewal and cancer of the gut: two sides of a coin." Science. **307**(5717): 1904-1909.
- Rallu, M., J. G. Corbin and G. Fishell (2002). "Parsing the prosencephalon." Nat Rev Neurosci **3**(12): 943-951.
- Rasin, M. R., V. R. Gazula, J. J. Breunig, K. Y. Kwan, M. B. Johnson, S. Liu-Chen, H. S. Li, L. Y. Jan, Y. N. Jan, P. Rakic and N. Sestan (2007). "Numb and Numbl are required for maintenance of cadherin-based adhesion and polarity of neural progenitors." Nat Neurosci **10**(7): 819-827.
- Rathjen, F. G., J. Wolff and R. Chiquet-Ehrismann (1991). "Restrictin: a chick neural extracellular matrix protein involved in cell attachment co-purifies with the cell recognition molecule F11." Development **113**(1): 151-164.
- Readhead, C., B. Popko, N. Takahashi, H. David Shine, R. A. Saavedra, R. L. Sidman and L. Hood (1987). "Expression of a myelin basic protein gene in transgenic shiverer mice: Correction of the dysmyelinating phenotype." Cell **48**(4): 703-712.
- Reynolds, N. D., N. W. Lukacs, N. Long and W. J. Karpus (2011). "Delta-like ligand 4 regulates central nervous system T cell accumulation during experimental autoimmune encephalomyelitis." J Immunol **187**(5): 2803-2813.
- Rhodes, K., G. Raivich and J. Fawcett (2006). "The injury response of oligodendrocyte precursor cells is induced by platelets, macrophages and inflammation-associated cytokines." Neuroscience **140**(1): 87-100.
- Rios, J. C., C. V. Melendez-Vasquez, S. Einheber, M. Lustig, M. Grumet, J. Hemperly, E. Peles and J. L. Salzer (2000). "Contactin-associated protein (Caspr) and contactin form a complex that is targeted to the paranodal junctions during myelination." The Journal of Neuroscience **20**(22): 8354-8364.
- Rivers, L. E., K. M. Young, M. Rizzi, F. Jamen, K. Psachoulia, A. Wade, N. Kessar and W. D. Richardson (2008). "PDGFRA/NG2 glia generate myelinating oligodendrocytes and piriform projection neurons in adult mice." Nat Neurosci **11**(12): 1392-1401.
- Robins, S. C., I. Stewart, D. E. McNay, V. Taylor, C. Giachino, M. Goetz, J. Ninkovic, N. Briancon, E. Maratos-Flier, J. S. Flier, M. V. Kokoeva and M. Placzek (2013). "alpha-Tanycytes of the adult hypothalamic third ventricle include distinct populations of FGF-responsive neural progenitors." Nat Commun **4**: 2049.
- Roca, C. and R. H. Adams (2007). "Regulation of vascular morphogenesis by Notch signaling." Genes Dev. **21**(20): 2511-2524.
- Rodilla, V., A. Villanueva, A. Obrador-Hevia, A. Robert-Moreno, V. Fernandez-Majada, A. Grilli, N. Lopez-Bigas, N. Bellora, M. M. Alba, F. Torres, M. Dunach, X. Sanjuan, S. Gonzalez, T. Gridley, G. Capella, A. Bigas and L. Espinosa (2009). "Jagged1 is the pathological link between Wnt and Notch pathways in colorectal cancer." Proc Natl Acad Sci U S A **106**(15): 6315-6320.
- Rolando, C. and V. Taylor (2014). "Neural stem cell of the hippocampus: development, physiology regulation, and dysfunction in disease." Curr Top Dev Biol **107**: 183-206.

- Rotshenker, S., F. Reichert, M. Gitik, R. Haklai, G. Elad - Sfadia and Y. Kloog (2008). "Galectin - 3/MAC - 2, Ras and PI3K activate complement receptor - 3 and scavenger receptor - AI/II mediated myelin phagocytosis in microglia." *Glia* **56**(15): 1607-1613.
- Roy, K., J. C. Murtie, B. F. El-Khodori, N. Edgar, S. P. Sardi, B. M. Hooks, M. Benoit-Marand, C. Chen, H. Moore, P. O'Donnell, D. Brunner and G. Corfas (2007). "Loss of erbB signaling in oligodendrocytes alters myelin and dopaminergic function, a potential mechanism for neuropsychiatric disorders." *Proc Natl Acad Sci U S A* **104**(19): 8131-8136.
- Rutz, S., B. Mordmüller, S. Sakano and A. Scheffold (2005). "Notch ligands Delta-like1, Delta-like4 and Jagged1 differentially regulate activation of peripheral T helper cells." *European Journal of Immunology* **35**(8): 2443-2451.
- Sainson, R. C. A., D. A. Johnston, H. C. Chu, M. T. Holderfield, M. N. Nakatsu, S. P. Crampton, J. Davis, E. Conn and C. C. W. Hughes (2008). "TNF primes endothelial cells for angiogenic sprouting by inducing a tip cell phenotype." *Blood* **111**(10): 4997-5007.
- Sakamoto, K., O. Ohara, M. Takagi, S. Takeda and K. Katsube (2002). "Intracellular cell-autonomous association of Notch and its ligands: a novel mechanism of Notch signal modification." *Dev Biol* **241**(2): 313-326.
- Samanta, J. and J. A. Kessler (2004). "Interactions between ID and OLIG proteins mediate the inhibitory effects of BMP4 on oligodendroglial differentiation." *Development* **131**(17): 4131-4142.
- Sansom, S. N. and F. J. Livesey (2009). "Gradients in the brain: the control of the development of form and function in the cerebral cortex." *Cold Spring Harb Perspect Biol* **1**(2): a002519.
- Sasai, Y., R. Kageyama, Y. Tagawa, R. Shigemoto and S. Nakanishi (1992). "Two mammalian helix-loop-helix factors structurally related to Drosophila hairy and Enhancer of split." *Genes Dev* **6**(12b): 2620-2634.
- Schwamborn, J. C., E. Berezikov and J. A. Knoblich (2009). "The TRIM-NHL Protein TRIM32 Activates MicroRNAs and Prevents Self-Renewal in Mouse Neural Progenitors." *Cell* **136**(5): 913-925.
- Scolding, N., R. Franklin, S. Stevens, C.-H. Heldin, A. Compston and J. Newcombe (1998). "Oligodendrocyte progenitors are present in the normal adult human CNS and in the lesions of multiple sclerosis." *Brain* **121**(12): 2221-2228.
- Seib, D. R., N. S. Corsini, K. Ellwanger, C. Plaas, A. Mateos, C. Pitzer, C. Niehrs, T. Celikel and A. Martin-Villalba (2013). "Loss of Dickkopf-1 restores neurogenesis in old age and counteracts cognitive decline." *Cell Stem Cell* **12**(2): 204-214.
- Seifert, T., J. Bauer, R. Weissert, F. Fazekas and M. K. Storch (2007). "Notch1 and its ligand Jagged1 are present in remyelination in a T-cell- and antibody-mediated model of inflammatory demyelination." *Acta Neuropathol* **113**(2): 195-203.
- Shen, Q., S. K. Goderie, L. Jin, N. Karanth, Y. Sun, N. Abramova, P. Vincent, K. Pumiglia and S. Temple (2004). "Endothelial cells stimulate self-renewal and expand neurogenesis of neural stem cells." *Science* **304**(5675): 1338-1340.
- Shen, Q., Y. Wang, J. T. Dimos, C. A. Fasano, T. N. Phoenix, I. R. Lemischka, N. B. Ivanova, S. Stifani, E. E. Morrisey and S. Temple (2006). "The timing of cortical neurogenesis is encoded within lineages of individual progenitor cells." *Nat Neurosci* **9**(6): 743-751.
- Shimizu, K., S. Chiba, N. Hosoya, K. Kumano, T. Saito, M. Kurokawa, Y. Kanda, Y. Hamada and H. Hirai (2000). "Binding of Delta1, Jagged1, and Jagged2 to Notch2 Rapidly Induces Cleavage, Nuclear Translocation, and Hyperphosphorylation of Notch2." *Molecular and Cellular Biology* **20**(18): 6913-6922.
- Shimizu, K., S. Chiba, K. Kumano, N. Hosoya, T. Takahashi, Y. Kanda, Y. Hamada, Y. Yazaki and H. Hirai (1999). "Mouse jagged1 physically interacts with notch2 and other notch receptors assessment by quantitative methods." *Journal of Biological Chemistry* **274**(46): 32961-32969.
- Shimojo, H., T. Ohtsuka and R. Kageyama "Oscillations in Notch Signaling Regulate Maintenance of Neural Progenitors." *Neuron* **58**(1): 52-64.
- Shimokita, E. and Y. Takahashi (2011). "Secondary neurulation: Fate-mapping and gene manipulation of the neural tube in tail bud." *Dev Growth Differ* **53**(3): 401-410.
- Silbereis, J. C., E. J. Huang, S. A. Back and D. H. Rowitch (2010). "Towards improved animal models of neonatal white matter injury associated with cerebral palsy." *Disease Models & Mechanisms* **3**(11-12): 678-688.

- Sim, F. J., C. Zhao, J. Penderis and R. J. Franklin (2002). "The age-related decrease in CNS remyelination efficiency is attributable to an impairment of both oligodendrocyte progenitor recruitment and differentiation." The Journal of neuroscience **22**(7): 2451-2459.
- Smart, I. H. (1973). "Proliferative characteristics of the ependymal layer during the early development of the mouse neocortex: a pilot study based on recording the number, location and plane of cleavage of mitotic figures." J Anat **116**(Pt 1): 67-91.
- Sorg, B. A., M. M. Smith and A. T. Campagnoni (1987). "Developmental expression of the myelin proteolipid protein and basic protein mRNAs in normal and dysmyelinating mutant mice." Journal of neurochemistry **49**(4): 1146-1154.
- Spassky, N., C. Goujet-Zalc, E. Parmantier, C. Olivier, S. Martinez, A. Ivanova, K. Ikenaka, W. Macklin, I. Cerruti, B. Zalc and J.-L. Thomas (1998). "Multiple Restricted Origin of Oligodendrocytes." The Journal of Neuroscience **18**(20): 8331-8343.
- Spassky, N., K. Heydon, A. Mangatal, A. Jankovski, C. Olivier, F. Queraud-Lesaux, C. Goujet-Zalc, J. L. Thomas and B. Zalc (2001). "Sonic hedgehog-dependent emergence of oligodendrocytes in the telencephalon: evidence for a source of oligodendrocytes in the olfactory bulb that is independent of PDGFR α signaling." Development **128**(24): 4993-5004.
- Spinner, N. B., R. P. Colliton, C. Crosnier, I. D. Krantz, M. Hadchouel and M. Meunier-Rotival (2001). "Jagged1 mutations in alagille syndrome." Hum Mutat **17**(1): 18-33.
- Spinner, N. B., R. P. Colliton, C. Crosnier, I. D. Krantz, M. Hadchouel and M. Meunier - Rotival (2001). "Jagged1 mutations in Alagille syndrome." Human mutation **17**(1): 18-33.
- Sprinzak, D., A. Lakhanpal, L. Lebon, L. A. Santat, M. E. Fontes, G. A. Anderson, J. Garcia-Ojalvo and M. B. Elowitz (2010). "Cis-interactions between Notch and Delta generate mutually exclusive signalling states." Nature **465**(7294): 86-90.
- Srinivasan, K., J. Roosa, O. Olsen, S.-H. Lee, D. S. Bredt and S. K. McConnell (2008). "MALS-3 regulates polarity and early neurogenesis in the developing cerebral cortex." Development **135**(10): 1781-1790.
- Srinivasan, R., G. Sun, S. Keles, E. A. Jones, S.-W. Jang, C. Krueger, J. J. Moran and J. Svaren (2012). "Genome-wide analysis of EGR2/SOX10 binding in myelinating peripheral nerve." Nucleic acids research **40**(14): 6449-6460.
- Stallcup, W. and L. Beasley (1987). "Bipotential glial precursor cells of the optic nerve express the NG2 proteoglycan." The Journal of Neuroscience **7**(9): 2737-2744.
- Stanley, P. and T. Okajima (2010). "Roles of Glycosylation in Notch Signaling." **92**: 131-164.
- Staudinger, J., J. Lu and E. N. Olson (1997). "Specific interaction of the PDZ domain protein PICK1 with the COOH terminus of protein kinase C- α ." J Biol Chem **272**(51): 32019-32024.
- Stidworthy, M. F., S. Genoud, W. W. Li, D. P. Leone, N. Mantei, U. Suter and R. J. Franklin (2004). "Notch1 and Jagged1 are expressed after CNS demyelination, but are not a major rate-determining factor during remyelination." Brain **127**(Pt 9): 1928-1941.
- Stolt, C. C., S. Rehberg, M. Ader, P. Lommes, D. Riethmacher, M. Schachner, U. Bartsch and M. Wegner (2002). "Terminal differentiation of myelin-forming oligodendrocytes depends on the transcription factor Sox10." Genes Dev **16**(2): 165-170.
- Stump, G., A. Durrer, A. L. Klein, S. Lutolf, U. Suter and V. Taylor (2002). "Notch1 and its ligands Delta-like and Jagged are expressed and active in distinct cell populations in the postnatal mouse brain." Mech Dev **114**(1-2): 153-159.
- Suh, H., A. Consiglio, J. Ray, T. Sawai, K. A. D'Amour and F. H. Gage (2007). "In vivo fate analysis reveals the multipotent and self-renewal capacities of Sox2⁺ neural stem cells in the adult hippocampus." Cell Stem Cell **1**(5): 515-528.
- Sun, Y., S. K. Goderie and S. Temple (2005). "Asymmetric Distribution of EGFR Receptor during Mitosis Generates Diverse CNS Progenitor Cells." Neuron **45**(6): 873-886.
- Sun, Y., M. Nadal-Vicens, S. Misono, M. Z. Lin, A. Zubiaga, X. Hua, G. Fan and M. E. Greenberg (2001). "Neurogenin Promotes Neurogenesis and Inhibits Glial Differentiation by Independent Mechanisms." Cell **104**(3): 365-376.
- Takahashi, T., R. Nowakowski and V. Caviness (1993). "Cell cycle parameters and patterns of nuclear movement in the neocortical proliferative zone of the fetal mouse." The Journal of Neuroscience **13**(2): 820-833.

- Takahashi, T., R. S. Nowakowski and V. S. Caviness, Jr. (1995). "The cell cycle of the pseudostratified ventricular epithelium of the embryonic murine cerebral wall." *J Neurosci* **15**(9): 6046-6057.
- Tam, P. P. and D. A. Loebel (2007). "Gene function in mouse embryogenesis: get set for gastrulation." *Nat Rev Genet* **8**(5): 368-381.
- Tamura, K., Y. Taniguchi, S. Minoguchi, T. Sakai, T. Tun, T. Furukawa and T. Honjo (1995). "Physical interaction between a novel domain of the receptor Notch and the transcription factor RBP-J kappa/Su(H)." *Curr Biol* **5**(12): 1416-1423.
- Tanigaki, K., F. Nogaki, J. Takahashi, K. Tashiro, H. Kurooka and T. Honjo (2001). "Notch1 and Notch3 instructively restrict bFGF-responsive multipotent neural progenitor cells to an astroglial fate." *Neuron* **29**(1): 45-55.
- Taniike, M., I. Mohri, N. Eguchi, C. T. Beuckmann, K. Suzuki and Y. Urade (2002). "Perineuronal oligodendrocytes protect against neuronal apoptosis through the production of lipocalin-type prostaglandin D synthase in a genetic demyelinating model." *The Journal of neuroscience* **22**(12): 4885-4896.
- Taverna, E. and W. B. Huttner (2010). "Neural progenitor nuclei IN motion." *Neuron* **67**(6): 906-914.
- Tenenbaum, L., A. Chtarto, E. Lehtonen, T. Velu, J. Brotchi and M. Levivier (2004). "Recombinant AAV - mediated gene delivery to the central nervous system." *The journal of gene medicine* **6**(S1): S212-S222.
- Tiberi, L., P. Vanderhaeghen and J. van den Aemele (2012). "Cortical neurogenesis and morphogens: diversity of cues, sources and functions." *Curr Opin Cell Biol* **24**(2): 269-276.
- Tkachev, D., M. L. Mimmack, M. M. Ryan, M. Wayland, T. Freeman, P. B. Jones, M. Starkey, M. J. Webster, R. H. Yolken and S. Bahn (2003). "Oligodendrocyte dysfunction in schizophrenia and bipolar disorder." *The Lancet* **362**(9386): 798-805.
- Tong, C. K. and A. Alvarez-Buylla (2014). "SnapShot: Adult Neurogenesis in the V-SVZ." *Neuron* **81**(1): 220-220 e221.
- Trapp, B. D., S. B. Andrews, C. Cootauco and R. Quarles (1989). "The myelin-associated glycoprotein is enriched in multivesicular bodies and periaxonal membranes of actively myelinating oligodendrocytes." *The Journal of cell biology* **109**(5): 2417-2426.
- Trapp, B. D., L. Bernier, S. B. Andrews and D. R. Colman (1988). "Cellular and Subcellular Distribution of 2' , 3' - Cyclic Nucleotide 3' - Phosphodiesterase and Its mRNA in the Rat Central Nervous System." *Journal of neurochemistry* **51**(3): 859-868.
- Tsuji, M., R. Shinkura, K. Kuroda, D. Yabe and T. Honjo (2007). "Msx2-interacting nuclear target protein (Mint) deficiency reveals negative regulation of early thymocyte differentiation by Notch/RBP-J signaling." *Proceedings of the National Academy of Sciences* **104**(5): 1610-1615.
- Tzartos, J. S., M. A. Friese, M. J. Craner, J. Palace, J. Newcombe, M. M. Esiri and L. Fugger (2008). "Interleukin-17 production in central nervous system-infiltrating T cells and glial cells is associated with active disease in multiple sclerosis." *The American journal of pathology* **172**(1): 146-155.
- Vadodaria, K. C. and F. H. Gage (2014). "SnapShot: Adult Hippocampal Neurogenesis." *Cell* **156**(5): 1114-1114 e1111.
- Vallejo, D. M., E. Caparros and M. Dominguez (2011). "Targeting Notch signalling by the conserved miR-8/200 microRNA family in development and cancer cells." *EMBO J* **30**(4): 756-769.
- Van Praag, H., T. Shubert, C. Zhao and F. H. Gage (2005). "Exercise enhances learning and hippocampal neurogenesis in aged mice." *The Journal of Neuroscience* **25**(38): 8680-8685.
- Vartanian, T., A. Goodearl, A. Viehöver and G. Fischbach (1997). "Axonal neuregulin signals cells of the oligodendrocyte lineage through activation of HER4 and Schwann cells through HER2 and HER3." *The Journal of cell biology* **137**(1): 211-220.
- Wang, S., A. D. Sdrulla, G. diSibio, G. Bush, D. Nofziger, C. Hicks, G. Weinmaster and B. A. Barres (1998). "Notch receptor activation inhibits oligodendrocyte differentiation." *Neuron* **21**(1): 63-75.
- Weber, P., U. Bartsch, M. N. Rasband, R. Czaniera, Y. Lang, H. Bluethmann, R. U. Margolis, S. R. Levinson, P. Shrager, D. Montag and M. Schachner (1999). "Mice Deficient for Tenascin-R Display Alterations of the Extracellular Matrix and Decreased Axonal Conduction Velocities in the CNS." *The Journal of Neuroscience* **19**(11): 4245-4262.

- Weinmaster, G., V. J. Roberts and G. Lemke (1991). "A homolog of *Drosophila* Notch expressed during mammalian development." *Development* **113**(1): 199-205.
- Weller, M., N. Krautler, N. Mantei, U. Suter and V. Taylor (2006). "Jagged1 ablation results in cerebellar granule cell migration defects and depletion of Bergmann glia." *Dev Neurosci* **28**(1-2): 70-80.
- Werner, P., D. Pitt and C. S. Raine (2001). "Multiple sclerosis: Altered glutamate homeostasis in lesions correlates with oligodendrocyte and axonal damage." *Annals of Neurology* **50**(2): 169-180.
- Wexler, E. M., A. Paucer, H. I. Kornblum, T. D. Palmer and D. H. Geschwind (2009). "Endogenous Wnt Signaling Maintains Neural Progenitor Cell Potency." *STEM CELLS* **27**(5): 1130-1141.
- Wilson, H. C., N. J. Scolding and C. S. Raine (2006). "Co-expression of PDGF α receptor and NG2 by oligodendrocyte precursors in human CNS and multiple sclerosis lesions." *Journal of neuroimmunology* **176**(1): 162-173.
- Woodhead, G. J., C. A. Mutch, E. C. Olson and A. Chenn (2006). "Cell-Autonomous β -Catenin Signaling Regulates Cortical Precursor Proliferation." *The Journal of Neuroscience* **26**(48): 12620-12630.
- Wright, G. J., J. D. Leslie, L. Ariza-McNaughton and J. Lewis (2004). "Delta proteins and MAGI proteins: an interaction of Notch ligands with intracellular scaffolding molecules and its significance for zebrafish development." *Development* **131**(22): 5659-5669.
- Wu, Z., H. Yang and P. Colosi (2010). "Effect of genome size on AAV vector packaging." *Molecular Therapy* **18**(1): 80-86.
- Xue, Y., X. Gao, C. E. Lindsell, C. R. Norton, B. Chang, C. Hicks, M. Gendron-Maguire, E. B. Rand, G. Weinmaster and T. Gridley (1999). "Embryonic lethality and vascular defects in mice lacking the Notch ligand Jagged1." *Hum Mol Genet* **8**(5): 723-730.
- Xue, Y., X. Gao, C. E. Lindsell, C. R. Norton, B. Chang, C. Hicks, M. Gendron-Maguire, E. B. Rand, G. Weinmaster and T. Gridley (1999). "Embryonic lethality and vascular defects in mice lacking the Notch ligand Jagged1." *Human molecular genetics* **8**(5): 723-730.
- Xue, Y., X. Gao, C. E. Lindsell, C. R. Norton, B. Chang, C. Hicks, M. Gendron-Maguire, E. B. Rand, G. Weinmaster and T. Gridley (1999). "Embryonic lethality and vascular defects in mice lacking the Notch ligand Jagged1." *Hum Mol Genet* **8**(5): 723-730.
- Ye, F., Y. Chen, T. Hoang, R. L. Montgomery, X.-h. Zhao, H. Bu, T. Hu, M. M. Taketo, J. H. van Es and H. Clevers (2009). "HDAC1 and HDAC2 regulate oligodendrocyte differentiation by disrupting the β -catenin-TCF interaction." *Nature neuroscience* **12**(7): 829-838.
- Yoon, K. and N. Gaiano (2005). "Notch signaling in the mammalian central nervous system: insights from mouse mutants." *Nat Neurosci* **8**(6): 709-715.
- Yu, Y., Y. Chen, B. Kim, H. Wang, C. Zhao, X. He, L. Liu, W. Liu, L. M. Wu, M. Mao, J. R. Chan, J. Wu and Q. R. Lu (2013). "Olig2 targets chromatin remodelers to enhancers to initiate oligodendrocyte differentiation." *Cell* **152**(1-2): 248-261.
- Yu, Y., Y. Chen, B. Kim, H. Wang, C. Zhao, X. He, L. Liu, W. Liu, L. M. N. Wu and M. Mao (2013). "Olig2 targets chromatin remodelers to enhancers to initiate oligodendrocyte differentiation." *Cell* **152**(1): 248-261.
- Yuan, Z. R., N. Kobayashi and T. Kohsaka (2006). "Human Jagged 1 mutants cause liver defect in Alagille syndrome by overexpression of hepatocyte growth factor." *J Mol Biol* **356**(3): 559-568.
- Yuan, Z. R., T. Kohsaka, T. Ikegaya, T. Suzuki, S. Okano, J. Abe, N. Kobayashi and M. Yamada (1998). "Mutational analysis of the Jagged 1 gene in Alagille syndrome families." *Hum Mol Genet* **7**(9): 1363-1369.
- Zeng, Y. A. and R. Nusse (2010). "Wnt proteins are self-renewal factors for mammary stem cells and promote their long-term expansion in culture." *Cell Stem Cell* **6**(6): 568-577.
- Zhang, J., G. J. Woodhead, S. K. Swaminathan, S. R. Noles, E. R. McQuinn, A. J. Pisarek, A. M. Stocker, C. A. Mutch, N. Funatsu and A. Chenn (2010). "Cortical neural precursors inhibit their own differentiation via N-cadherin maintenance of β -catenin signaling." *Developmental cell* **18**(3): 472-479.
- Zhang, Y., A. T. Argaw, B. T. Gurfein, A. Zameer, B. J. Snyder, C. Ge, Q. R. Lu, D. H. Rowitch, C. S. Raine, C. F. Brosnan and G. R. John (2009). "Notch1 signaling plays a role in regulating precursor differentiation during CNS remyelination." *Proc Natl Acad Sci U S A* **106**(45): 19162-19167.

References

- Zhao, C., W. Deng and F. H. Gage (2008). "Mechanisms and functional implications of adult neurogenesis." Cell **132**(4): 645-660.
- Zhu, X., H. Zuo, B. J. Maher, D. R. Serwanski, J. J. LoTurco, Q. R. Lu and A. Nishiyama (2012). "Olig2-dependent developmental fate switch of NG2 cells." Development **139**(13): 2299-2307.
- Zinin, N., I. Adameyko, M. Wilhelm, N. Fritz, P. Uhlen, P. Ernfors and M. A. Henriksson (2014). "MYC proteins promote neuronal differentiation by controlling the mode of progenitor cell division." EMBO Rep **15**(4): 383-391.
- Zuchero, J. B. and B. A. Barres (2013). "Intrinsic and extrinsic control of oligodendrocyte development." Curr Opin Neurobiol **23**(6): 914-920.

8 Appendix

8.1 Published Article

8.1.1 Background for Published Article

N-cadherins play a critical role in maintaining tissue structure and the stem cell niche in the developing neocortex (Kadowaki, Nakamura et al. 2007). Spatial and temporal regulation of N-cadherin expression throughout development is carefully controlled, however the mechanisms underlying this remain for the most part unknown. miRNAs have been shown to regulate neurogenesis, with many being specific for neural development (Lagos-Quintana, Rauhut et al. 2002, Landgraf, Rusu et al. 2007, Bak, Silaharoglu et al. 2008, He, Liu et al. 2012). This study aimed to address the regulation of N-cadherin expression through miRNAs, specifically the miR379–410 cluster.

8.1.2 Statement of Contribution

For this paper, I participated in performing the IUE experiments in which the miR379–410 cluster were either over expressed or abolished in the developing neocortex of E13.5 embryos.

8.1.3 Key Findings

One of the key findings of this study is that miRNAs from the miR379-410 cluster (miR369-3p, miR496 and miR543) can directly modulate the expression level of N-cadherin in the developing neocortex, and subsequently regulate the development of NSCs, neuronal migration and the timing of neurogenesis. In previous studies, insufficient levels of N-cadherins resulted in an increased number of cells leaving cell cycle and premature neuronal differentiation (Zhang, Woodhead et al. 2010). In this study, through the overexpression of three miRNAs using IUE, premature neuronal differentiation and migration was observed, which recapitulates findings from previous studies. Additionally, N-cadherin rescue experiments were able to rescue the phenotype.



miR379–410 cluster miRNAs regulate neurogenesis and neuronal migration by fine-tuning N-cadherin

Luciano Rago^{1,2}, Robert Beattie³, Verdon Taylor³ & Jennifer Winter^{1,4,*}

Abstract

N-cadherin-mediated adhesion is essential for maintaining the tissue architecture and stem cell niche in the developing neocortex. N-cadherin expression level is precisely and dynamically controlled throughout development; however, the underlying regulatory mechanisms remain largely unknown. MicroRNAs (miRNAs) play an important role in the regulation of protein expression and subcellular localisation. In this study, we show that three miRNAs belonging to the miR379–410 cluster regulate N-cadherin expression levels in neural stem cells and migrating neurons. The overexpression of these three miRNAs in radial glial cells repressed N-cadherin expression and increased neural stem cell differentiation and neuronal migration. This phenotype was rescued when N-cadherin was expressed from a miRNA-insensitive construct. Transient abrogation of the miRNAs reduced stem cell differentiation and increased cell proliferation. The overexpression of these miRNAs specifically in newborn neurons delayed migration into the cortical plate, whereas the knockdown increased migration. Collectively, our results indicate a novel role for miRNAs of the miR379–410 cluster in the fine-tuning of N-cadherin expression level and in the regulation of neurogenesis and neuronal migration in the developing neocortex.

Keywords microRNAs; N-cadherin; neural differentiation; neural migration
Subject Categories Cell Adhesion, Polarity & Cytoskeleton; Neuroscience; Stem Cells

DOI 10.1002/embj.201386591 | Received 13 August 2013 | Revised 29 January 2014 | Accepted 29 January 2014

Introduction

Mammalian neocortical development is characterised by the differentiation of ventricular zone (VZ) neural stem cells into neurons that migrate from the VZ into the cortical plate (CP). These neurons migrate towards the pial surface of the neocortex to reach their final position just below the marginal zone (MZ) (Noctor *et al.*, 2004;

Gotz & Huttner, 2005; Cooper, 2008). Most radial glial cells (RGCs) differentiate into neurons indirectly via intermediate progenitor cells (IPCs). IPCs reside in the subventricular zone (SVZ) and divide symmetrically to produce either two neurons or two IPCs. After leaving the cell cycle, newborn neurons become multipolar and appear to migrate in a random motion (multipolar migration) within the SVZ and lower intermediate zone (IZ) (Tabata & Nakajima, 2003; LoTurco & Bai, 2006). In the IZ, neurons acquire a bipolar morphology characterised by a short trailing process and a long leading process that extends towards the CP. In the bipolar stage, neurons migrate radially by intertwining their leading process along RGCs processes (Noctor *et al.*, 2004).

Radial glial cells, derived from neuroepithelial cells, retain some epithelial characteristics and are tightly interconnected by N-cadherin (Ncad)-mediated apical adherens junctions (AJ) (Hatta & Takeichi, 1986; Hatta *et al.*, 1987; Gumbiner, 1996; Takeichi, 2007). Ncad is a type I cadherin that mediates calcium-dependent cell adhesion (Takeichi, 1995). The conditional knockout of Ncad in the developing neocortex results in the disorganisation of the tissue and internal structures of the cortex (Kadowaki *et al.*, 2007). Furthermore, Ncad regulates the proliferation of RGCs by activating β -catenin signalling (Zhang *et al.*, 2010).

In addition to RGC proliferation, Ncad regulates neuronal migration in the developing neocortex by mediating the interaction between migrating neurons and RGC fibres (Shikanai *et al.*, 2011). Ncad is also crucial for polarising post-mitotic neurons (Gartner *et al.*, 2012). It is clear that Ncad levels must be precisely regulated to achieve RGC differentiation, and during neuronal migration so that neurons reach their specific layer in the CP. Changes in the Ncad expression level result in neuronal differentiation (Zhang *et al.*, 2010) and migration defects (Kawauchi *et al.*, 2010; Zhang *et al.*, 2010; Franco *et al.*, 2011; Jossin & Cooper, 2011; Shikanai *et al.*, 2011).

Recently, miRNA-mediated regulation of Ncad has been shown to be highly important for the suppression of tumour metastasis *in vitro* (Meng *et al.*, 2010) and *in vivo* (Gao *et al.*, 2013). miRNAs are short, non-coding RNAs of approximately 22 bases. They are synthesised in the nucleus as immature pre-miRNAs and exported to the cytoplasm where they are processed by Dicer to mature

¹ Department of Molecular Embryology, Max Planck Institute of Immunobiology and Epigenetics, Freiburg, Germany

² University of Freiburg Faculty of Biology, Freiburg, Germany

³ Department of Biomedicine, University of Basel, Basel, Switzerland

⁴ Institute of Human Genetics, University Medical Centre of the Johannes Gutenberg University, Mainz, Germany

*Corresponding author. Tel: +49 6131 179684; Fax: +49 6131 175690; E-mail: jewinter@uni-mainz.de

miRNAs and associate with the RISC silencing complex. This complex recognises portions of the 3' untranslated region (3'UTR) in the target messenger RNAs (mRNAs), and this recognition results in either the degradation of the mRNA or the inhibition of its translation. miRNAs bind their target mRNAs through multiple imperfect base pairings. The complementarity of the so-called seed sequence, which comprises nucleotides 2–8, is largely responsible for determining the specificity of target recognition (Kim & Nam, 2006; Bartel, 2009). Several compelling studies indicate that miRNAs play important roles during mammalian brain development. miR134, a miRNA belonging to the miR379–410 cluster, promotes cell proliferation, reduces cell migration *in vivo* (Gaughwin *et al.*, 2011) and negatively regulates the size of dendritic spines *in vitro* (Schratt *et al.*, 2006; Fiore *et al.*, 2009).

Even though it is widely accepted that the level of cell surface Ncad must be precisely regulated to ensure proper neurogenesis and neuronal migration, the underlying regulatory mechanisms are poorly understood. The aim of this study was to investigate the regulation of Ncad expression by miRNAs; therefore, we made use of an *in vivo* approach to show that at least three miRNAs belonging to the miR379–410 cluster are essential for proper mammalian neocortical development. miR369-3p, miR496 and miR543 bind directly to the 3'UTR of the Ncad transcript and fine-tune the expression level of Ncad in VZ progenitors and migrating neurons and control neuronal differentiation and migration. Additionally, miR369-3p regulates expression of Adam10 and TrappC8 during development of the neocortex, which suggests a regulatory network of this miRNA cluster.

Results

miRNAs belonging to the miR379–410 cluster are expressed in neural progenitors and neurons in the developing neocortex

Using the prediction softwares Targetscan, Miranda and PicTar, we identified 21 candidate miRNAs that were predicted to bind to conserved target sequences in the Ncad 3'UTR (Supplementary Table S2). Interestingly, five of the predicted miRNAs, namely miR329, miR369-3p, miR495, miR496 and miR543, belong to the miR379–410 cluster, which is conserved in mammals and located on chromosome 12 in mice. Other members of the miR379–410 cluster have been reported to be expressed in the central nervous system and to be essential for neurogenesis and neuronal function (Fiore *et al.*, 2009; Christensen *et al.*, 2010; Gao *et al.*, 2010; Gaughwin *et al.*,

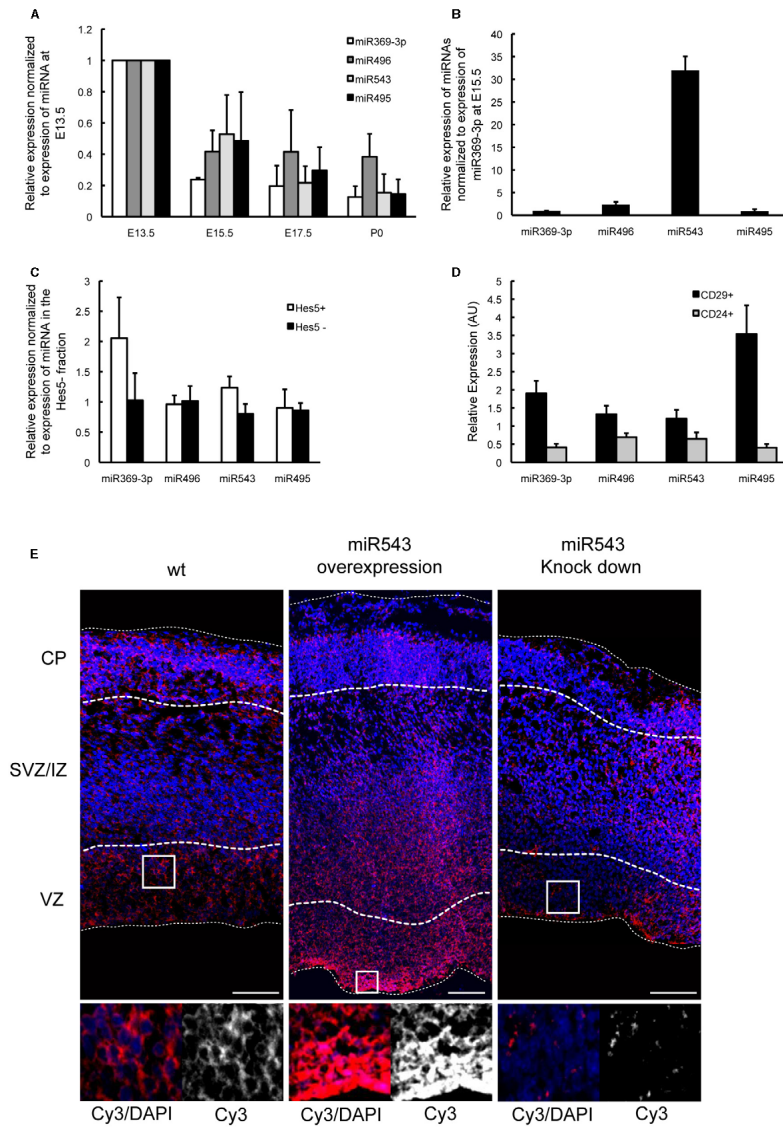
2011). Thus, the miRNAs belonging to the miR379–410 cluster appear to be promising candidates for regulating Ncad expression in the developing brain. Therefore, we focused on these miRNAs for the remainder of this study.

We found that miR369-3p, miR495, miR496 and miR543 are present in the developing forebrain at high levels at embryonic day E13.5 and that their expression levels decrease later during embryonic development (Fig 1A). Notably, miR543 is approximately fifteen times more abundant than miR369-3p, miR495 and miR496 at E15.5 (Fig 1B). miR329 was not included in these analyses because we could not confirm the regulation of Ncad expression by this miRNA in subsequent experiments (data not shown).

To determine which specific cell populations express the miR379–410 cluster miRNAs, we isolated Notch signalling neural progenitors from transgenic mice that express GFP under the control of the *Hes5* regulatory elements (Basak & Taylor, 2007). We sorted GFP⁺ and GFP⁻ cells from E15.5 embryos, isolated the small RNAs and performed specific qRT-PCR for four of the miR379–410 cluster miRNAs. Whereas the expression level of miR369-3p is approximately twofold higher in the neural progenitors (GFP⁺) compared with the differentiated cell populations (GFP⁻), miR495, miR496 and miR543 are expressed at approximately the same level in the neural progenitor and more differentiated cell (GFP⁻) populations (Fig 1C). Presumably, the more differentiated cell (GFP⁻) population represents a mixture of various cell types including *Hes5* neural progenitors, IPCs and neurons. Similar to what has been described for the human neural lineage (Pruszkowski *et al.*, 2009), we and others found that neural progenitors specifically express CD29, whereas neurons express CD24 (Supplementary Fig 1C; www.gene-paint.org). To test whether the four miR379–410 cluster miRNAs are also expressed by neurons, in addition to neural progenitors, we made use of these surface markers to fluorescence-activated cell sorting (FACS)-sort neural precursor cells and differentiating neurons from E15.5 embryos. To confirm the specificity of the sorting, we analysed the fractions for the expression of the three nuclear markers Pax6 (RGCs), Tbr2 (IPCs) and Tbr1 (neurons) (Supplementary Fig S1A). We observed that all four miR379–410 cluster miRNAs are expressed in the neural precursor cell population as well as in the neuronal cell population; however, expression in neurons is lower than in precursors (Fig 1D). To further confirm these results, we took neocortical cells from E15.5 embryos into culture under either non-differentiating or differentiating conditions. In agreement with the *in vivo* data, we found a higher expression of all four miR379–410 cluster miRNAs in neural precursors than in neurons *in vitro* (Supplementary Fig S1B).

Figure 1. miRNAs belonging to the miR379–410 cluster are expressed in cortical progenitors and neurons.

- A, B The forebrains were collected at the indicated developmental stages. Small RNAs were extracted and subjected to qRT-PCR using specific primers that recognise mature miRNAs. The relative expression levels of the miRNAs normalised to their expression in the forebrain at E13.5 are shown in (A). The relative expression levels of the miRNAs normalised to the expression of miR369-3p at E15.5 are shown in (B). At E15.5, miR543 is fifteen times more abundant than miR369-3p, miR495 and miR496 in the developing forebrain.
- C The forebrains of *Hes5::GFP* transgenic mice were collected, and single-cell suspensions were prepared and fluorescence-activated cell sorting (FACS)-sorted to isolate the GFP⁺ and GFP⁻ cell fractions. The relative expression levels of the miRNAs in *Hes5*⁺ (GFP⁺) and *Hes5*⁻ (GFP⁻) fractions are shown.
- D The forebrains of E15.5 mice were collected, and single-cell suspensions were stained for CD29 and CD24 followed by FACS sorting. Small RNAs were isolated and subjected to qRT-PCR.
- E *In situ* hybridisation was conducted to detect mature miR543. A miR543-specific locked nucleic acid (LNA) probe was hybridised on cryosections of E13.5 wt brains and E15.5 brains that had undergone *in utero* electroporation at E13.5 with either a pcDNA3.1-pre-miR543 construct or anti-miR543 LNAs. Images of the boxed regions are shown at a higher magnification. Scale bars, 100 μ m. VZ: ventricular zone, SVZ/IZ, subventricular zone, intermediate zone; CP, cortical plate.



To further study the expression of miR543, the most abundant of the four miR379–410 cluster miRNAs in the developing forebrain, we performed *in situ* hybridisation on E13.5, E15.5 and E17.5 brain slices using a probe that specifically detects mature miR543. Consistent with the qRT-PCR results, we detected miR543 expression by neural progenitors (in the VZ), as well as by differentiating neurons (in the CP). In the IZ, which is mainly composed of migrating newborn neurons, miR543 expression is weaker but still detectable (Fig 1E, Supplementary Fig S1D). To determine the specificity of the *in situ* hybridisation signal, we used a scramble probe (Supplementary Fig S1D). Moreover, we overexpressed or knocked down the expression of miR543 in the developing neocortex by the *in utero* electroporation (Tabata & Nakajima, 2001). As expected, miR543 overexpression enhanced the *in situ* hybridisation signal, and miR543 depletion significantly decreased the signal (Fig 1E).

Taken together, these results show that miR369-3p, miR495, miR496 and miR543 are expressed in the neural progenitors and differentiating neurons of the developing neocortex, which suggests that these miRNAs may play important roles in multiple neurogenic processes.

miRNAs belonging to the miR379–410 cluster interact directly with the Ncad 3'UTR

To test for the direct binding of the predicted miRNAs to the Ncad 3'UTR, we performed luciferase reporter assays. The pGL3P reporter plasmid carrying the Ncad 3'UTR downstream of the firefly luciferase cDNA was co-transfected with the pcDNA3.1 vector expressing one of the 21 candidate miRNAs and the pRL vector containing the *Renilla* luciferase cDNA for normalisation. It was previously shown that one of the 21 candidate miRNAs, miR194-1, binds directly to Ncad 3'UTR, downregulating its expression *in vitro* and *in vivo* (Meng et al, 2010), and therefore, we used this as a positive control. Interestingly, three out of the five miR379–410 cluster miRNAs significantly downregulate the reporter gene expression compared with the empty vector control (Fig 2A). Quantitative RT-PCR confirmed the expression of all five miR379–410 cluster miRNAs at comparable levels (Supplementary Fig 2A). The overexpression of miR369-3p and miR496 decreases the luciferase expression level by approximately 50% comparable to the known Ncad regulator miR194-1. The overexpression of miR543 decreases reporter expression by approximately 35%. No significant decrease in reporter expression is observed following overexpression of miR495 (Fig 2A). Therefore, we used miR495 as a negative control in the remainder of the study. Additionally, overexpression of miR499 or

miR129-1 also significantly decreases reporter expression (data not shown).

To determine whether there is a direct interaction between the miRNAs and the Ncad 3'UTR, we replaced the miRNA seed sequence within the corresponding pcDNA3.1-pre-miRNA construct and the predicted miRNA binding sites within the pGL3P-Ncad-3'UTR construct with the corresponding complementary sequences (Supplementary Fig S2B). It is predicted that miR194-1 and miR543 bind to two different sites in the Ncad 3'UTR, and therefore, these sites were mutated separately. Mutation of either the seed sequence or the predicted binding sites abolishes reporter activity (Fig 2B). These results indicate that there is a direct interaction between these miRNAs and the Ncad 3'UTR.

The miRNAs, which are encoded in a genomic cluster, may be co-expressed *in vivo*. Therefore, these miRNAs may independently or cooperatively bind to their targets and act in a synergistic or additive manner. To determine whether the miRNAs belonging to the miR379–410 cluster act in this manner to regulate the Ncad expression level, we co-transfected different combinations of two of the three miRNAs and carried out the reporter assays. We found that the reporter activity is downregulated by approximately 70% when miR369-3p and miR496 are co-expressed (Fig 2C). These results suggest that this pair has an additive effect.

To determine whether miR369-3p, miR496 and miR543 downregulate the endogenous expression of Ncad, we overexpressed them in NIH3T3 fibroblasts and carried out an immunoblot analysis using specific antibodies. The overexpression of each miRNA significantly decreases the Ncad protein level compared with the overexpression of non-functional miRNAs containing mutations in their seed sequences, or the pcDNA empty vector (Fig 2D).

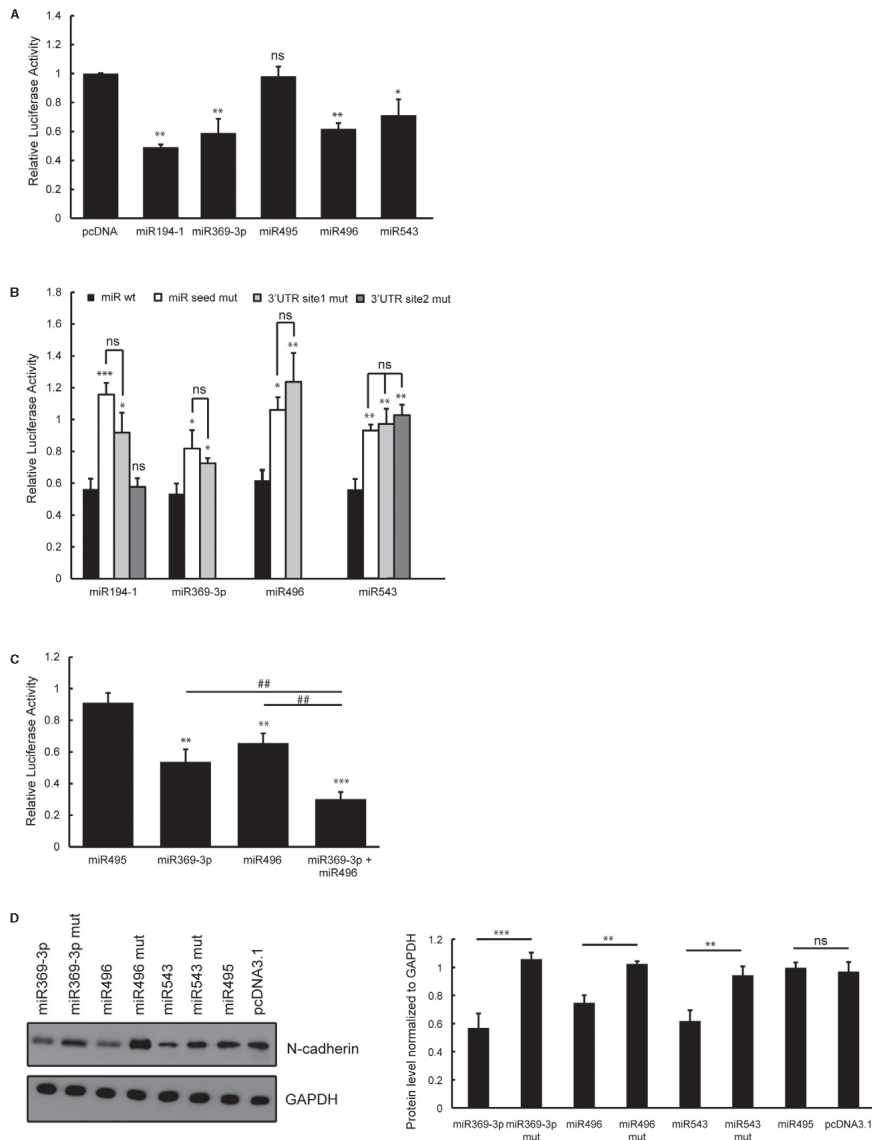
miR369-3p, miR496 and miR543 downregulate Ncad expression *in vivo* in the developing neocortex

To study the miRNA-dependent regulation of Ncad expression in the developing neocortex *in vivo*, we overexpressed or abrogated miR369-3p, miR496 and miR543 expression in RGCS *in vivo*. We co-expressed the miRNAs with pCAG-mCherry vector to identify transfected cells. We found that the overexpression of miR543 results in a reduction in Ncad protein, which is only evident in the areas containing transfected cells, but not in the adjacent areas (Supplementary Fig S3A and B). However, changes in Ncad expression are not detected when miR369-3p or miR496 is overexpressed (data not shown), suggesting that the overexpression of these two miRNAs alone is not sufficient for significant downregulation of the Ncad

Figure 2. miRNAs belonging to the miR379–410 cluster regulate Ncad expression by binding directly to the Ncad 3' untranslated region (UTR).

A–C. Luciferase reporter assays were performed in HEK-293 cells. The entire Ncad 3'UTR was cloned into the pGL3P promoter vector. Pre-miRNA sequences were cloned into the pcDNA3.1 vector. Forty-eight hours after transfection, the cells were harvested, and the luciferase activity was measured. For normalisation, a *Renilla* luciferase plasmid was co-transfected ($n = 4$; ns, not significant; * $P < 0.05$; ** $P < 0.01$; *** $P < 0.001$; **** $P < 0.001$; ***** $P < 0.01$). Three miRNAs belonging to the miR379–410 cluster significantly downregulated the luciferase activity (A). Direct interaction of miRNAs with the Ncad 3'UTR (3'UTR site mut) were replaced with the corresponding complementary sequences by *in vitro* mutagenesis. The co-transfection of two miRNAs belonging to this cluster has an additive effect that decreases the reporter activity even more when compared with the transfections of single miRNAs (C).

D. One week after transfecting with the indicated miRNA construct and selecting with G418, the NIH3T3 cells were lysed and subjected to immunoblot analysis using an Ncad-specific antibody. Bands were quantified using ImageJ software. Normalised intensity to GAPDH is plotted ($n = 4$; ns, not significant; ** $P < 0.01$; *** $P < 0.001$).



protein level *in vivo*. Nonetheless, the co-expression of miR369-3p with miR496 significantly reduces Ncad protein levels in the developing neocortex, supporting our earlier findings that specific pairs of these miRNAs have an additive effect (Fig 3A and B).

The overexpression of miR543 alone or miR369-3p with miR496 severely disrupts the RGC AJs and results in the disorganisation of the developing neocortex (Supplementary Fig S3A and B). The lack of PKC ζ staining, a polarity complex protein, at the apical membrane and the lower β -catenin level at the membrane of transfected cells confirmed disruption of the ventricular surface (Fig 3C and D, Supplementary Fig S3C and D). These results phenocopy the loss of Ncad (Kadowaki *et al*, 2007). Furthermore, this phenotype is rescued by expressing an exogenous HA-tagged Ncad that lacks the 3'UTR and is therefore resistant to miRNA-mediated regulation (Fig 3A–D, Supplementary Fig S3A–D). Anti-HA immunostaining confirmed that all transfected cells expressed the HA-Ncad rescue vector (Supplementary Fig S3E). Taken together, these results indicate that the disruption of the AJs at the ventricular surface is caused by the downregulation of Ncad and that Ncad is a primary target of miR543, miR369-3p and miR496 in the developing neocortex.

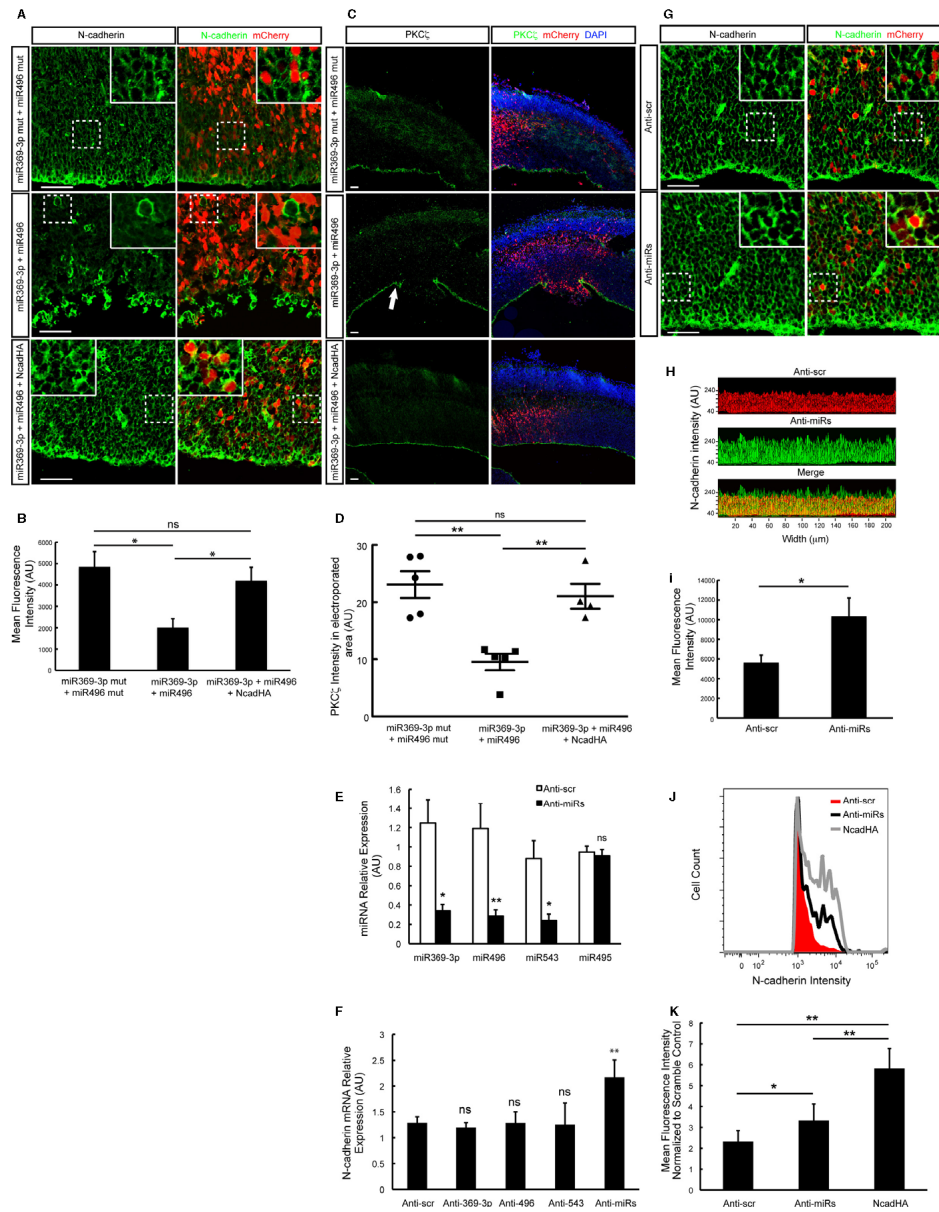
To test whether the endogenous miR369-3p, miR496 and miR543 regulate the expression of Ncad in the developing neocortex, we knocked down these miRNAs using commercially available anti-miRNAs locked nucleic acids (LNAs; GeneCopoeia) co-electroporated with pCAG-mCherry reporter construct. We confirmed that the LNAs can effectively downregulate the expression of the three miRNAs, by micro-dissecting the electroporated regions of the brains, isolating the small RNAs and performing qRT-PCR. We detected a miRNA knockdown efficiency of 65% to 70%. We used expression of miR495 as a specificity control (Fig 3E). Total mRNA was also isolated from the electroporated brain regions. Ncad mRNA levels do not change when miR369-3p, miR496 or miR543 is knocked down individually. Nevertheless, when all three miRNAs are knocked down simultaneously, levels of Ncad mRNA are significantly increased by 40% (Fig 3F). We used equal amounts of scramble LNA and control for the double or triple miRNA knockdown.

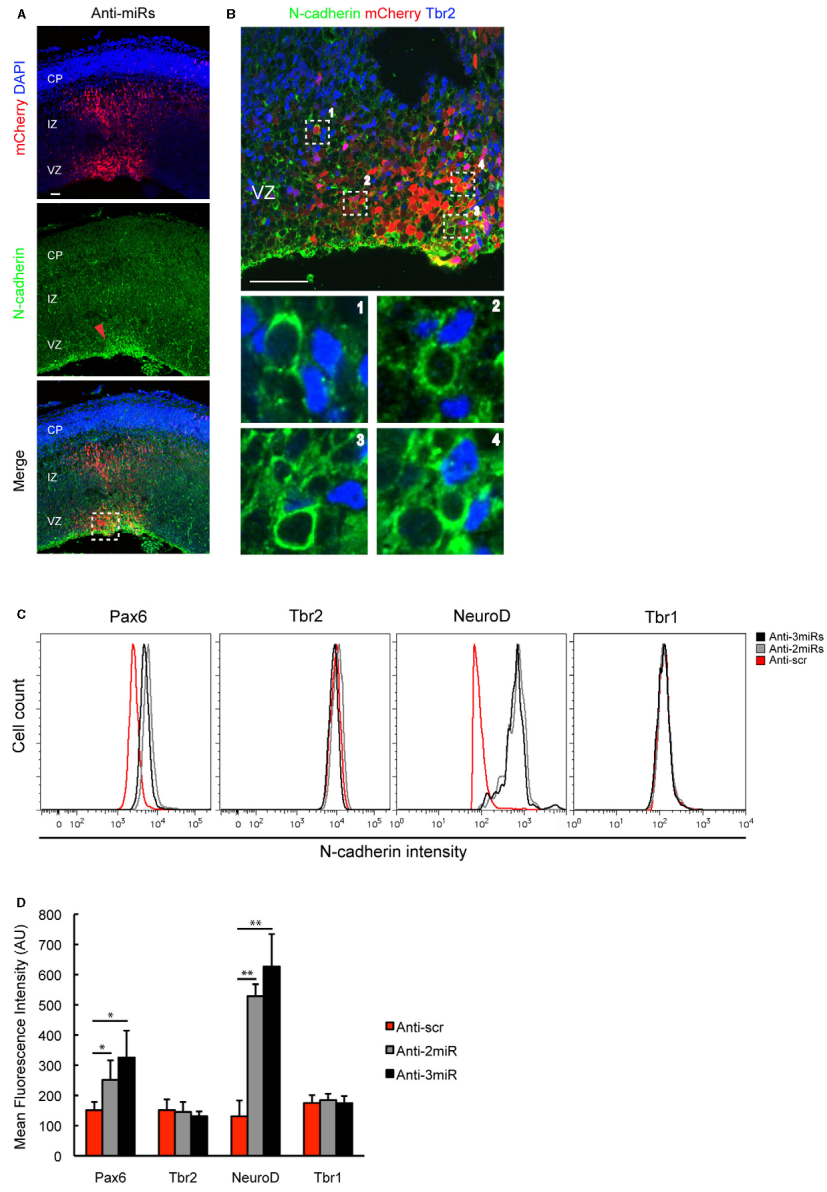
Immunostaining for Ncad confirmed these results. Only when all three miRNAs (miR369-3p, miR496 and miR543) are knocked down simultaneously is Ncad protein expression significantly increased compared with the scrambled control (Fig 3G–I).

To confirm our results, we performed FACS analysis to examine the surface expression of Ncad by mCherry⁺, miRNA-expressing cells using single-cell suspensions prepared from electroporated brains. Knockdown of all three miRNAs results in a significant increase of approximately 40% in the Ncad cell surface expression compared with the scrambled LNA control (Fig 3J and K). Overexpression of Ncad served as a positive control (Fig 3J and K). Next, we investigated which cell populations in the developing neocortex upregulated Ncad expression as a result of miRNA knockdown. Immunostaining showed an enhanced Ncad level mainly in the VZ, suggesting that the cell populations in this region are more affected by the miRNA knockdown (Fig 4A). A thorough analysis of the transfected areas of neocortex revealed that the electroporated cells with enhanced Ncad staining are Tbr2⁺ putative progenitors, suggesting that Tbr2⁺ IPCs are not affected by the miRNA knockdown (Fig 4B). To analyse which cell populations upregulated Ncad expression as a result of miRNA knockdown in more detail, we performed FACS analysis of four different cell populations (RGCs, IPCs, newborn migrating neurons in the IZ and neurons in the CP) that were identified based on the expression of the nuclear markers Pax6 (RGCs), Tbr2 (IPCs), NeuroD1 (IZ neurons) and Tbr1 (CP neurons) (Englund *et al*, 2005). The depletion of each miRNA individually does not significantly affect Ncad expression (Supplementary Fig S4A and B), but the depletion of miR369-3p with miR496 and the depletion of all three miRNAs (miR369-3p, miR496 and miR543) simultaneously significantly upregulate the amount of Ncad at the cell surface in RGCs and IZ neurons, but not in IPCs or CP neurons (Fig 4C and D), as evidenced by the peak shift towards higher Ncad intensity. In summary, these results suggest that miR369-3p, miR496 and miR543 regulate Ncad expression mainly in the RGCs and migrating IZ neurons, but not in the IPCs or CP neurons of the developing neocortex, and that

Figure 3. miR369-3p, miR496 and miR543 downregulate Ncad expression in the developing neocortex *in vivo*.

- A, B Forty-eight hours after electroporating the brain tissue at E13.5, the brains were fixed, sectioned and subjected to immunostaining experiments with an Ncad- or PKC ζ -specific antibody. The simultaneous overexpression of miR369-3p and miR496 downregulates the Ncad protein level, and the co-expression of an HA-tagged Ncad lacking its endogenous 3' untranslated region (UTR) rescues this effect. Ventricular surfaces are shown at 40 \times magnification. Scale bars, 50 μ m. Insets are indicated in dashed boxes in the original pictures. The bar graph in (B) shows the mean fluorescence intensity calculated from pictures of independent experiments for each treatment using the ZEN2010 software (Zeiss) ($n = 4$; ns, not significant; * $P < 0.05$).
- C The simultaneous overexpression of miR369-3p and miR496 disrupts the AJ, as evidenced by the loss of the PKC ζ protein, and the co-expression of an HA-tagged Ncad lacking its endogenous 3'UTR rescues this effect. Cortices are shown at 10 \times magnification. Scale bars, 50 μ m.
- D Quantification of the PKC ζ intensity in the electroporated area is shown.
- E, F Brains were electroporated with anti-miRNAs locked nucleic acids (LNAs) control (Anti-scr) against miR369-3p (Anti-369-3p), miR496 (Anti-496), miR543 (Anti-543) or all three together (Anti-miRs). Forty-eight hours later, the electroporated regions were micro-dissected and small RNAs or total mRNA was isolated. qRT-PCR that detects specifically mature miRNAs was conducted to determine the knockdown efficiency (E). qRT-PCR was performed to determine Ncad mRNA abundance (F). Data were normalised to HPRT expression.
- G–K Knockdown of all three miRNAs, miR369-3p, miR496 and miR543, increases the Ncad protein level. Forty-eight hours after the electroporation of anti-miR control LNAs (Anti-scr) or anti-miR LNAs against miR369-3p, miR496 and miR543 (Anti-miRs), the brains were fixed, sectioned and subjected to immunohistochemistry with an Ncad-specific antibody. Ventricular surfaces are shown at 40 \times magnification. Scale bars, 50 μ m (G). Images of the VZ of electroporated brains stained for Ncad were subjected to 2.5D projection using the ZEN2010 software (Zeiss) (H). The mean fluorescence intensity was calculated from pictures of independent experiments for each treatment as in (G) using the ZEN2010 software (Zeiss) ($n = 4$; * $P < 0.05$) (I). Forty-eight hours after the electroporation of Anti-scr or Anti-miRs, the electroporated regions were micro-dissected and single-cell suspensions were stained for cell surface Ncad and analysed by fluorescence-activated cell sorting. The overexpression of Ncad served as a positive control (Ncad-HA) (J). The mean fluorescence intensity was calculated using the FlowJo software (Tree Star) (K) ($n = 5$; * $P < 0.05$; ** $P < 0.01$).





there is a partial redundancy in function and cooperation among these miRNAs.

miR369-3p, miR496 and miR543 regulate neuronal differentiation *in vivo*

To determine whether miR369-3p, miR496 and miR543 regulate RGC proliferation and neuronal differentiation, we transfected RGCs in the mouse brain with miRNA overexpression constructs or anti-miR LNAs at E13.5 by *in utero* electroporation. Electroporated brains were analysed at E15.5 by immunostaining with antibodies against markers for RGCs (Pax6), IPCs (Tbr2) and differentiated neurons (Tbr1) (Englund et al., 2005).

The overexpression of miR543 or miR369-3p with miR496 results in premature neuronal differentiation, as shown by a significant decrease in Pax6⁺ RGCs and an increase in Tbr1⁺ neurons (Supplementary Fig S5, Fig 5A and B). Furthermore, co-electroporation of the plasmid encoding the HA-tagged Ncad without its endogenous 3'UTR at a low concentration rescues this differentiation phenotype (Fig 5A and B, Supplementary Fig S5). There is no evidence of increased apoptosis after miRNA overexpression (Supplementary Fig S6A).

The knockdown of the individual miRNAs did not result in significant changes in the proliferation or differentiation of RGCs (Supplementary Fig S6B). However, when miR369-3p, miR496 and miR543 are knocked down simultaneously, neuronal differentiation is significantly reduced at the time of analysis (Fig 5C and D), suggesting a redundant function of these three miRNAs. Furthermore, there is a significant increase in apical but not basal mitoses—which suggests an increase in RGC, but not IPC proliferation (Supplementary Fig S6C and D)—in agreement with the FACS results that show higher Ncad levels in RGCs, but not in IPCs. We observe similar effects when we overexpress Ncad. Taken together, these results indicate that by fine-tuning Ncad levels, miR369-3p, miR496 and miR543 regulate cell proliferation and differentiation.

miRNAs belonging to the miR379–410 cluster regulate neuronal migration *in vivo*

Because we observed that miR369-3p, miR496 and miR543 were also expressed in differentiating neurons (Fig 1C and D), we investigated whether these miRNAs regulate neuronal migration, in addition to neuronal differentiation.

We overexpress miR543 or miR369-3p with miR496 at E13.5 and analyse the distribution of electroporated cells 2 days later. We find an increase in the migration of cells out of the VZ, which we can rescue by expressing low amounts of the HA-tagged Ncad lacking

the endogenous 3'UTR (Supplementary Fig S7A, Fig 6A). Conversely, the simultaneous knockdown of all three miRNAs results in a decreased migration of cells out of the VZ, which is phenocopied by overexpressing the HA-tagged Ncad (Fig 6A).

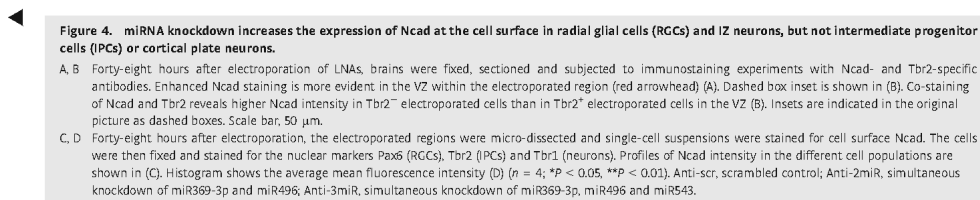
However, these migrational changes may be a secondary effect resulting from the differentiation defects previously described in our results. In addition, they may reflect changes in radial glia-independent VZ to IZ migration. To further investigate the relationship between the differentiation and migration defects and to analyse potential changes in radial glia-dependent migration from the IZ to the CP, we overexpressed the three miRNAs and the mCherry reporter under the control of the NeuroD1 promoter, which is active in newborn neurons, but not RGCs at E13.5, and analysed the distribution of the transfected cells at E17.5.

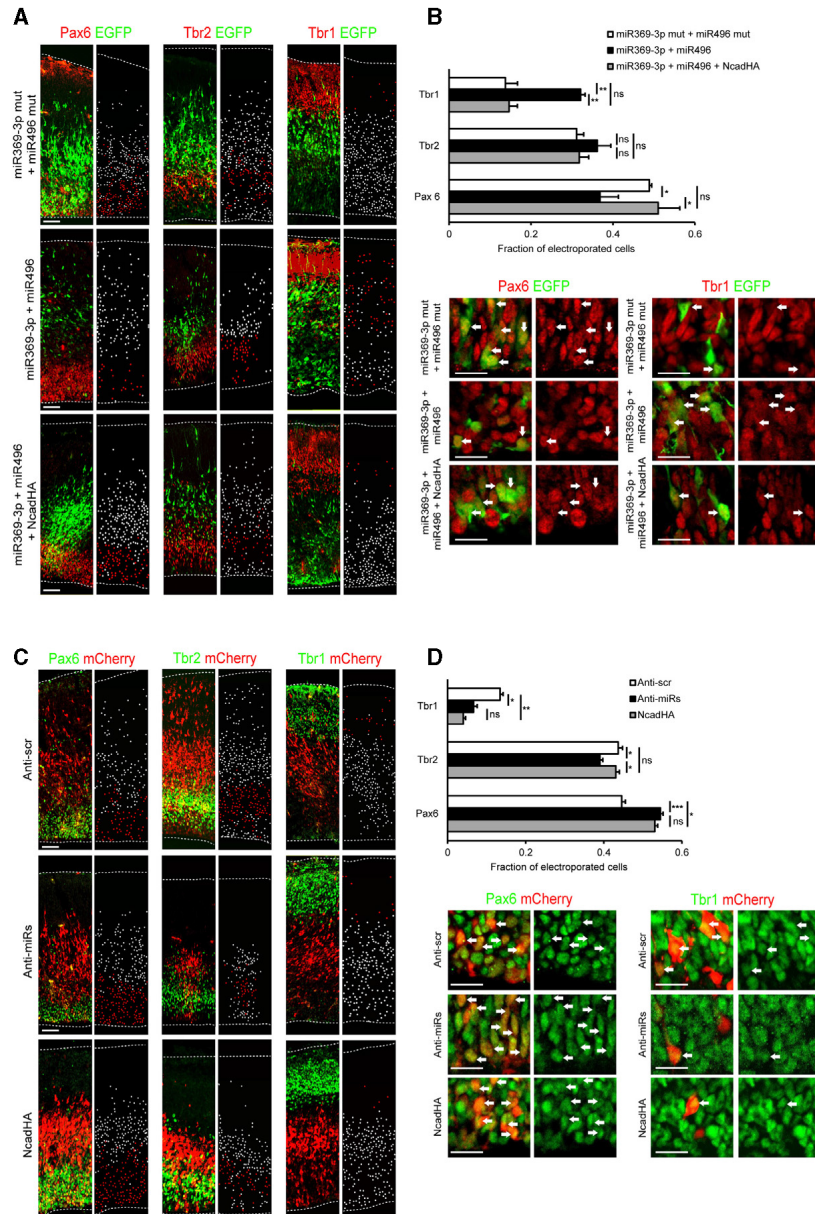
Although the overexpression of each miRNA has no effect, co-expression of miR369-3p and miR496 results in fewer cells migrating into the upper cortical plate (UCP) and more cells remaining in the lower cortical plate (LCP) and IZ (Supplementary Fig S7B and Fig 6B). Conversely, when miR369-3p with miR496 (Anti-2miR), or these together with miR543 (Anti-3miR) are knocked down simultaneously, more transfected cells migrate into the UCP and fewer electroporated cells migrate into the LCP. Of note, the overexpression of Ncad from the NeuroD1 promoter phenocopies this phenotype (Fig 6B). Furthermore, the migrating neurons appeared to have morphological abnormalities. We observed a higher proportion of rounded cells in the SVZ and a higher proportion of migrating neurons with branched leading processes in the CP compared with the scrambled control at E15.5. Additionally, the leading processes appear to be thicker at E17.5 when the expression of all three miRNAs was knocked down (Supplementary Fig S7C–E).

Taken together, these results suggest that miR369-3p, miR496 and miR543 regulate neuronal migration and that Ncad is an important target of these miRNAs in migrating neurons. This is in agreement with the previous results showing enhanced Ncad expression levels in NeuroD1⁺ cells (Fig 4C and D). Notwithstanding, we cannot rule out the possibility that the effects on migration and morphology of differentiating neurons could be caused by a misregulation of not only Ncad, but also other as yet to be identified miRNA targets.

Additional targets are only regulated in their expression by individual miRNAs, but not by miR369-3p, miR496 and miR543 together

miRNAs typically regulate the expression of numerous targets. Phenotypes that arise upon interfering with the expression of





particular miRNAs might be a consequence of the misregulation of several of these targets. With an *in silico* approach, we identified 16 putative targets that were predicted to be regulated by at least two of the miRNAs (Supplementary Table S3). Of these, only genes with a known expression pattern in the developing neocortex were chosen for further analysis, namely Adam10, TrappC8, Cxadr, Pax6, PlxnA2 and Mbnl1.

The 3'UTRs of the selected target genes were cloned downstream of the Firefly luciferase gene in the pGL3P vector, and reporter assays were performed. Overexpression of miR369-3p significantly decreased luciferase expression of vectors containing the 3'UTRs of Adam10, a metalloprotease that regulates Ncad turnover on the cell surface (Reiss *et al.*, 2005), PlxnA2, a receptor of the semaphorin signalling pathway that plays a role in neuronal migration (Renaud *et al.*, 2008), and TrappC8, a member of the endocytic pathway trafficking complex (Zong *et al.*, 2011). This was not the case, however, when miR496 or miR543 was overexpressed (Supplementary Fig S8A). To confirm the regulation of these targets *in vivo* in the developing neocortex, we micro-dissected brains electroporated with LNAs against each of the miRNAs and carried out qRT-PCR experiments. Only the knockdown of miR-369-3p significantly increased the expression of Adam10 and TrappC8, but not that of PlxnA2 (Supplementary Fig S8B).

In contrast to the simultaneous overexpression or knockdown of miR369-3p and miR496 in newborn neurons or RGCs, the overexpression or knockdown of miR369-3p alone in the respective cell population did not cause a neuronal migration defect or differentiation effect (Supplementary Fig S8C and data not shown). Together, these results suggest that the neuronal migration phenotype we observed upon the simultaneous knockdown or overexpression of miR369-3p, miR496 and miR543 in newborn neurons might not be caused primarily by changes in the expression of Adam10, PlxnA2 and TrappC8. Nevertheless, other targets of these miRNAs may also play a role during neuronal migration.

Discussion

In the developing neocortex, Ncad plays important roles, such as maintaining the tissue architecture and regulating neural stem cell proliferation, neuronal differentiation and neuronal migration. For the correct execution of all of these processes, the level of Ncad

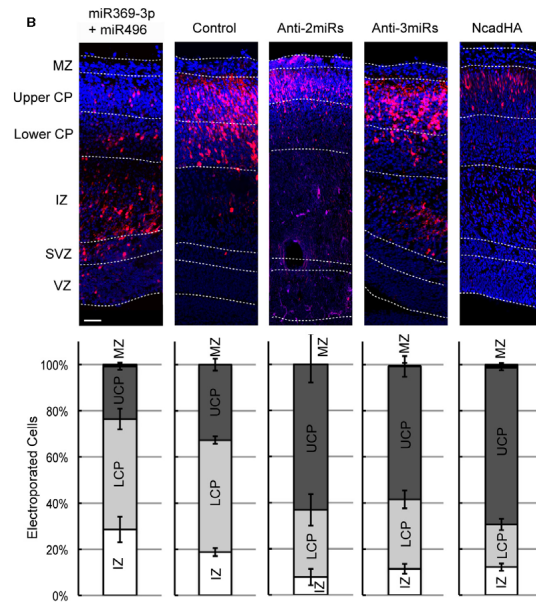
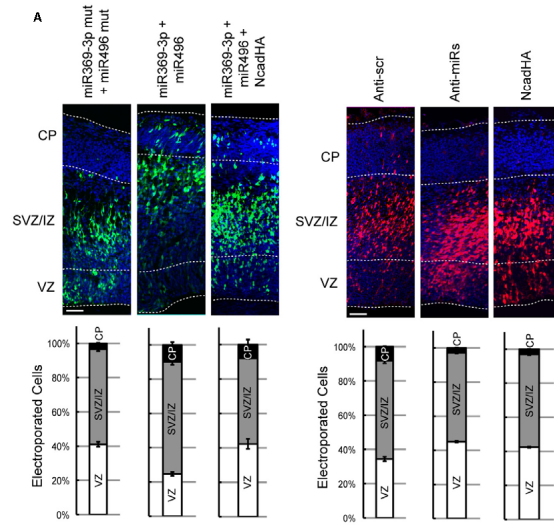
must be precisely regulated. Recently, it has been shown that Ncad activity is controlled by endocytosis and the Reelin pathway in migrating neurons, but much less is known about the transcriptional and post-transcriptional regulation of Ncad expression (Kawauchi *et al.*, 2010; Franco *et al.*, 2011; Jossin & Cooper, 2011). In this study, we show that three miRNAs belonging to the miR379–410 cluster, miR369-3p, miR496 and miR543, fine-tune the expression level of Ncad in the developing neocortex and regulate neural stem cell proliferation and neurogenesis as well as neuronal migration.

Similar to Ncad, these three miRNAs are expressed throughout the neocortex during development. They are expressed in neural stem cells and differentiating neurons, and their expression levels are higher during early developmental stages and lower during the late developmental stages. The overlapping expression patterns of Ncad and its regulatory miRNAs indicate that these do not function by turning Ncad expression on and off. Rather, our results suggest that miRNAs from the miR379–410 cluster form a regulatory network that keep the Ncad expression level within a physiological range that allows for proper neuronal differentiation and migration. Several studies highlight the importance of an accurate expression level in the developing neocortex. In the VZ, maintenance of the stem cell niche is achieved through adhesion-dependent β -catenin signalling. In this previous study, an insufficient Ncad level, generated by an shRNA-mediated knockdown technique, resulted in an increased number of cells exiting the cell cycle and premature neuronal differentiation (Zhang *et al.*, 2010). In our study, overexpression of the three miR379–410 cluster miRNAs produces a phenotype similar to the premature neuronal differentiation described previously. More importantly, this phenotype can be rescued by co-expression of an Ncad variant that is resistant to miRNA-mediated regulation. On the other hand, the simultaneous knockdown of miR369-3p and miR496 or all three of these miRNAs results in an increase in the amount of Ncad at the cell surface of RGCs, an increase in RGC proliferation and a reduction in neuronal differentiation. This suggests that miR369-3p, miR496 and miR543 regulate RGCs proliferation and differentiation by repressing Ncad expression and that fine-tuned Ncad levels are required for proper neurogenesis to occur.

In previous studies, different effects on the migratory behaviour of newborn neurons were observed depending on the developmental stage and the specific cell type in which Ncad expression had been reduced. Zhang *et al.* showed that neuronal migration

Figure 5. miR379–410 cluster miRNAs regulate neuronal differentiation.

- A, B Simultaneously overexpressing miR369-3p and miR496 results in early neuronal differentiation. miRNA expression constructs were co-electroporated with pCAG-eGFP at E13.5. Forty-eight hours later, the electroporated brains were analysed. Images double immunostained for GFP (green) and markers (red) for radial glial cells (RGCs) (Pax6), intermediate progenitor cells (Tbr2) and neurons (Tbr1) illustrate that miR369-3p and miR496 induce neuronal differentiation. The co-expression of an HA-tagged Ncad rescues this early differentiation phenotype. Images next to the respective immunostaining images show visual representations where all electroporated cells that also express Pax6, Tbr2 or Tbr1 are labelled red, while all electroporated cells that do not express Pax6, Tbr2 or Tbr1 are labelled white (A). Histogram showing the percentage of GFP⁺ Pax6⁺, GFP⁺ Tbr2⁺ and GFP⁺ Tbr1⁺ cells over the total population of GFP⁺ electroporated cells is given (B). Higher magnification images show a representative region of the VZ (Pax6⁺) and of the cortical plate (CP) (Tbr1⁺). Arrows indicate electroporated cells that express the respective marker. Scale bars: 50 μ m for images at the left, 20 μ m for magnified images (B).
- C, D Knockdown of miR369-3p, miR496 and miR543 results in a decrease in cell differentiation. Anti-miR locked nucleic acids were co-electroporated with pCAG-mCherry at E13.5. The electroporated brains were analysed 48 h later. Immunostaining (green) for Pax6, Tbr2 and Tbr1 is shown. mCherry is shown in red. Representative pictures illustrating the delay in neuronal differentiation after knockdown of miR369-3p, miR496 and miR543. Overexpressing the HA-tagged Ncad results in a similar delay in cell differentiation. Scale bars: 50 μ m (C). The histogram shows the percentage of mCherry⁺ Pax6⁺, mCherry⁺ Tbr2⁺ and mCherry⁺ Tbr1⁺ cells over the total population of mCherry⁺ cells. Higher magnification images show representative regions of the VZ (Pax6⁺) and the CP (Tbr1⁺). Arrows indicate those electroporated cells that express the respective marker. Scale bars: 50 μ m for images at the left, 20 μ m for magnified images (D).



increased 30 h after an shRNA inhibiting Ncad expression was expressed in RGCs, an effect we also observe 48 h after we overexpressed miR543 or miR369-3p together with miR496. This increase in neuronal migration may be a consequence of a premature exit from the cell cycle and premature neuronal differentiation. In contrast, when miR369-3p and miR496 were overexpressed together under the control of the NeuroD1 promoter, neuronal migration was impaired 4 days after electroporation. Specifically downregulating the Ncad expression level in migrating neurons may possibly delay the migration of neurons because of adhesion defects. Conversely, knocking down the expression of the miRNAs resulted in an increase in migration at later stages with a higher proportion of neurons migrating to the upper cortical plate. Overexpressing Ncad specifically in newborn neurons phenocopied this effect. These apparently opposite findings may be the result of the different functions of Ncad in different cell populations. While in RGCs it is required for stem cells niche maintenance, in migrating neurons it is required for motility of the cell towards the CP. Also, the different modes of migration that are affected may play a role. While the overexpression of the miRNAs in RGCs predominantly affects glia-independent VZ to IZ migration, the specific overexpression in newborn neurons affects glia-dependent migration into the CP. However, the regulation of different sets of targets of these miRNAs in RGCs versus migrating neurons cannot be ruled out.

It is widely accepted that miRNAs regulate the expression of numerous targets. Therefore, Ncad might not be the only target that is regulated in its expression by miR369-3p, miR496 and miR543. In this study, we identify two more targets of miR369-3p, namely Adam10 and TrappC8. None of these targets, however, is in addition regulated by one of the other two miRNAs. The sole action of miR369-3p seems to be insufficient to affect neuronal differentiation or migration *in vivo*. Nevertheless, changes in expression of these targets, together with other targets of miR496 yet to be identified, and in addition to changes in the expression of Ncad, might contribute to the neuronal differentiation and migration defects observed upon the simultaneous knockdown or overexpression of miR369-3p and miR496.

In contrast to Drosha- and Dicer-knockout studies, which showed no effect on RGCs proliferation, the knockdown of the three miRNAs of the miR379–410 cluster in our study enhanced RGCs proliferation (De Pietri Tonelli *et al.*, 2008; Knuckles *et al.*, 2012). This discrepancy

might be due to the fact that mature miRNAs have been shown to be very stable in the developing neocortex (Knuckles *et al.*, 2012). Therefore, a genetic depletion of components of the miRNA-processing machinery might not be as effective as a knockdown approach targeting mature miRNAs. However, it might as well be that compensatory mechanisms are activated in a genetic knockout but not in a system such as the *in utero* electroporation technique, which targets only a subset of cells.

The miR379–410 cluster, located within the *Gtl2/Dlk1* locus, is composed of more than 50 miRNAs (Khudayberdiev *et al.*, 2009), which are expressed in the developing and adult brain (Seitz *et al.*, 2004). Three of these miR379–410 cluster miRNAs (miR134, miR329 and miR381) are necessary for activity-dependent dendritogenesis (Fiore *et al.*, 2009), and miR134 negatively regulates the dendritic spine size in hippocampal neurons (Schrott *et al.*, 2006). During embryonic development, miR134 regulates neural stem cell proliferation and neuronal migration by repressing the expression of chordin-like 1 and doublecortin (Gaughwin *et al.*, 2011). Taken together with our study, these results suggest that the miR379–410 cluster forms a large regulatory network that controls different aspects of neuronal development and function. Because the cluster encodes more miRNAs than the ones that have been currently investigated, other miRNAs belonging to this cluster may have additional functions that have not yet been identified. Future studies investigating which of these miR379–410 cluster miRNAs are necessary for specific aspects of neuronal development and function and which targets they regulate will be of great interest in this field.

Materials and Methods

Animals

Hes5::GFP mice have been described elsewhere (Basak & Taylor, 2007). All mice were on a C57BL/6J background and 8–12 weeks old. The mice were maintained on a 12-h day/night cycle with adequate food and water under specific pathogen-free conditions. They were treated according to Max Planck Institutional and German Federal regulations under licence numbers 0-06/02 and G-09/18 (Ethical Commission Freiburg, Germany).

Figure 6. miR379–410 miRNAs regulate neuronal migration.

A The brains were electroporated at E13.5 and analysed at E15.5. miR369-3p and miR496 constructs were co-electroporated with pCAG-eGFP. The histograms show the percentage of GFP⁺ cells in each cortical area. miRNAs vs. mut miRNAs $\chi^2 = 66.21$, $P < 0.001$, miRNAs vs. miRNAs rescued with NcadHA $\chi^2 = 80.61$, $P < 0.001$ (mut miRNAs $n = 3$ brains, 1165 cells; miRNAs $n = 4$ brains, 1155 cells; miRNAs + NcadHA rescue $n = 3$ brains, 1031 cells). Knockdown of miR369-3p, miR496 and miR543 delays the cell migration towards the CP. Anti-miR locked nucleic acids (LNAs) were co-electroporated with pCAG-mCherry. The histograms show the percentage of mCherry⁺ cells in each cortical area. Scrambled control (Anti-scr) vs. anti-miR LNAs (Anti-miRs) $\chi^2 = 49.83$, $P < 0.001$, Anti-scr vs. NcadHA $\chi^2 = 52.21$, $P < 0.001$ (Anti-scr $n = 4$ brains, 1187 cells; Anti-miRs $n = 4$ brains, 1520 cells; NcadHA $n = 4$ brains, 1307 cells). Scale bars, 50 μ m.

B The overexpression of miR369-3p with miR496 delays migration, whereas the knockdown of miR369-3p, miR496 and miR543 together enhances migration during later developmental stages. The overexpression of NcadHA under the control of the NeuroD1 promoter phenocopies the miRNA knockdown phenotype. The brains were electroporated at E13.5 with pNeuroD1-mCherry, pNeuroD1-miR369-3p and pNeuroD1-miR496, pNeuroD1-mCherry and the anti-miR LNAs or with pNeuroD1-mCherry and pNeuroD1-NcadHA as indicated, and analysed at E17.5. The electroporation of pNeuroD1-pre-miRNAs mutated in the seed sequence was used as a control. The histograms show the percentage of mCherry⁺ cells in each cortical area. Control vs. miR369-3p + miR496 $\chi^2 = 88.21$, $P < 0.001$, control vs. Anti-2miRs $\chi^2 = 133.0$, $P < 0.001$, control vs. Anti-3miRs $\chi^2 = 97.15$, $P < 0.001$, control vs. NcadHA $\chi^2 = 229.6$, $P < 0.001$ (control $n = 6$ brains, 1435 cells; miR369-3p + miR496 $n = 7$ brains, 1007 cells; Anti-2miRs $n = 3$ brains, 558 cells; Anti-3miRs $n = 5$ brains, 1112 cells; NcadHA $n = 5$ brains, 726 cells). Scale bar, 50 μ m.

Data information: Images result from merging two different pictures of the same tissue sample. VZ, ventricular zone; SVZ/Z, subventricular zone, intermediate zone; CP, cortical plate; MZ, marginal zone.

In utero electroporation

In utero electroporation was performed exactly as described elsewhere (Knuckles *et al.*, 2012). A brief description of the *in utero* electroporation experiments as well as plasmid and antibody information are given in Supplementary Materials and Methods.

Cell culture, reporter assays and immunoblot experiments

Neurons were cultured in neurobasal medium supplemented with 10% B27 and 200 μ M of L-glutamine. Neural precursor cells were cultured in the same medium with the addition of 100 μ g/ml of EGF and 100 μ g/ml of FGF.

HEK-293 and NIH3T3 cells were cultured in DMEM supplemented with 10% FCS, 1% non-essential amino acids, 15 mM HEPES, 10 units/ml of penicillin and 10 μ g/ml of streptomycin. For luciferase assays, 2.5×10^4 cells/well were seeded and transfected with 100 ng of the constructs cloned in pGL3P vector, 20 ng of the pRL control vector and 200 ng of the pcDNA3.1-pre-miRNA plasmid using the calcium-phosphate method. After 48 h, the cells were lysed, and the enzymatic activity was analysed using a Centro LB 960 luminometer (Berthold Technologies).

For immunoblot analysis, NIH3T3 cells were transfected with Lipofectamine 2000 (Invitrogen) according to the manufacturer's instructions. After 1 week of selection with G418, the cells were lysed. Thirty micrograms of protein was resolved by electrophoresis on SDS-10% acrylamide gels. The gels were blotted on PVDF membranes, and Western blot analyses were performed with an antibody directed against Ncad (BD Transduction Laboratories). For normalisation, an antibody against GAPDH (Santa Cruz Biotechnology) was used. Quantification of the bands was performed with ImageJ and normalised to GAPDH band intensity. Plasmids and constructs are listed in Supplementary Materials and Methods. Primer sequences are given in Supplementary Table S1.

Real-time RT-PCR

Mice were sacrificed by cervical dislocation, and the embryos were collected. Embryonic brains were dissected, and the cortices were isolated. The tissue was homogenised using an Ultra-Turrax T25 homogeniser (IKA Labortechnik). Small RNAs were isolated using the miRPremier microRNA Isolation Kit, and total mRNA was isolated using the High Pure RNA Isolation Kit (Roche) according to the manufacturer's instructions.

Real-time RT-PCR experiments for miRNAs were performed using the TaqMan MicroRNA Assays (Applied Biosystems) according to the manufacturer's instructions. All miRNA quantities are relative to U6 snRNA.

In situ hybridisation and immunohistochemistry

For *in situ* hybridisation, the commercially available miR543 and scramble LNA probes, which are 5'-3'DIG labelled, were purchased from Exiqon. *In situ* hybridisation was performed on frozen brain sections using the EDC method as previously described (Pena *et al.*, 2009). For immunohistochemistry, brains were dissected, fixed, cryosectioned and stained with the respective antibodies.

Fluorescence-activated cell sorting

For cell population sorting, E15.5 forebrains were homogenised and single-cell suspensions incubated with commercially available anti-CD29 (BD Transduction Laboratories) and anti-CD24 (Santa Cruz Biotechnology) antibodies for 1 h on ice. A secondary antibody (anti-rat-Alexa594, Invitrogen) was used to detect CD29.

Electroporated brains were dissected, and the tissue was disrupted. For cell surface Ncad staining, living cells were incubated in a mouse anti-Ncad antibody (BD Transduction Laboratories), fixed, permeabilised and incubated in the indicated primary and secondary antibodies (primary: rabbit anti-Pax6, rabbit anti-Tbr1, rabbit anti-Tbr2 from Abcam; secondary: anti-mouse-Alexa488, anti-rabbit-Cy5, Invitrogen). FACS analysis was performed with a LSR II Cytometer (BD) immediately after treatment.

Statistics

All statistical analyses were performed with Prism (GraphPad Softwares). For reporter assays, qRT-PCR experiments, mean fluorescence intensity plots and cell counting in the electroporated brains, treatments were compared with controls using Student's *t*-test. For the statistics on the cell distribution for the electroporated brains, a contingency test followed by a chi-squared test was applied. All the samples were tested for normality and equal variances, and correction tests were performed when necessary. All bar graphs represent mean \pm s.e.m.

Supplementary information for this article is available online: <http://emboj.embopress.org>

Acknowledgments

We thank M.-J. Tsai for providing the pBS-Beta2 plasmid. We are grateful to R. Kemler for helpful discussions and for critically reading the manuscript. L.R. was a PhD student of the International Max Planck Research School Molecular and Cellular Biology and of the Faculty of Biology, University of Freiburg. This work was supported by the Swiss National Science Foundation and the SystemsX.ch project NeuroStemX (M.T.).

Author contribution

LR wrote the manuscript, conceived or designed the experiments, performed the experiments and analysed the data. RB performed the experiments. VT designed the experiments. JW wrote the manuscript and conceived or designed the experiments.

Conflict of interest

The authors declare that they have no conflict of interest.

References

- Bartel DP (2009) MicroRNAs: target recognition and regulatory functions. *Cell* 136: 215–233
- Basak O, Taylor V (2007) Identification of self-replicating multipotent progenitors in the embryonic nervous system by high Notch activity and Hes5 expression. *Eur J Neurosci* 25: 1006–1022
- Christensen M, Larsen LA, Kauppinen S, Schratt G (2010) Recombinant adeno-associated virus-mediated microRNA delivery into the postnatal

- mouse brain reveals a role for miR-134 in dendritogenesis in vivo. *Front Neural Circuits* 3: 16
- Cooper JA (2008) A mechanism for inside-out lamination in the neocortex. *Trends Neurosci* 31: 113–119
- De Pietri Tonelli D, Puivers JN, Haffner C, Murchison EP, Hannon CJ, Huttner WB (2008) miRNAs are essential for survival and differentiation of newborn neurons but not for expansion of neural progenitors during early neurogenesis in the mouse embryonic neocortex. *Development* 135: 3911–3921
- Englund C, Fink A, Lau C, Pham D, Daza RA, Bulfone A, Kowalczyk T, Hevner RF (2005) Pax6, Tbr2, and Tbr1 are expressed sequentially by radial glia, intermediate progenitor cells, and postmitotic neurons in developing neocortex. *J Neurosci* 25: 247–251
- Fiore R, Khudayberdiev S, Christensen M, Siegel G, Flavell SW, Kim TK, Greenberg ME, Schmitt C (2009) Mef2-mediated transcription of the miR379-410 cluster regulates activity-dependent dendritogenesis by fine-tuning Pimilio2 protein levels. *EMBO J* 28: 697–710
- Franco SJ, Martínez-Garay I, Gil-Sanz C, Harkins-Perry SR, Müller U (2011) Reelin regulates cadherin function via Dab1/Rap1 to control neuronal migration and lamination in the neocortex. *Neuron* 69: 482–497
- Gao J, Wang WY, Mao YW, Craff J, Guan JS, Pan L, Mak G, Kim D, Su SC, Tsai LH (2010) A novel pathway regulates memory and plasticity via SIRT1 and miR-134. *Nature* 466: 1105–1109
- Gao P, Xing AY, Zhou GY, Zhang TG, Zhang JP, Gao C, Li H, Shi DB (2013) The molecular mechanism of microRNA-145 to suppress invasion-metastasis cascade in gastric cancer. *Oncogene* 32: 491–501
- Gärtner A, Fornasiero EF, Munck S, Vennekens K, Seuntjens E, Huttner WB, Valtorta F, Dotti CC (2012) N-cadherin specifies first asymmetry in developing neurons. *EMBO J* 31: 1893–1903
- Caughwin P, Ciesla M, Yang H, Lim B, Brundin P (2011) Stage-specific modulation of cortical neuronal development by Mmu-miR-134. *Cereb Cortex* 21: 1857–1869
- Cotz M, Huttner WB (2005) The cell biology of neurogenesis. *Nat Rev Mol Cell Biol* 6: 777–788
- Gumbiner BM (1996) Cell adhesion: the molecular basis of tissue architecture and morphogenesis. *Cell* 84: 345–357
- Hatta K, Takagi S, Fujisawa H, Takeichi M (1987) Spatial and temporal expression pattern of N-cadherin cell adhesion molecules correlated with morphogenetic processes of chicken embryos. *Dev Biol* 120: 215–227
- Hatta K, Takeichi M (1986) Expression of N-cadherin adhesion molecules associated with early morphogenetic events in chick development. *Nature* 320: 447–449
- Jossin Y, Cooper JA (2011) Reelin, Rap1 and N-cadherin orient the migration of multipolar neurons in the developing neocortex. *Nat Neurosci* 14: 697–703
- Kadowaki M, Nakamura S, Machon O, Krauss S, Radice CL, Takeichi M (2007) N-cadherin mediates cortical organization in the mouse brain. *Dev Biol* 304: 22–33
- Kawauchi T, Sekine K, Shikanai M, Chihama K, Tomita K, Kubo K, Nakajima K, Nabeshima Y, Hoshino M (2010) Rab GTPases-dependent endocytic pathways regulate neuronal migration and maturation through N-cadherin trafficking. *Neuron* 67: 588–602
- Khudayberdiev S, Fiore R, Schmitt C (2009) MicroRNA as modulators of neuronal responses. *Commun Integr Biol* 2: 411–413
- Kim VN, Nam JW (2006) Genomics of microRNA. *Trends Genet* 22: 165–173
- Knuckles P, Vogt MA, Lugert S, Milo M, Chong MM, Hautbergue CM, Wilson SA, Littman DR, Taylor V (2012) Drosha regulates neurogenesis by controlling Neurogenin 2 expression independent of microRNAs. *Nat Neurosci* 15: 962–969
- LoTocco JJ, Bai J (2006) The multipolar stage and disruptions in neuronal migration. *Trends Neurosci* 29: 407–413
- Meng Z, Fu X, Chen X, Zeng S, Tian Y, Jove R, Xu R, Huang W (2010) miR-194 is a marker of hepatic epithelial cells and suppresses metastasis of liver cancer cells in mice. *Hepatology* 52: 2148–2157
- Noctor SC, Martínez-Cerdeno V, Ivic L, Kriegstein AR (2004) Cortical neurons arise in symmetric and asymmetric division zones and migrate through specific phases. *Nat Neurosci* 7: 136–144
- Pena JT, Sohn-Lee C, Rouhanifard SH, Ludwig J, Hafner M, Mihailovic A, Lim C, Holloch D, Berninger P, Zavolan M, Tuschl T (2009) miRNA in situ hybridization in formaldehyde and EDC-fixed tissues. *Nat Methods* 6: 139–141
- Pruszkowski J, Ludwig W, Blak A, Alavian K, Isacson O (2009) CD15, CD24, and CD29 define a surface biomarker code for neural lineage differentiation of stem cells. *Stem Cells* 27: 2928–2940
- Reiss K, Maretzky T, Ludwig A, Tousseyn T, de Strooper B, Hartmann D, Saftig P (2005) ADAM10 cleavage of N-cadherin and regulation of cell-cell adhesion and beta-catenin nuclear signalling. *EMBO J* 24: 742–752
- Renaud J, Kerjan G, Sumita I, Zagar Y, Georget V, Kim D, Fouquet C, Suda K, Sanbo M, Suto F, Ackerman SL, Mitchell KJ, Fujisawa H, Chédotal A (2008) Plexin-A2 and its ligand, Sema6A, control nucleus-centrosome coupling in migrating granule cells. *Nat Neurosci* 11: 440–449
- Schmitt C, Tuebing F, Nigh EA, Kane CC, Sabatini ME, Kiebler M, Greenberg ME (2006) A brain-specific microRNA regulates dendritic spine development. *Nature* 439: 283–289
- Seitz H, Rojo H, Bortolin ML, Lin SP, Ferguson-Smith AC, Cavaille J (2004) A large imprinted microRNA gene cluster at the mouse Dlk1-Ct12 domain. *Genome Res* 14: 1741–1748
- Shikanai M, Nakajima K, Kawauchi T (2011) N-cadherin regulates radial glial fiber-dependent migration of cortical locomoting neurons. *Commun Integr Biol* 4: 326–330
- Tabata H, Nakajima K (2001) Efficient in utero gene transfer system to the developing mouse brain using electroporation: visualization of neuronal migration in the developing cortex. *Neuroscience* 103: 865–872
- Tabata H, Nakajima K (2003) Multipolar migration: the third mode of radial neuronal migration in the developing cerebral cortex. *J Neurosci* 23: 9996–10001
- Takeichi M (1995) Morphogenetic roles of classic cadherins. *Curr Opin Cell Biol* 7: 619–627
- Takeichi M (2007) The cadherin superfamily in neuronal connections and interactions. *Nat Rev Neurosci* 8: 11–20
- Zhang J, Woodhead GJ, Swaminathan SK, Noles SR, McQuinn ER, Pisarek AJ, Stocker AM, Mutch CA, Funatsu N, Chenn A (2010) Cortical neural precursors inhibit their own differentiation via N-cadherin maintenance of beta-catenin signalling. *Dev Cell* 18: 472–479
- Zong M, Wu XG, Chan CW, Choi MY, Chan HC, Tanner JA, Yu S (2011) The adaptor function of TRAPPC2 in mammalian TRAPPs explains TRAPPC2-associated SEDT and TRAPPC9-associated congenital intellectual disability. *PLoS One* 6: e23350

8.2 Curriculum Vitae

Robert J. Beattie

Socinstrasse 1
Basel, Switzerland, 4051
Mobile: +41-78929-9497
Work: +41-61695-53092
robert.beattie@unibas.ch

Citizenship: Canadian, German

Education

- 2009 – Present **PhD**
Department of Biomedical Science
The University of Sheffield, Sheffield, England
University of Basel, Basel, Switzerland
- 2004 – 2009 **Bachelor of Science**, Honours (Co-op)
Major: Microbiology
University of Manitoba, Winnipeg, Canada

Relevant Courses/ Projects

Postgraduate

- RNA-Sequencing (Switzerland)
- R-programing (Switzerland)
- LTK module 1 animal license (Switzerland)
- EMBO Animal Models for Physiology and Disease (England)
- International Max Planck Research School for Molecular and Cellular Biology Practical Course (Germany)
- Home Office Animal License Modules 1-4 (England)
- Biotechnology YES (England)

Undergraduate (3000 & 4000 level)

- Honours Project
- Developmental Biology
- Mechanisms of Microbial Disease
- Molecular Biology of Eukaryotes
- Molecular Biology of Prokaryotes
- Microbial Fermentations
- Reg. of Biochemical Processes
- Immunology
- Virology
- Biological Energy Transduction
- Microbial Systematics

Research Experience

09.2009 – Present **PhD Student**, University of Basel, Basel, Switzerland
Supervisor: Prof. Verdon Taylor, Biomedicine

Jagged1 signaling pathway seems to be a hub for the regulation of many signaling transduction pathways involved in neural stem cell differentiation. My project addressed this signaling crosstalk *in vivo* and *in vitro*.

Technical skills gained through this research:

- *In utero* electroporation
- Stereotaxic injections for gene delivery (AAV and retrovirus)
- Designing BAC mouse transgenics
- Chromatin immunoprecipitation of proteins of interest
- Subcellular fractionation and analysis by western blotting
- Maintenance and analysis of neurosphere cultures (NSCs)

- 09.2008 – 09.2009 **Honours Student**, University of Manitoba, Winnipeg, Canada
 Supervisor: Dr. Steve Whyard, Biological Sciences
- Gene knock-down in mosquitos using dsRNA
 - Histological analysis of mosquito tissue samples
 - qRT-PCR analysis of cDNA samples derived from mosquitos treated with dsRNA
 - Tissue preparation for use in electon microscopy
 - Ultrastructural anaylsis by electron microscopy
 - Time point analysis of gene expression
- 05.2008 – 09.2008 **Student Internship (Co-op)**, Max-Planck Institute of Immunobiology and Epigenetics, Freiburg, Germany
 Supervisor: Prof. Verdon Taylor, Developmental Embryology
- Generation of a transgenic mouse from scratch
 - Creation of a bacterial artificial chromosome used to generate the transgenic mice
 - Preparation and sectioning of tissue samples for immunological analysis of protein expression
 - Handling and working with mice
 - DNA fragment and plasmid analysis
- 01.2007 – 04.2008 **Co-op Student**, National Microbiology Lab, Public Health Agency of Canada, Winnipeg, Canada
 Supervisor: Dr. Ute Stroehrer, Special Pathogens Group
- Worked with Rabies Virus vectors expressing foreign proteins
 - Advanced cloning techniques involving Ebola and Marburg viral nucleic acids (level 2)
 - Immunofluorescence microscopy for detection of protein expression in cells
 - Western blots for detecting protein expression levels
 - Maintained and worked with multiple cell lines

Projects

- 06.2011 – 11.2011 **Biotechnology YES Competition**, Manchester, England
 Together with an enthusiastic team of PhD students, we developed and marketed an innovative new product for use in the cancer screening industry, utilizing the latest innovative biotechnology advancements.
- Skills gained through this competition:*
- Strong team building, partnerships and cooperation
 - Creation and delivery of clear, concise business plans for venture capitalists
 - Knowledgeable on marketing demands and prerequisites
- 04.2011 **School Outreach**, The University of Sheffield, Sheffield, England
- Taking my love of science and discovery from the lab to the classroom, I worked one on one with elementary students to inspire and teach them about the world of biology
- 09.2010 – 09.2011 **BMS PhD Society**, The University of Sheffield, Sheffield, England
- I successfully established a PhD Society in the department of Biomedical Science from scratch. This involved organizing social events, charity fundraisers and the first annual BMS PhD Retreat.

Skills gained during this experience:

- Thorough planning and management from an initial idea to the final implementation
- Applying and securing adequate funds through various grants
- Designing workshops and lecture series
- Inviting guest speakers for lectures

Technical Skills

- **Animal handling:** Basic mouse and rat care, PCR based genotyping, *in utero* electroporation of mouse embryos, gene delivery through stereotactic injections in postnatal and adult, intracranial infusions, trochar implantations,
- **Biochemistry:** Chromatin immunoprecipitation, SDS-PAGE, Western blot, Subcellular fractionation
- **Cell Culture:** Culturing and maintaining classical lines (N2A, NIH3T3, HEK293, Platinum-E), Primary neural stem cell cultures (Neural stem cell), Lipid reagent and calcium phosphate based cell culture transfection, primary cell culture nucleofection (Amaxa system) and viral transduction.
- **Data Analysis:** Basic RNA and ChIP sequencing analysis, R programming language, cloning and DNA analysis software (Lasergene, SeqMan), TierBase animal software.
- **Histochemical:** Immunofluorescence, cryostat tissue sectioning, proliferation assays (Thymidine analog incorporation, EdU).
- **Microscopy:** Conventional light and Fluorescence microscopy, Confocal microscopy (experience with Zeiss LSM 510 confocal, Zeiss Observer Apotome, Leica DMI 4000, Leica video microscope, Zeiss Zen and Leica application suite.)
- **Molecular Biology:** RNA/DNA extraction and purification, cloning DNA fragments and plasmid analysis, BAC cloning (transgenic mice), RT-PCR, qRT-PCR (SYBR green), RNA-Sequencing.

Professional Skills

- Comfortable working independently or within a group.
- Strong communication, interpersonal, and leadership skills gained through volunteer experiences as well as in my time as PhD representative.
- Skilled program developer and conference planner exemplified by the PhD society and annual PhD weekend retreat I founded in our department.
- Robust problem-solving skills.
- Enthusiastic and self motivated to work long hours having high energy and integrity.
- Highly organized with extensive multi-tasking abilities as displayed at my lab while carrying out several experiments simultaneously.
- Highly adaptable to new situations and cultures as demonstrated by my international research experience in Canada, Germany, England, and Switzerland.
- Knowledgeable on the biotechnology industry, entrepreneurship and business start-ups.

Grants

- SSN travel grant (2012)
- Career Development and Transferable Skills Training Grant (2010)

Societies and Memberships

01.2012 – Present Swiss Society of Neuroscience (SSN)
04.2013 – 04.2014 International Society for Stem Cell Research (ISSCR)
10.2012 – 10.2013 British Neuroscience Association (BNA)

Publications

Beattie, R., C. Rolando, E. Boda, R. Ivanek, A. Buffo, V. Taylor, “Jagged1 regulates a fate switch of neural stem cells to oligodendrocyte precursor cells in vivo.” *Manuscript being prepared.*

Beattie, R.*, A. Grabosch*, M. Rukavina*, V. Taylor., “PICK1 and PKC α Link Jagged1 to TBLR1 and Histones to Regulate Neurogenesis.” *Manuscript being prepared.*

Beattie, R.*, T. Mukhtar*, V. Taylor (2014). “Fundamentals of Neurogenesis and Neural Stem Cell Development.” Neural Surface Antigens: From Basic Biology Towards Biomedical Applications. J. Pruszek.

Rago, L. **R. Beattie**, V. Taylor and J. Winter (2014). “miR379-410 cluster miRNAs regulate neurogenesis and neuronal migration by fine-tuning N-cadherin.” EMBO J.

Meetings and Symposia

2014 The 8th Notch Meeting – Athens, Greece

2014 The 9th FENS Forum of Neuroscience – Milan, Italy – Poster to be presented

2013 The 11th ISSCR Meeting – Boston, USA – Poster presented

2012 The 8th FENS Forum of Neuroscience – Barcelona, Spain – Poster presented

2011 Cambridge Neural Stem Cell Symposium – Cambridge, England – Poster presented

Awards

- White Cross Guild Scholarship (2004)
- Steeltown Insurance Award (2004)
- Grade 12 Valedictorian (2004)
- Grade 12 Citizenship Award (2004)
- Nominated for MTS Young Humanitarian Award (2004)
- HSC Volunteer Leaders in Service Excellence (2007)
- Manitoba Co-op Student of the year award (2008)
- Honourary mention Canadian Co-op Student of the year award (2008)
- Millennium Student Success Grant (2008)
- U of M bursary (2008)
- UMSU bursary (2008)
- 3M Canada Company Bursary (2008)
- Max Planck Institute of Immunobiology and Epigenetics International Student Ambassador Award (2010)